Timber-glass shear wall stabilised timber modules

Application of a timber-glass shear wall as stabilising element in a mid-rise modular timber building

CIE5060-9 MSc Thesis

Jippe van Daalen

Delft University of Technology

TU Delft

BURO HAPPOLD

Timber-glass shear wall stabilised timber modules

Application of a timber-glass shear wall as stabilising element in a mid-rise modular timber building

by

Jippe van Daalen

in partial fulfilment of the requirements for the degree of

Master of Science
in Civil Engineering

Track
Building engineering

Specialisation
Structural design

at the Delft University of Technology,
to be defended publicly on February 21st, 2024 at 16:00.

Student number: 4677528

Thesis committee

Prof. dr. ir. C. Louter	TU Delft (chair)
Ir. S. Pasterkamp	TU Delft
Ir. M. Felicita	TU Delft
Ir. T. Uijtenhaak	BuroHappold (daily supervisor)

Cover: https://finchbuildings.com/finch-buildings-gaat-bouwen-voor-woonwaard/

An electronic version of this thesis is available at http://repository.tudelft.nl/.

TU Delft

BURO HAPPOLD

Preface

This master thesis concludes the final part of my studies at the TU Delft. This thesis fulfills the final part of the requirements for my Master of Science in Civil Engineering.

First and foremost, I would like to thank the members of my graduation committee: Prof.dr.ir. Christian Louter, Ir. Sander Pasterkamp, Ir. Maria Felicita and Ir. Tijl Uijtenhaak. Thank you for your guidance and expertise throughout the process. Your experience and knowledge have been extremely valuable in my research. Especially your feedback and suggestions during the progress meetings have been extremely motivating and sometimes even overwhelming. Nevertheless, I always got a lot of new energy after those meetings to dive deeper into the topic.

Special thanks to Tijl Uijtenhaak for providing me with all the resources and connections within Buro-Happold. You made it feel like I was part of the company and team in Rotterdam, and not just working on my own project. Your enthusiasm about modular buildings and timber buildings has been contagious and also made me enthusiastic about the topic. I appreciated all the discussions and your refreshing view on the topic.

I would also like to thank all my (future) colleagues at Burohappold for always being helpful and open to questions and discussions.

Finally, I would like to thank the people who have not directly been involved but were a huge support along the journey. A massive thank you to my parents and brother for their continuous support, not just during this project but during my entire studies here in Delft. Also a big thank you to my roommates and friends, for making my time here in Delft unforgettable.

Jippe van Daalen
Delft, February 2024

Summary

In the Netherlands, there is a huge demand for housing. The Dutch government is planning to build 900.000 houses by 2030, which is an enormous challenge. Modular construction could offer a solution to this challenge. Modular construction offers many advantages over traditional construction methods. Modular buildings can be built faster, more efficiently, with less waste, and to a higher standard.

Currently, most of the modular building can be fabricated off-site, except for the stability system. This is traditionally a concrete core or a steel frame. Therefore, the question arises: Could modules be designed such that there is no need for an additional stability system? As modules are typically built in a rectangular shape, incorporating stability elements such as bracings along the longer side of the module is not the problem. The main challenge lies in the limited length available for stability elements on the shorter side of the module, combined with the fact that this shorter side is commonly used for windows and openings for door frames. This introduces a conflicting interest between structural capacity and daylight within the module. This conflicting interest becomes more and more prominent as the building height goes up. A possible solution to this problem can be found in the use of a load-bearing window frame with glass infill as a stability element, often referred to in literature as a timber-glass shear wall (TGSW). A typical build-up of a TGSW consists of a timber substructure, a timber adapterframe, screws connecting the adapterframe to the substructure, a structural adhesive, and a glass pane.

Therefore, this thesis will answer the main research question: 'To what extent can the structural performance of a timber-glass shear wall as a stability element in a timber module be used to accommodate for the stability of a mid-rise modular timber building?' The goal of this thesis is to gain insight into the structural capacity of a TGSW, such that it can be used as a stability element in a modular timber building.

The approach to answering the main research question consists of several steps. First, a literature study was conducted on modular buildings and timber-glass shear walls. The outcome of the study has provided insight into how modular buildings are constructed in general and how relevant aspects such as progressive collapse, fire safety design, and foundation design influence structural design. The study also resulted in an analytical prediction model for the load-bearing capacity and stiffness of the TGSW. Through this prediction model, it became clear how the properties of individual components (substructure, screws, frame, adhesive and glass pane) relate to the load-bearing capacity and stiffness of the total TGSW-system.

The second step was to propose a design for a modular timber building composed of timber modules. To save on computational time, the stability elements of the building are modelled using steel diagonals as an equivalent system for the TGSW. The cross-sectional area of the steel diagonals is directly related to the properties of the TGSW. Therefore, the steel diagonals have identical stability properties as the TGSW. In this study, varying the type of adhesive and the spacing of the screws was found to have the most significant impact on the overall structural properties of the TGSW. The horizontal connections are made of steel plates fastened with screws. The vertical connections are realised by shear plate connectors. The entire building was modelled in a 3D FEM programme to assess the structural behaviour of the building and its compliance with building regulations. Several building configurations ranging from 1:1 to 1:3 height-to-width ratio were investigated. For each building configuration, the cross-sectional area of the steel diagonals was adjusted within a specified range. This range corresponds to variations in adhesive type or screw spacing. As a result, design graphs were produced, which present the requirements for the load-bearing capacity and stiffness of the stability system. These can be compared to the load-bearing capacity and stiffness of the TGSW. This comparison can be used as a validation method to determine the viability of the TGSW stability element in a modular building.

The results of this study indicate that a modular building can be stabilised by a TGSW up to six stories within the height-to-width ratio of 1:1 to 1:3. The minimum building configurations per story height are: 3 modules high by 5 modules wide, 4 modules high by 8 modules wide, 5 modules high by 12 modules wide, and 6 modules high by 18 modules wide. These slenderness ratios were governed by the strength of the TGSW. The limiting factor in the load-bearing capacity is the shear strength of

the adhesive. These slenderness ratios could only be reached with elastic adhesives such as silicones. The next step is to create a more extensive FEM model that could predict the load-bearing capacity and stiffness of the TGSW in a more accurate way compared to an analytical model. Furthermore, exploring the performance of the TGSW under different horizontal loads, such as earthquakes, would give valuable insight.

Contents

Nomenclature

Abbreviations

Abbreviation	Definition
TGSW	Timber-glass shear wall
ALPA	Alternative load path analysis
ULS	Ultimate limit state
SLS	Serviceability limit state
ALS	Accidental limit state
CLT	Cross laminated timber
GLT	Glue laminated timber
MCA	Multi criteria analysis
FEM	Finite element method

1

Introduction

1.1. Context

In the Netherlands, there is a significant housing shortage due to a growing population, permit approval precedures and lack of available building space. Therefore the Dutch government is planning to build 900.000 houses by 2030 (Ministerie van Algemene Zaken 2023). This challenge requires a rapid construction method. Modular building could offer a solution to this challenge. Modular building is an innovative and rapid construction method in which buildings are composed of standardised prefabricated modules or units. The advantage of modular building is that the construction process becomes safer, faster, cheaper, less construction space is required, better quality is delivered, is more reusable, and reduces waste material (Ferdous et al. 2019). Currently, the maximum building height of stacked modules is mainly determined by horizontal forces like wind and earthquake loads (Gunawardena 2016). This means that the horizontal stability of the building cannot be ensured by the stacked modules alone, and additional stability systems are necessary. Two commonly used examples of these systems are presented in Figure 1.1 and Figure 1.2:

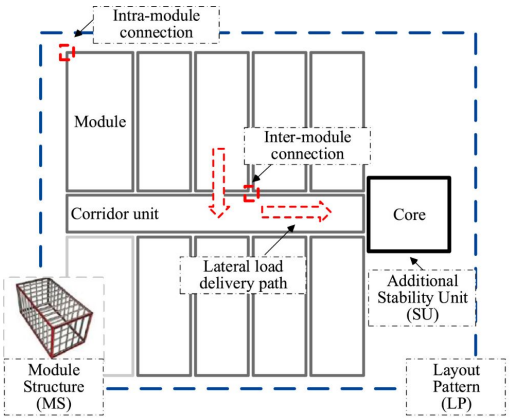

Figure 1.1: Stability provided by a core (Ye et al. 2021).

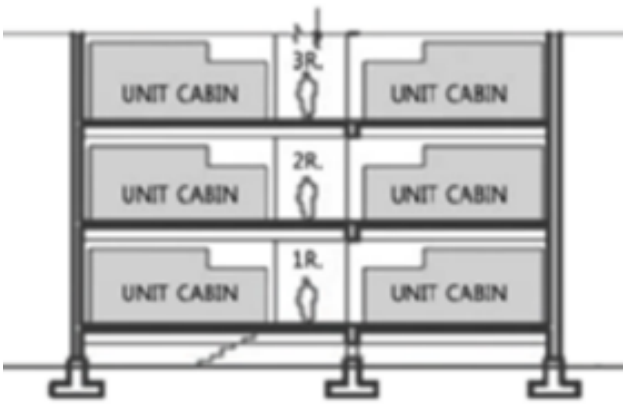

Figure 1.2: Stability provided by a modular in-fill method (Park and Ock 2016).

In Figure 1.1 stability is provided by adding a concrete or steel core. The modules are then placed around the core and attached to the core, allowing the horizontal forces to be transferred via the core to the foundation. Vertical forces are transferred through the modules to the foundation (Park and Ock 2016). The second system consists of a concrete or steel frame combined with the Modular infill method, which is an effective way to improve the structural stability of a building. With this method, modules are prefabricated and then installed in the frame. Both the vertical and horizontal forces are transferred through the frame (Park and Ock 2016). The major disadvantage of both methods is that they are not modular, demountable, or reusable. To create an entirely modular building, stability must therefore be ensured in a different way.

Stability can be ensured by incorporating the stability elements inside each module creating 'stability modules'. Connecting the stability modules should allow for force transfer between the modules, thus coupling all the stability elements from a structural point of view. All the coupled stability elements together form the global stability system for the entire building. The primary challenge for stability modules is the limited length available for stabilising elements in the transverse direction, in combination with the necessary openings required for door frames and windows. As the building height goes up and the horizontal forces increase, more space is required for the stability elements inside the module. As a consequence, to create a stability module, the windows should become smaller to increase the space for stabilising elements. However, this reduces the natural daylight in the module. This conflicting interest can be solved by using the window, and more specifically the timber frame and glass pane, as stabilising element. The literature commonly refers to this concept as the Timber-Glass Shear Wall (TGSW) element as shown in Figure 1.3.

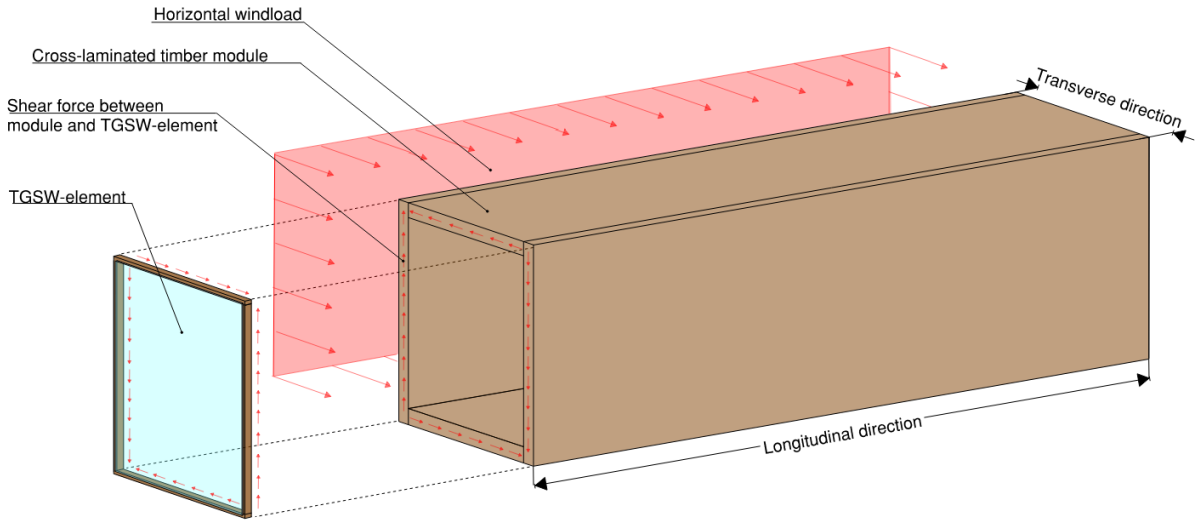

Figure 1.3: Timber-glass shear wall as stabilising element in a cross-laminated timber module

In this way, the interests of both transparency and stability aspects of the module are aligned. The problem is that there is no precedent in the application of glass as a stability element in a module. Therefore, to create a safe, ductile and warning stability system more knowledge is desired about this timber-glass composite system applied in a module. Furthermore, more insight must be gained on a suitable way to connect the window frame to the timber module.

1.2. Problem statement

In the Context section, a conflicting interest between transparency and stability of a timber module is introduced. To solve this conflict, the window, more specifically the timber frame and glass pane acting as a composite, can potentially serve as a stabilising element. However, the application of a structural timber-glass composite within a module lacks precedent. The main problem originates from insufficient knowledge and understanding of this subject necessitating the need for further knowledge and understanding of the timber-glass composite system applied in a timber modular building.

Some research has been done on the structural performance of the timber-glass shear wall itself, which indicates the potential of the system, but again the application in modular buildings lacks. Currently, the structural capacity of a window is fully neglected in strength- and stiffness calculations of modular buildings as building standards only recently introduced guidelines for in-plane loaded windows as well as load-bearing adhesive connections (Felix Nicklisch, Hernandez, et al. 2015). Nevertheless, the strength and stiffness of a timber-glass composite are yet to be specified. Hence, the realisation of modular buildings using this principle requires more research into the structural performance of the TGSW.

From the viewpoint of modular construction, it remains unclear how the horizontal forces are distributed across the stability elements of the modular building. Therefore, a full-scale FEM-model is

necessary to demonstrate how forces are distributed over the stability elements of the modular building. This model should include the properties of the stability elements, the modules, and the connections between the modules. Concequently, a comparison can be made between the required strength and stiffness of the entire building and those offered by the stability element (TGSW). This comparison serves as a validation method to determine the viability of the Timber-Glass Shear Wall (TGSW) as a stability element for modular buildings.

Additionally, there is a need to identify an effective method for connecting window frames to timber modules, in order to develop a stabilising module that successfully combines transparency and stability.

1.3. Scope

In this section, the scope of this research is given. As modular construction is a broad topic, not all aspects can be considered within the given time frame. The scope of this research is limited by the following boundary conditions:

- Typology: The purpose of the stabilising modules is limited to residential use. The height of the buildings is focused on mid-rise structures thus limited to 3 to 10 stories.
- Materials: The materials used for the design of the modules is limited to glass and cross-laminated timber (CLT). In the connections, optionally steel is used to create stronger connections.
- Type of loading: Lateral forces included in this research are limited to wind loads. Blast loading, seismic loading and impact loading are not considered. The vertical loads included are the standard permanent and variable loads for residential buildings as described in the Eurocode.
- Fire safety: The fire safety aspects of a timber module are assessed qualitatively during the literature study. Options to improve the fire safety of the structural elements of the module are given but no calculations will be performed in this thesis.
- Progressive collapse: Progressive collapse in modular buildings is described qualitatively in the literature research but the robustness of the building will not be assessed. In theory, the connections provide both horizontal and vertical ties. However, no calculations are performed to verify whether these connections can indeed contribute to a robust design in case of progressive collapse.
- Foundation: The design of the foundation is out of the scope of this research. For the global FEM-model the foundation is modelled with rigid line supports under each side of the modules. The stiffness of the foundation is therefore not included.
- Building physics: No attention is paid to the building physics of the modules. This means that acoustics, thermal comfort and thermal insulation, ventilation and lighting are not within the scope of this research. One exception is made in the detailing of the timber-glass wall as this should be a realistic design including for example weather tightness.
- Building services: Building services such as electrical wiring, air ducts, plumbing and elevator shafts are out of the scope of this research.

1.4. Research goal

The goal of this research is to gain insight into the structural capacity of the timber-glass composite wall in a new application as a shear wall in stabilising modules. With this insight, it becomes possible to apply a timber-glass wall in a timber module and stabilise a modular building without an additional stabilising system. Plus, the gained insight can be used to identify critical parameters and components which can be used to improve the structural performance of the timber-glass wall within the module requirements. As a consequence, modular buildings can be built more slender, without the need for additional stability systems.

To achieve this main goal four sub-goals are specified:

- **The first goal is to propose an initial design for the timber glass shear wall based on the literature study.** Several properties of the timber-glass shear wall itself have already been researched. Within these research projects, various design proposals were suggested for the detailing of the timber-glass wall. These include the type of timber, cross-section of the timber frame,

type of glass, dimensions of the glass pane, type of structural adhesive, thickness of the adhesive, and number of bond lines. Combining the findings of these researches, a design for the timber-glass shear wall will be proposed with a focus on the application in a timber module.

- **The second sub-goal is to develop a prediction model that quantifies the structural performance of the timber-glass wall.** Using this model, the structural performance of the timber-glass wall can be improved by adjusting parameters within the module requirements. The following parameters will remain unchanged: the timber frame dimensions, glass dimensions, and structural adhesive dimensions. Two parameters will be varied: The shear modulus of the structural adhesive within a specific range and the screw spacing.
- **The third sub-goal is to understand how a modular building which is composed of 'stability' modules structurally behaves.** Two aspects are specifically of interest: how the horizontal force is distributed over the stability elements and the total deflection of the building. A full-scale FEM-model of the modular building, including properties of the stability elements, modules and connections, should provide this understanding. A better understanding of the structural performance of the building results in requirements for the structural performance of the stability elements. These requirements can be compared to the actual structural performance of the stability element (TGSW). This comparison is used as a validation method to determine the viability of the Timber-Glass Shear Wall (TGSW) as a stability element for modular buildings.
- **The forth sub-goal is to identify an effective method for connecting the timber window frame to the timber module.** To use the timber-glass wall as a stabilising element in a timber module, it must be connected to the timber module.

1.5. Research questions

1.5.1. Main research question

The main research question is:

To what extent can the structural performance of a timber-glass shear wall as a stability element in a timber module be used to accommodate for the stability of a mid-rise modular timber building?

1.5.2. Sub research questions

In order to answer the main research question several sub-questions have been formulated:

1. How does the existing literature relate the in-plane stiffness and load-bearing capacity of the timber-glass shear wall to the properties of its individual components like the adhesive, glass pane, timber frame, screws, and timber substructure?
2. What connection can be used to create an intra-modular connection between the timber-glass shear wall and the load-bearing elements of the timber module?
3. What are common solutions to create an inter-modular connection between timber modules?
4. How can the analytical spring-model be used to improve the in-plane stiffness and load-bearing capacity of the timber-glass shear wall within the module requirements?
5. How can the results of a finite element model be used to determine the load-bearing capacity and stiffness of a mid-rise modular timber building, including the strength and stiffness of the inter and intra-modular connections?

1.6. Methodologies

In this chapter, the methodologies which will be used to answer the sub-research questions will be specified. This is split into three parts and shown in Figure 1.4.

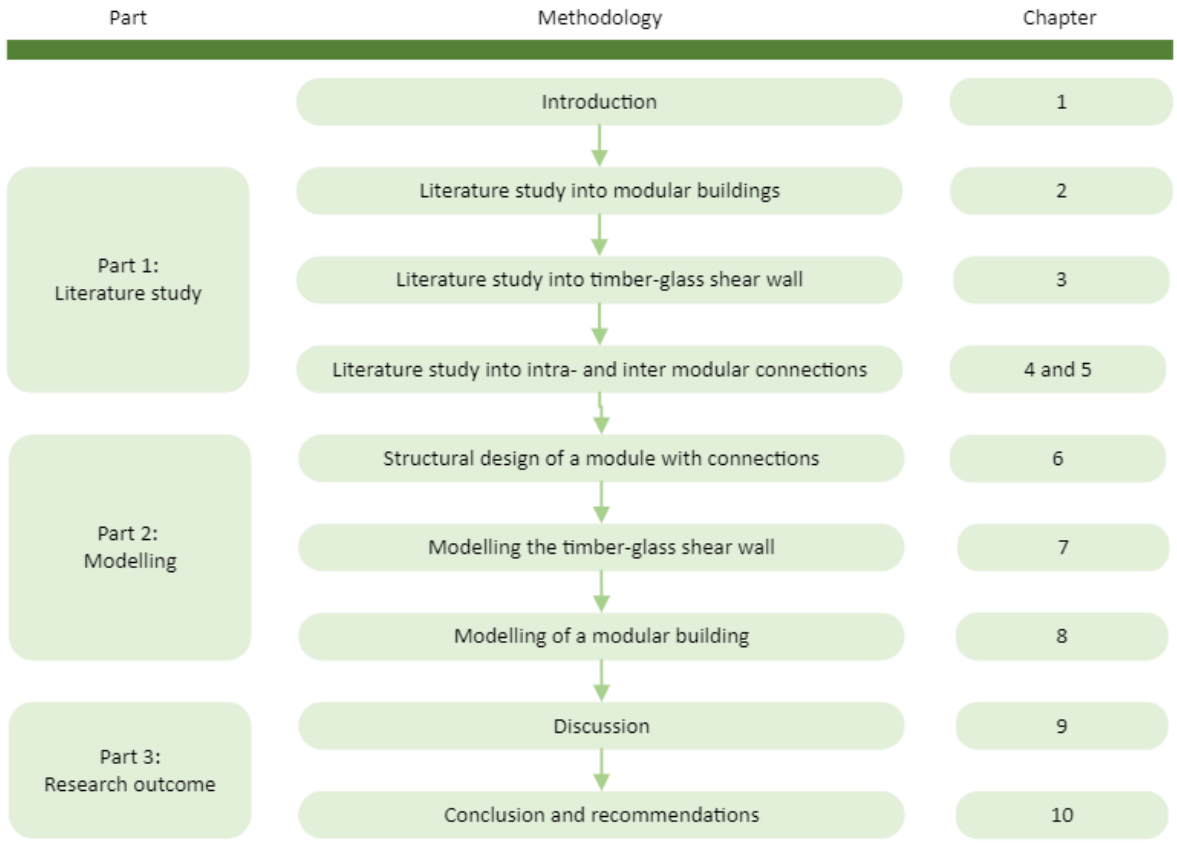

Figure 1.4: Research methodology outline.

The first part consists of literature research and focusses on mid-rise modular buildings and on timber-glass composite walls. Relevant topics within mid-rise modular buildings such as progressive collapse, fire safety of modules, building regulations for modular construction, inter- and intra-module connections and types of foundations suitable for modular construction will be discussed. Additionally, relevant aspects within timber-glass composite walls such as timber joints, the type of adhesive, and glass- and timber properties will be discussed. This can be summarized as defining the properties of the individual components of the TGSW-system, which is visualised in part (a) in Figure 1.5.

The second part starts with a design proposal for a modular timber building based on the literature study. An example of a CLT-module is presented, with dimensions and properties. Furthermore all connections, will be presented along with the properties of these connections. In essence, an example building design of a modular timber building is given. Within this proposed design, the load-bearing capacity and stiffness of the TGSW is investigated. At this point the TGSW is modelled as a spring model as can be seen in Figure 1.5 as part (b). Two parameters will be adjusted to explore their relation with the load-bearing capacity and the stiffness of the TGSW: the shear modulus of the adhesive and the screw spacing.

Lastly the complete modular timber building is modelled in a FEM programme. The TGSW will be modelled with the less time-consuming fictive diagonal method which is shown in part (c) in Figure 1.5. The model will be used to assess whether the modular building complies with the ULS and SLS regulations from the Eurocode. Through reverse engineering, the building regulations can be translated into specific requirements for the Timber-Glass Shear Wall (TGSW), to ensure that the building complies with regulations.

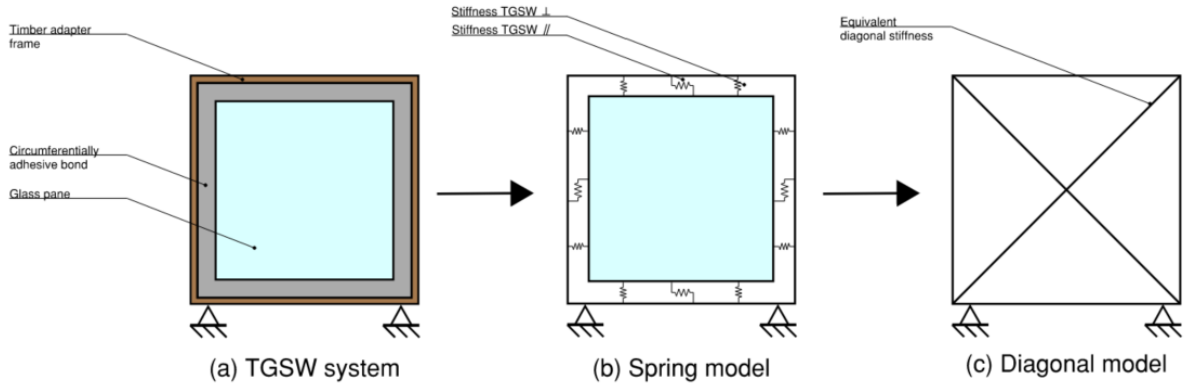

Figure 1.5: Modelling the TGSW

2

Modular construction

This chapter serves as an introduction to modular buildings. It will give an overview of the structural aspects of modular construction. First, a general description is given to inform the reader about important definitions and typologies within modular construction. Relevant literature will be presented regarding fire safety design, progressive collapse and foundation design. This chapter is used as a basis for the building design given in Chapter 7.

2.1. General

For many years the construction industry has lagged behind other sectors in terms of productivity. By shifting the production process to the factory, it is possible to increase productivity by 50 percent. This is due to a controlled and safe environment in the factory, the ability to coordinate and repeat activities, and a greater level of automation. Furthermore, construction costs can be reduced by 20% due to more efficient material use, reduced labour on site, and economies of scale (Nick Bertram et al. 2019). As a consequence of producing the majority of the building components in the factory, only the assembly process of the prefabricated elements is done on-site. This workflow is known as modular construction and can be done on several scales. Prefabricated beams and columns are examples of one-dimensional elements representing the smallest scale of prefabrication. A higher level of prefabrication is achieved when producing two-dimensional panels. This can be used for walls equipped with insulation and boarding. The largest scale of prefabrication is achieved with 3 dimensional or volumetric units which come equipped with all the essential mechanical, electrical, and plumbing components. The latter option fully utilises the potential of modular construction, allowing for 70 to 95 percent of a building to be prefabricated (M. Lawson et al. 2014). In this thesis, modular construction refers to the use of 3D volumetric units.

2.1.1. Pros and cons of modular construction

Besides the reduced construction costs and -time, additional advantages in terms of improving building quality are presented by M. Lawson et al. 2014. First of all, it gives greater opportunities for recycling and reuse of modules because of the demountable inter-modular connections. Moreover, there is less disturbance to the neighbourhood since the majority of the on-site labour is shifted toward the factory. In addition, the double-skin nature of modular construction results in excellent acoustic and thermal insulation.

Modular construction offers not only benefits but also drawbacks. The main drawback of modular construction lies in its limited flexibility regarding building design due to the repetitive nature of the modules. Furthermore, there is a trade-off between transportation costs and size limitations. For road transportation without police escort, a maximum width of 3,5 meters is permitted. This either limits the maximum size of a module or increases the transportation costs (Nick Bertram et al. 2019). Also, there is a trade-off between hoisting costs of the crane and weight limitations. A 100- or 200-tonne capacity mobile crane is required to lift modules that can weigh up to 25 tonnes. Besides the weight capacity, the radius of lifting affects the lifting capacity as this is reduced significantly at maximum crane extension. Therefore, a strategic location of the mobile crane is as important as the lifting capacity to minimise

costs (M. Lawson et al. 2014).

2.1.2. Development of timber modules

Presumably, the first concrete room module in the form of a serially manufactured house was produced in 1896 by the French firm Hennebique. This module was more or less a by-product of the industrialisation of concrete construction. After that, the developments in modular construction were slow. However, due to the post-war demand for social housing and rapid construction, the development of modular construction regained attention. Starting in the 1960s in the United States, reinforced concrete modules were used in highrises to fulfil the need for housing. Additionally, mobile housing in the form of a timber module was introduced during this period. These mobile homes can be seen as the first timber room modules.

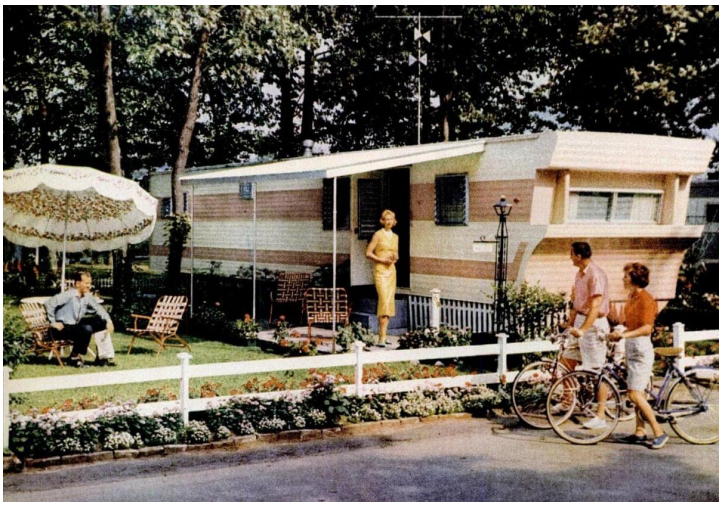

Figure 2.1: Example of a mobile home in 1960's (Americana 2021).

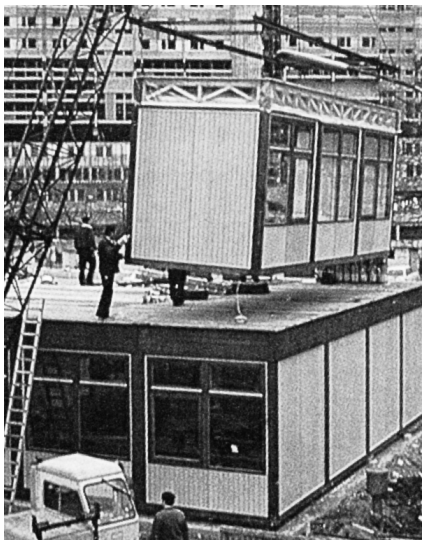

Figure 2.2: Youth centre made of timber room modules, Hanover Germany (Huß et al. 2019).

In Central Europe, the first timber modules originated in the early 1970s and were restricted to single-story buildings. These modules had standard dimensions ranging from 3x3 meters to 3x12 meters and were based on a glulam timber framework structure. Such an example is shown in Figure 2.2 where timber modules, developed by the Holtman company, are placed. These modules were used in various projects for both temporary and permanent buildings.

Up until the 1990s, all timber modular buildings were single-story buildings, but in the 1990s multi-story room modules were developed in Austria and Switzerland. In Austria, engineers started to develop a frame-constructed timber module for extendable two-storey single-family houses. In Switzerland, engineers developed a flexible system which could go even higher, up to four stories. This system was applied in the modular-T office building in Neuchâtel and was made of 57 room modules. It consists of an elevated base level for a loading zone made of a steel structure, two full office floors made of wooden containers, and a recessed top floor. The next step was taken in 2010 when the development of timber modules advanced to include structures of up to five stories. The Alpenhotel Ammerwald was constructed in 10 days and consists of a total of 96 modules on a two-story concrete base. All surfaces of the timber module, including the floor, were made of cross-laminated timber.

Figure 2.3: Modular-T building in Neuchâtel (*Modular-T* n.d.).

Figure 2.4: Alpenhotel Ammerwald (Huß et al. 2019).

Nowadays, the development of timber modules is still going on. Especially the scale in which the timber modules are applied is increasing, as projects involving 200 to 300 modules are becoming more common. Alongside the increase in scale, the building height is also being pushed higher and higher as new developments in construction methods progress. An example of this is the Puukuokka residential building in Finland, which was constructed in 2015 using only modular construction, with seven to eight floors stacked on top of each other. Another example is Hotel Jakarta in Amsterdam that has eight floors stacked of timber modules. Both the Puukuokka building and Hotel Jakarta will be discussed in more detail in the Application of modular buildings section.

Figure 2.5: Hotel Jakarta in Amsterdam (*172 hotelrooms - Hotel Jakarta - Ursem Modular Building systems* 2019).

Figure 2.6: Puukuokka Housing Block (*EUMiesAward* n.d.)

2.1.3. Application of modular buildings

Modular timber construction is used for both temporary buildings and permanent buildings. The demountability and lightweight modules make it perfect for quick and short-term purposes in case of emergencies or refugee accommodation. On the other hand, modular construction can also compete with traditional construction methods. Based on the level of prefabrication, various applications can be seen. For modular construction, the main applications are in the sectors of social housing, student housing, military housing, hospitals, prisons, or hotels since these buildings have a high level of standardisation (M. Lawson et al. 2014).

This research will focus on mid-rise modular timber buildings with a residential function. To get familiar with this kind of building, several existing projects will be reviewed:

- Hotel Jakarta
- Puukuokka
- Woodie Student Hostel
- Sara Cultural center

An extended description of each project can be found in Appendix A. The summarised results of the case study are presented in Table 2.1 and Table 2.2 below.

Project	Number of stacked modules	Number of modules	Modules type	Continuously supported / corner supported	Module manufacturer
Hotel Jakarta	8	176	CLT walls + Concrete floor	Continuously supported	Ursem
Puukuokka	8	116	CLT walls + CLT floor	Continuously supported	StoraEnso
Woodie Student Hostel	6	371	3 layered CLT walls + floor	Continuously supported	Kaufman bausystemen
Sara cultural center	13	205	CLT walls + GLT columns + CLT floors	Continuously supported + corner supported	Derome

Table 2.1: General information per project

Project	Stability system	Vertical force transferring system	Foundation type	Fire safety	Progressive collapse
Hotel Jakarta	3 reinforced concrete cores	CLT walls of the module	Pile foundation	90 min + 30 min with sprinkler	No information available
Puukuokka	CLT shear walls	CLT walls of the module	Concrete raft foundation	Gypsum board layer + sprinkler system	No information available
Woodie Student Hostel	3 reinforced concrete cores	CLT walls of the module	Pile foundation	REI 90 minutes	No information available
Sara cultural center	2 CLT cores	CLT walls + GLT columns of the module	Concrete foundation	R90/R60 + sprinkler system	No information available

Table 2.2: Structural related information per project

From the case study, several conclusions can be drawn. First of all, a core structure is mainly applied but, this should not necessarily be the case as can be seen from the Puukuokka project. Secondly, the walls are able to carry the load for at least 8 layers of stacked modules. Between 8 and 13 floors a tipping point is achieved in which the walls alone cannot provide for the vertical forces. In this case, GLT columns are required additionally. Thirdly, the foundation in all case studies is found to be made of concrete. Based on the location and the strength of the soil, piles are required additionally. Finally, from a fire safety perspective, it can be seen that sprinkler systems are often applied in mid-rise buildings to increase fire safety. Regulations prescribe 120 minutes of fire safety for the load-bearing structure. However, if sprinklers are installed, this requirement can be reduced by 30 minutes. Furthermore, according to the Finnish regulation, the load-bearing elements should be covered with non-combustible material like gypsum board. Progressive collapse is not described in any of the projects.

2.2. Structural design of timber modules

In general, three types of load-bearing modules can be distinguished:

- Continuously supported modules
- Corner-supported modules
- Non-load bearing modules, often called pods.

Continuously supported modules are modules where the walls are load-bearing. Usually, the longitudinal walls are used to transmit the vertical loads. The main reason for this is that these walls serve as a barrier between individual apartments, and thus have no openings or windows. The thickness of the CLT itself varies according to the building height (2-7 stories) and fire application between 79 and 140 mm per module wall (Huß et al. 2019). Special care should be taken so that the fire does not spread within the cavity wall between the two modules. A commercial build-up of a load-bearing wall

that can be applied up to 7 stories consists of gypsum board (≈ 25 mm), CLT (≈ 120 mm), air gap (≈ 50 mm), insulation (≈ 30 mm), CLT (≈ 120 mm) and gypsum board (≈ 25 mm) resulting in a total thickness of 370 mm. This buildup by StoraEnso is also used in the Puukuokka one building and is shown in Figure 2.7.

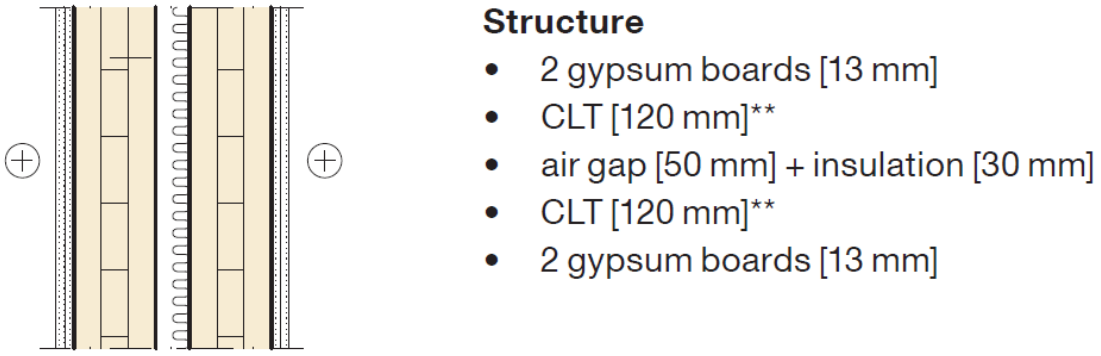

Figure 2.7: Commercial build-up CLT wall by StoraEnso

Corner-supported modules are modules where the corner posts and optional intermediate posts are load-bearing. The posts are connected via edge beams which span between the posts creating an open module. In order to reduce the thickness of the edge beams or for transportation purposes, intermediate posts can be introduced. The downside of corner-supported modules is that they have relatively weak post-beam connections in terms of rotational stiffness. To improve the stability of such a module, additional bracing elements should be applied. In timber construction, the safety of these types of modules in midrise buildings is still being investigated. For example, the robustness and the ability to form alternative load paths were investigated by Joep Knudde in his master thesis (Knuppe 2022). As a consequence, no case studies have been found with a timber corner-supported module used in a residential building.

Non-load bearing modules or often called 'pods' are non-structural modular units which are directly supported on the floors of the building. Common applications of pods are highly serviced areas such as prefabricated bathrooms, toilets, kitchens or small plant rooms. As pods usually include many services, they are often located around the shared service risers back-to-back with other pods. As a result up to four pods may be concentrated around one area of the floor slab (M. Lawson et al. 2014).

2.3. Fire safety in modular timber buildings

The main two goals of a fire safe design are to prevent any casualties and avoid damage to adjacent buildings. This means that building preservation or preventing damage to the building is of no interest although the owner of the building might take additional measures (J. Maljaars and A.J. Breunese 2015).

2.3.1. Fire safety regulations: Building Decree 2012

To meet these two goals, the Dutch government has created minimum regulations which are set out in the Building Decree 2012. This decree contains technical regulations that represent minimum requirements for all structures in the Netherlands. The requirements for fire safety from a structural point of view are described in Chapter 2 of the Building Decree and will be explained below.

Fire resistance values

The first requirement is related to the fire resistance of a building. The fire resistance of a building can be explained as a specific period of time a structure should be able to withstand the fire without the risk of structural failure. The basis for this regulation is that the building should be evacuated and searched for a reasonable amount of time during a fire, without the risk of collapse. For new residential buildings the following requirements are defined:

Heighest floor level	Fire resistance in minutes	Fire resistance in minutes for fire load <= 500 MJ/m^2
<= 7 m	60	30
7 - 13 m	90	90
>= 13 m	120	120

Table 2.3: Fire resistant level based on highest floor level (Rijksoverheid 2023)

For low-rise buildings (<= 7 meters) the fire resistance period can be shortened by 30 minutes if the permanent fire load is less than 500 MJ/m^2. For a mid-rise timber modular building, this requirement implies that the fire resistant time should be at least 120 minutes.

Fire performance characteristics

Besides the fire-resistant values, there are also additional fire performance characteristics for timber elements. For load-bearing elements three important characteristics are described in the Eurocode (NEN-EN 13501-2 2023):

- Load-bearing capacity (R): The ability of the element of building construction to withstand fire exposure under specified mechanical actions, on one or more faces, for a period of time, without any loss of structural stability.
- Integrity (E): The ability of the element of building construction that has a separating function, to withstand fire exposure on the exposed side only (not from both sides simultaneously), without the transmission of fire to the unexposed side as a result of the passage of flames or hot gases
- Thermal insulation (I): the ability of the element of building construction to withstand fire exposure on the exposed side only (not from both sides simultaneously), without the transmission of fire as a result of significant transfer of heat from the exposed side to the unexposed side.

The effects are visualised in Figure 2.8

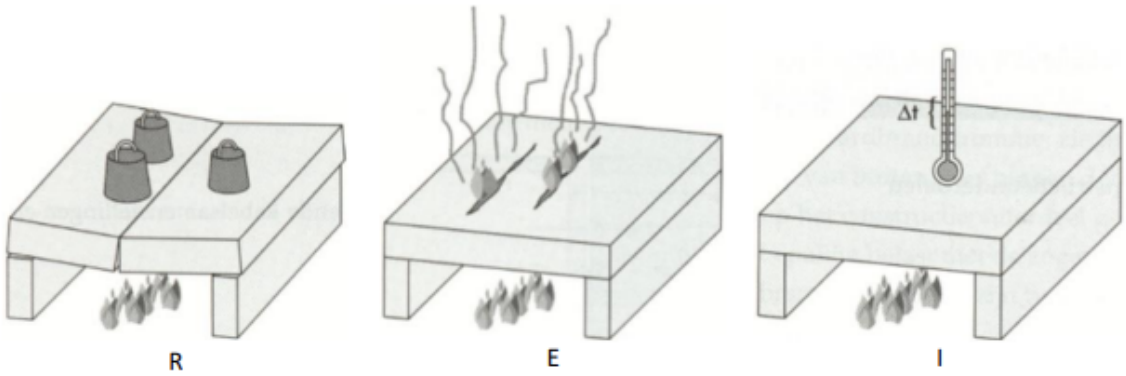

Figure 2.8: Visualisation of the three performance characteristics (Zandbergen 2016)

The first characteristic is applied to all load-bearing elements in a structure. The other two characteristics are important for compartmentalising the building which will be discussed in the next section.

Fire compartments

To prevent fire and smoke spread, the building is separated into fire compartments. These compartments are designed to be fire-resistant for 60 minutes. Within these 60 minutes, the fire and smoke should be contained within the compartment and must not spread to other compartments. In addition, the load-bearing elements should not fail within these 60 minutes, possibly causing a progressive collapse of the whole structure.

As discussed, the integrity and thermal insulation characteristics are important for constructing fire compartments. The elements and joints that separate the fire compartments must maintain their function in the event of a fire to prevent the fire from spreading. To prevent the spread of hot gases or

flames, cracks or openings cannot be formed during a fire. This is related to the integrity aspect. The second aspect is the thermal insulation, and this should prevent the temperature to rise above the ignition temperature on the unexposed fireside.

Modular buildings are compartmentalised by the way the buildings are constructed. As each module is designed to be an individual compartment, this is beneficial for fire safety design. Especially if fire stoppings are applied between two modules, it becomes harder for the fire to spread to another module. Fire stopping prevent the fire from spreading in the cavity between two modules. The double-skin nature of modular buildings complements perfectly with a fire-safe design.

Fire protection system

Besides the passive measures prescribed in the Dutch Building Decree, there are also active measures that should be applied in buildings. These are in the form of fire protection systems. The main objective of these systems is to detect and locate a fire in an early stage. In addition, the occupants and the fire brigade must be alerted. The first system that is required for all new residential buildings is the presence of smoke alarms. These should be placed in closed escape routes between the exit of a living space and an exit of a compartment. In addition, fire hoses should be present in the same way.

Another common fire protection system, that is used especially in mid-rise and high-rise buildings is a sprinkler system. A sprinkler system could control or suppress a fire in an early. This slows down the spread of the fire and gives people more time to egress the building. In the Netherlands, the application of sprinkler systems can be used to reduce the fire resistance time of the load-bearing structure with 30 minutes. For a modular midrise building, the fire resistance time can be reduced from 120 minutes to 90 minutes if a sprinkler system is applied. Looking at the examples from case study, 3 out of 4 buildings made use of the sprinkler system, indicating that this is a very useful fire protection system.

2.3.2. Structural fire design: Eurocode 5

The fire-resistant values prescribed in the Building Degree can be realised by the engineer by following the guidelines for a structural fire design given in the Eurocode EN 1995-1-2. The Eurocode describes two design procedures for determining the mechanical resistance of timber:

- Reduced cross-section method: This method uses a conservative estimation of the reduced cross-section while no reduction of the material properties is applied.
- Reduced properties method: This method estimates the reduced cross-section while also reducing the material properties.

The Eurocode and the Dutch National Annex state that the reduced cross-section method shall be applied and therefore the reduced cross-section method will be elaborated on. The reduced properties method will not be discussed any further.

It should be noted that more advanced methods can also be applied. These methods can include a FEM analysis based on parametric fire loading or computer simulations that involve computational fluid dynamics models. In the more advanced models smoke spread, visibility at different cross-sections and heat transfer within solids can be analysed. These analyses are out of the scope of this research.

Reduced cross-section method

Timber is a combustible material, but has a low coefficient of conductivity. This means that as timber is exposed to fire, the surface becomes hot but the core remains relatively cool. The heated surface of timber will pyrolyse if the temperate exceeds about 250 degrees Celsius. At this point, the timber releases gasses of decomposition from the surface after which the gases mix with oxygen and burn (J. Maljaars and A.J. Breunese 2015). As a consequence of the burning of timber, the cross-section gradually reduces. The speed at which the cross-section reduces is called the charring rate.

In the Eurocode, the charring rate is used to calculate the residual section of a wooden cross-section. The reduction is described by Equation 2.1

$$d_{ef} = d_{char,n} + k_0 d_0 \tag{2.1}$$

$d_{char,n}$ represents the charring depth and is calculated by multiplying the charring rate with the time of fire exposure. $k_0 d_0$ represents the heat-affected zone. It is assumed that the timber within the heat-affected zone and close to the char line has zero strength and stiffness. The thickness of this layer

for unprotected timber increases linearly from 0 to 7 mm within 20 minutes and remains 7 mm after 20 minutes. In the new Eurocode 5, this unprotected timber layer is increased to 14 mm.

The basic design charring rate for one-dimensional charring is described by the parameter β_0. This is the charring rate which occurs when flat wood is exposed to fire from one side. However, this basic situation is rarely the case. Therefore the notional charring rate (β_n) is introduced which incorporates several factors which influence the charring rate. Klippel and Schmid 2017 proposes a relationship between β_0 and β_n by multiplying with k-coefficients as shown in Equation 2.2. This model is also intended to be used in the updated Eurocode 5 (Wiesner and Bisby 2019).

$$\beta_n = k_s \cdot k_{pr} \cdot k_n \cdot k_g \cdot k_{cr} \cdot k_j \cdot k_{co} \cdot \beta_0 \tag{2.2}$$

The factors are explained in Table 2.4.

Coefficient	Description	Explanation
k_s	Section coefficient	Considers the influence of the width of the timber member. This parameter is only significant for the charring rate on the narrow side.
k_{pr}	Protection coefficient	Coefficient addresses the behaviour of protected timber surfaces, for which different charring rates should be applied during different phases of fire exposure.
k_n	Corner rounding	Since charring is greater near cross-section corners, gaps and fissures, β_n should be used to transform the irregular shape of residual cross-sections into simple rectangular cross-sections
k_g	Gaps between boards	
k_{cr}	Cracks and char fissures	
k_j	Joint coefficient	Considers the influence of joints in panels not backed by battens or structural members or panels and their influence on the protection and insulation time of these layers.
k_{co}	Connection coefficient	Considers increased charring for connections with metal fasteners, which conduct heat into the core of the cross-section.

Table 2.4: Definitions of k-coefficients to determine the initial charring rate β_n (Klippel and Schmid 2017)

For solid wood or glue-laminated timber, standard values are used in Eurocode 5 based on the type and density of the wood. For hardwoods, the charring rate varies linearly with the density between 290 kg/m^3 and 450 kg/m^3. The charring rate of softwood and hardwood is given in Table 2.5:

Wood type		β_n mm/min	β_0 mm/min
Softwood and beech	GLT with a characteristic density of $\geq$ 290 kg/m^3	0,65	0,7
	Solid timber with a characteristic density of $\geq$ 290 kg/m^3	0,65	0,8
Hardwood	Solid or glued laminated hardwood with a characteristic density of $\geq$ 290 kg/m^3	0,65	0,7
	Solid or glued laminated hardwood with a characteristic density of $\geq$ 450 kg/m^3	0,50	0,55

Table 2.5: Design charring rates β_0 and β_n of timber (EN 1995-1-2 2004)

The charring rate for cross-laminated timber is different compared to solid wood due to the layered, glued composition and joints between the timber boards (Klippel and Schmid 2017). When assuming the charring rate, a distinction should be made between the situation where charring layers fall off the CLT panel and where charring layers don't fall off. At around 300 °Cthe glue will fail and charring layers will fall off. If the charring layer falls, the fire protection function of the charcoal is lost. After that, twice the charring rate is expected due to the exposure of uncharred timber directly to the fire environment.

This effect continues for 25 mm and after that, the charring rate returns to its original charring rate. This principle is illustrated in Figure 2.9.

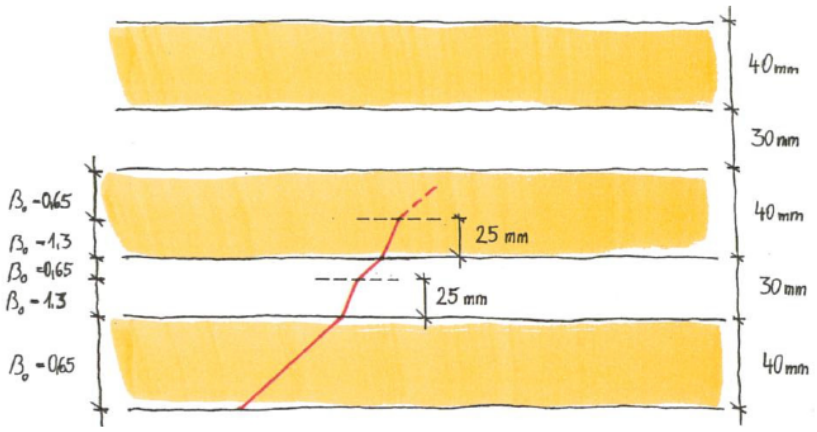

Figure 2.9: Charring rate of a CLT floor panel when the char layer falls off

If the charring layer doesn't fall off, the formed charcoal layer protects the remaining CLT. In this case, the CLT panel has similar behaviour as solid wood in fire. For wall elements, the falling off of charred layers was less common. Nevertheless, Klippel and Schmid 2017 suggests using at least five-layer CLT elements for load-bearing and unprotected wall elements to provide a robust solution. For a CLT wall panel with a gap width of less than 2 mm, Wiesner and Bisby 2019 uses a charring rate of 0.65 mm/min where only the outermost layer is charred and 0.8 mm/min where the charring progresses past the first layer.

Based on the charring depth, the reduced cross-section can be derived as a function of time. Subsequently, the loading can be compared to the resistance of the timber elements with a reduced cross-section. If the resistance remains higher than the loading during the fire-resistant time prescribed in the Building Decree, the design is assumed to be safe.

2.3.3. Glass and fire safety design

Only small parts of the building will be composed of glass but these elements are part of the main load-bearing structure, therefore it is important to look at the effect of fire on a glass pane.

Currently, NEN-EN 15998 2020 refers to the standard guidelines for load-bearing walls in case of fire. The same fire performance characteristics for timber, which were shown in Figure 2.8 apply to glass. This means that the glass used in the buildings should maintain its load-bearing capacity, integrity, and thermal insulation for a certain period of time. This classification can only be done based on fire experiments as described in the Eurocode (Bedon 2017). Glass manufacturers can classify their glass accordingly for 30, 60 90, or 120 minutes of fire performance.

For calculations on the strength of glass after a fire load of a certain time, no guidelines are given in the Eurocode. As the behaviour of glass in fire situations is relatively unknown, more research is required to develop guidelines. Nevertheless, two approaches can be made to improve the fire safety of a design according to Feldmann et al. 2014: use protection measures for example additional fire glazing, or improve the redundancy of the building. For this thesis, the second option will be incorporated in the design.

2.4. Progressive collapse

The ability of a structure to prevent progressive collapse can be described by the robustness or structural integrity of a structure. Robustness is described in the Eurocode as the ability of a structure to withstand events such as fire, explosions, impact or the consequences of human error, without being damaged to an extent disproportionate to the original cause (EN 1991-1-7 2006). This implies that a failure of a small part of the building doesn't lead to the failure of a bigger part or, even worse the entire building. It is advised that the damage should be less than either 100 m^2 or 15% of the floor area.

This can be done by looking at the ability of the structure to redistribute loads in case it is subjected to damage.

2.4.1. Design methods to prevent progressive collapse

In literature, five common design methods are proposed that use the redistribution of loads to assess the robustness. Two of these design methods are indirect meaning they are scenario-independent strategies. The other three methods are direct methods and address a specific damage scenario. These methods are shown in Figure 2.10.

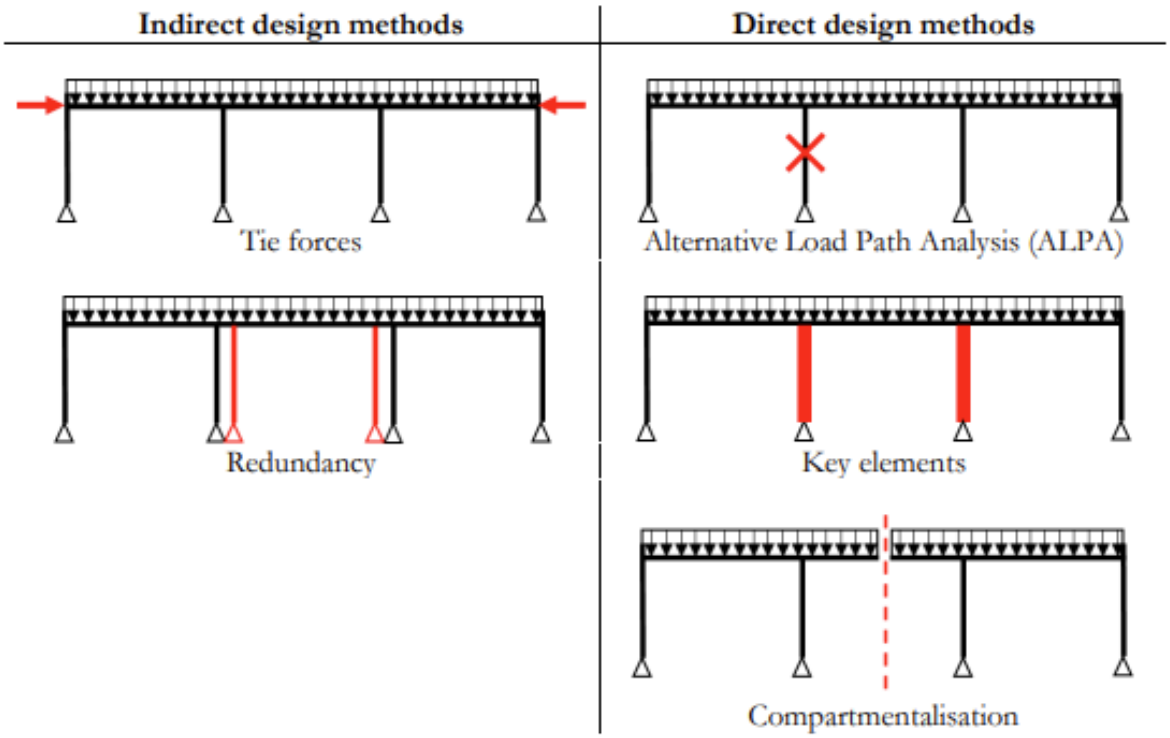

Figure 2.10: Direct and indirect robustness design measures (Voulpiotis 2021)

Tie forces

Tie forces can be provided by creating continuous horizontal and vertical load paths along and around the perimeter of the structure. The ties can be realised by connecting structural elements with mechanical connections or additional elements. The redistribution of the load is then realised by the catenary action of the connected structural elements. This can be seen as an alternative load path but is indirect as it does not require the analysis of the damaged scenario (Huber et al. 2019).

Redundancy

Redundancy can be seen as the existence of alternative load paths. Redundancy can be achieved passively or actively. In case the load is shared among parallel members already at low load levels, it is called active redundancy. In case the parallel members start to take up loads after a certain amount of damage, it is called passive redundancy. In a redundant system, ductile failure is preferred over brittle failure as this allows for load-sharing. If a brittle element fails after overload, the remaining elements must take over all the overload. However, if the failure is ductile, the remaining elements only need to support the additional load above the yield point of the failed element (Huber et al. 2019).

Alternative load path design

Alternative Load Path design relies on an alternative load path analysis (ALPA) in case of a notional removal of a structural element. In this design approach, a specific type of damage, such as the removal of a column, is applied to the structure. Subsequently, an assessment is made to ensure that there

is adequate capability for the redistribution of loads (Voulpiotis 2021). For modular construction, the extreme cases are the loss of a notional module at the bottom floor. Therefore this design approach will be further explained based on two extreme cases shown in Figure 2.11.

Key elements

Key elements are critical load-bearing elements that are designed to withstand a certain impact or damage on top of normal loading. This means that these elements are dimensioned for accidental loading conditions and are over-dimensioned for normal loading conditions. This method should be used as a last resort if no other ways are possible to form alternative load paths within the tolerated building design. The reason for this is that when this element fails, despite its overcapacity, the structure loses significant strength and progressive collapse is probable (Huber et al. 2019).

Compartmentalisation

Compartmentalisation is based on the division of the structure into independent structural parts which themselves are robust. If a certain part collapses, this should have no consequence for other compartments and thus progressive collapse is prevented. This strategy can be applied by strengthening the borders of compartments to resist high loads or allow for large displacements. This approach is suitable for large horizontal low-rise buildings however less applicable for high-rise buildings (Ellingwood et al. 2007).

2.4.2. Progressive collapse in modular buildings

For modular construction, alternative load path design and the tie-forces method are the most suitable. In practice, the principle of both methods collides and results in one design solution: adequately tying the modules together at the intra-modular connections. In the case of the removal of a module, the forces can be redistributed via the connections, and an alternative load path is created assuming the connections are capable of transferring the tying forces. To assess the robustness of a modular building, two extreme cases are regarded and are shown in Figure 2.11

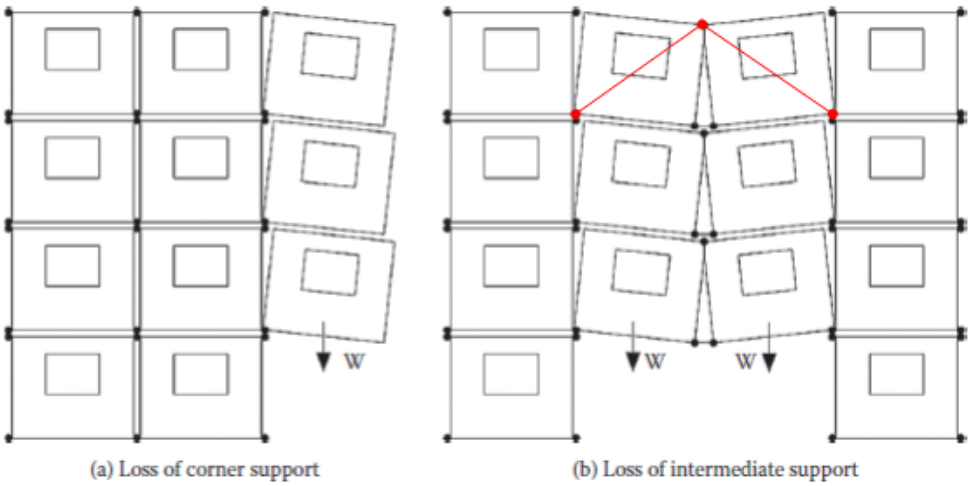

Figure 2.11: Robustness scenarios in modular construction (P. M. Lawson et al. 2008)

It turns out that the loss of a corner support module tends to be the worst case. As for the loss of an intermediate support 'bridging' action can occur. This basically means that as the middle modules rotate, the diagonal of the module should shorten to the width of the module assuming the outside modules are fixed horizontally. As the load required to shorten the diagonal remains higher than the acting load, a stable equilibrium is found and the collapse will not progress. This system is visualised with the red lines in Figure 2.11. However, if the load is high enough the system will move past its equilibrium and fail, which is known as snap-trough instability.

Zooming in on failure case (a), it is assumed that the ties should only accommodate the loads on the adjacent module and not the sum of loads of the modules on top. According to M. Lawson et al.

2014 the minimum value of the horizontal tying force for a robust design is one-third of the load applied to the module.

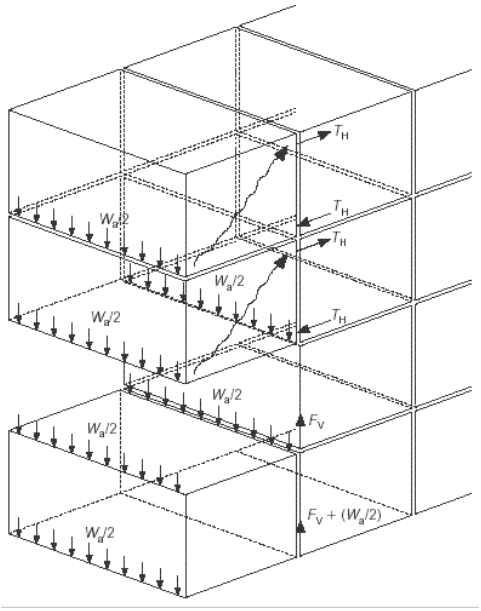

Figure 2.12: Tying action in a group of modules(P. M. Lawson et al. 2008)

Especially for modular units which make use of a timber-glass shear wall, this extreme load case should be considered. The loss of a module results in a tensile force in the perpendicular wall as shown in Figure 2.12. The tensile capacity of the timber-glass shear wall should be able to accommodate this tensile force otherwise, the modules will fail regardless of the tensile strength in the connection. However, due to time constraints, this thesis does not include accidental loading as a load case in further analysis.

2.5. Foundation design in modular construction

The foundation of a modular building can have several layouts as depicted in Figure 2.13.

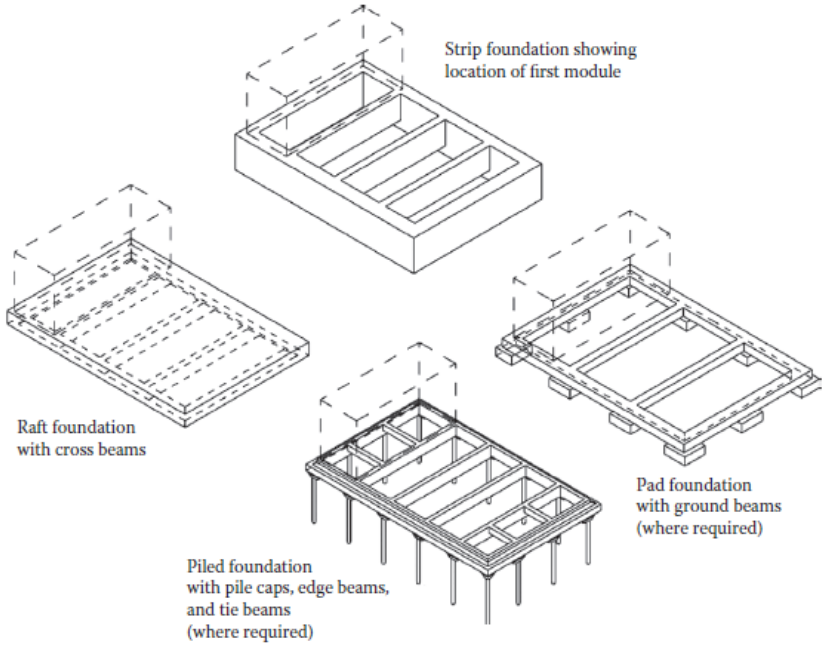

Figure 2.13: Foudation systems (M. Lawson et al. 2014)

For load-bearing modules, strip footings or ground beams supported by pile caps are common solutions. For corner-supported modules, highly concentrated loads should be accounted for in the foundation. By applying piles at strategic locations under the ground beams, sufficient load-bearing capacity can be created for these concentrated loads. In general, a lower spacing of the foundation piles leads to smaller-sized ground beams and vice versa (M. Lawson et al. 2014). Generally speaking, the low weight of the timber modules is favourable for the loads on the foundation. However, in some cases, this can also lead to uplifting forces in the foundation. This depends mainly on the height of the building and the plan of the building (M. Lawson et al. 2014). For timber modular buildings the foundation is usually constructed of another material than timber e.g. concrete. This design trend is also clearly visible in the buildings assessed in the case study as they all have a concrete foundation on piles. This is mainly because the load-bearing capacity of a concrete foundation is higher and is not affected by decay due to fungus or termites.

2.6. Conclusion

In the scope of this research is was stated that aspects like fire safety, progressive collapse and foundation design were discussed in a quantitative manner and not in a qualitative manner. For a complete building design, these aspects should be integrated and assessed in a qualitative manner. Due to time constraints, the requirements for these aspects are given but not integrated nor verified in the design proposed in Chapter 7. The conclusions from this chapter are:

The stability of a midrise modular timber building is influenced by the aspects of fire safety design, progressive collapse and foundation design. It is important to note that the building is constructed of load-bearing modules. This means that the walls, floors and ceilings not only have a separating function but also a structural function. This essentially means that when talking about the structural components, this is the entire building.

With respect to the fire safety design, several requirements should be met. First of all the stability system and overall load-bearing structure should withstand a fire for 120 minutes. The fire gradually reduces the thickness of the structural components and therefore the reduced cross-section should be used for calculation with fire loads. As a consequence, the load-bearing system is over-dimensioned for normal loading conditions to account for this reduction of the cross-section. Furthermore, the building codes specify that fire compartments should retain their integrity, insulation, and structural capacity for 60 minutes.

Progressive collapse has mostly implications for the forces in the connection design. For modular

buildings, the ALPA and tie methods are the most suitable approaches to prevent progressive collapse. In case of removal of a module, this would result in tensile forces in the connections in horizontal direction. This force should be resisted by horizontal tensile ties created along the building.

The first two aspects are part of the loads acting on the the structure and have a direct impact on how the building should be designed. The foundation design however influences the resistance part of the building. This essentially means that the foundation design is influenced by the lateral forces instead of the other way around. Nevertheless, there are two specific considerations for the foundation design. The first consideration is that for lightweight buildings, tension could occur in the foundation, which can be handled by applying tensile foundation piles. The other consideration would be related to the nature of load-bearing modules. As the walls are load-bearing they should ideally be continuously supported by a strip foundation optionally supported by piles.

3

Timber-glass shear wall

In this chapter, the aspects related to the timber-glass shear wall will be discussed. First, a general introduction to the build-up of the wall will be given. Subsequently, the properties of the components will be related to the in-plane stiffness and load-bearing capacity of the timber-glass shear wall system. At the end of this chapter, the following research question is answered:

How does the existing literature describe the influence of the properties of the adhesive layer, glass pane, and timber frame on the in-plane stiffness and load-bearing capacity of the overall timber-glass shear wall?

3.1. General

In the Introduction it was mentioned that a timber frame in combination with a glass pane could serve as a stabilising element. Felix Nicklisch, Hernandez, et al. 2015 formulated this in a more technical way suggesting that load-bearing timber glass composites (LBTGC) can be used as shear walls in buildings. The general build-up of timber-glass shear wall is illustrated in Figure 3.1.

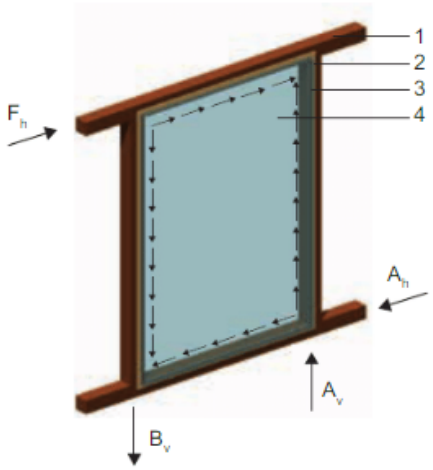

Figure 3.1: General build-up and the load-bearing principle of a timber-glass shear wall element (Štrukelj et al. 2015).

The build-up consists of (1) main timber frame, (2) optional adapter frame with screwed connection,(3) adhesive joint, (4) glass pane. In literature, three types of LBTGC systems can be found: Only shear adhesive bonding, only blockings, and a combination of both. Two example build-ups of the first and last system are designed by Holzforschung Austria (HFA) and Vienna University of Technology (VUT). The system with only blockings is not considered. The two example build-ups will be explained in Section 3.1.1 and Section 3.1.2. The advantage of both methods being screwed to the substructure

is that this allows for easy replacement in the event that the glass pane breaks. Especially for modular buildings, this concept is favourable as only the window could be replaced instead of the whole module.

3.1.1. Build-up Holzforschung Austria (HFA)

The design was created by the wood research centre in Austria. This design is shown in Figure 3.2. It can be seen that the glass panel is glued to the adapter frame with a shear adhesive bonding. Therefore, this detail only allows for shear forces along the adhesive and the perimeter of the glass pane. The shear forces in the adhesive can be determined with the theory of shear field beams, which is further elaborated on in Section 3.4.

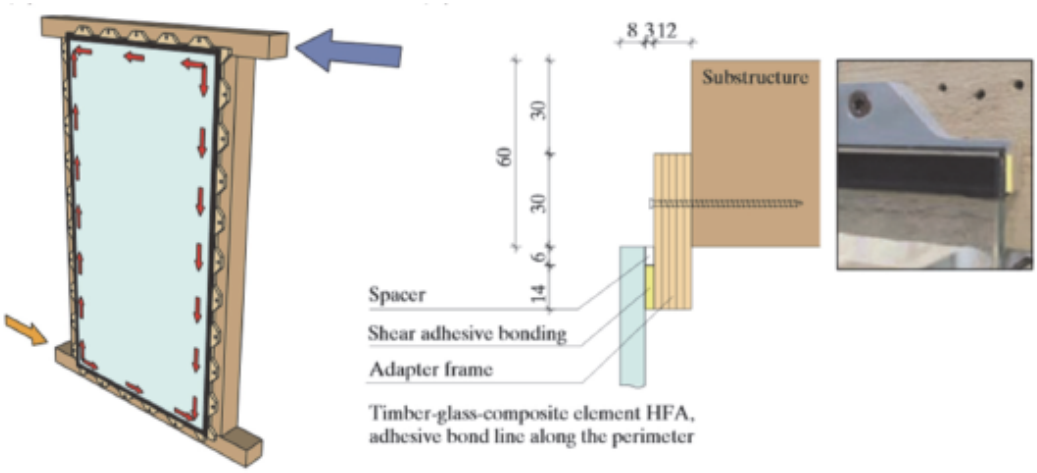

Figure 3.2: (a) Shear bonding with adapter frame system HFA (b) detail [mm] (Fadai, Holzinger, et al. 2021)

In this case, the displacement of the system u_k is related to the horizontal force H with Equation 3.1. As the system is loaded by shear alone, the stiffness of the system is determined by the individual shear stiffness of each component. These individual shear stiffness values are then combined in an overall stiffness factor, denoted as K_{shear}

$$H = u_k * K_{shear} \tag{3.1}$$

3.1.2. Build-up Vienna University of Technology (VUT)

This timber-glass shear wall was designed during the process of research work at the University in Vienna. In this design, the glass panel is again glued to the adapter frame, but also spaced by a blocking. This setup allows for an additional compression diagonal to be formed in the glass pane, next to the shear field. By introducing an extra load-bearing principle, the maximum force the system can transmit, is higher while also increasing the stiffness of the system (Fadai, Rinnhofer, et al. 2017). In figure 3.3 the compression diagonal is green and the shear bonding is red.

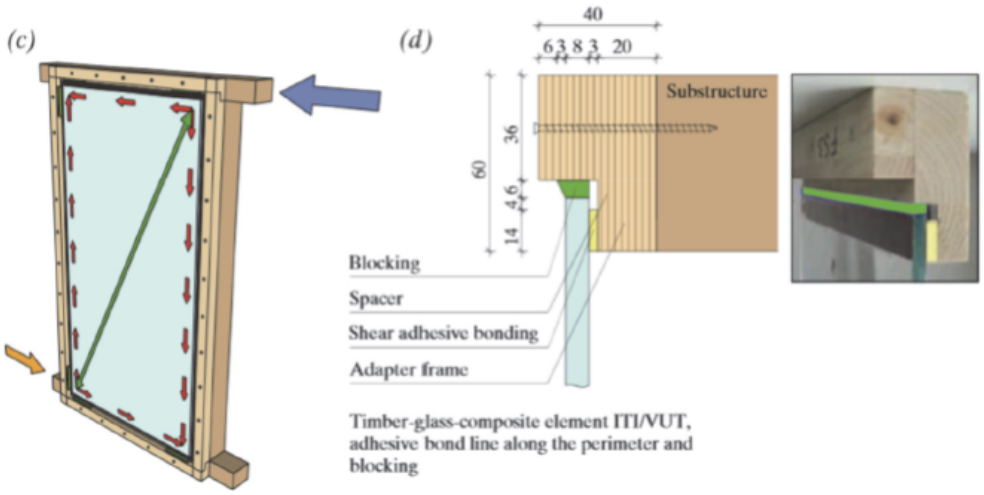

Figure 3.3: (c) Shear bonding and blocking system VUT (d) detail [mm] (Fadai, Holzinger, et al. 2021)

Again, the displacement of the system u_k can be related to the horizontal force H. The introduction of an extra load-bearing principle parallel to the shear field introduces an additional stiffness factor, denoted as $K_{diagonal}$.

$$H = u_k * (K_{shear} + K_{Diagonal}) \tag{3.2}$$

This thesis focuses on the HFA build-up as the force transfer in this detail remains clear even when dealing with tolerances and thermal expansion. In addition, more data was available on detail (a) compared to detail (c). This data can be used to verify the theoretical model with experimental data.

3.2. Properties of the glass, timber and adhesive

The properties of the materials used are inherently related to the properties of the composite. In this section, the different materials will be discussed. The stress-strain curve is examined for each material to determine the elastic zone for that material. From the stress-strain curve, the stiffness of each material within the elastic zone is derived. Plus, the maximum stress within the elastic zone is determined for each material. These two properties will be used to assess the strength and stiffness of the timber-glass shear wall. The plastic region provides ductilty for the system but is not included for the strength and stiffness of the system. This is driven by the fact that, the TGSW should remain in the elastic region in order to function properly. Entering the plastic region will go hand in hand with irreversible strains and damage, which is not desired during the lifetime of the building. This is similar to for example the yield strength and ultimate strength for a steel beam.

3.2.1. Adhesive

The adhesive connects the timber to the glass. As glass is a brittle material and vulnerable for stress concentrations, a smooth force transmission from the timber to the glass should be initiated. Using a proper selection of the type of adhesive, this goal is realised.

Types of adhesives

In general, there are three types of adhesive:

- Rigid adhesive e.g. epoxy (high strength high stiffness (> 1000 MPa))
- semi-elastic adhesive e.g. polyurethane, acrylate (balanced strength and elasticity (100-500 MPa))
- elastic adhesive e.g. silicone (low strength, low stiffness (<10 MPa))

The stress-strain behavior of an adhesive is dependent on the type of adhesive used. In Kozłowski 2014, a suggestion is proposed to characterise the stress-strain curves for each adhesive type, as

shown in Figure 3.4. The same characterisation is used in this thesis for the shear-strain characterisation.

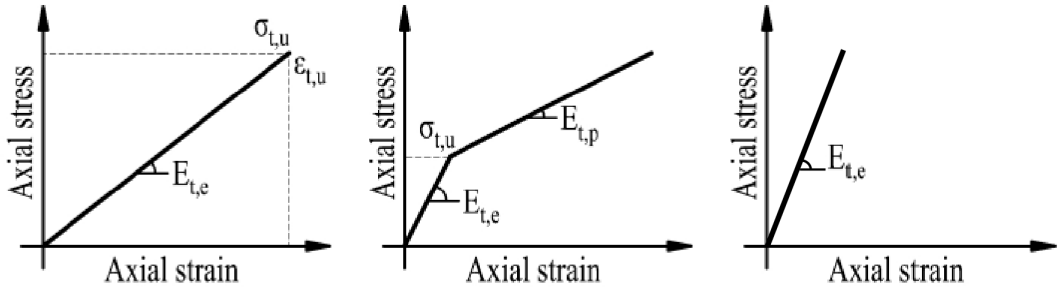

Figure 3.4: Mechanical characteristics of silicones (left), semi-elastic adhesives (middle), epoxies (right)

The silicones will be modelled with linear elastic shear - strain behaviour. The semi-elastic adhesives will be modelled with bi-linear shear-strain behaviour. Here, the first part of the graph is assumed to be the elastic strain, whereafter the plastic strain starts. The epoxies are modelled with linear shear-strain behaviour.

Several examples of adhesive are selected in each category to determine the properties of the three types of adhesive. The properties are deducted from product data sheets[1], Felix Nicklisch, Dorn, et al. 2014[2], Nicklisch et al. 2016[3], Blyberg 2011[4] Kozłowski 2014[5] and Felix Nicklisch 2016[6] The adhesives with their corresponding properties are presented in Table 3.1

Type	Adhesive	Type	E $[N/mm^2]$	G $[N/mm^2]$	$\tau_{max}[N/mm^2]$	$\tau_{elastic}[N/mm^2]$	μ	ϵ_{max}
A	OTTOCOLL S660	Silicone	3 [3]	1	0,87 [6]		0,5 [3]	1,65 [3]
A	Sikasil SG-20	Silicone	1 [5]	0,33	0,93 [4]		0,5 [5]	4,5 [1]
A	Sikasil SG500	Silicone	3,17 [5]	1,09	0,8 [2]		0,46 [5]	2,5 [1]
B	Nolax C44.8505	Modified epoxy	18 [3]	6,4	5,2 [2]	1,8 [6]	0,39 [3]	1,99 [3]
B	Sikafast 5215	Acrylate	78 [5]	27	3,4 [2]	2,3 [4]	0,46 [5]	1,5 [1]
B	Delo-PUR 9895	Polyurethane	100 [6]	35	5,1 [2]		0,42 [6]	0,3 [6]
B	Araldite 2029	Polyurethane	414 [6]	146	0,9 [6]		0,42 [6]	0,39 [6]
C	Scotch-Weld DP490	Epoxy	1442 [3]	504	11,9 [2]		0,43 [3]	0,05 [3]
C	Delo-DUOPOX AD840	Epoxy	1700 [6]	594	7,9 [2]		0,43 [6]	0,06 [6]

Table 3.1: General adhesive properties

Several remarks must be made about the data shown in Table 3.1:

- First of all, Delo-Pur 9885 and Araldite 2029 have no value for $\tau_{elastic}$. This is because there was no data available of the shear -strain behaviour of these adhesives. Therefore $\tau_{elastic}$ could not be determined.
- For isotropic materials, the E-modulus, G-modulus, and poisons ratio are related to each other with Equation 3.3.

$$E = 2G(1 + \mu) \tag{3.3}$$

  In case, two of the three properties are known, the third can be calculated. Sometimes, different E-modulii were presented in research compared to the manufacturers data sheet. Usally the values presented in research papers were less optimistic compared to the values presented in the data sheets. Hence, the values of the research papers are chosen when differences occur.
- The maximum shear stress is tested for small plywood-glass specimens. The maximum shear stress is presented as a material property solely related to the adhesive. However, it is stated in the tests, that the shear strength is limited by the plywood strength or adhesion to the timber surface. Hence, the maximum shear stress is not a characteristic of the adhesive alone, but a characteristic of an adhesive used in a plywood-to-timber bond. For example, Felix Nicklisch 2016 stated that Araldite 2029, showed poor adhesion to the timber surface, which resulted in a relatively low maximum shear strength.

- Finally, it should be mentioned that epoxy's have the best performance in terms of stiffness and strength however, this comes at the cost of ductility.

Failure mechanisms adhesive bonding

In this section, the different failure patterns according to ISO 10365 will be explained. The failure patterns are shown in Figure 3.5.

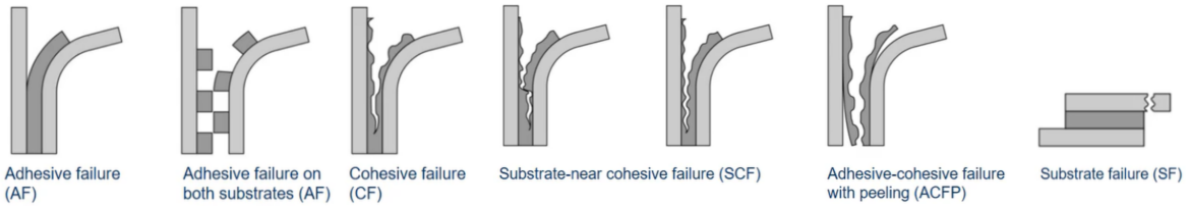

Figure 3.5: Failure patterns in adhesive bonding according to ISO 10365

The seven failure patterns can be distinguished into four categories:

- Adhesive failure (AF): Adhesion failure between the adhesive and the substrate at the interface between the adhesive and the substrate. Adhesive failure may occur on both the glass-adhesive interface as well as the timber-adhesive interface.
- Cohesive failure (CF and SCF): Failure inside the adhesive itself, which can be in middle of the adhesive but also near substrate.
- Mixed-mode failure (ACFP): A combination of partial adhesive failure and partial cohesive failure.
- Substrate failure (SF): The substrate itself fails, while the adhesive remains intact. This means that either the timber or the glass itself fails.

The type of failure pattern and the strength of the bond is greatly influenced by the combination of the substrate and adhesive used. Simply using a substrate and adhesive that can withstand higher stresses does not automatically lead to a bond with greater strength. For instance, the individual components (adhesive and substrate) are stronger, but the adhesion between the adhesive and adherent can be much lower. In that case, a different failure mechanism can occur, ultimately leading to a lower bond strength regardless of the individual strength of the components. Therefore, when comparing test results, it is crucial to ensure that different types of adhesives are only compared when the adherents are also similar.

Stress concentrations in elastic timber-glass adhesive connections: Volkersen model

In adhesive bonds, stresses are much harder to predict than a simple average shear stress along the bondline. In research performed by Niedermaier 2004 the Volkersen method is proposed to account for these stress concentrations. This method is based on the closed differential equal for shear forces along an adhesive bond. Instead of assuming that the adherents/substrates are infinitely stiff, which results in average shear stresses, the adherents do have a stiffness. The difference can be seen in Figure 3.6 and Figure 3.7.

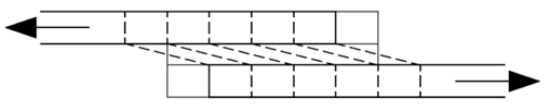

Figure 3.6: Adhesive deformation average (Floor 2014)

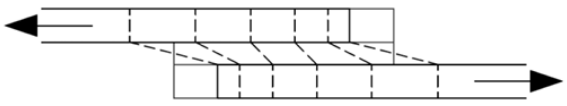

Figure 3.7: Adhesive deformation Volkersen (Floor 2014)

The main assumptions in this Volkersen model are:

- Adhesive and adherent are assumed to behave in a linear elastic manner.
- The bending moment due to load eccentricity is not considered thus only shear stresses occur in the adhesive bonding. Peel and bending stresses are neglected.
- The adherents show no shear deformation.

- Perfect bonding of the adhesive to the adherent.

A comment should be made about the application of the Volkersen model for this project. The assumption that the adherent does not show shear deformation is valid if the shear modulus of the adhesive is far lower compared to the shear modulus of the adherent. For the stiffer adhesives, this becomes no longer valid, as the shear modulus of the adhesive becomes similar to the shear modulus of the timber. In Tsai et al. 1998, an improved Volkersen model is proposed which includes shear deformation of the adherent. From that model, it can be concluded that the original Volkersen overestimates the peak stresses and therefore is more conservative. Consequently, it is safe to assume that the adherent does not show shear deformation. The derivation of the solution to the differential equation is presented in Niedermaier 2004. In this thesis only the solution is presented. The following variables are defined in the following way:

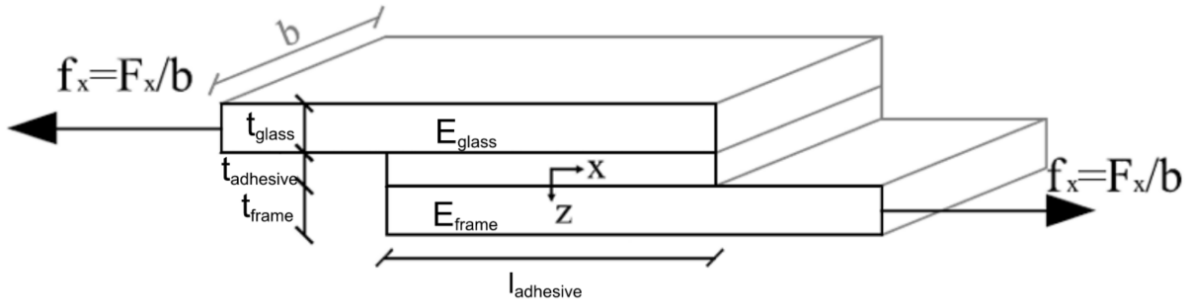

Figure 3.8: Variable definition Volkersen model

The solution results in a shear-force along the length of the bondline and the magnitude is given by Equation 3.4:

$$\tau(x) = \frac{\omega \cdot \tau_m}{(\beta+2)\cdot(\cosh\omega - 1)} \cdot [\sinh(\omega(1 - \frac{x}{l_{adhesive}})) + (\beta+1)\cdot\sinh(\omega\frac{x}{l_{adhesive}})] \tag{3.4}$$

With:

$$\omega = \sqrt{\frac{G_{adhesive}\cdot(E_{glass}\cdot t_{glass} + E_{frame}\cdot t_{frame})\cdot l^2_{adhesive}}{E_{glass}\cdot t_{glass}\cdot E_{frame}\cdot t_{frame}\cdot t_{adhesive}}} \tag{3.5}$$

$$\beta = \frac{(E_{frame}\cdot t_{frame} - E_{glass}\cdot t_{glass})\cdot G_{adhesive}\cdot l^2_{adhesive}}{E_{glass}\cdot t_{glass}\cdot(G_{adhesive}\cdot l^2_{adhesive} + E_{frame}\cdot t_{frame}\cdot t_{adhesive})} \tag{3.6}$$

Maximum shear stresses are found at the start and end of the bond. The maximum stress is related to the average stress along the bondline τ_m with a stress concentration factor K_{stress}.
At $x = 0$:

$$\tau_{max,start} = \frac{\omega\cdot\tau_m\cdot\sinh\omega}{(\beta+2)\cdot(\cosh\omega-1)} = K_{stress,start}\cdot\tau_m \tag{3.7}$$

At $x = L$:

$$\tau_{max,end} = \frac{\omega\cdot\tau_m\cdot(\beta+1)\cdot\sinh\omega}{(\beta+2)\cdot(\cosh\omega-1)} = K_{stress,end}\cdot\tau_m \tag{3.8}$$

The stress concentration factor increases as the stiffness of the adhesive increases and vice versa. Stiffer adhesives deform a less compared to more flexible adhesives, which results in less redistribution of stresses in the bondline. As a result, the peak stresses in the bond increase as the stiffness of the adhesive is increased.

Mullins effect

The Mullins effect is a stress-softening phenomenon which occurs in elastomers and rubbers under cyclic loading. This mechanism of stress softening is characterised by a decrease of the stress on unloading compared to the stress on loading at the same strain. The most important assumption of

Mullins model is that the reloading path is the same as the unloading path as long as the maximum strain of the first loading is not reached. This is shown in Figure 3.9. In other words, the stress-strain curve of an adhesive depends on the maximum loading previously experienced.

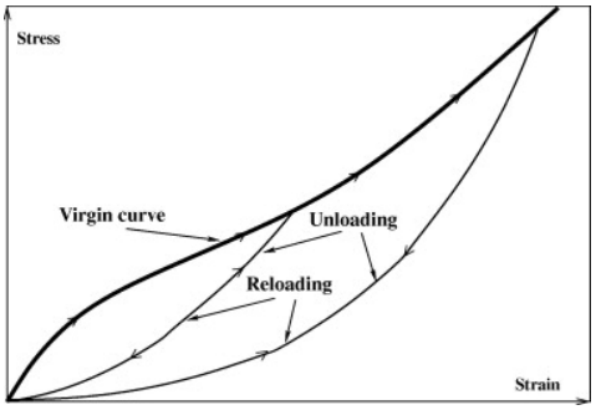

Figure 3.9: Idealised Mullins mechanical behaviour (Cantournet et al. 2009)

For the timber-glass shear wall system this doesn't lead to a reduction of the maximum load-bearing capacity as the maximum allowable stress is not lowered. However, for the stiffness of the TGSW system, a decreasing initial stiffness is observed after multiple loading cycles. This results in larger deformations at lower loads compared to the first load cycle. That being said, the stress-strain diagram will still ultimately reach the final position, albeit with a different route. Therefore, in the rest of this thesis, the Mullins effect is not included in determining the load-bearing capacity and stiffness of the TGSW system.

Glass transition temperature

The glass transition temperature is an important mechanical property of adhesives. At the glass transition temperature, the adhesive changes from a hard and glassy material to a soft and rubbery material. This means that the mechanical properties of the same adhesive can vary drastically at different temperatures. This is visualised in Figure 3.10. Therefore it is important to look at the glass transition temperature of the selected adhesives, in order to know what mechanical behaviour can expected within the operating temperature range. The operating temperature range prescribed in the ETAG 002 guideline for façade elements, and thus the timber-glass wall, is between -20 °Cand +80 °C. If opaque glazing is applied an even higher maximum surface temperature of +100 °Cshould be used.

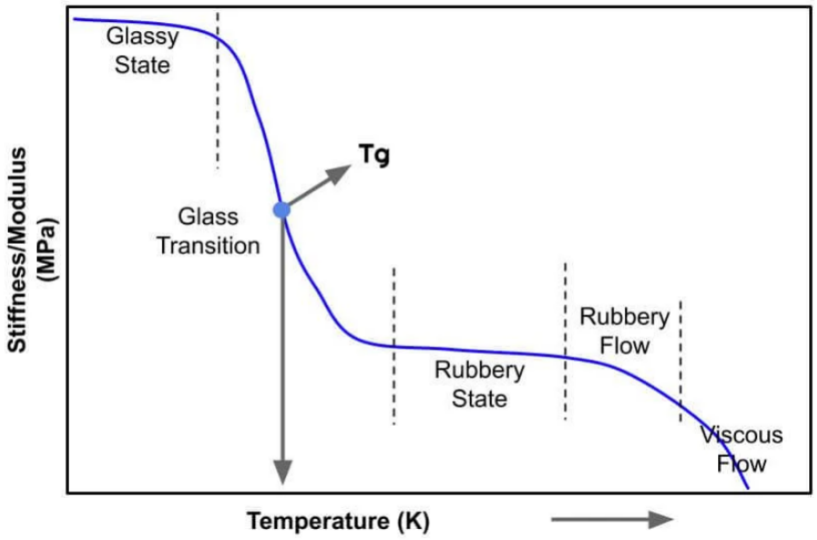

Figure 3.10: Glass transition temperature graph (Raghvendra Gopal 2021)

For silicones the glass transition temperature is typically between -140 °Cand -40 °C. This means that silicones at room temperatures behave as rubbery materials. This can also be observed when looking at the E-modulus of several silicones (see Table 3.1), which are low compared to the other types of adhesives (Lindberg 2023). For epoxy's the glass transition temperature can be within the operating range of façade elements. Typically the glass transition temperature of epoxy's is between 30 °Cand 100 °C. This is the reason why epoxy's have a high stiffness compared to silicones because epoxy's are in their glassy state at room temperature. Nevertheless, it can be seen that the glass transition temperature for epoxy's corresponds to the operating temperature range of façade elements. Therefore, it is important to know where exactly the glass transition temperature of a specific epoxy is, in order to use the right mechanical properties.

For the specific adhesives presented in Table 3.1 the following glass transition temperature's are used:

Type	Adhesive	T_g [°C]
Silicone	OTTOCOLL S660	-
	Sikasil SG-20	-
	Sikasil SG500	-
Semi-elastic adhesive	Nolax C44.8505	88
	Sikafast 5215	55
	Delo-PUR 9895	32
Epoxy	Scothc-Weld DP490	68
	Delo-DUOPAX AD840	79

Table 3.2: Glass transition temperature (Felix Nicklisch 2016)

Within the operating temperature range, the glass transition temperature has no influence on the stiffness of the silicones. Therefore, no values are presented in Table 3.2. Besides, it can be seen that the glass transition temperature of the stiffer adhesives, except for Nolax C44.8505, are all within the operating temperature range. This means that, they are less suitable as adhesive for a TGSW as their stiffness will massively decrease at higher temperatures. Extra research should be put into the mechanical properties of these adhesives in their rubbery phase to see if those adhesive can fulfil their task in their rubbery phase.

3.2.2. Glass

There are different types of glass. For this project single pane soda-lime silicate glass will be used. This has the following properties:

Property	Value	Unit
Density	2500	kg/m^3
Young's modulus	70000	MPa
Shear modulus	28455	MPa
Coefficient of thermal expension	9×10^{-6}	K^{-1}
Poisson's ratio	0,23	-
Float glass strength ($f_{g,k}$)	45	N/mm^2

Table 3.3: General properties of glass

Glass is a linear-elastic, isotropic and homogeneous material that fails brittle (Pölzl 2017). As a consequence glass does not show any plastic behaviour and the maximum allowable stress corresponds to the elastic limit stress. This is shown in Figure 3.11. To ensure the ductile behavior of the system, it is crucial that the timber-glass shear wall does not exhibit brittle failure. Consequently, the governing failure mechanism shouldn't involve the glass pane as this would result in brittle failure.

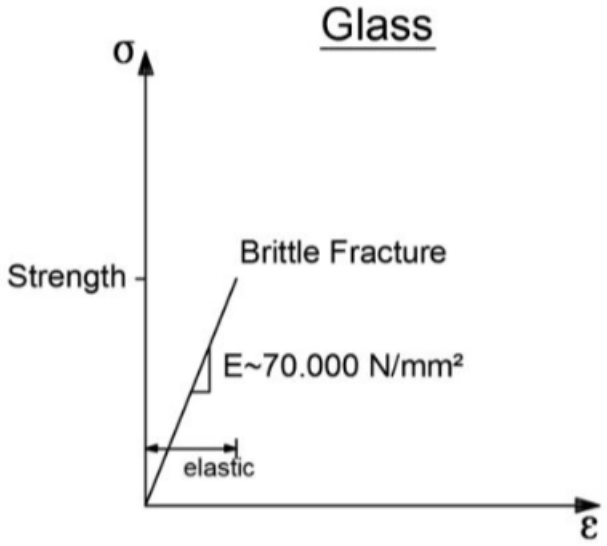

Figure 3.11: Stress-strain relation glass (Pölzl 2017)

For the relation between Young's modulus and shear modulus Equation 3.3 can be used, since glass is an isotropic material.

3.2.3. Timber

The timber used for the adapter frame is laminated veneer lumber (LVL) whose veneers are laid in the same direction as the frame member (Kerto-S). The properties of LVL Kerto-S are given in Table 3.4:

Property	Value	Unit
Characteristic density	480	kg/m^3
Mean density	510	kg/m^3
Young's modulus parallel to the grain	11600	MPa
Shear modulus parallel to the grain, flatwise	270	MPa
Shear strength parallel to the grain, flatwise ($f_{v,0,flat,k}$)	2,3	MPa
Shear strength perpendicular to the grain, flatwise ($f_{v,90,flat,k}$)	0,6	MPa
Tensile strength parallel to the grain ($f_{t,0,k}$)	35	MPa

Table 3.4: General properties of LVL Kerto-S (Metsä n.d.)

Laminated veneer lumber is created by using a rotary peeling technique on a log. Thin layers of veneer are peeled off and defects are eliminated. Next, these veneer layers are glued together with the grain orientation all in the same direction. This results in good properties parallel to the grain, while having weak properties perpendicular to the grain (Hiziroglu 2016). This manufacturing method results in higher capacities and more reliable mechanical properties for LVL compared to sawn timber (Gilbert et al. 2017).

Despite the differences in strength it is assumed that the failure mechanisms of LVL are similar to sawn timber. The reason for this assumption is that the theory behind the failure remains unchanged. However, the point at which this failure mechanism occurs is higher for the stronger LVL compared to sawn timber. For timber, tension failure is a brittle failure mechanism and compressive failure shows a ductile failure mechanism. The type of failure is independent of the loading direction, although the magnitude at which this occurs is significantly lower when the load is applied perpendicular to the grain compared to parallel to the grain. This is shown in Figure 3.12

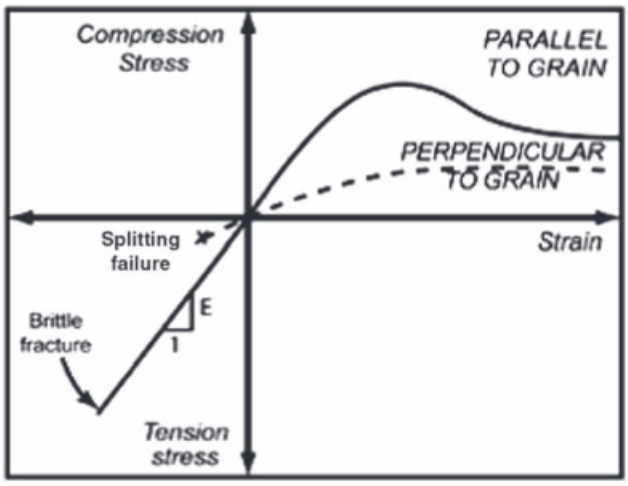

Figure 3.12: Stress-strain relation timber (Gilbert et al. 2017)

As timber is an orthotopic material, Equation 3.3 cannot be used and shear failure is considered separately. Shear failure is characterised by a sliding of the fibres and results in cracking parallel to the grain and is regarded as a brittle failure (Franke et al. 2015). Therefore, the ultimate shear stress of LVL parallel to the grain is equal the elastic limit stress parallel to the grain. Loading up until the elastic limit stress is assumed to be linear elastic.

3.3. Stiffness of the timber-glass shear wall

In order to relate the deformation of the TGSW system to the force, the stiffness of the system must be determined. Several methods are used to model this relation. An exact solution has been derived based on differential equations, with a constitutive model for the connection and different boundary conditions. The downside of this method is the relatively long calculation time. Another option is to

apply the spring model proposed by Kreuzinger and Niedermaier 2005. Later, an extension to this model was given by Hochhauser. The latter two options are explained below.

3.3.1. Stiffness: Spring model by Kreuzingen and Niedermaier

The first option to derive the system stiffness is to apply a spring model where the spring stiffness refers to the stiffness of the individual components. The most basic spring model was proposed by Kreuzinger and Niedermaier 2005. In this model, it is assumed that the stiffness of the adhesive is much lower than the stiffness of the timber and glass. Hence, it can be concluded that the deformation of the adhesive is much greater than the deformation of the glass and timber. Therefore it is assumed that for low-stiffness adhesives, the timber and glass are rigid. The simplified spring model is shown in Figure 3.13.

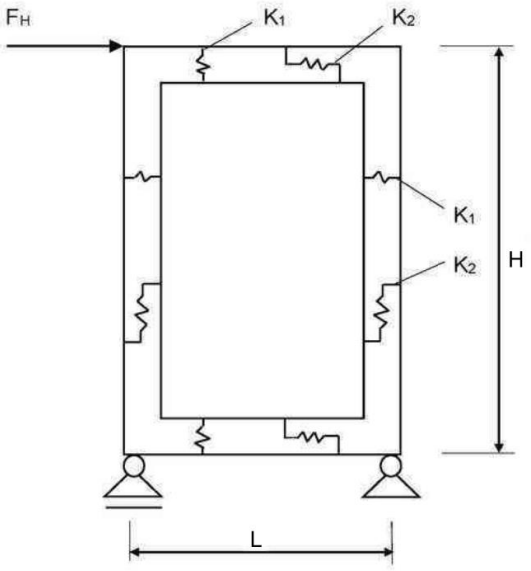

$$K_1 = \frac{G_{perpendicular,adhesive} * (w_{adhesive} * l_{adhesive})}{t_{adhesive}} \tag{3.9}$$

$$K_2 = \frac{G_{parallel,adhesive} * (w_{adhesive} * l_{adhesive})}{t_{adhesive}} \tag{3.10}$$

$$u = F_h \cdot \frac{2}{K_2 \cdot L} \left(\frac{1}{1 + \frac{K_1}{K_2}\frac{H}{3L}} + \frac{\frac{H}{L}}{1 + \frac{K_1}{K_2}\frac{L}{3H}} \right) \tag{3.11}$$

$$K_{shear} = \frac{2}{K_2 \cdot L} \left(\frac{1}{1 + \frac{K_1}{K_2}\frac{H}{3L}} + \frac{\frac{H}{L}}{1 + \frac{K_1}{K_2}\frac{L}{3H}} \right)^{-1} \tag{3.12}$$

Figure 3.13: Spring model introduced by Kreuzinger and Niedermaier

In Figure 3.13, the stiffness of the adhesive is given by K_1 and K_2, which are respectively the stiffness in the direction perpendicular to the connected timber frame and the shear stiffness parallel to the connected timber frame. $G_{parallel,adhesive}$ and $G_{perpendicular,adhesive}$ correspond to the shear modulus of the adhesive in two directions and are assumed equal (Felix Nicklisch 2016). As a result the spring stiffness of both of springs $K_1 = K_2$ are equal. The thickness and width of the adhesive are given by parameters $t_{adhesive}$ and $w_{adhesive}$. Finally, as the adhesive is a continuous connection and the springs act as a point connection, the spring stiffness is adjusted according to the spring spacing. The impact length per spring is given by $l_{adhesive}$ and is equal to the spring spacing. Finally, the relation between the force and the displacement is given by Equation 3.11. For completeness the system stiffness K_{shear} is given in Equation 3.12. This factor relates the displacement to force as in Equation 3.1.

3.3.2. Stiffness: Spring model by Hochhauser

A more general spring model was developed by Hochhauser in 2011. Contrary to the previous spring model, this model takes into account the stiffness of the other components. For systems where a stiffer adhesive is used, it can no longer be assumed that the deformation of the adhesive is much greater compared to the deformation of the timber and glass. Therefore those components cannot be regarded as rigid and hence their stiffness is included in a serial system. This system is visualised in Figure 3.14. The stiffness of these more extensive springs, should substitute the stiffness of the springs K_1 and K_2.

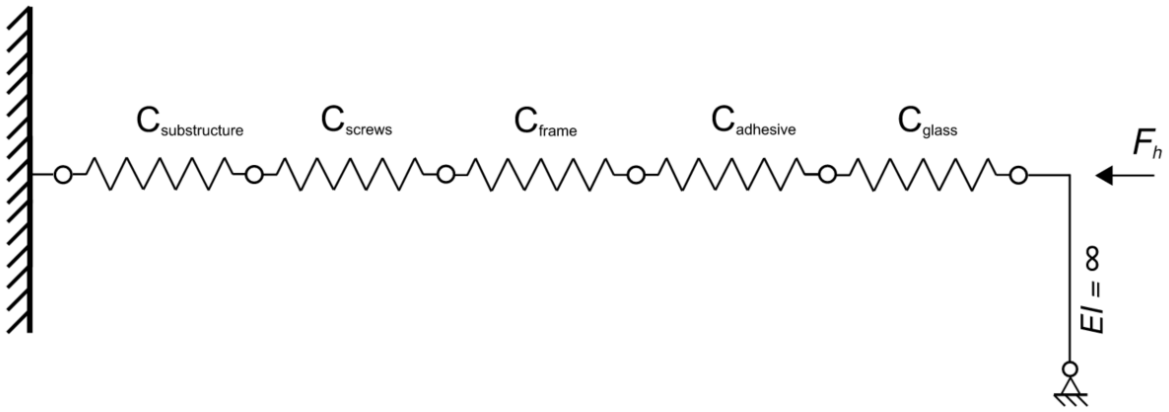

Figure 3.14: Spring model shear only (Felix Nicklisch 2016)

$C_{substructure}$, C_{screw}, C_{frame}, $C_{adhesive}$, C_{glass} refer to the stiffness of the following components: substructure, screws, adapter frame, adhesive, and glass pane. The equivalent stiffness can now be described with the standard equation for combined serial stiffnesses. The result is shown in Equation 3.13.

$$C_{equivalent,shear} = \frac{1}{\frac{1}{C_{substructure}} + \frac{1}{C_{screws}} + \frac{1}{C_{adapterframe}} + \frac{1}{C_{adhesive}} + \frac{1}{C_{glass}}} \tag{3.13}$$

A better understanding of the stiffness of the components can be achieved by looking at parameters influencing the stiffness. For this specific system, the parameters are shown in Figure 3.15

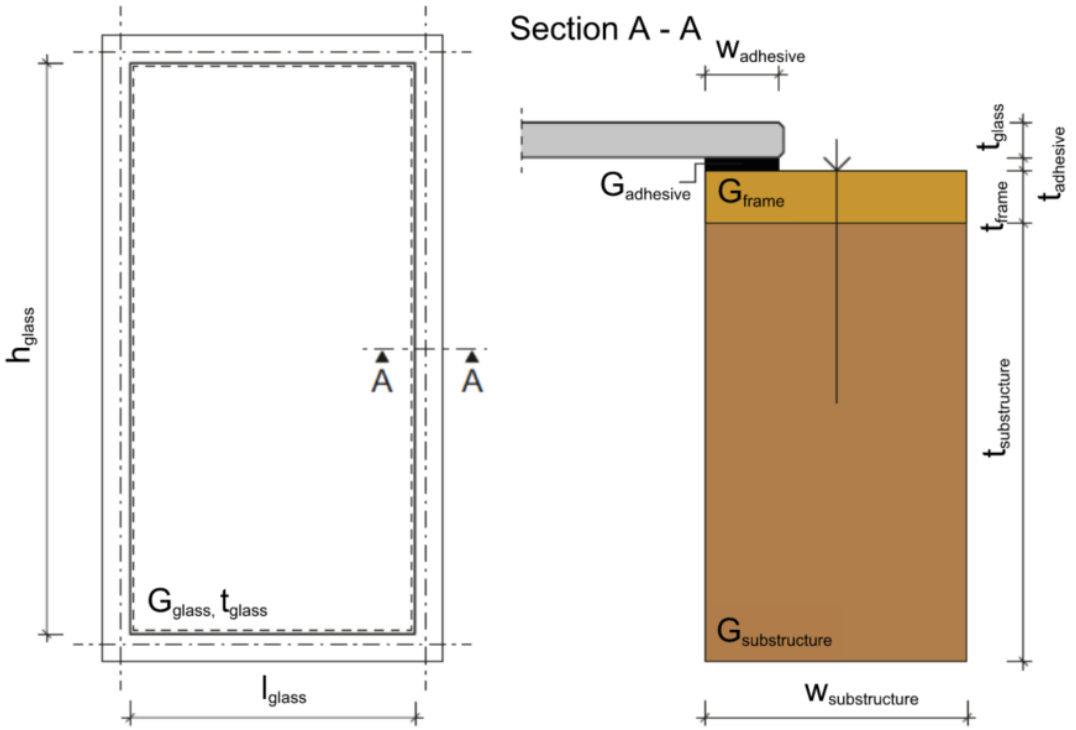

Figure 3.15: Properties HFA (Felix Nicklisch 2016)

The equations describing the stiffness of each component are presented below. The influence of the substructure in the longitudinal direction is determined based on the shear modulus and dimensions of the wood cross-section:

$$C_{substructure} = \frac{G_{substructure} \cdot w_{substructure}}{t_{substructure}} \tag{3.14}$$

The deformations at the interface between the adapter frame and the substructure result from the flexibility of the screw connection. In addition to the distance and diameter of the screws, the density of the connected wood-based materials influences the stiffness.

$$C_{screws} = m \cdot K_{ser} = \frac{n}{l} \cdot \rho_m^{1,5} \cdot \frac{d_{screw}}{23} \tag{3.15}$$

The shear stiffness of the adapter frame in the longitudinal direction is:

$$C_{frame} = \frac{G_{frame} \cdot w_{frame}}{t_{frame}} \tag{3.16}$$

The shear stiffness of the adhesive joint in the longitudinal direction is determined by the shear modulus of the adhesive and the cross-sectional area of the joint:

$$C_{adhesive} = \frac{G_{adhesive} \cdot w_{adhesive}}{t_{adhesive}} \tag{3.17}$$

Finally, the shear strain of the glass under plane stress is accounted for by the spring stiffness of the glass pane:

$$C_{glass} = \frac{2 \cdot G_{glass} \cdot t_{glass}}{h_{glass}} \cdot \left(1 + \frac{h_{glass}}{l_{glass}}\right) \tag{3.18}$$

According to Felix Nicklisch 2016, the longitudinal stiffness, transversal stiffness and equivalent stiffness from equation 3.13 are assumed equal meaning $C_{equivalent,shear}$ = K_1 = K_2. The stiffness of the system can now be determined by inserting $C_{equivalent}$ in Equation 3.12 resulting in Equation 3.19.

$$K_{shear} = \frac{F_h}{u} = \left[\frac{2}{C_{equivalent,shear} \cdot l_{glass}} \cdot \left(\frac{1}{1 + \frac{h_{glass}}{3 \cdot l_{glass}}} + \frac{\frac{h_{glass}}{l_{glass}}}{1 + \frac{l_{glass}}{3 \cdot h_{glass}}}\right)\right]^{-1} \tag{3.19}$$

3.4. Load-bearing capacity of the timber-glass shear wall

The load-bearing capacity of the timber-glass shear wall is calculated analytically. As the strength of the shear wall is determined by the strength of the weakest component, the strength of each component is calculated. In order to do so, the timber glass wall is assumed to behave similarly to a shear beam. Under the assumption that the the glass is loaded only in-plane, and does not buckle out of plane due to the horizontal load, the theory of the shear beam can be applied. In this theory, the edge members are considered rigid and connected with hinges in the corners. The glass pane only transfers shear forces. Based on these assumptions, a constant shear force is created along the edge of the glass pane. This shear force then becomes a normal force in the edge members. The shear field theory is shown in the middle in Figure 3.16. Additionally, due to the high in-plane stiffness of the glass pane, the glass pane will not show shear deformation but a rotation. This rotation introduces additional shear forces perpendicular to the edge of the glass pane. These are shown on the right in Figure 3.16.

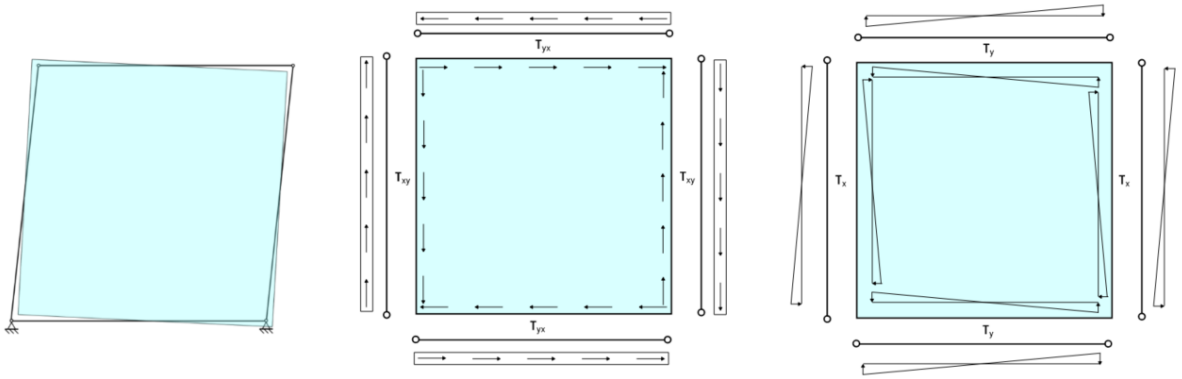

Figure 3.16: Deformation and corresponding stresses on the timber frame and glass pane(Niedermaier Peter and Kreuzinger Heinrich 2005)

The magnitude of shear forces along the perimeter of the glass are derived with the energy method. This is done according to Källsner and Girhammar 2009 who use an elastic model to analyse light-frame timber shear walls. The shear wall consisted of a sheathing board that was connected to timber studs with fasteners. In that case, the fasteners were regarded as discrete point connections. In this case, a similar derivation is performed but now the adhesive is regarded as a continuous connection. The result has already been presented in Niedermaier Peter and Kreuzinger Heinrich 2005. The magnitude of the shear forces resulting from it is given by the following equations:

$$\tau_{xy} = \frac{F}{l} \frac{1}{1 + \frac{K_1}{K_2} \frac{L}{3H}} \tag{3.20}$$

$$\tau_{yz} = \frac{F}{l} \frac{1}{1 + \frac{K_1}{K_2} \frac{H}{3L}} \tag{3.21}$$

$$\tau_{x} = \frac{F}{l} \frac{\frac{6L}{H}}{2 + \frac{K_1}{K_2} \frac{6L}{H}} \tag{3.22}$$

$$\tau_{y} = \frac{F}{l} \frac{\frac{6H}{L}}{2 + \frac{K_1}{K_2} \frac{6H}{L}} \tag{3.23}$$

Based on this stress distribution, the maximum load-bearing capacity is calculated.

Strength glass

The characteristic shear stress of glass is not known. As glass is a brittle material the shear stress is converted to the maximum principal stress which can be compared with the characteristic tensile strength of glass. The conversion is done based on the circle of Mohr and results in Equation 3.24

$$\sigma_1 = -\sigma_2 = \frac{\sigma_x + \sigma_y}{2} + \sqrt{(\frac{\sigma_x + \sigma_y}{2})^2 + \tau_{xy}^2} \tag{3.24}$$

As the glass panel is solely loaded in shear Equation 3.24 is simplified to $\sigma_1 = -\sigma_2 = \tau_{xy}$. The compressive strength of glass is much higher than the tensile strength so σ_2 is not considered. This results in the assumption that the characteristic shear stress is equal to the characteristic tensile strength of glass. Subsuquently, the shear strength of the glass pane is calculated by the shear plane with the adhesive loaded in shear multiplied by the tensile strength of the glass:

$$F_{max} = w_{adhesive} * h_{glass} * f_{\mathsf{g,k}} \tag{3.25}$$

According to the shear field theory, the glass pane should not buckle out of plane. Therefore the buckling force for a glass pane loaded in shear is also considered. In the dissertation of Mocibob 2008 about glass panes in shear loading Equation 3.26 is given, to calculate the critical shear buckling stress.

$$\tau_{cr} = \frac{\pi^2 E}{12\,(1 - v^2)} \cdot \left(\frac{t_{glass}}{l_{glass}}\right)^2 \cdot k_\tau \cdot k_{VSG} \tag{3.26}$$

With:
For a simply supported square pane ($\alpha = 1$)

$$k_\tau = 5.34 + \frac{4}{\alpha^2} = 9,34 \tag{3.27}$$

For laminated glass panels of the same thickness

$$k_{VSG} = 1.5 \tag{3.28}$$

Again, assuming the characteristic shear stress is equal to the characteristic tensile strength of glass the slenderness ratio is given:

$$\bar{\lambda}_P = \sqrt{\frac{f_{\mathsf{g,k}}}{\tau_{\mathsf{crit}}}} \tag{3.29}$$

The reduction factor from the buckling curve is given by:

$$\chi\left(\bar{\lambda}_P\right) = \frac{1}{\Phi + \sqrt{\Phi^2 - \bar{\lambda}_P}} \tag{3.30}$$

With:

$$\phi = \frac{1}{2} \cdot (1 + 0,49 \cdot (\bar{\lambda}_P - 0,8) + \bar{\lambda}_P) \tag{3.31}$$

The buckling force is given by:

$$F_{h,max} = \chi \cdot l_{glass} \cdot \Sigma t * f_{\text{g,k}} \tag{3.32}$$

Strength adhesive

The strength of the adhesive is given by Equation 3.33:

$$F_{h,max} = \tau_m \cdot h_{glass} \cdot w_{adhesive} \cdot K_{stress,Volkersen} \tag{3.33}$$

Strength LVL Kerto-s

The shear force along edge of the glass pane, results in a normal force in the frame. The characteristic tensile strength parallel to the grain of the LVL Kerto-s frame is used to calculate the maximum horizontal force. The maximum horizontal force is given by Equation 3.34:

$$F_{h,max} = f_{\text{t,0,k}} \cdot w_{frame} \cdot t_{frame} \tag{3.34}$$

The shear force along edge of the glass pane (shown in the middle in Figure 3.16), acts on the interface between the glass and the LVL frame. The LVL frame must be able to support this parallel shear force. The characteristic shear strength parallel to the grain (flatwise) of the LVL Kerto-s frame is used to calculate the maximum horizontal force. The maximum horizontal force is given by Equation 3.35:

$$F_{h,max} = f_{\text{v,0,flat,k}} \cdot h_{glass} \cdot w_{adhesive} \tag{3.35}$$

The shear force perpendicular to the edge of the glass pane (shown on the right in Figure 3.16), also acts on the interface between the glass and the LVL frame. The characteristic shear strength perpendicular to the grain (flatwise) of the LVL Kerto-s frame is is used to calculate the maximum horizontal force. The maximum horizontal force is given by Equation 3.36:

$$F_{h,max} = f_{\text{v,90,flat,k}} \cdot h_{glass} \cdot w_{adhesive} \tag{3.36}$$

4

Timber to timber intra-modular connections

In this chapter, the connections between elements that form one module are discussed. These connections are called intra-modular connections. Special attention is required for the connection between the module and the timber-glass shear wall as this should allow the element to function as stability element for the module. At the end of this chapter, the following research question is answered:

What are common solutions for the intra-modular connection between the timber-glass shear wall and the load-bearing elements of the timber module?

4.1. Type of intra-modular connections

First, a clear overview of the type of connections required to construct a single module is given. These intra-modular connections consists of:

- Connection between the wall and the floor
- Connection between the wall and the ceiling
- Connection between the timber-glass shear wall and the module

For simplicity, identical connections are used between the wall and the ceiling, as well as between the wall and the floor.

4.2. Connection between the wall and ceiling/floor

The connection of the wall to the ceiling or the floor depends on the type of construction chosen for the modules. There are two options:

- The balloon structure
- The frame structure

Both are shown in Figure 4.1:

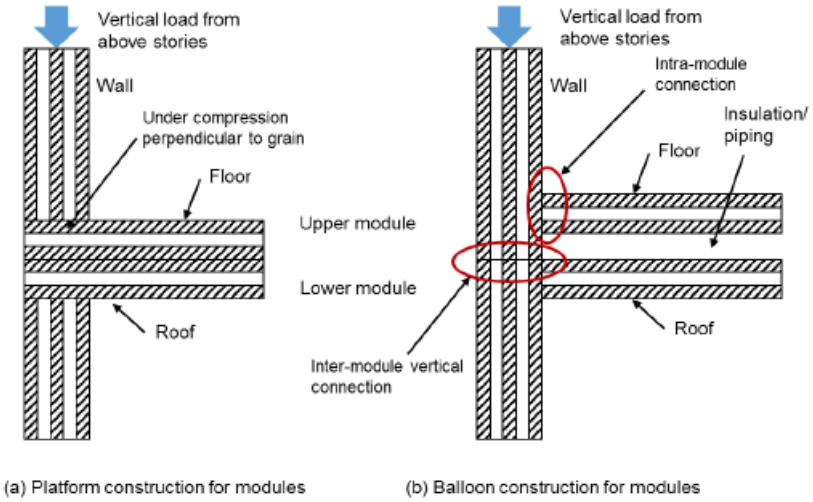

Figure 4.1: Type of construction methods to stack modules

For a platform type construction walls are placed on top of the floor. As a consequence, all the vertical loads of the stories above pass through the floor and the ceiling. For mid-rise to tall timber buildings the floors of the lower levels are under high compressive stresses perpendicular to the grain. This can lead to excessive shrinkage and compression creep over time. This can be solved by creating special connections and reinforcements.

A more simple solution would be to avoid compression perpendicular to the grain. This results in a balloon-type construction. It can be seen that, in the case of a balloon-type of construction, the walls are continuous along the height of the building. The floors should only carry the loads of one floor to the walls. For this reason, the balloon-type construction is chosen in this thesis. For the balloon type of construction, the walls are connected to the edge of the floors. This type of connection can be constructed in three common ways according to the CLT handbook:

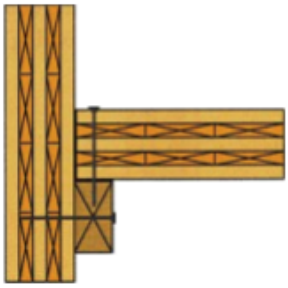

Figure 4.2: Floor to wall connection with timber ledger.

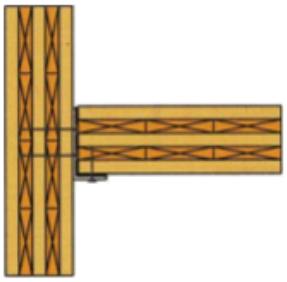

Figure 4.3: Floor to wall connection angle bracket top.

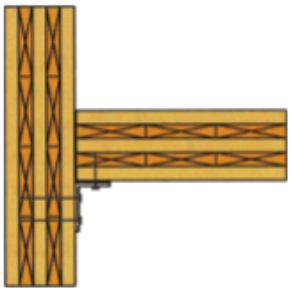

Figure 4.4: Floor to wall connection angle bracket bottom.

For this thesis, the angle bracket top will be used. The primary reason for this is that it requires minimal structural height due to the integration of the floor within the bracket. Especially for modular buildings that already have separate ceilings and floors, the structural height should be kept limited. An industry example is the Titan S angle bracket from Rothoblaas shown in Figure 4.5. The shear capacity of a Rothoblaas titan S connection for a timber-to-timber application is given by the manufacturer. In this case, screws with a diameter of 8 mm and length of 80 mm are used, the shear capacity is 33,9 kN per bracket. This connection is assumed to have no rotational capacity, resulting in zero stiffness.

Figure 4.5: Industry example angle bracket: Rothoblaas Titan-S

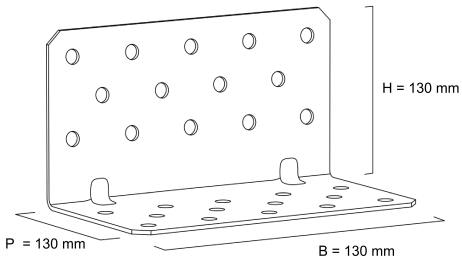

Figure 4.6: Dimensions of the Rothoblaas Titan-S

The same connection will be used for the ceiling to wall connection.

4.3. Connection between the timber-glass wall and the module

The connection between the timber-glass shear wall and the module itself is very important. This connection should transfer the horizontal forces exerted on the module to the timber-glass shear wall, in order to stabilise the the module. For this reason, the adapter frame will be screwed to the module. Screws realise a simple connection and can be applied along the perimeter of the adapter frame. This will prevent peak stresses as the connection between the two components can be regarded as continuous if enough screws are used. Furthermore, the capacity and stiffness of this connection are predictable. In addition, such a connection allows for easy replacement in case a glass panel breaks. The panel can be screwed off and a new timber-glass shear wall can be screwed to the face of the module.

4.3.1. Strength of a LVL-to-CLT screwed connection

The strength of a screwed timber-to-timber connection depends on several characteristics of the individual components:

- The embedment strength of the CLT and LVL
- The bending strength of the screw
- The pull-out strength of the screw
- The failure modes for screws in single shear

In the end, the strength of the connection is determined by the capacity of the lowest component.

The embedment strength of the CLT and LVL

The embedment strength of solid timber depends on the density of the timber, the fastener diameter, and the angle between the load and the grain direction. Due to the anisotropic nature of the timber, the embedment strength parallel to the grain is much higher than the embedment strength perpendicular to the grain. The embedment strength of solid timber for both load directions is given in Equation 4.1 and 4.2. The embedment strength of timber loaded parallel to the grain is:

$$f_{h,0,k} = 0,082 \cdot (1 - 0,01 \cdot d_{screw}) \cdot \rho_k \tag{4.1}$$

The relation between the embedment strength parallel to the grain ($\alpha = 0°$) up to perpendicular to the grain ($\alpha = 90°$) was proposed by Johanson and is implemented in Eurocode 5. This relation is shown below:

$$f_{h,\alpha,k} = \frac{f_{h,0.k}}{k_{90} \cdot \sin(\alpha)^2 + \cos(\alpha)^2} \tag{4.2}$$

Where:

$$k_{90} = \begin{cases} 1,35 + 0,015 d_{screw} & \text{for softwoods} \\ 1,30 + 0,015 d_{screw} & \text{for LVL} \\ 0,90 + 0,015 d_{screw} & \text{for hardwoods} \end{cases} \tag{4.3}$$

For CLT, two extra parameters are introduced to derive the embedment strength. These two parameters are the orientation of the load application relative to the panel, and the thickness of the CLT layers. The orientation of the load application relative to the panel can be in the panel face or at the panel edge. The two extra parameters are visualised in Figure 4.7.

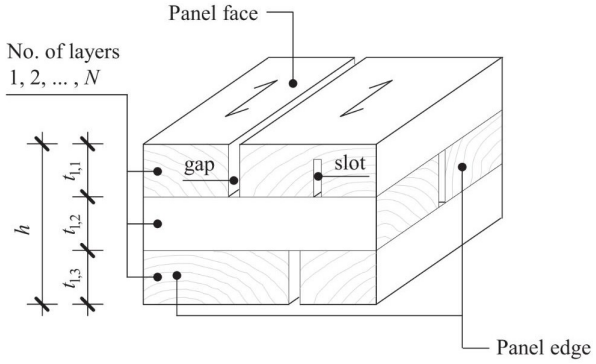

Figure 4.7: Definition panel orientation (Mohammad et al. 2018)

Uibel and Blaß 2013 propose Equation 4.4 and 4.5 to calculate the characteristic embedment strength specifically for nails and screws in the panel edge and panel face of CLT. These formulas are the result of regression analysis of numerous tests. The embedment strength of screws and nails in the panel face and panel edge of CLT are respectively:

$$f_{h,k,face} = 0,112 \cdot d_{screw}^{-0,5} \cdot \rho_k^{1,05} \tag{4.4}$$

$$f_{h,k,edge} = 0,862 \cdot d_{screw}^{-0,5} \cdot \rho_{layer,k}^{0,56} \tag{4.5}$$

According to Uibel and Blaß 2013 Equation 4.4 and 4.5 are only valid for panels with a maximum layer thickness of 9 mm. In other cases, the embedment strength of solid timber could be used. This means that for CLT the embedment strength of solid timber can be used. For LVL, Equation 4.4 and 4.5 can be used because the veneer layers are usually less than 9 mm thick. However, for this thesis, the formulas from Eurocode 5 are used for LVL. Remarkably, Equation 4.4 and 4.5 are independent of the angle between the load and the grain direction. This could be explained by the fact that the anisotropic nature of timber is reduced by applying different orientations of timber layers in CLT. This effect is even more present when thin layers (< 9 mm) are used. This effect can also be seen in the embedment strength calculation for dowels. In the same paper, a k_{90} factor of 1,1 is proposed for dowels compared to 1,35 given in Equation 4.3 for softwoods.

In case the screws penetrate multiple layers of CLT, certain layers are loaded perpendicular to the grain while others are loaded parallel to the grain. For calculations, it is assumed that both layers are loaded perpendicular to the grain. This simplifies the calculations while underestimating the embedment strength of the timber loaded parallel to the grain. This means that the calculation is conservative, thus on the safe side.

The bending strength of the fastener

According to Johanson, it is assumed that the bending strength of the dowel is equal to the elastic moment capacity of the screw's cross-section. This results in the bending strength of the dowel:

$$M_{y,Rk} = 0,3 \cdot f_{u,k} \cdot d_{screw}^{2,6} \tag{4.6}$$

The characteristic axial withdrawal capacity of the fastener

In case the bending strength of the fastener is governing, the so-called 'rope effect' should be taken into account. Due to the bending deformation, the fastener will try to elongate however, for some types of fasteners this is restricted. The restricted elongation of the fastener results in axial tensile forces that develop as the bending deformation increases. This axial tensile force hinders more bending deformation thus contributing to the load-bearing capacity of the connection. The extent to which the 'rope effect' contributes to the load-bearing capacity depends on how much the elongation is restrained

per type of fastener. In the Eurocode it is specified that the 'rope effect' should be limited to the following percentages of the Johansen part:

- Screws 100 %
- Other nails 50 %
- Square and grooved nails 25 %
- Bolts 25%
- Round nails 15 %
- Dowels 0 %

For screws, it can be concluded that the 'rope effect' cannot exceed the Johansen part. The 'rope effect' is given by the $\frac{F_{ax,Rk}}{4}$ part in Equation 4.11. In Uibel and Blaß 2013 the results are presented of 119 withdrawal tests of screws in the panel face of the CLT, and 268 tests with screws in the edge of the CLT panel. This resulted in the following expression which can be used to calculate the axial withdrawal capacity of a screw fastener is given by:

$$F_{ax,k,Rk} = \frac{0,35 \cdot d^{0,8} \cdot l_{ef}^{0,9} \cdot \rho_k^{0,75}}{1,5\cos(\epsilon)^2 + \sin(\epsilon)^2} \tag{4.7}$$

This formula can be used for both screws in the face and the edge of the CLT panel according to Uibel and Blaß 2013. Contrary to this, Mohammad et al. 2018 suggests using the withdrawal capacity of screws in solid timber stated in the Eurocode 5. This formula is presented in Equation 4.8 and results in slightly higher values compared to Equation 4.7. The reason for this is that experiments have shown that there is no significant difference in withdrawal capacity for screws in CLT compared to solid timber if the CLT does not have significant gaps. Plus, the probability of placing a screw along its whole inserted tread length in a gap is much lower in the case of face application than in the case of edge application.

$$F_{ax,k,Rk} = \frac{f_{ax,k} \cdot d \cdot l_{ef} \cdot k_d}{1,2\cos(\alpha)^2 + \sin(\alpha)^2} \tag{4.8}$$

Where:

$$f_{ax,k} = 0,52 \cdot d^{-0,5} \cdot l_{ef}^{-0,1} \cdot \rho_k^{0,8} \tag{4.9}$$

$$k_d = min \begin{cases} \frac{d}{8} \\ 1 \end{cases} \tag{4.10}$$

The results of the paper of Mohammad et al. 2018 are used in this thesis and therefore the withdrawal capacity of screws are calculated with Equation 4.8 according to Eurocode 5.

Strength of a timber-to-timber screwed connection

In the Eurocode, six failure mechanisms are described for a fastener single shear connecting two timber elements. These are presented in Figure 4.8 with corresponding strength formula in Equation 4.11.

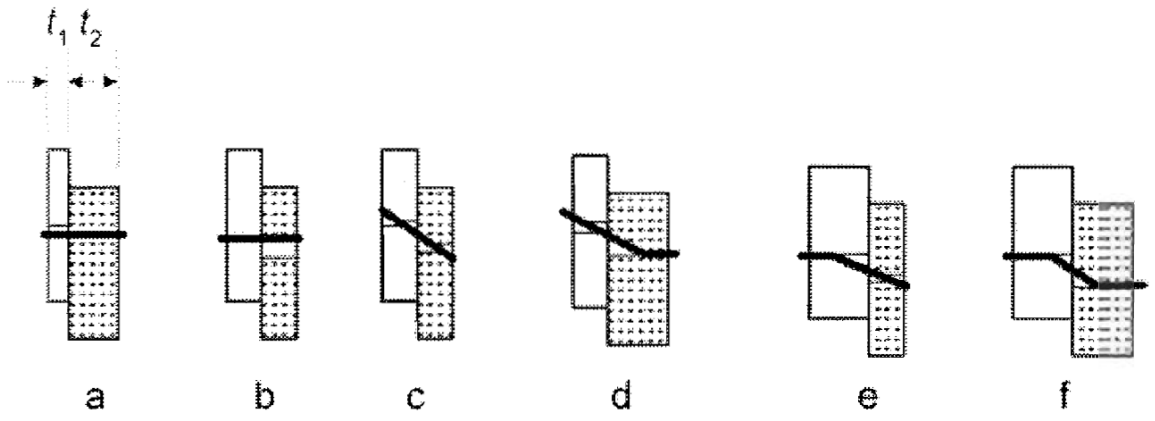

Figure 4.8: Failure modes fasteners in single shear timber-timber

$$F_{v,Rk} = \min \begin{cases} f_{h1,k} \cdot t_1 \cdot d & (a) \\ f_{h2,k} \cdot t_2 \cdot d & (b) \\ \frac{f_{h1,k} \cdot t_1 \cdot d}{1+\beta}[\sqrt{\beta + 2\beta^2[1 + \frac{t_2}{t_1} + \frac{t_2}{t_1}^2] + \beta^3(\frac{t_2}{t_1})^2} - \beta(1 + \frac{t_2}{t_1})] + \frac{F_{ax,Rk}}{4} & (c) \\ 1,05\frac{f_{h1,k} \cdot t_1 \cdot d}{2+\beta}[\sqrt{2\beta(1+\beta) + \frac{4\beta(2+\beta)M_{y,Rk}}{f_{h,1,k} \cdot d \cdot t_1^2}} - \beta] + \frac{F_{ax,Rk}}{4} & (d) \\ 1,05\frac{f_{h1,k} \cdot t_2 \cdot d}{1+2\beta}[\sqrt{2\beta^2(1+\beta) + \frac{4\beta(1+2\beta)M_{y,Rk}}{f_{h,1,k} \cdot d \cdot t_2^2}} - \beta] + \frac{F_{ax,Rk}}{4} & (e) \\ 1,15\sqrt{\frac{2\beta}{1+\beta}}\sqrt{2M_{y,Rk} \cdot f_{h,1,k} \cdot d} + \frac{F_{ax,Rk}}{4} & (f) \end{cases} \tag{4.11}$$

Where:

$$\beta = \frac{f_{h,2,k}}{f_{h,1,k}} \tag{4.12}$$

The variables $f_{h1,k}$, $f_{h2,k}$ and $M_{y,Rk}$ refer to the embedment strength of timber element 1 and 2, and the bending strength of the fastener. Timber element 1 is the LVL kerto-S frame and timber element 2 is the CLT module.

4.3.2. Geometrical boundary conditions for the placement of screws in CLT and LVL

In the Mohammad et al. 2018 multiple boundary conditions for the placements of fasteners in CLT are specified, which are also implemented in the Austrian national application document of the Eurocode (ÖNORM B 1995-1-1). Currently, there are no extra requirements in the Eurocode itself and therefore this annex is used as a guideline.

Minimum spacing, minimum edge distance and minimum end distance for screws in CLT

Boundary conditions are given for the minimum spacing, minimum edge distance and minimum end distance. These boundaries are specified to ensure that brittle failure mechanisms, like the tensile or shear splitting of timber, do not occur prior to the ductile failure mechanism. In other words, this guarantees that the calculated maximum load-bearing capacity of the connection can be reached before brittle failure occurs.
First, the definition of the distances are shown in Figure 4.9:

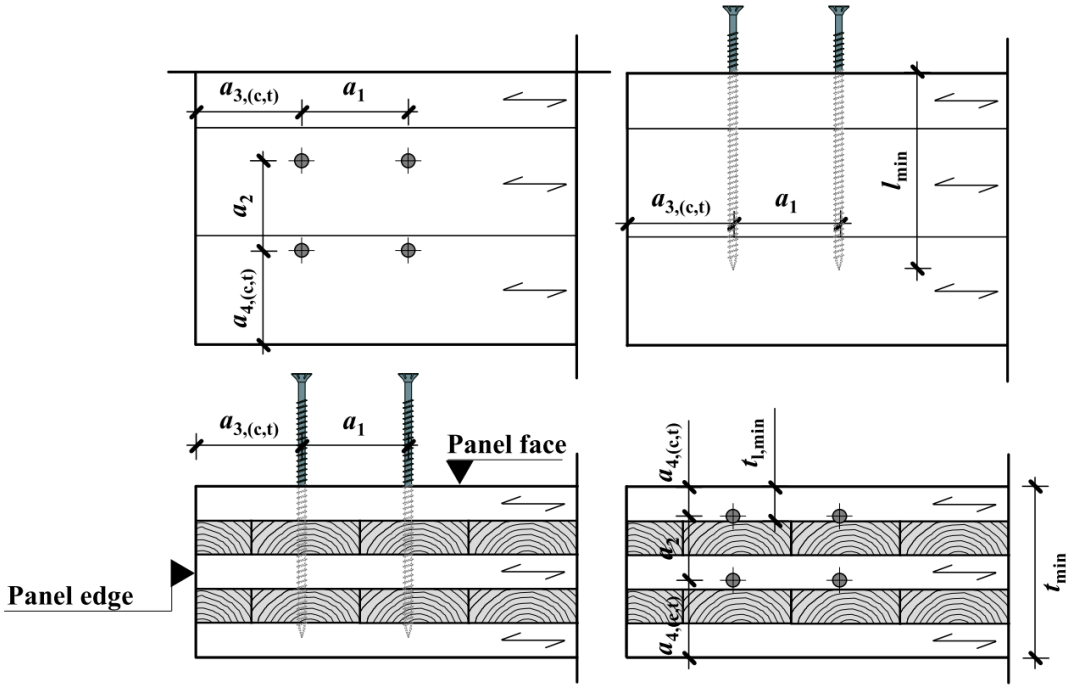

Figure 4.9: Definition of geometrical boundary conditions for fasteners in CLT. Screws in the panel face (left) and screws in the panel edge (right) (Mohammad et al. 2018)

The minimum values suggested by Mohammad et al. 2018 are given in Table 4.1

Fastener type	Position	a_1	a_2	$a_{3,t}$	$a_{3,c}$	$a_{4,t}$	$a_{4,c}$
Self-tapping screws	Face	4 d	2,5 d	6 d	6 d	6 d	5 d
	Edge	10 d	3 d	12 d	7 d	5 d	5 d

Table 4.1: Minimum requirement for the edge distance, end distance and spacing of dowelled-type fasteners in CLT

The advantage of CLT is that, due to it's build-up, it is less prone to brittle failure when loaded in the panel face. When comparing the edge distance of CLT to softwood, the result shows lower edge distances for CLT. On the contrary, it can be concluded that the panel edge is much more sensitive to brittle failure mechansisms, because the edge distances are much higher.

Additional geometrical requirements for screws in CLT

Furthermore, for self-tapping screws, additional geometrical requirements are prescribed in Mohammad et al. 2018:

Fastener type	Position	n_{min}	t_{min}	$t_{1,min}$	l_{min}	d_{min}
Self-tapping screws	Face	4				6 mm
	Edge		10 d	d $\geq$ 8: 3d	10 d	8 mm

Table 4.2: Additional geometrical requirements for screws in CLT

It should be noted that according to the ÖNORM B 1995-1-1, it is not allowed to axially load screws in the face of a CLT panel. The reason for that is that the gap width in CLT has similar dimensions as commonly used screw diameters, and therefore the withdrawal capacity can not be guaranteed if the screw is located in a gap. Again, these extra requirements are introduced to prevent brittle failure mechanisms, mainly for axially loaded screws. For example, block shear, which is a brittle failure mechanism, was observed in an axially loaded group of screws when the penetration depth was not sufficient.

Minimum spacing, minimum edge distance and minimum end distance for screws in LVL
For LVL the boundary conditions are given in the Eurocode. If the screw diameter is bigger than 6 mm, it is regarded as a bolt and therefore the boundary conditions for bolts are given:

Spacing and edge/end distances	Angle to grain	Minimum spacings and egde/end distances
a_1 (parallel to grain)	$0° \leq \alpha \leq 360°$	$(3 + 2\lvert\cos\alpha\rvert)d$
a_2 (perpendicular to grain)	$0° \leq \alpha \leq 360°$	$3d$
$a_{3,t}$ (loaded end)	$-90° \leq \alpha \leq 90°$	max $(7d; 80mm)$
$a_{3,c}$ (unloaded end)	$90° \leq \alpha \leq 150°$ $150° \leq \alpha \leq 210°$ $210° \leq \alpha \leq 270°$	max$(a_{3,t}; \lvert\sin\alpha\rvert d; 3d)$ $3d$ max$(a_{3,t}; \lvert\sin\alpha\rvert d; 3d)$
$a_{4,t}$ (loaded end)	$0° \leq \alpha \leq 180°$	max $(2 + 2\lvert\sin\alpha\rvert d; 3d)$
$a_{4,c}$ (unloaded end)	$180° \leq \alpha \leq 360°$	$3d$

Table 4.3: Minimum requirement for the edge distance, end distance and spacing of bolts (EN 1995-1-2 2004)

Effective number of fasteners
Lastly, the requirements for the effective number of fasteners are presented. The strength of the connection can't simply be calculated by the multiplication of the number of fasteners with the strength of an individual fastener. The factor that reduces the strength of a group of fasteners is n_{eff} and only depends on the geometrical conditions. The value is presented in Table 4.4

Fastener type	Position	Axially loaded	Laterally loaded
Self-tapping screws	Face	$n^{0,9}$	n
	Edge	$n^{0,9}$	min $\begin{cases} n \\ n^{0,9} \cdot \sqrt[4]{\frac{a_1}{13d}} \end{cases}$

Table 4.4: Effective number of screws in CLT

4.3.3. Stiffness of a timber-to-timber screwed connection

Zooming in on the stiffness behaviour of a single fastener type of connection one can observe a non-linear load-displacement relation. This is shown in Figure 4.10:

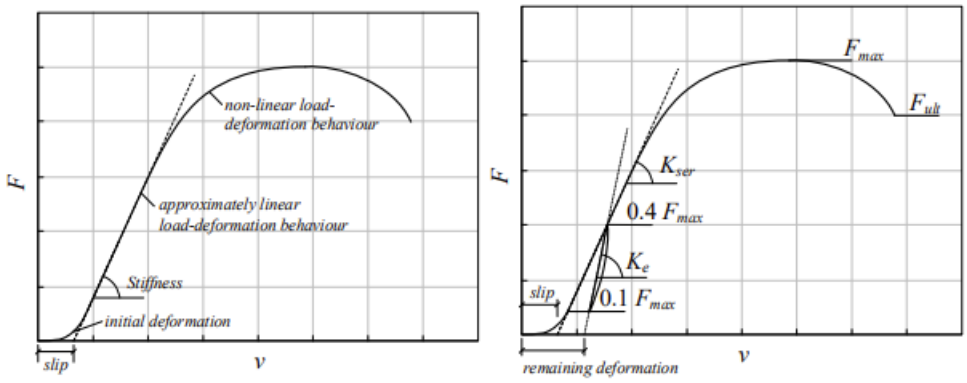

Figure 4.10: Characteristics of the load-deformation diagram of a dowelled-type connection (Mohammad et al. 2018)

From the left graph, two important parameters should be pointed out. First of all, the initial part of the graph shows a deformation already present at zero to low loads. This is the slip of the connection and is introduced by hole tolerances. For screws in timber, this is usually not considered.

The second important parameter is the stiffness of the connection, which is equal to the slope of the curve. For calculation purposes, the non-linear graph is approximated with a linear line, resulting in a constant stiffness. The approximation which is used in the Eurocode is shown in the right graph. The stiffness K_{ser} is used in the serviceability limit state (SLS). For a dowell-type connection, K_{ser} is equal to the secant stiffness between $0,1F$ and $0,4F$. On the basis of many tests the empirical equation 4.13 is given in the Eurocode to calculate the value for K_{ser}. The variable ρ_m refers to the density of the timber element.

$$K_{ser} = 2 \ \cdot {\rho_m}^{1,5} \cdot \frac{d}{23} \tag{4.13}$$

Looking at Figure 4.10, K_{ser} is the stiffness at the load level of approximately 60 to 70 percent of the maximum load (Sandhaas et al. 2018). Failure of the screws can therefore be regarded as a ductile failure mechanism.

In case the density of the connected timber elements differ, Equation 4.14 can be used to calculate ρ_m.

$$\rho_m = \sqrt{\rho_{m,1} \cdot \rho_{m,2}} \tag{4.14}$$

5

Timber to timber inter-modular connections

In this chapter, the module-to-module connections are discussed. These connections are called inter-modular connections and should allow for force transfer between the modules. At the end of this chapter, the following research question is answered:

What connection can be used to create an inter-modular connection between the timber modules?

5.1. Type of forces

The first step in the selection of a suitable connection is to investigate which forces should be transferred between the modules. These forces are a result of the horizontal and vertical forces. The horizontal loading is only wind loading. The vertical loading is self-weight, superimposed dead loads and live loads. These loads result in the following type of forces in the connections:

- Shear force between the upper and lower module in y-direction
- Shear force between the upper and lower module in x-direction
- Shear force between two adjacent modules in y-direction
- Compressive force between two adjacent modules
- Compressive force between the upper and lower module

It should be noted that the compressive forces, could turn into tensile forces in case of progressive collapse. The connections will not be calculated for tension, nor will the tensile force be quantified in this thesis. However, for this thesis, it is taken into consideration that the connection should in principle be able to transfer a tensile force.

The advantage of the balloon-type construction is that the compressive force between the upper and lower modules can be transferred directly from the upper sidewall to the lower sidewall. Hence, no connection is necessary for this force.

5.2. Type of inter-modular connections

This thesis provides several common options to create inter-modular connections. The objective for the inter-modular connections is to create:

- A demountable connection
- Ductile connection
- Provide space for thermal and acoustic insulation. Between adjacent modules mainly thermal insulation is used. Between vertical modules, sound insulation is applied.

5.2.1. Horizontal connection: Steel plate with screws

For force transfer between horizontal modules, the connection design will consist of screws and steel plates. This connection is simple in execution, and was used multiple times in projects investigated during the case study in Chapter 2. This connection is designed to accommodate the following forces:

- Shear force between two adjacent modules in y-direction
- Compressive force between two adjacent modules

5.2.2. Vertical connection: Shear plate connector

The vertical connection is more complicated, as shear in two directions should be transferred. In the direction of the sidewalls, the shear can easily be transferred over the length of the wall. Shear perpendicular to the wall could also be transferred over the entire length of the wall if a linear shear distribution is present. Unfortunately, this is not the case as the stability element of the module is present on one side of the module. This means that the horizontal force, which is transferred as shear force, is concentrated on one side of the module. To assess the possibilities, a multi-criteria analysis is made to decide which connection is best suitable. This is shown in Table 5.1

Connection	Glued in rods	Tooth-plate connector	Ring plate connector	Shear plate connector	Steel plate and screws	Steel plate and dowels
Demountability	- -	+-	++	++	+	++
Ductility	++	++	++	++	++	++
Provide spacing	++	- -	- -	++	++	++
Required work onsite	-	+	+	+	-	+-
Applicable in both walls	- -	++	++	++	- -	- -
Visibility	++	++	++	++	+-	+-
Simplicity	-	+	+-	+-	++	++
Progressive collapse (Possible tension)	+	- -	- -	- -	++	++
Fire safety	+	+	+	+	-	-
Total	29	32	33	37	32	34

Table 5.1: Multi-criteria analysis for the vertical inter-modular connection

Based on this analysis the shear plate connector will be used to provide the shear connection. This connection is designed to accommodate the following forces:

- Shear force between the upper and lower module in y-direction
- Shear force between the upper and lower module in x-direction

It was previously stated that the connection should in principle be able to transfer tensile forces, which is not possible with this connection. So, this connection is combined with a steel plate and screws, which should transfer the tensile forces.

5.3. Steel plate with screws: Strength and stiffness

A simple and affordable connection is made by combining steel plates with screws. In this case, the screws are used to transfer the force from the timber element to the steel plate and vice versa. A detailed drawing of a possible connection is shown in Figure 5.1

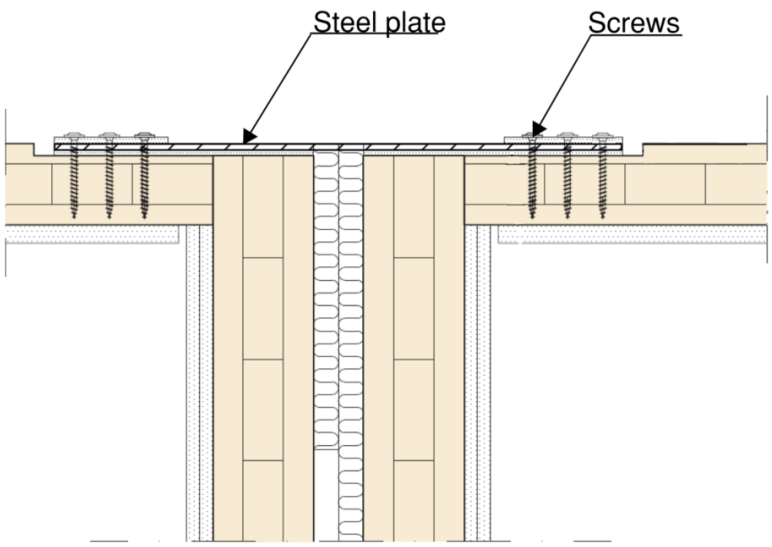

Figure 5.1: Example of a horizontal connection with a steel plate and self-tapping screw fasteners

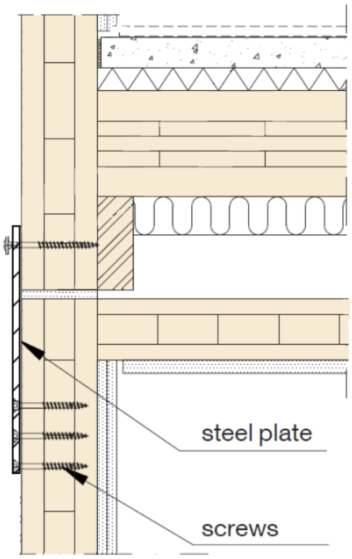

Figure 5.2: Example of a vertical connection with a steel plate and self-tapping screw fasteners

5.3.1. Strength of timber-to-steel connection

The strength of the connection depends on several characteristics of the individual components:

- The embedment strength of the CLT
- The bending strength of the screw
- The pull-out strength of the screw
- The failure modes for screws in single shear
- The strength of the steel plate

In the end, the strength of the connection is determined by component with the lowest capacity.

The embedment strength of the CLT

This is already discussed in Section 4.3.1

The bending strength of the fastener

This is already discussed in Section 4.3.1

The characteristic axial withdrawal capacity of the fastener

This is already discussed in Section 4.3.1

The failure modes for steel-to-timber fasteners in single shear

In the Eurocode five different failure mechanisms for steel-to-timber fasteners are described. The five failure mechanisms are shown in Figure 5.3: The following five failure modes:

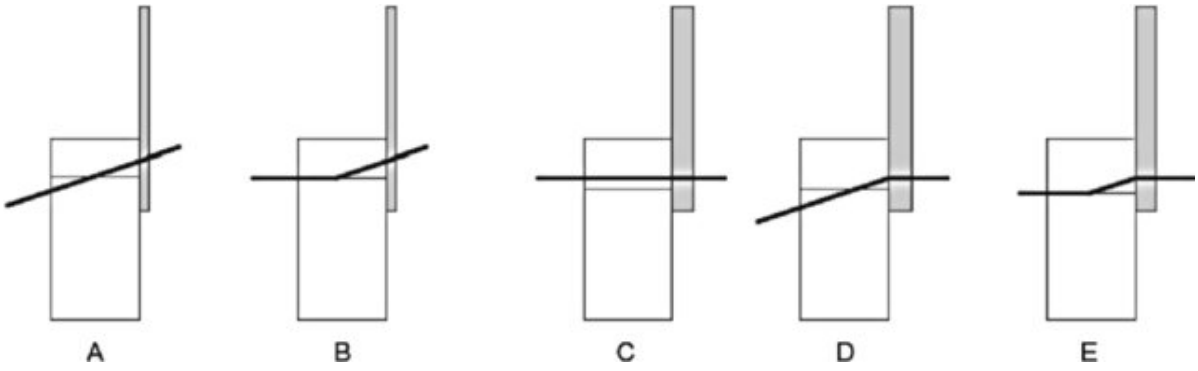

Figure 5.3: Failure modes fasteners in single shear

The different failure mechanisms are based on embedment failure of the timber, yielding of the fastener or a combination of both. Embedment failure of the timber and yielding of the fastener both result in ductile failure.

The last parameter that influences the possible failure modes is the distinction between thick and thin steel plates. This distinction is made based on the thickness of the steel plate (t_{plate}) compared to the diameter of the fastener (d_{screw}). For a timber-to-steel connection with a thin steel plate ($t_{plate} \leq 0,5 \cdot d_{screw}$) the fastener is able to rotate freely in the plate. In Figure 5.3 it can be seen that for failure modes (a) and (b) the dowel exits the steel plate under an angle. In other words, the steel plate is too thin to bend the dowel horizontally again. This means that for thin steel plates only failure mechanisms (a) and (b) can occur. In thick steel plates ($t_{plate} \geq d$) the dowel can't rotate freely and will therefore be bent by the steel plate until the dowel is horizontal. This can be seen in failure modes (c) till (e) as the dowel exits the steel plate horizontally. This means that for thick steel plates failure mechanisms (c), (d) and (e) can occur. The characteristic strength for thin plates is given by the minimum of failure mode (a) and (b):

$$F_{v,rk,thin} = min \begin{cases} 0,4 \ \cdot \ f_{h,90,k} \cdot d_{screw} \cdot l_{screw} & (a) \\ 1,15 \ \sqrt{2 \cdot M_{y,Rk} \cdot f_{h,90,k} \cdot d_{screw}} + \frac{F_{ax,Rk}}{4} & (b) \end{cases} \tag{5.1}$$

The characteristic strength for thick steel plates is given by the minimum of failure mode (c), (d) and (e):

$$F_{v,rk,thick} = min \begin{cases} f_{h,90,k} \cdot l_{screw} \cdot \ d_{screw} & (c) \\ f_{h,90,k} \cdot l_{screw} \cdot d_{screw} \cdot \left[\sqrt{2 + \frac{4 \cdot M_{y,Rk}}{f_{h,90,k} \cdot d_{screw} \cdot {l_{screw}}^2}} - 1 \right] + \frac{F_{ax,Rk}}{4} & (d) \\ 2,3 \cdot \sqrt{2 \cdot M_{y,Rk} \cdot f_{h,90,k} \cdot d_{screw}} + \frac{F_{ax,Rk}}{4} & (e) \end{cases} \tag{5.2}$$

If the thickness of the plate is between thin and thick plates, linear interpolation is applied between the governing failure modes.

The strength of the steel plate

In general, the strength of the steel plate will not govern the design of a screwed connection. However, if the thickness of the plate is too thin, the strength of the plate could become governing. Therefore the buckling strength and net area strength of the plate are given.

In this case, the wind load would result in a compressive force through the plate, which means that buckling can be a possible failure mechanism. Especiallly for thinner plates, this failure mechanism could become governing.

It is assumed that the buckling length is equal to the centre-to-centre distance between the screws. Whenever multiple rows of screws are used, the distance between the inner screws is used. The Euler buckling load of the plate is given:

$$N_{cr} = \frac{\pi^2 \cdot E_s \cdot I_{plate}}{{L_{cr}}^2} \tag{5.3}$$

Where:

$$I_{plate} = \frac{1}{12} \cdot b_{plate} \cdot {t_{plate}}^3 \tag{5.4}$$

Subsequently, the design buckling resistance of the plate can be calculated:

$$N_{b,rd} = \frac{\chi \ \cdot A_{plate} \cdot f_y}{\gamma_{M1}} \tag{5.5}$$

Where:

$$\chi = \frac{1}{\Phi + \sqrt{\Phi^2 - \lambda^2}} \tag{5.6}$$

$$\Phi = 0,5 \cdot [1 + \alpha \cdot (\lambda - 0,2) + \lambda^2] \tag{5.7}$$

α is an imperfection factor for buckling curves

$$\lambda = \sqrt{\frac{A_{plate} \cdot f_y}{N_{cr}}} \tag{5.8}$$

$$A_{plate} = b_{plate} \cdot t_{plate} \tag{5.9}$$

Next, the net area of the plate should be checked. The section where holes for the screws are located, is the weakest part. The holes in the plate are 1 mm larger than the diameter of the screws. The net area of the steel plate is:

$$A_{net} = (b_{plate} - n \cdot (1 + d)) \cdot t_{plate} \tag{5.10}$$

$$N_{net,rd} = A_{net} \cdot f_y \tag{5.11}$$

5.3.2. Geometrical boundary conditions for the placement of screws in CLT

This is already discussed in Section 4.3.1

Effective number of fasteners

This is already discussed in Section 4.3.1

5.3.3. Stiffness of the connection

The stiffness of the connections has a great impact on the total stiffness of the building and the force distribution across the modules. First of all, there is no external stability mechanism which means that all the lateral forces should be transferred via the inter-modular connections. On top of that, the lateral forces pass through an inter-modular connection to the adjacent modules. For an efficient force transfer across the modules, the stiffness of the connection cannot be too low. A low stiffness of the connection will result in a relatively high deformation of the connection. As the number of adjacent modules increases, the number of horizontal connections increases, and thus the deformation. As a result, the first module will deform too much, while the last module is not activated.

On the basis of many tests the empirical equation 5.12 is given in the Eurocode to calculate the value for K_{ser}. The variable ρ_m refers to the density of the timber element.

$$K_{ser} = 2 \cdot {\rho_m}^{1,5} \cdot \frac{d}{23} \tag{5.12}$$

This equation is the same equation as for a timber-to-timber connection, except for a factor of two. The factor two is introduced for steel-to-timber connections assuming infinite stiffness of the steel. It can be observed that the stiffness of the connection is independent of the load direction or the failure mechanism. It was previously discussed that the slip of the connection for timber is not considered. However for prefabricated holes in the steel plate, this is taken into consideration. No value for the initial slip of the connection is prescribed in the Eurocode. Due to the fact that the slip is created by hole tolerances, the hole tolerance could be used as an estimation of the slip value. For steel connections, this is usually equal to 1 mm. The stiffness that should be used for the ultimate limit state (ULS) is given in the Eurocode in Equation 5.13

$$K_u = \frac{2}{3} \cdot K_{ser} \tag{5.13}$$

For connections with multiple fasteners, each fastener can be regarded as a spring with the spring stiffness K_{ser} or K_u depending on the limit state. The total stiffness of the connection can be derived by applying the springs in parallel for the screws on one side of the connection and in series with the screws on the other side of the connection. This concept is visualised in Figure 5.4. The stiffness of the steel plate is much higher than the stiffness of the screws and is therefore assumed to be rigid.

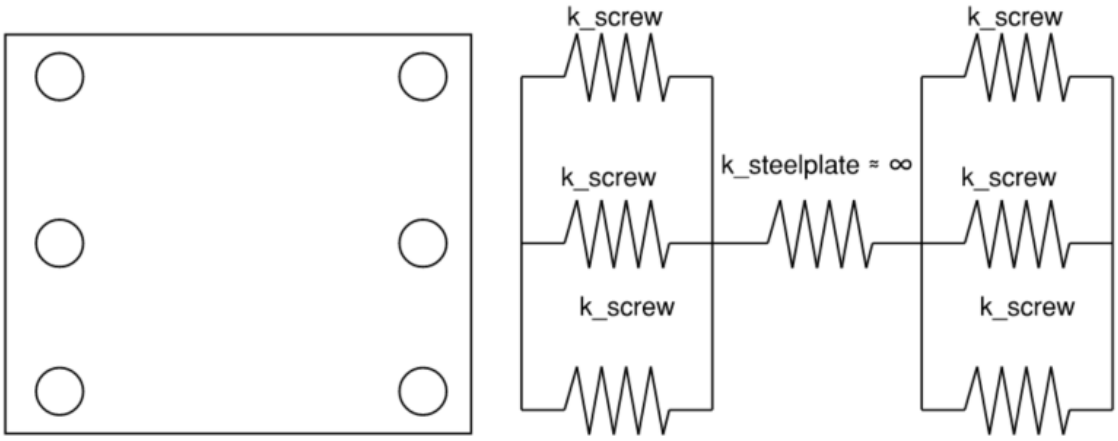

Figure 5.4: Schematic drawing of the stiffness of the connection represented as springs

The stiffness of the connection can also be explained in a more mathematical way as in Equation 5.14. Again it can be seen that inserting an infinite stiffness for the steel plate, results in no contribution to the total stiffness of the connection. This means that the steel plate doesn't deform.

$$K_{connection} = \frac{1}{\frac{1}{n \cdot K_{screw}} + \frac{1}{K_{steelplate}} + \frac{1}{n \cdot K_{screw}}} \tag{5.14}$$

5.4. Shear plate connector type B with dowel: Strength and stiffness

The second connection is again a cheap and demountable connection created with a shear plate connector. Typically, this connector is used to strengthen dowelled connections by increasing the shear area with an additional circular flanged plate. The shear plates are made of steel, a aluminium cast alloy or cast iron. The assembly of this connection starts with predrilling a hole for the bolt and a groove for the steel flange in both timber elements. Next, the shear plate is inserted in both timber elements, which can already be done off-site. Then, a bolt is put through the timber elements and the connectors. To finish the connection, the nut at the end of the bolt is tightened, closing the space between the two timber elements. Optionally a washer can be used to spread the clamping force over a greater area. This lowers the stress perpendicular to the grain of the timber and prevents crushing of the timber. The connection can be seen in Figure 5.5.

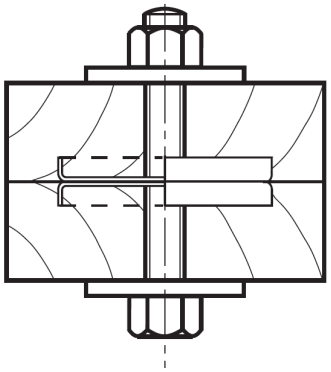

Figure 5.5: Shear plate connector

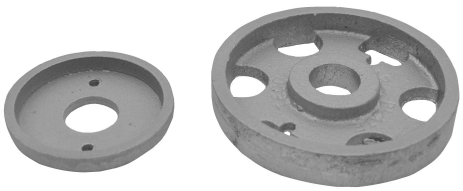

Figure 5.6: Shear plate connector Type B2 - B3

In the Dutch Annex for fasteners(NEN-EN 912) standard dimensions are visualised in Figure 5.7 and 5.8:

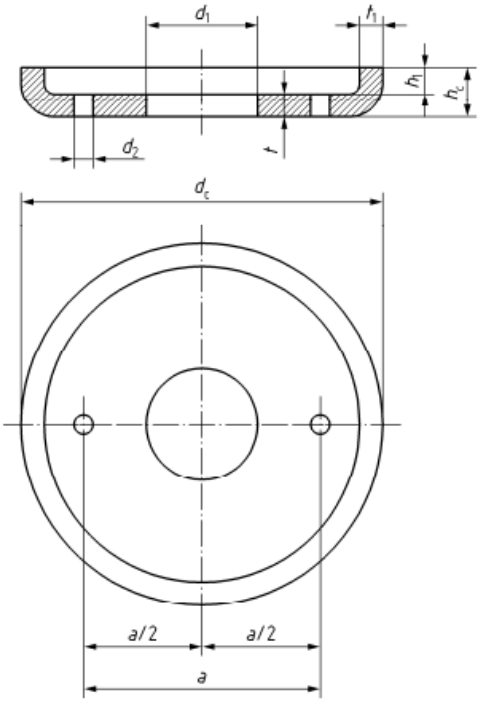

Figure 5.7: Shear plate connector type B2 (NEN-EN 912 2011)

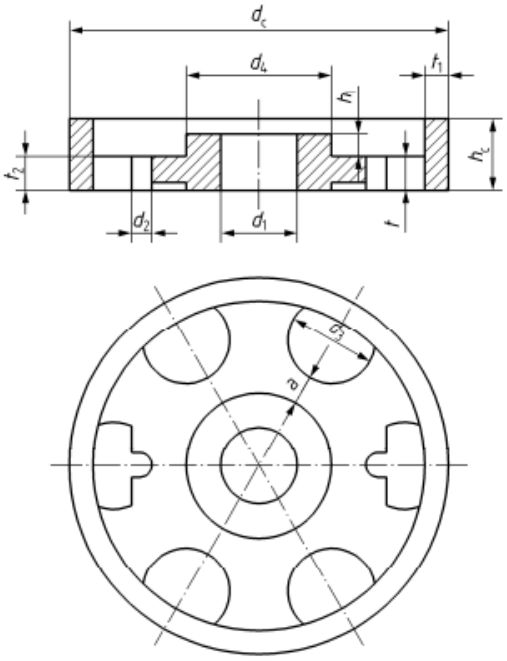

Figure 5.8: Shear plate connector type B3 (NEN-EN 912 2011)

	Diameter of plate d_c [mm]	Height h_c [mm]	Thickness of plate T [mm]	Thickness of flange t_1 [mm]	Diameter of centre hole d_1 [mm]	Diameter of nail holes d_2 [mm]
Type B2	66,7	10,7	4,4	4,4	20,5	4,0
Type B3	102,0	15,7	5,0	6,0	20,5	4,0

Table 5.2: Dimensions of connectors of type B2 and B3 in mm(NEN-EN 912 2011).

Shear plate type B2 is a circular flange plate with a bolt-hole trough the centre. In addition, two nail holes are drilled into the plate. Shear plate type B3 is slightly different but functions similarly. This type is made of a perforated circular flanged plate with an integral cylindrical centre. Again, two nail holes are predrilled into the plate. This means that both shear plates can already be installed off-site in the modules. On-site the dowel can be inserted in the bolt-hole, after which the upper module can be lifted over the dowel. This means that no drilling of holes or screwing is required on-site to create the connection. For this connection, it is not possible to tighten the connection with nuts. This is not necessary as the self weight of the modules ensures a tight connection.

5.4.1. Strength of connection

The strength of this connection is purely given by the shear plate, while the strength of the dowel is disregarded. The strength of a shear plate connector is given by:

$$F_{v,0,Rk} = min \begin{cases} k_1 \cdot k_2 \cdot k_3 \cdot k_4 \cdot 35 \cdot d_c^{1,5} & (a) \\ k_1 \cdot k_3 \cdot h_e \cdot 31,5 \cdot d_c & (b) \end{cases} \tag{5.15}$$

Where:

$$k_1 = min \begin{cases} 1 \\ \frac{t_1}{3h_c} \\ \frac{t_2}{5h_e} \end{cases} \tag{5.16}$$

k_2 applies for a loaded end $(-30° \leq \alpha \leq 30°)$:

$$k_2 = min \begin{cases} k_a \\ \frac{a_{3,t}}{2d_c} \end{cases} \tag{5.17}$$

$$k_a = \begin{cases} 1,25 & \text{for connections with one connector per shear plane} \\ 1,0 & \text{for connections with more than one connector per shear plane} \end{cases} \tag{5.18}$$

For other values of α, $k_2 = 1$.

$$a_{3,t} = max \begin{cases} 1,1d_c \\ 7d \\ 80 \end{cases} \tag{5.19}$$

$$k_3 = min \begin{cases} 1,5 \\ \frac{\rho_k}{350} \end{cases} \tag{5.20}$$

$$k_4 = \begin{cases} 1,0 & \text{for timber-to-timber connections} \\ 1,1 & \text{for steel-to-timber connections} \end{cases} \tag{5.21}$$

In Equation 5.15 condition (a) refers to the strength which corresponds to block shear of the shear plate. Condition (b) refers to the embedment failure of the timber caused by the shear plate. The factors k_1 till k_4 take into account different aspects which influence the strength of the connection:

- k_1 is a modification factor taking into account thickness of the timber member. For the connection of just two timber members, t_2 is not applicable as this refers to the thickness of the middle member.
- k_2 refers to the block shear strength. If the edge distance reduces, the area which shears out becomes lower, thus reducing the strength.
- k_3 is a modification factor for the timber density. Tests conducted by Blass et al. 1994, which formed the basis for the Eurocode for shear plates, were conducted using C24 softwood timber. For higher densities, a higher strength of the timber is observed.
- k_4 is related to the connected material. This factor should only be applied when block shear is governing. This means that block shear is less likely to occur if a timber-to-steel connection is used compared to a timber-to-timber connection.

Similar to the embedment strength for timber for nails, the Johansen formula can be used to calculate the strength at an angle α to the grain:

$$F_{v,\alpha,Rk} = \frac{F_{v,Rk}}{k_{90} \cdot \sin(\alpha)^2 + \cos(\alpha)^2} \tag{5.22}$$

Where:

$$k_{90} = 1,3 + 0,001 \cdot d_c \tag{5.23}$$

5.4.2. Geometrical boundary conditions for the placement of shear plates

In the Eurocode minimum spacing, edge- and end distances are given for shear plate connectors. These are shown in Table 5.3. These distances are provided to make sure that no brittle failure mechanisms occur, such as tensile splitting of the timber.

Spacing and edge/end distances	Angle to grain	Minimum spacings and egde/end distances
a_1 (parallel to grain)	$0° \leq \alpha \leq 360°$	$(1,2 + 0,8\lvert \cos \alpha \rvert)d_c$
a_2 (perpendicular to grain)	$0° \leq \alpha \leq 360°$	$1,2d_c$
$a_{3,t}$ (loaded end)	$-90° \leq \alpha \leq 90°$	$1,5d_c$
$a_{3,c}$ (unloaded end)	$90° \leq \alpha \leq 150°$ $150° \leq \alpha \leq 210°$ $210° \leq \alpha \leq 270°$	$(0,4 + 1,6\lvert \sin \alpha \rvert)d_c$ $1,2d_c$ $(0,4 + 1,6\lvert \sin \alpha \rvert)d_c$
$a_{4,t}$ (loaded end)	$0° \leq \alpha \leq 180°$	$(0,6 + 0,2\lvert \sin \alpha \rvert)d_c$
$a_{4,c}$ (unloaded end)	$180° \leq \alpha \leq 360°$	$0,6d_c$

Table 5.3: Minimum requirement for the edge distance, end distance and spacing of shear plate connectors (EN 1995-1-2 2004)

The distances given in Table 5.3 are visualised in Figure 5.9:

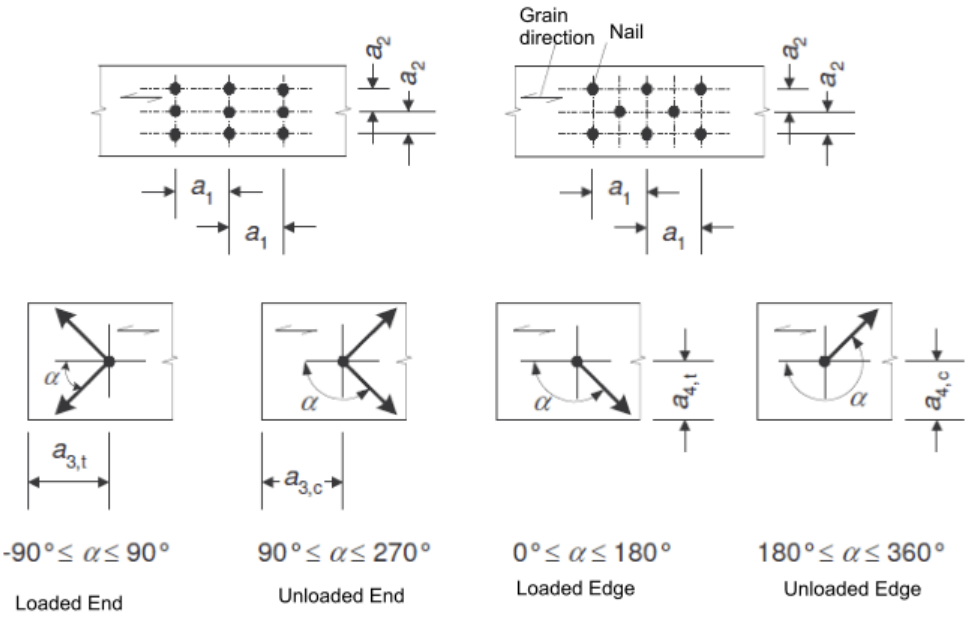

Figure 5.9: Edge distance and spacing

5.4.3. Stiffness of the connection

The stiffness of the connection in SLS is given in the Eurocode. For shear plates, this is given by Equation 5.24.

$$K_{ser} = 2 \cdot \rho_m \cdot \frac{d_c}{4} \tag{5.24}$$

Comparing this to other mechanical fasteners, this is results in a stiff connection considering it is just a dowelled connection. The stiffness in ULS situation is given in a similar way:

$$K_u = \frac{2}{3} \cdot K_{ser} \tag{5.25}$$

6

Drawings of the timber module and connections

In this chapter, all the schematic drawings of the timber module and connections are presented. The dimensions which are presented in this chapter, will be used in the following chapters. In addition, the design choices will be discussed.

6.1. Design choices

During the design of the module and timber-glass shear wall, many design choices were made. The most important decisions were:

- The size of the module was governed by transportation requirements. To reduce transportation costs, the module must be able to be transported by truck. This limited the size of the module to 3 meters in width, 3 meters in height, and 10 meters in length.
- The ratio between the width and thickness of the adhesive is limited by the ETAG 002. This guideline states that this should be lower than a 3:1 ratio to ensure a hinged connection for the glass in case of in-plane loads. For this design a width and thickness of respectively 50 mm to 6 mm are chosen. This is larger than the prescribed 3:1 ratio. However Descamps et al. 2017 concludes that using a larger thickness-to-width ratio leads to acceptable errors in the range of a few percent.
- The TGSW does not cover the entire front of the module because of the space required to install the vertical plate connection. This can be seen on the bottom right of Figure 6.5.
- Inside the module a traditional window is installed. This window has multiple purposes. The first one is that the TGSW does not provide any insulation, therefore a traditional double-glazing system is installed inside the module. Another reason is that this extra window is an extra layer of protection for the TGSW. The final reason is that the cavity between the TGSW and the traditional window could be filled with fire-protective foam in case of fire in the module. In this case, the TGSW will not be exposed to the fire directly but is protected by a layer of foam.

6.2. 3D renders of the modular building, timber module, and connections

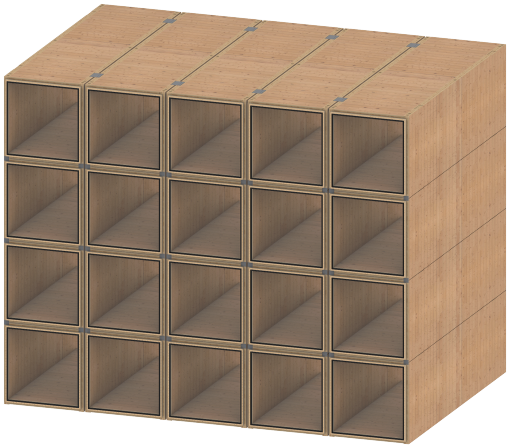

Figure 6.1: 4 x 5 modules modular building

Figure 6.2: Timber module

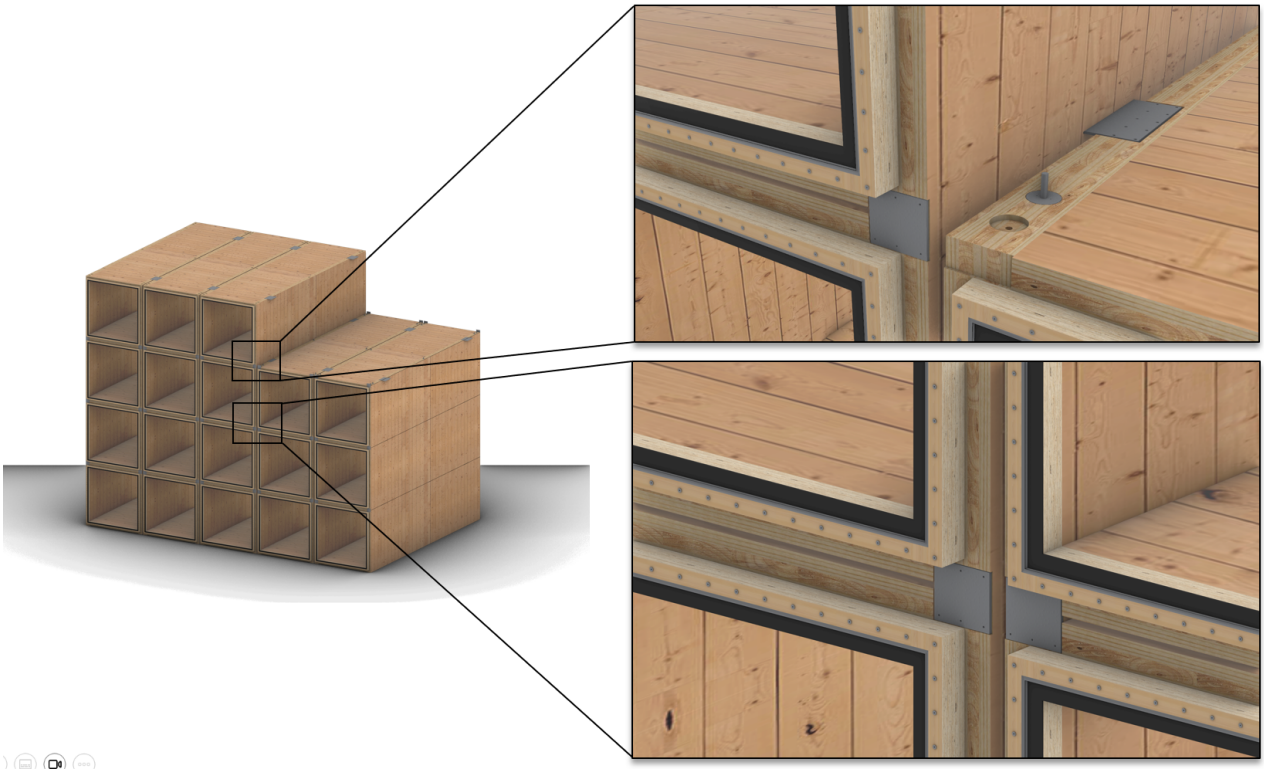

Figure 6.3: Location of the inter-modular connections

6.3. Schematic drawings of the modular building, timber module, and connections

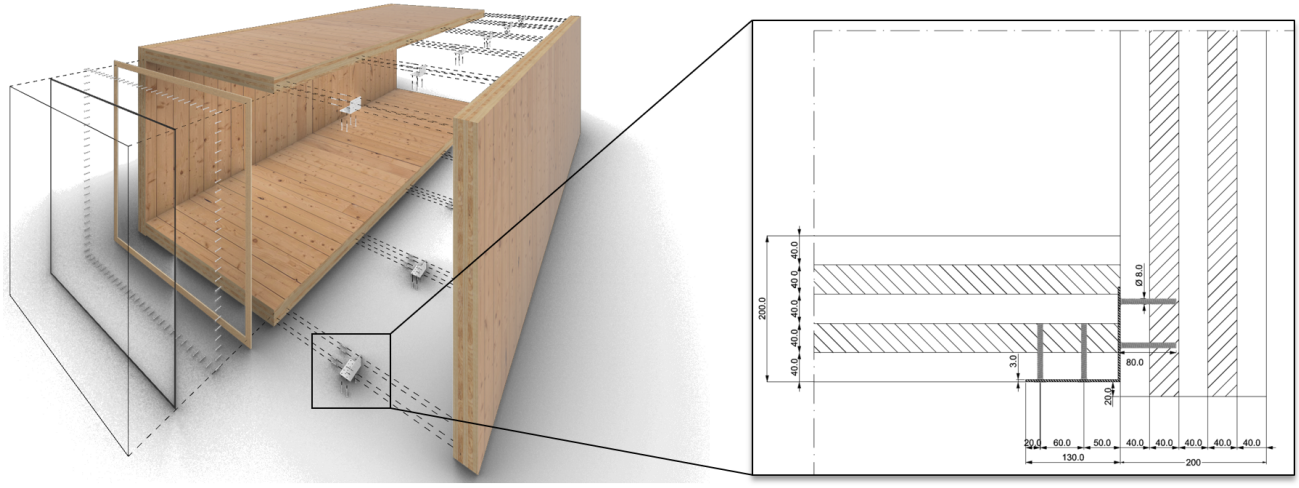

Figure 6.4: Exploded view of the timber modules and steel bracket detail

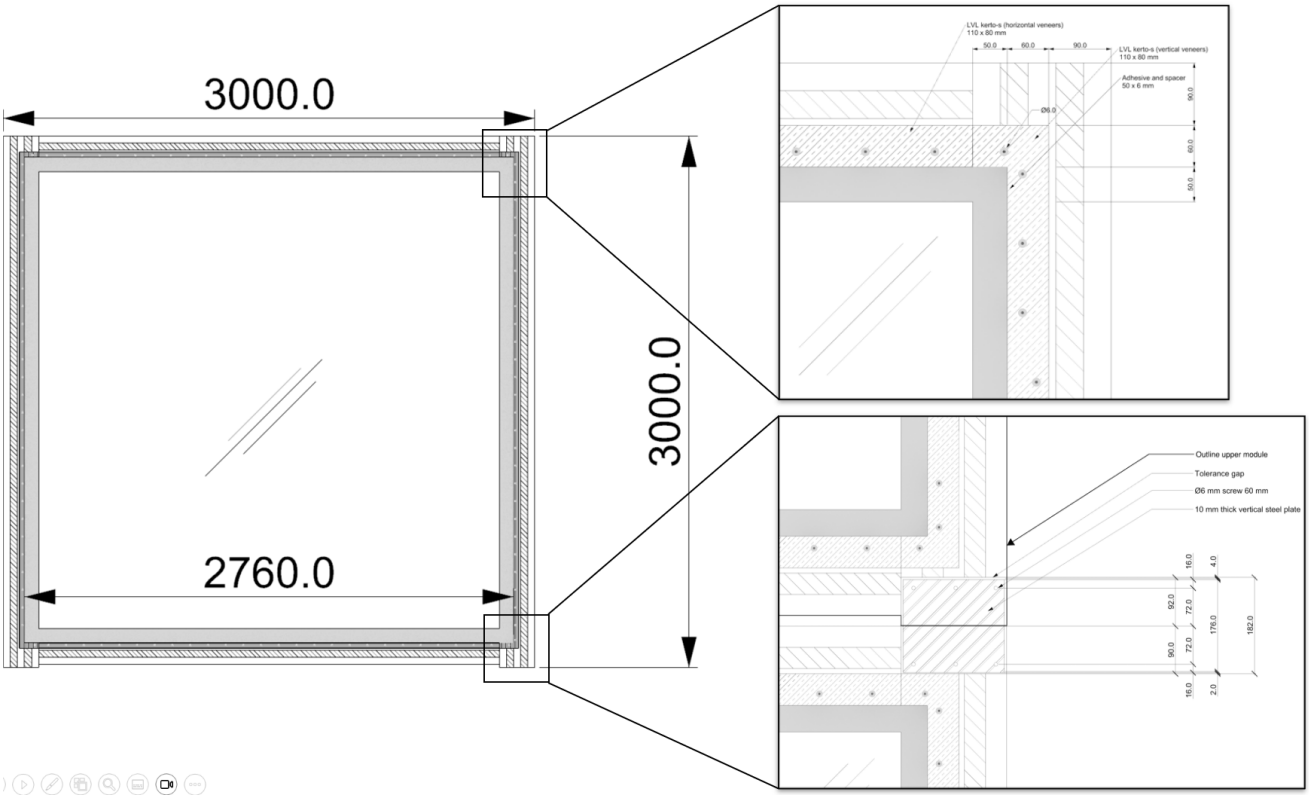

Figure 6.5: Dimensions of the module and top and bottom corner detail

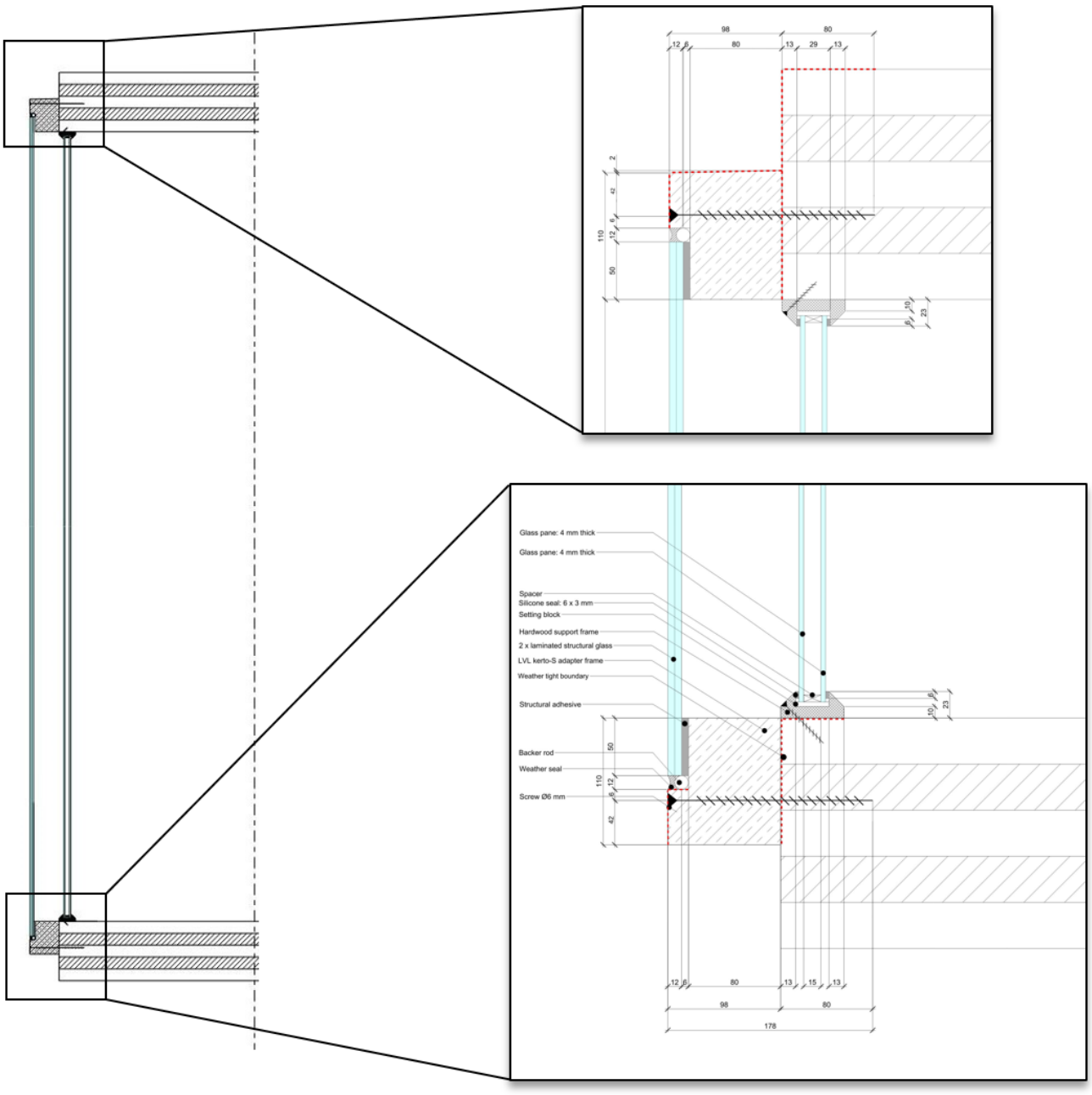

Figure 6.6: Section of timber module with top and bottom detail of the TGSW

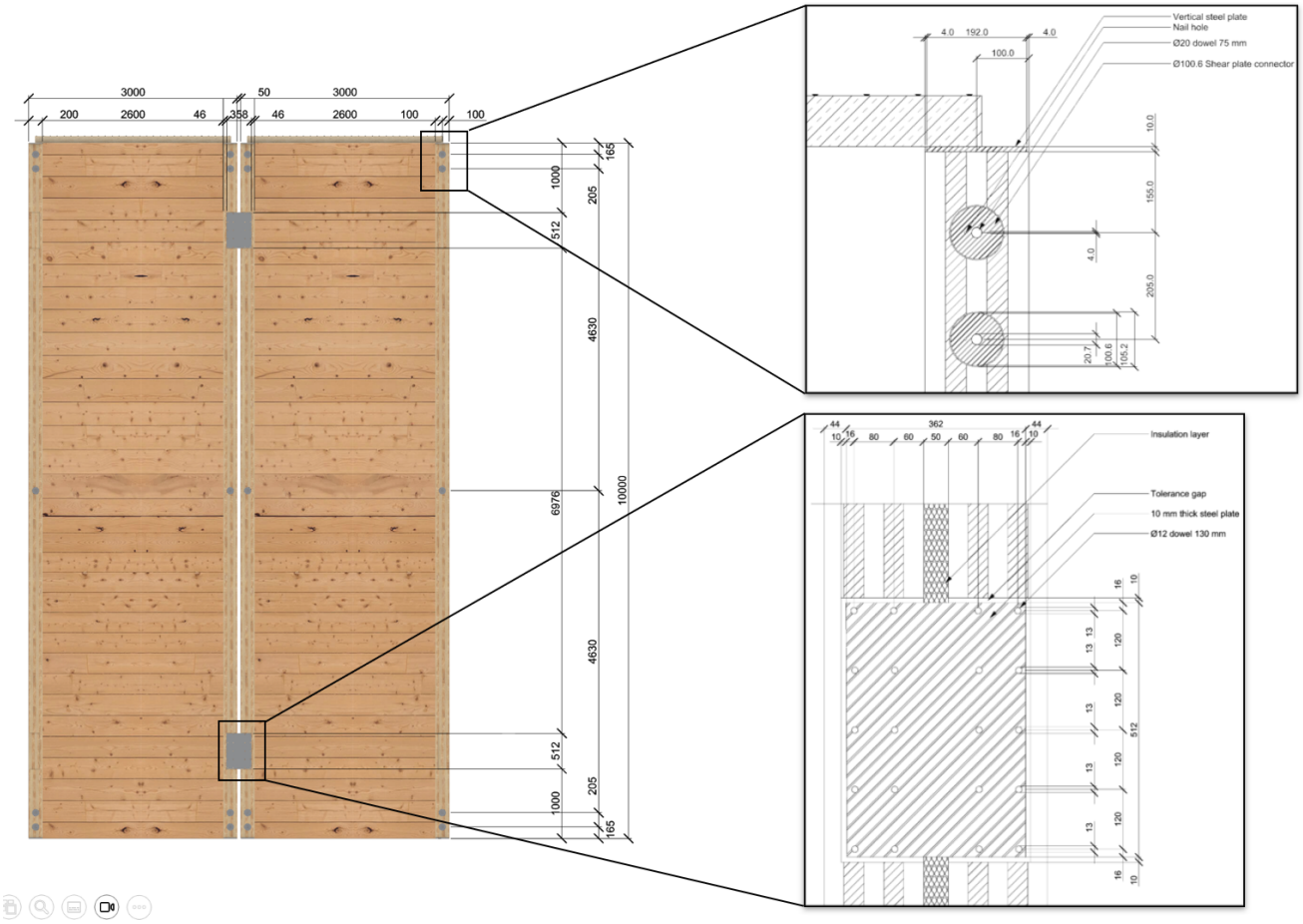

Figure 6.7: Locations of the steel plates and shear plate connectors with details

7

Parameter analysis of the TGSW

In this chapter, the in-plane stiffness and load-bearing capacity of the TGSW are calculated for the design presented in Chapter 6. In relation to these calculations, two specific parameters are varied. These parameters are the shear modulus of the adhesive and the spacing of the screws. These two parameters are the most flexible parts of the TGSW and therefore changing these parameters is expected to have the greatest influence. At the end of this chapter, the following research question is answered:

How can the result of the Hochhauser spring model be used to calculate and improve the in-plane stiffness and load-bearing capacity of the timber-glass shear wall within the module requirements?

7.1. Parameter analysis of the stiffness of the TGSW

The module design presented in Chapter 6 is used as guide for the term 'module requirements' presented in the research question. This means that the sizes and dimensions of the TGSW are kept constant. Only the shear modulus and the spacing of the screws are varied during the stiffness and load-bearing capacity calculations of the TGSW. The properties of each component of the TGSW are presented in Table 7.1.

Adhesive	LVL frame	Glass pane	CLT C30	Screw
$t_{adhesive}$ = 6 mm	t_{frame} = 80 mm	h_{glass} = 2760 mm	w_{timber} = 200 mm	d_{screw} = 6 mm
$w_{adhesive}$ = 50 mm	w_{frame} = 110 mm	l_{glass} = 2760 mm	t_{timber} = 80 mm	s_{screw} = **100** mm
$G_{adhesive}$ = **10** N/mm^2	G_{frame} = 270 N/mm^2	t_{glass} = 12 mm	G_{timber} = 750 N/mm^2	l_{screw} = 160 mm
	ρ_{frame} = 510 kg/m^3	G_{glass} = 28455 N/mm^2	ρ_{timber} = 460 kg/m^3	

Table 7.1: Properties TGSW

For a start, two example numbers are underlined and given in bold for the shear modulus of the adhesive and the spacing to give an indication of the calculation. For these properties, the stiffness of the TGSW can be calculated with Equation 3.14 till Equation 3.19. These equations give the stiffness of each component and combine the stiffness in series. With Equation 3.19 K_{shear} is calculated based on C_{total}. The result is presented in Table 7.2.

Component	G [N/mm^2]	w [mm]	t [mm]	$C_{equivalent}$ [N/mm^2]
Substructure	750	200	80	1875
Screws	d_{screw} = 6 mm	s_{screw} = 100 mm		27,81
Frame	270	110	80	371,25
Adhesive	10	50	6	83,3
Glass pane	28455	2276 x 2276	12	494,87
C_{total}				18,79
K_{shear}				17290

Table 7.2: Stiffness of the TGSW with properties presented in Table 7.1

7.1.1. Shear modulus of the adhesive

The adhesive is a crucial element of the TGSW as this part transfers all shear forces from the LVL-frame to the glass pane. As the thickness and width of the adhesive are kept constant, the shear modulus of the adhesive is the only parameter that can be varied to influence the stiffness of the TGSW. Again, the different adhesives characterising the three types of adhesives are examined. Again, Equation 3.14 till Equation 3.19 are used to calculate K_{shear} for each adhesive. The outcome is presented in Table 7.3.

Type	Adhesive	G [N/mm^2]	Stiffness TGSW [N/mm]
Silicone	OTTOCOLL S660	1	5706
	Sikasil SG-20	0,33	2272
	Sikasil SG500	1,09	6081
Semi-elastic adhesive	Nolax C44.8505	6,4	15343
	Sikafast 5215	27	20152
	Delo-PUR 9895	35	20610
	Araldite 2029	146	21888
Epoxy	Scothc-Weld DP490	504	22197
	Delo-DUOPAX AD840	594	22216

Table 7.3: Stiffness TGSW per adhesive

For these specific adhesives, a system stiffness is presented. This can also be done in a more general way. The shear stiffness of the adhesive is varied from 0,1 N/mm^2 up to 1000 N/mm^2. The result is presented in Figure 7.1:

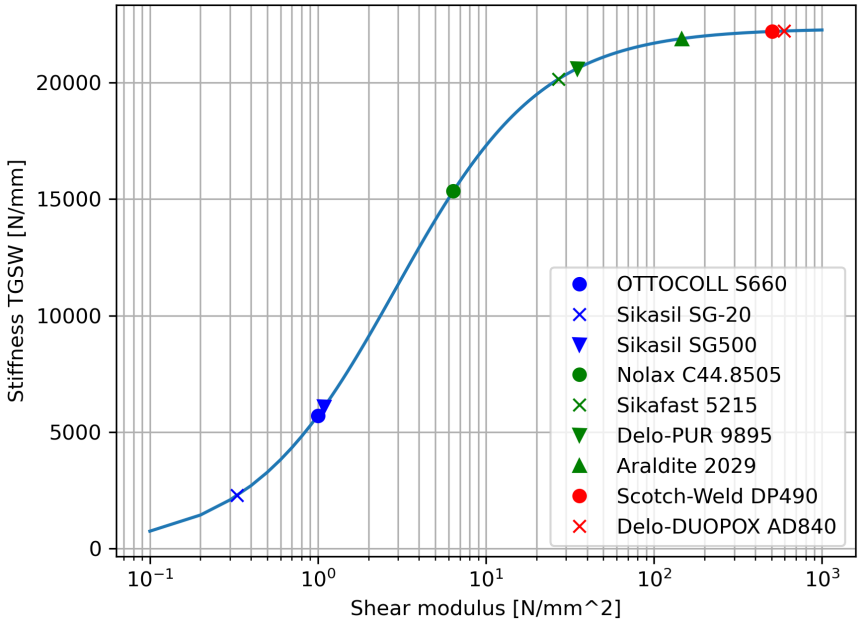

Figure 7.1: Stiffness vs shear modulus

The main takeaways from this graph include:

- Within these module requirements, the stiffness of the TGSW ranges from approximately 2000 N/mm to 22500 N/mm.
- The lower boundary is governed by the shear modulus of the adhesives as this typically does not go lower than 0.1 N/mm^2 for structural adhesives. In theory, this graph would coincide with the origin of the graph. However, this scenario would also give no load-bearing capacity and therefore the realistic limit of 0.1 N/mm^2 is used.
- The upper boundary is governed by the stiffness of the other components in the TGSW. The stiffness of the TGSW is determined by the individual stiffness in series. Therefore, increasing the shear stiffness to infinity would not result in an infinite stiffness of the TGSW, but simply exclude the influence of the stiffness of the adhesive.
- The slope of the curve is steepest from approximately 1 to 10 N/mm^2 meaning a change within this range would have the highest impact on the stiffness of the TGSW. This suggests that elastic or semi-elastic adhesives that are within this stiffness range, offer greater design flexibility. A small change within this range has a relatively high impact on the total stiffness of the TGSW. On the contrary, swapping a stiff semi-elestic adhesives with an epoxy would result in a negligible increase in the stiffness of the TGSW.

Ultimately, the stiffness of the TGSW is closely related to the displacement of the module, consequently affecting the overall displacement of the building.

7.1.2. Screw dimensions and spacing

The connection between the module and the TGSW is made with simple screws. However, the screws greatly influence the stiffness of the entire TGSW. Essential for the connection is that this doesn't limit the load-bearing capacity of the wall. Within this requirement, there is still a lot of freedom in the combination of screw size and spacing. The penetration length of the screw has no relation with the stiffness of the TGSW and is therefore not considered. This design configuration limits the maximum screw diameter to 6 mm due to requirements imposed by the end distances for screws. However, if the thickness of the adhesive or the wall of the module is increased, thicker screws could optionally be used. For a screw diameter of 6 mm different spacings are plotted. It should be noted that the spacing

is also inherent to the number of screws used and thus the shear capacity of the TGSW. This means that the maximum spacing is determined by the shear force that is transferred through the screws. The minimum spacing is prescribed by the Eurocode and states a distance of $5d = 30mm$.

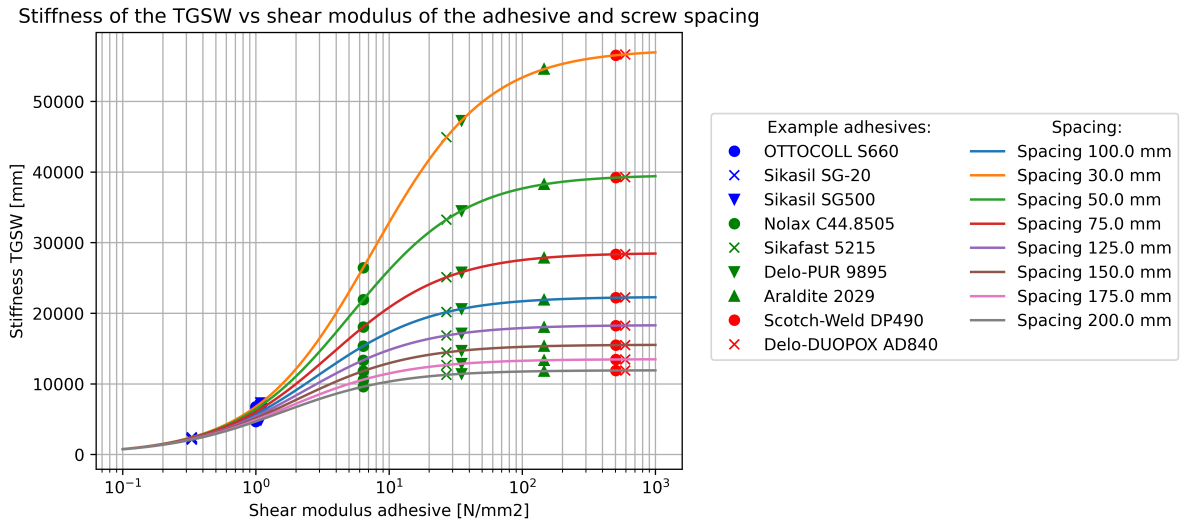

Figure 7.2: Stiffness vs screw spacing and shear modulus

The difference in stiffness between the different spacings per adhesive type indicate the importance of the stiffness of the screws on the total stiffness of the TGSW. For the stiffer adhesives this difference is clearly visible, but for the more ductile adhesives this isn't. Therefore Table 7.4 is given which present the upper and lower boundary stiffness per adhesive.

	Sikasil SG20	OTTOCOLL S660	Sikasil SG500	Nolax C44.8505	Sikafast 5215	Delo-PUR 9895	Araldite 2029	Scotch-Weld DP490	Delo-DUOPOX AD840
30 mm	2423	6762	7294	26447	44921	47265	54573	56531	56657
200 mm	2087	4666	4912	9591	11272	11414	11796	11885	11890
Difference [N/mm^2]	336	2096	2382	16856	33649	35851	42777	44646	44767
Difference [%]	14	31	39	64	75	76	78	79	79

Table 7.4: Difference in stiffness between a screw spacing of 200 mm and 30mm per adhesive

The main takeaways from this graph and table are:

- Changing the screw spacing from the lower boundary of 200 mm to 30 mm has significant effect on the stiffness of the TGSW for stiffer adhesives e.g. stiff semi-elastic adhesives and epoxy's. Increasing the screw spacing can result in 5 times more stiffer TGSW comparing the at the upper and lower boundary.
- This effect is almost neglectable when considering the most ductile adhesives such as Sikasil SG20. This can be explained by the fact that the stiffness of the screws should be in a similar range as that of the adhesive in order to notice an effect. If the adhesive becomes less stiff than the screws, any changes in the stiffness of the screws will have a negligible impact on the overall stiffness of the TGSW. Therefore increasing the screw spacing will have less effect for the elastic adhesives.

7.2. Parameter analysis on the strength of the TGSW

In this section the relation between the strength of the TGSW and the stiffness of the adhesive is investigated. Furthermore, the maximum horizontal force is determined per component. The weakest component determines the strength of the TGSW.

7.2.1. Adhesive strength

The stress concentration in each adhesive is modelled with the Volkersen theory as explained in Chapter 3. Shear force τ_{xy} acts parallel to the glass edge and therefore the bondlength is considered equal to the length of the glass pane. The shear force τ_{xy} also acts parallel to the grain orientation of the LVL-frame, thus the E-modulus of LVL parallel to the grain is used. Shear force τ_x acts perpendicular to the glass edge, and varies over the length of the glass panel edge. The second direction in which the Volkersen theory is applied is in x-direction over a much smaller bond length. It is applied to the maximum value of τ_x at the edge of the glass pane. τ_x acts perpendicular to the grain direction of the LVL-frame and therefore the much lower E-modulus of LVL perpendicular to the grain is used. Due to shear forces acting in two directions, stress concentrations also occur in two directions. The magnitude of the stress concentrations is different for these directions as the stiffness of the LVL and bondlength are different for both directions (see Table 7.5). The two directions are visualised in Figure 7.3

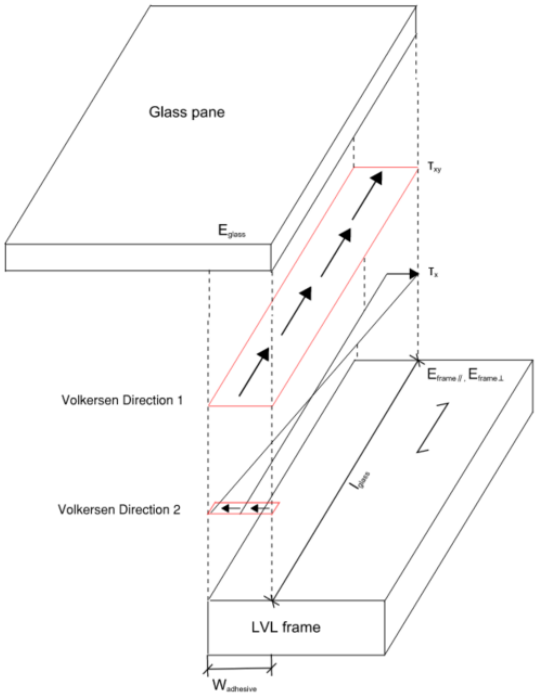

Figure 7.3: Volkersen properties

Variable	Direction 1	Direction 2
$E_{glass}[N/mm^2]$	70.000	70.000
$t_{glass}[mm]$	12	12
$G_{adhesive}[N/mm^2]$	Varies	Varies
$t_{adhesive}[mm]$	6	6
$E_{frame}[N/mm^2]$	11600	350
$t_{frame}[mm]$	80	80
$l_{adhesive}[mm]$	2760	50

Table 7.5: Input values for direction 1 and 2 for the Volkersen model

The most ductile adhesives show the lowest concentration of stresses along the bondline. This is shown in Figure 7.4 and Figure 7.5.

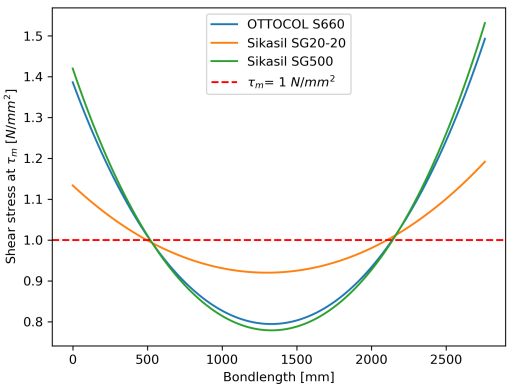

Figure 7.4: Stress concentration Silicones: Direction 1

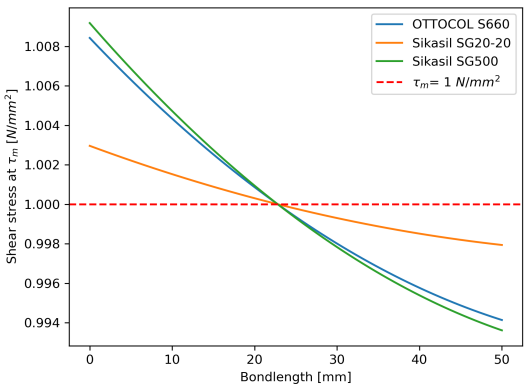

Figure 7.5: Stress concentration Silicones: Direction 2

Adhesive		$K_{stress,1}$	$K_{stress,2}$
Ottocol S660	x=0	1,39	1,008
	x=l	1,49	0,994
Sikasil SG20-20	x=0	1,13	1,003
	x=l	1,19	0,998
Sikasil SG500	x=0	1,42	1,009
	x=l	1,53	0,993

Table 7.6: K_{stress} for silicones

The semi-elastics show average stress concentrations:

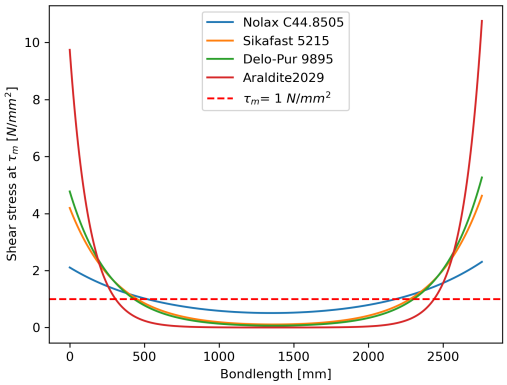

Figure 7.6: Stress concentration semi-elastics: Direction 1

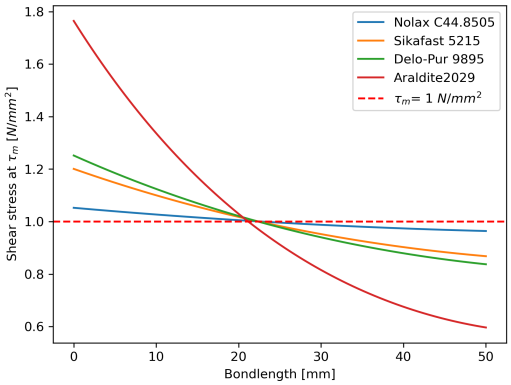

Figure 7.7: Stress concentration semi-elastics: Direction 2

Adhesive		$K_{stress,1}$	$K_{stress,2}$
Nolax C44.8505	x=0	2,91	1,05
	x=l	3,19	0,96
Sikafast 5215	x=0	5,93	1,20
	x=l	6,54	0,87
Delo-Pur 9895	x=0	6,74	1,25
	x=l	7,45	0,84
Araldite2029	x=0	13,78	1,76
	x=l	15,22	0,60

Table 7.7: K_{stress} for semi-elastic

The epoxies show the highest stress concentrations:

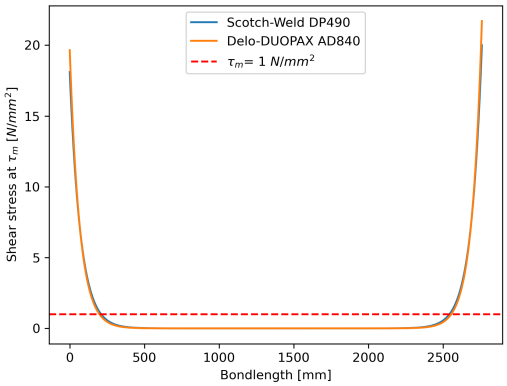

Figure 7.8: Stress concentration epoxy's: Direction 1

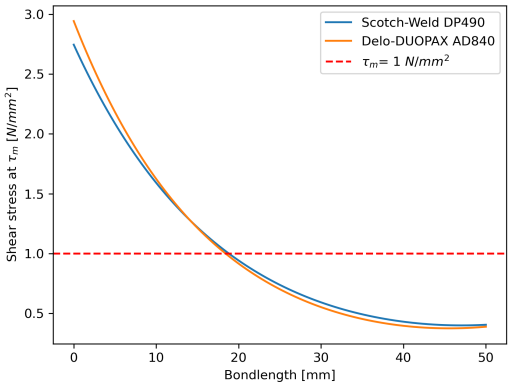

Figure 7.9: Stress concentration epoxy's: Direction 2

Adhesive		$K_{stress,1}$	$K_{stress,2}$
Scotch-Weld DP490	x=0	25,60	2,75
	x=l	28,28	0,40
Delo-DUOPAX AD840	x=0	27,79	2,94
	x=l	30,70	0,39

Table 7.8: K_{stress} for epoxy

If the maximum shear stress of the adhesive is reached somewhere in the bondline, the TGSW will fail. Therefore, the maximum K_{stress} factor per adhesive is applied as a reduction factor to the shear strength of the adhesive. The shear strength τ_{max} per adhesive was presented in Chapter 3 in Table 3.1. τ_{max} represents the maximum allowable stress in the adhesive and is deduced from the product data sheets and research articles. As the shear forces act in two directions (see Figure 3.16), and both have different reduction factors, some rewriting is required. τ_{xy} represents the shear stress parallel to the bondline (Volkersen direction 1), and τ_x represents the shear stress perpendicular to the bondline (Volkersen direction 2). In general, two perpendicular shear forces can be added by vector addition, and the result should be equal to or lower than the maximum allowable shear stress of the adhesive τ_{max}:

$$\tau_{max} = \sqrt{\tau_{xy}^2 + \tau_y^2} \tag{7.1}$$

As the maximum shear stress cannot be reached anywhere in the bondline, the peak stress factors are added to the equation:

$$\tau_{max} = \sqrt{(\tau_{xy} \cdot K_{stress,1})^2 + (\tau_y \cdot K_{stress,2})^2} \tag{7.2}$$

For rectangular glass panes, it holds that $\tau_{xy} = \tau_y$, which allows for a relation between τ_{max} and τ_{xy}. For other than 1:1 glass ratio's a different relation between τ_{xy} and τ_y can be derived. The relation between τ_{max} and τ_{xy} is:

$$\tau_{xy} = \tau_y = \sqrt{\frac{\tau_{max}^2}{K_{stress,1}^2 + K_{stress,2}^2}} = \tau_{max} \cdot \sqrt{\frac{1}{K_{stress,1}^2 + K_{stress,2}^2}} = \tau_{max} \cdot K_{total} \tag{7.3}$$

After applying the peak stress factors to either τ_{max} or $\tau_{elastic}$, a maximum shear force is introduced that includes stress concentrations, called τ_{peak}. This value is used to calculate the maximum horizontal force. The result is presented in the following table:

Type	Adhesive	E $[N/mm^2]$	G $[N/mm^2]$	$\tau_{max}[N/mm^2]$	$\tau_{elastic}[N/mm^2]$	$K_{total}[-]$	$\tau_{peak}[N/mm^2]$
A	OTTOCOLL S660	3	1	0,87	-	1,80	0,48
A	Sikasil SG-20	1	0,33	0,93	-	1,55	0,59
A	Sikasil SG500	3,17	1,09	0,8	-	1,83	0,44
B	Nolax C44.8505	18	6,4	5,2	1,8	3,36	0,54
B	Sikafast 5215	78	27	3,4	2,3	6,65	0,35
B	Delo-PUR 9895	100	35	5,1	-		-
B	Araldite 2029	414	146	0,9	-		-
C	Scotch-Weld DP490	1442	504	11,9	-	28,41	0,41
C	Delo-DUOPOX AD840	1700	594	7,9	-	30,84	0,26

Table 7.9: Shear strength properties adhesive

The relation between the maximum horizontal force on the timber glass shear wall and the shear stress τ_{xy} and τ_y was presented in Chapter 3 in Figure 3.16.

After combining Equation 7.3 with Equation 3.20 and rewriting, the following equation can be used to determine the maximum horizontal force per adhesive:

$$F_h = \frac{(1 + \frac{K_1}{K_2}\frac{L}{3H}) \cdot L \cdot w_{adhesive} \cdot \tau_{peak}}{\gamma_{tot}} = \frac{(1 + 1\frac{2760}{3 \cdot 2760}) \cdot 2760 \cdot 50 \cdot \tau_{peak}}{6} \tag{7.4}$$

The result for F_h per adhesive is shown:

Type	Adhesive	F_h [kN]
Silicone	OTTOCOLL S660	14,72
	Sikasil SG-20	18,09
	Sikasil SG500	13,49
Semi-elastic adhesive	Nolax C44.8505	16,56
	Sikafast 5215	10,73
	Araldite 2029	-
Epoxy	Scothc-Weld DP490	12,57
	Delo-DUOPAX AD840	7,97

Table 7.10: Maximum horizontal force per adhesive

The main takeaways from this section are:

- Epoxy's have the highest strength and stiffness of the three types of adhesives.
- After including the effect of stress concentrations in the adhesive bond, the more flexible adhesives have a better performance. The main reason is that as the stiffness of an adhesive increases, it leads to higher levels of stress concentration within the adhesive bond, thus reducing the performance of the adhesive.

Thermal expension glass

As the glass is circumferentially bonded to the timber frame, thermal expansion will lead to thermal stresses. It is assumed that the thermal expansion is accommodated for by the adhesive. In NVN-CEN/TS 19100-1 n.d. it is stated that stresses within the glass due to temperature difference should be verified neglecting all other variable actions. Therefore, these stresses are not considered in combination with other loads but as a separate case. The expansion of the glass is given by the following Equation:

$$\delta_L = \delta_T \cdot \alpha_t \cdot L \tag{7.5}$$

With:
$\delta_T = 80°\text{C} - 20°\text{C} = 60°\text{C}$
$\alpha_t = 9 \cdot 10^{-6} K^{-1}$
$L = 2760mm$

This results in an expansion of the glass pane of 1,44 mm in both the length and the width. The adhesive should therefore expand $\delta_L = \frac{1{,}44 \cdot \sqrt{2}}{2} = 1,02mm$. Depending on the type of adhesive, this results in a thermal stress in the 6 mm thick adhesive. The thermal stress is shown in Table 7.11

$$\tau_t = G \cdot \gamma = G \cdot \frac{\delta_L}{t_{adhesive}} \tag{7.6}$$

Type	Adhesive	τ_t $[N/mm^2]$
Silicone	OTTOCOLL S660	0,17
	Sikasil SG-20	0,06
	Sikasil SG500	0,19
Semi-elastic adhesive	Nolax C44.8505	1,09
	Sikafast 5215	4,60
	Delo-PUR 9895	5,95
	Araldite 2029	24,82
Epoxy	Scothc-Weld DP490	85,68
	Delo-DUOPAX AD840	100,98

Table 7.11: Thermal stresses per adhesive

It can be seen that the epoxies should cope with much higher thermal expansion stresses compared to the thermal stresses for the silicones. It should be noted that it is assumed that the adhesives should accommodate all the expansion. In reality, the other components will also deform slightly, resulting in lower thermal stresses in the stiffer adhesives.

7.2.2. Glas panel strength and buckling

Glass panel strength, first order

In order to verify the stresses in the glass a small FEM model is made. In this case the spring model is converted to a FEM model, with rigid edge beams. The glass panel is modelled as surface element and connected to the edge with line releases. The stiffness of the line release in both x- and y-direction represents a continuous spring connection. Next to the horizontal force exerted on the top of the frame, a surface load is exerted on the glass panel. This represents the wind-load directly to the glass panel. The calculation and loadcase is specified in Chapter 8, nevertheless the outcome is already used here:

$$q_{wind,ULS} = q_{wind} \cdot 1,5 = 0,59 \cdot 1,5 = 0,89kN/m^2 \tag{7.7}$$

The maximum tensile stress in the glass pane is calculated according to NVN-CEN/TS 19100-1 n.d. The maximum compressive stress in the glass is not relevant as this is much higher than the maximum tensile stress.

$$f_{g,d} = \frac{f_{g,k}}{\gamma_M} \cdot k_e \cdot k_{sp} \cdot k_{mod} \cdot \lambda_A \cdot \lambda_1 = \frac{45}{1,8} = 25N/mm^2 \tag{7.8}$$

With:
$f_{g,k} = 45N/mm^2$ for float glass
$\gamma_m = 1,8$ for CC2
$k_e = 1$ for polished edges
$k_{sp} = 1$ for float glass, as produced
$k_{mod} = 1$ for windloading (3s)
$\lambda_A = 1$ and $\lambda_1 = 1$ for the area of the pane $< 18m^2$

Lastly, the self-weight of the glass panel is included in the FEM analysis. The maximum horizontal force that can be combined with the windload and selfweight is given by the FEM analysis. When the maximum principal tensile stress is equal to $25N/mm^2$, the maximum horizontal force is found. This is at approximately 312 kN. For glass, the principal stresses are the governing stresses for the glass pane. As soon as the maximum tensile strength of the glass is reached in any direction of the glass pane, cracks could begin to form. Therefore, a closer look is taken at the principal stresses for the

three loadcases: the out-of-plane horizontal loading, the in-plane wind load and the combination of both. For convenience, an equal scale is used so that colors corresponds to similar stresses in the glass pane in the FEM results. First, the maximum principal stresses are shown for the horizontal load. The horizontal load is located at the top right corner of the frame, towards the left.

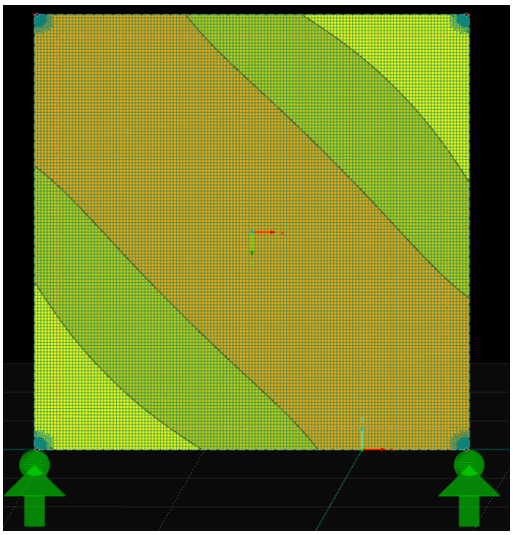

Figure 7.10: Maximum stress glass panel RFEM sigma 1 horizontal load

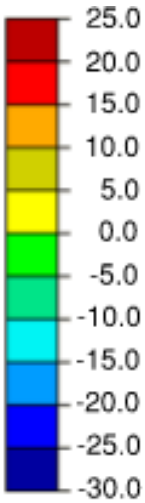

Figure 7.11: Principal stresses scaling

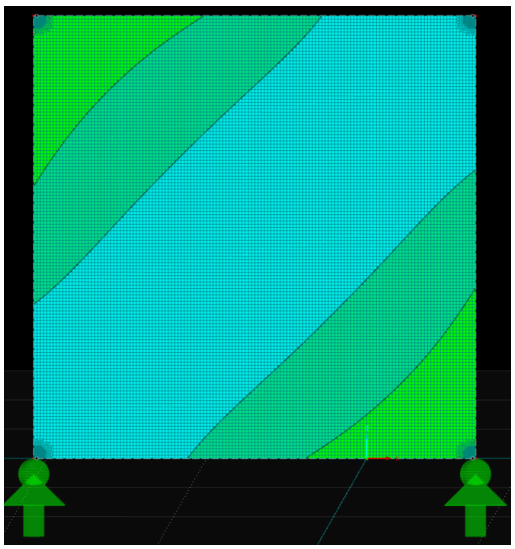

Figure 7.12: Maximum stress glass panel RFEM sigma 2 horizontal load

It can be seen that due to the horizontal loading, a tension diagonal from top left to bottom right is formed. Additionally, a compressive diagonal is formed from top right to bottom left. It can be seen that, regardless of the increase in mesh density, no stress concentration arise in the corners. Due to the elastic connection between the timber and the glass, the force introduction is spread over a greater area, thus limiting the stress concentrations.

The maximum principal stresses σ_1 and $\sigma 2$ for solely the in-plane wind load are shown too:

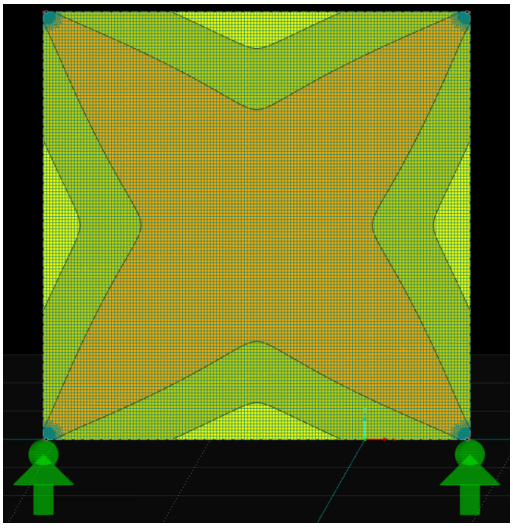

Figure 7.13: Maximum stress glass panel RFEM sigma 1 in-plane windload

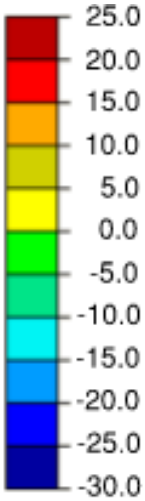

Figure 7.14: Principal stresses scaling

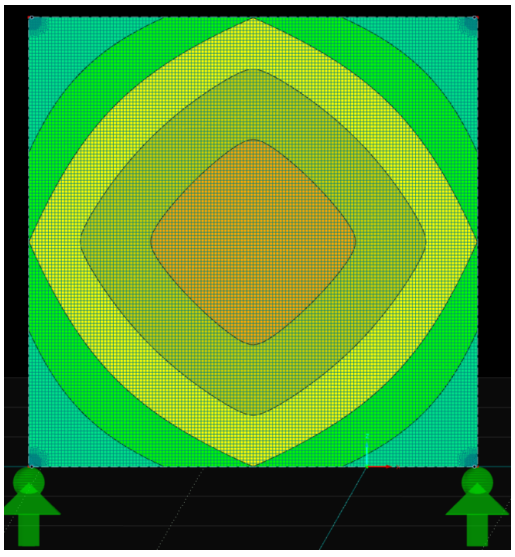

Figure 7.15: Maximum stress glass panel RFEM sigma 2 in-plane windload

The principal stresses due to the horizontal loading and windload combined are shown in Figure 7.13 and Figure 7.15:

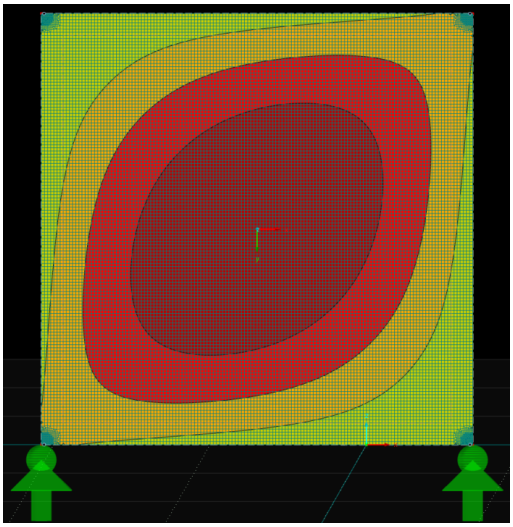

Figure 7.16: Maximum stress glass panel RFEM sigma 1

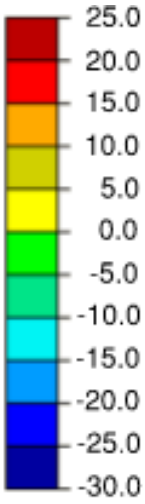

Figure 7.17: Principal stresses scaling

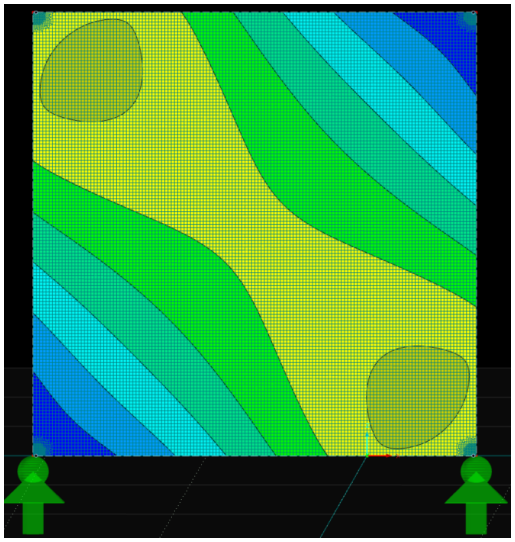

Figure 7.18: Maximum stress glass panel RFEM sigma 2

It can be concluded that the maximum horizontal force F_h is equal to 312 kN. Stress concentrations in the adhesive are not included in this FEM-model. Although, stiffer adhesives induce stress concentrations in the bondline and glass pane, it can be seen that the maximum tensile stress is at the centre of the glass pane. At the edges, where the stress concentrations arise, much lower stresses are observed.

Glass panel strength: second order plus initial bow

The glass pane is of substantial size and can therefore show significant second order effects. Especially with the combination of a horizontal load and an in-plane wind load. In addition, glass panes will never be completely flat, but will have an initial bow. This initial bow is generated with the RF-IMP module in RFEM. According to CEN 19100-3, an imperfection of $\frac{l_0}{333}$ should be used which results in an initial bow of 8,3 mm deflection at the centre. This imperfection is applied in the same direction as the in-plane load resulting in the most unfavourable situation. This is shown in Figure 7.19

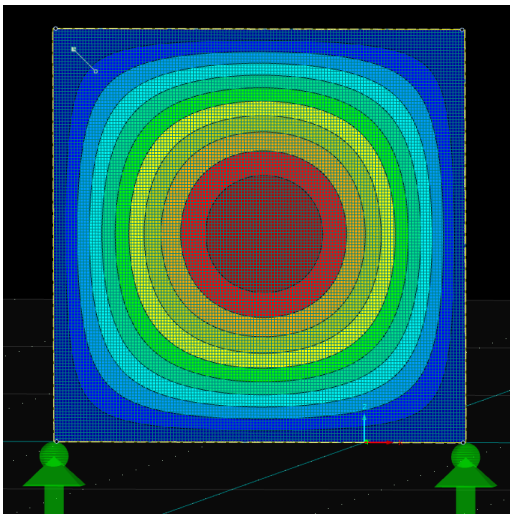

Figure 7.19: Initial imperfections as starting point for the model

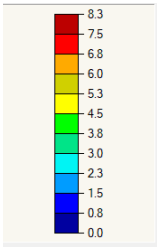

Figure 7.20: Initial imperfections

Again, the same model is calculated, but now also including second-order calculations and the initial deformation from the imperfections. Including both aspects will reduce the maximum capacity of the

glass pane to 189 kN. At this point maximum principal tensile stress is already equal to $25N/mm^2$. The maximum principle stresses are shown at this point.

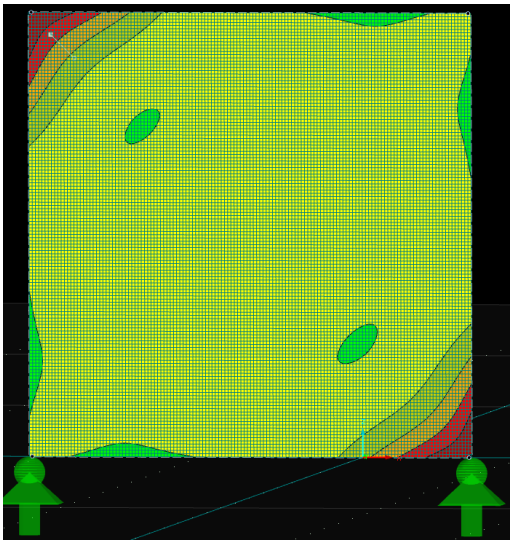

Figure 7.21: Maximum stress glass panel RFEM sigma 1 with second order calculations and initial bow

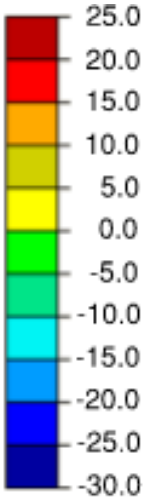

Figure 7.22: Principal stresses scaling

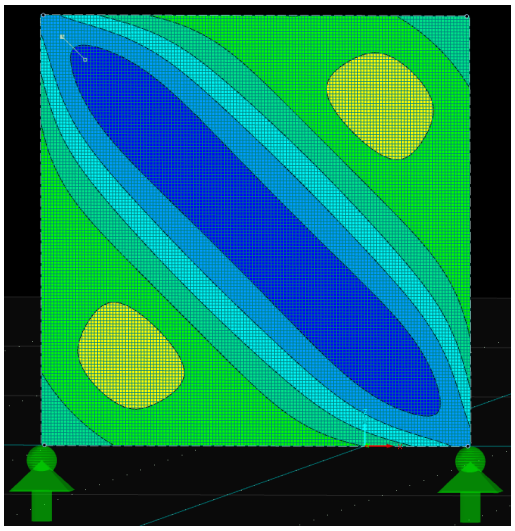

Figure 7.23: Maximum stress glass panel RFEM sigma 2 with second order calculations and initial bow

Finally, also the deflection of the glass is calculated and is 28,2 mm which is within the limit for the SLS load case. The deflection limit at centre for a glass pane continuously supported along all edges is $\frac{L}{50} = 55mm$ (NVN-CEN/TS 19100-1 n.d.). The deflected shape is given below:

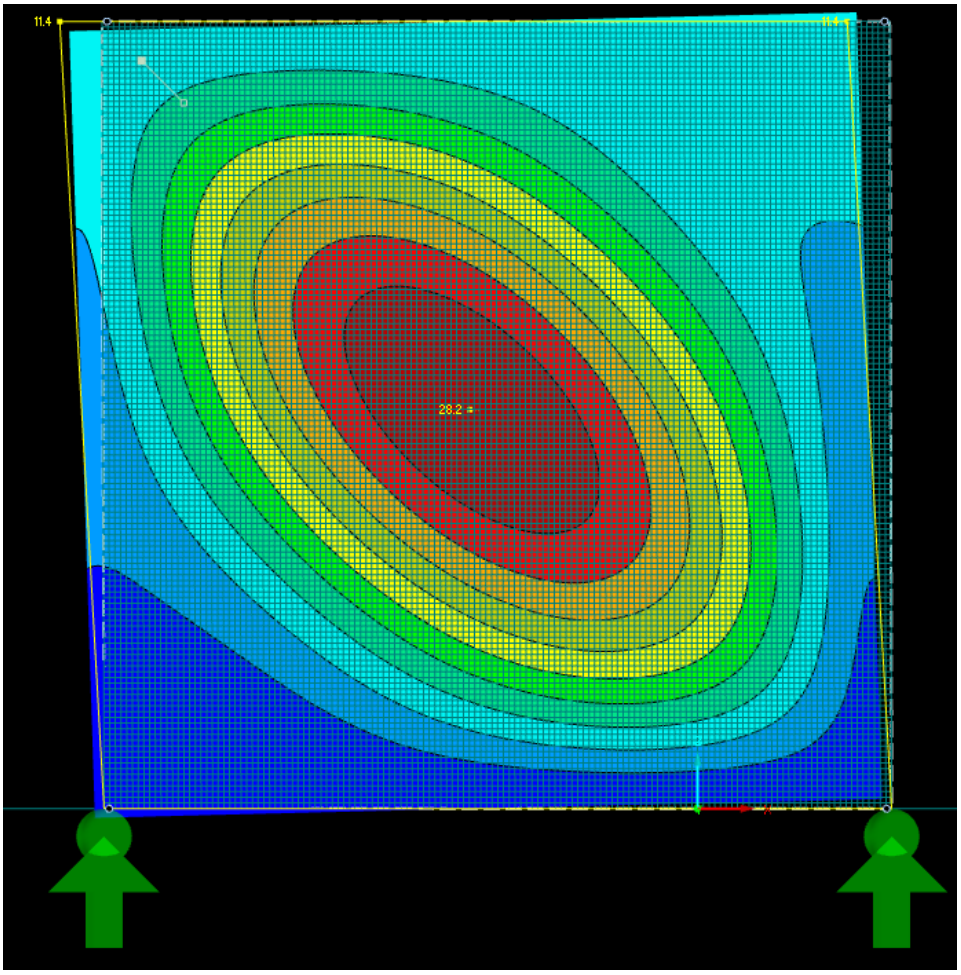

Figure 7.24: Deflected shape 2e order plus initial bow

It can be seen that the compression diagonal from top right to bottom left, is increasing the deflection over the other diagonal. This also explains why at the top left and bottom right corner, peak tensile stresses can be found. The glass is being pushed out by the compressive diagonal formed from top right to bottom left. But, since the frame is continuously supported, the glass should return to zero deflection at the top left corner and bottom right corner. The deflection gradient is relatively high at these points, which also indicates high stresses at the top left corner and bottom right corner.

Glass buckling

In Section 3.4 the equations for the buckling load of a glass pane are given. For safety, only one glass pane is considered instead of the laminated glass. The equations will not be repeated but the intermediate answers will be presented:
$\tau_{cr} = 16,1 N/mm^2$
$\lambda = 1,67$
$\phi = 1,55$
$\chi = 0,41$

$$H = \chi \cdot l \cdot t \cdot \frac{f_{g,k}}{\gamma_m} = 0,41 \cdot 2760 \cdot 12 \cdot \frac{45}{1,8} = 339kN \tag{7.9}$$

Buckling of the glass is not dependent on the stiffness of the adhesive.

7.2.3. Screw strength

The strength of the screws is related to the spacing of the screws. Spacings ranging from 30 mm till 200 mm are examined. The spacing can be increased up to the minimum value of 5 times the diameter

of the screw. In this case, that would be a minimum spacing of 30 mm. The maximum spacing is determined by the required strength. Increasing the spacing, reduces the number of screws and thus the strength of the connection. The available length for screws in the LVL-frame is presented below. The edge distance for screws in LVL is $7d_{screw}$. The screws have a diameter of 6 mm.

$$l = l_{total} - 2 * screw_{edgedistance} = 2820 - 2 \cdot 6 \cdot 7 = 2676mm \tag{7.10}$$

For a spacing of 100 mm it holds:

$$N = 2676/100 \approx 27screws. \tag{7.11}$$

The calculations for the screws are based the stress distribution presented in Figure 3.16. For rectangular glass panes, it holds that the maximum value of τ_{xy} equals the maximum value of τ_y, leading to a reduction factor of $\sqrt{2}$. The corners of the LVL frame represent the locations where these maximum values occur. To factor in stress concentrations within the bondline, peak stress factors were introduced into the adhesive calculation. These stress concentrations also continue to a certain extent in the LVL-frame and to the screws. Nevertheless, it is assumed that the 80 mm thick frame and screws have adequate capacity to redistribute the stress concentrations over the frame. As a result, the stress distribution presented in Figure 3.16 is used for the strength calculations of the screws.

The characteristic strength of one screw is 3043 N which was calculated in Appendix B. The final strength of the screws is:

$$H = \frac{N \cdot F_{v,rk} \cdot k_{def}}{\sqrt{2 \cdot \gamma_m}} = \frac{30 \cdot 3043 \cdot 1,1}{\sqrt{2} \cdot 1,3} = 49,15kN \tag{7.12}$$

This calculation can also be performed for the other spacings, and the results are summarised in Table 7.12

Spacing [mm]	Number of screws	H [kN]
30	90	163,86
50	53	96,50
75	36	65,54
100	27	49,15
125	21	38,23
150	18	32,77
175	15	27,31
200	13	23,67

Table 7.12: Screw strength per spacing

It can be seen that that a screw spacing of 200 mm, the strength of the screws almost become governing, as the strongest adhesive has a strength of 17 kN. Thus, a spacing lower than 200 mm is desirable.

7.2.4. Strength of the LVL adapter frame

The strength of the LVL is related to the shear strength of the LVL as this is much lower compared to the tensile or compressive stress of LVL. The characteristic shear strength parallel to the grain (flatwise) of the LVL Kerto-s frame 2,3 N/mm^2. Again a reduction factor of $\sqrt{2}$ is used for τ_{xy} and τ_y.

$$H = \frac{f_{v,0,flat,k} \cdot l \cdot w_{adhesive}}{\gamma_m \cdot \sqrt{2}} = \frac{2,3 \cdot 2760 \cdot 50}{\sqrt{2} \cdot 1,3} = 172kN \tag{7.13}$$

The characteristic shear strength perpendicular to the grain (flatwise) of the LVL Kerto-s frame 0,6 N/mm^2. Again a reduction factor of $\sqrt{2}$ is used for τ_{xy} and τ_y.

$$H = \frac{f_{v,90,flat,k} \cdot l \cdot w_{adhesive}}{\gamma_m \cdot \sqrt{2}} = \frac{0,6 \cdot 2760 \cdot 50}{\sqrt{2} \cdot 1,3} = 45kN \tag{7.14}$$

The strength of the LVL adapter frame is not dependent on the stiffness of the adhesive.

TGSW strength

The last step is to combine all the strengths of the individual components, and visualise them as function of the TGSW stiffness. The result is shown in Figure 7.25

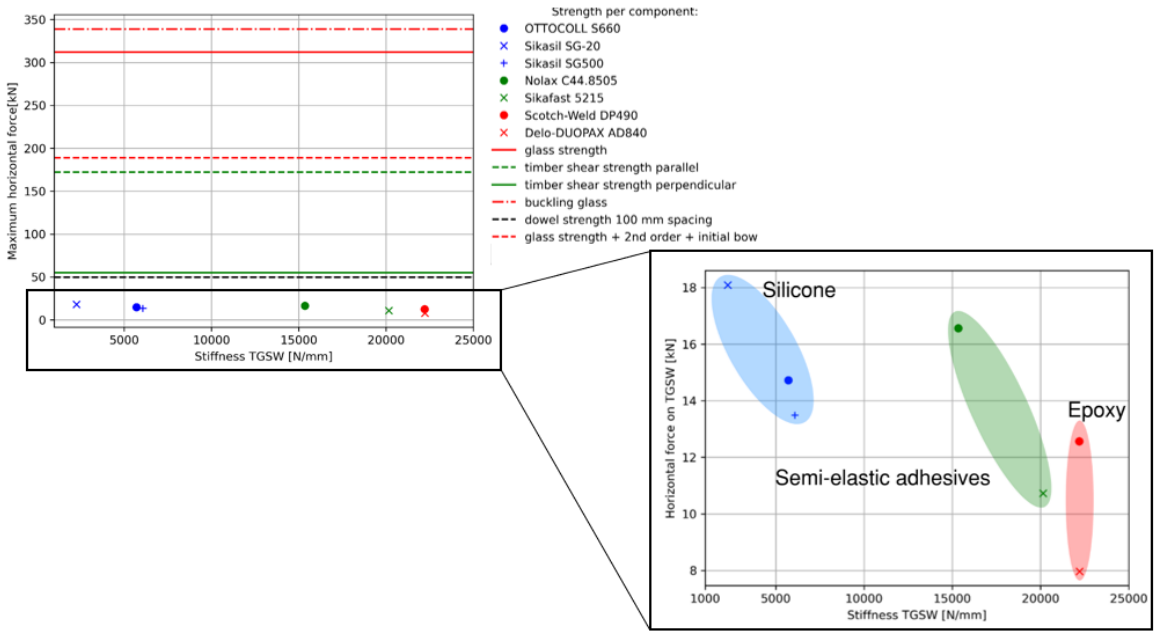

Figure 7.25: Strength TGSW vs stiffness of the TGSW

The main takeaways from this graph are:

- The adhesive is governing for strength of the TGSW design. Depending on the type of adhesive used, a different strength is acquired. Most suitable from this point of view are the elastic adhesives and possibly the most flexible semi-elastics. The epoxy's are not suitable for this purpose.
- Depending on the spacing of the screws, the strength of the screws comes closer to the strength of the adhesives. Especially with better performing adhesives, the screws could become governing for the design. However, this can easily be solved by decreasing the screw spacing. This will make the failure mechanism shift again towards adhesive failure rather than screw failure.

8

Modelling of a timber modular building

In this chapter, the global design of the modular building is assessed. A more extensive Finite Element Model is created to see how the stability elements are loaded across the modular building. The modular buildings have 3 to 6 stories and undergo assessment within a height-to-width ratio, ranging from 1:1 to 1:3. This means that the smallest building consists of 9 modules and the largest of 108 modules. After this chapter, the following research question is answered:
How can the results of a finite element model be used to determine the load-bearing capacity and stiffness of a mid-rise modular timber building, including the strength and stiffness of the inter and intra-modular connections?

8.1. Equivalent diagonal theory

In Chapter 7 the TGSW was modelled with springs. Due to computational limitations, the TGSW is simplified from the spring model (b) to a frame with two diagonals (c) with identical properties. This step is shown in Figure 8.1.

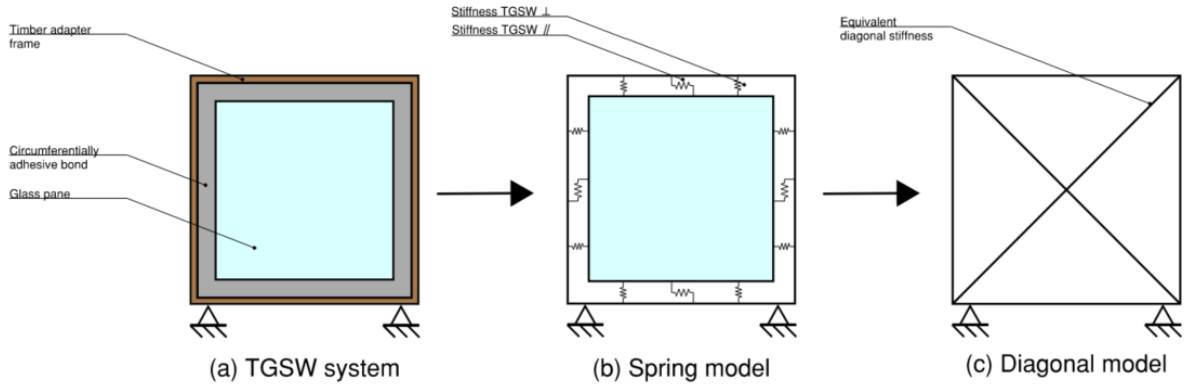

Figure 8.1: Schematic modelling of the TGSW

As a start, the stiffness of the spring model relates the horizontal force acting on the TGSW to the displacement of the TGSW. Similarly, an expression which relates horizontal force of the diagonal model to the displacement of the diagonal model can be found. The goal is to find an expression which relates the stiffness of the spring model to stiffness of the diagonal model. The derivation of this expression is shown below and results in Equation 8.2.

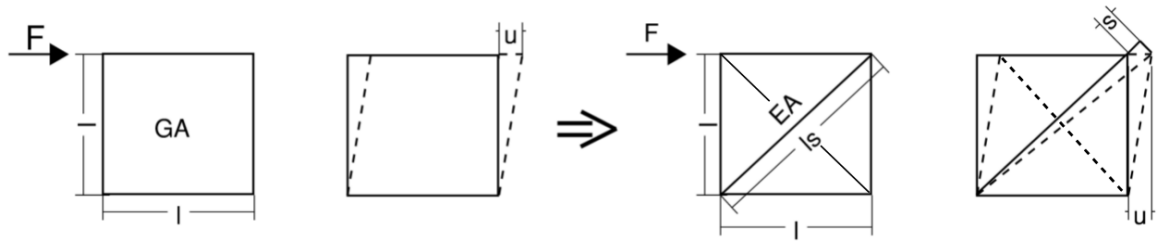

Figure 8.2: Relation stiffness shearwall and diagonal

$$u = \frac{F \cdot l}{GA}$$

$$u = \frac{F}{k}$$

With:

$$k = \frac{GA}{l}$$

$$l_s = \sqrt{2}l$$

$$\frac{s}{l} = \frac{u}{l_s} \rightarrow s = \frac{u}{\sqrt{2}}$$

$$N = \sqrt{2}F$$

$$s = \frac{N \cdot l_s}{EA}$$

$$u = \frac{\sqrt{2}F \cdot \sqrt{2}l \cdot \sqrt{2}}{EA}$$

Equalising the displacement of the shear wall to the displacement of the braced frame results in:

$$\frac{1}{k} = \frac{2\sqrt{2}l}{EA} \tag{8.1}$$

$$k = \frac{EA}{2\sqrt{2} \cdot l} \tag{8.2}$$

With:

$$A = b_{diagonal} \cdot h_{diagonal} \cdot 2 \tag{8.3}$$

Assuming the diagonal is replaced by a square steel profile, the stiffness of the TGSW can be converted into dimensions of the steel square profile. For example, a stiffness of 7 kN/mm of the TGSW results in two steel profiles of 11,89 mm by 11,89 mm which have equivalent stiffness.

8.2. The finite element model of the modular building

In order to assess how a modular building behaves structurally, a FEM-model with steel diagonals is created. This concept is shown in Figure 8.3.

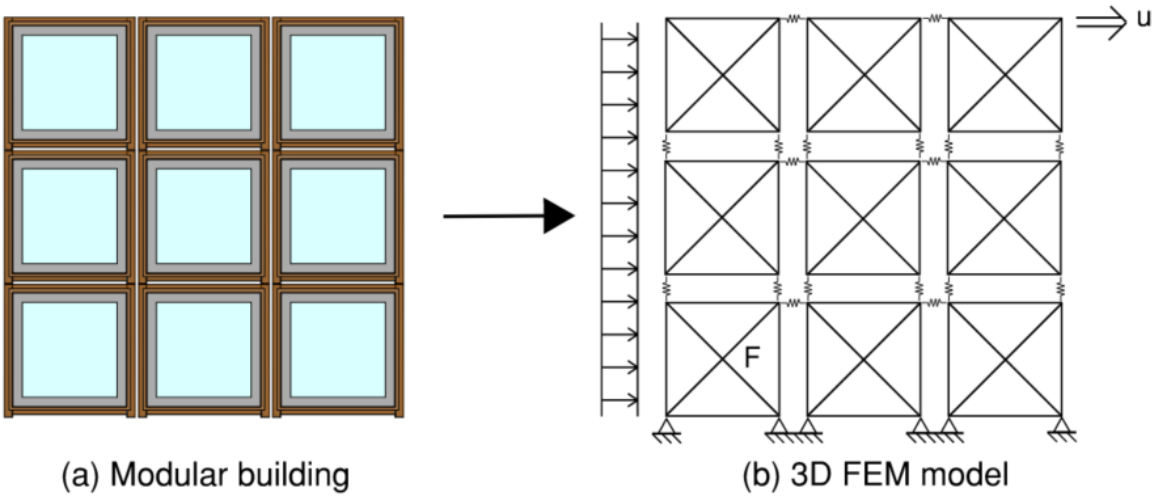

Figure 8.3: Schematic representation of the modular building

The FEM-model has two goals:

- Find out how the windload is distributed across the steel diagonals based on the stiffness of the diagonals. The force in the diagonals represents the force on the TGSW. This force gives the requirement for the strength of the TGSW.
- Exlore the relationship between the stiffness of the steel diagonals and the total displacement of the building. The displacement gives a requirement for the stiffness of the TGSW.

8.2.1. Geometry of the module in RFEM

The finite element model is made in RFEM 5. The walls, ceiling and floor of the module are modelled with surface elements representing the CLT panels. The connection between the walls, ceiling and floor is modelled as line hinge meaning that only a rotational release is applied. As a consequence, the frame itself has zero capacity against lateral loads. In reality, there will be some rotational capacity in the corners, giving some capacity against lateral loading. This is thus a conservative assumption. The diagonals are modelled as truss members (only N) which only have one longitudinal stiffness EA. The diagonals have moment hinges at both ends. The stiffness can be varied according to the stiffness of the TGSW. In Figure 8.4 the model of the module is shown.

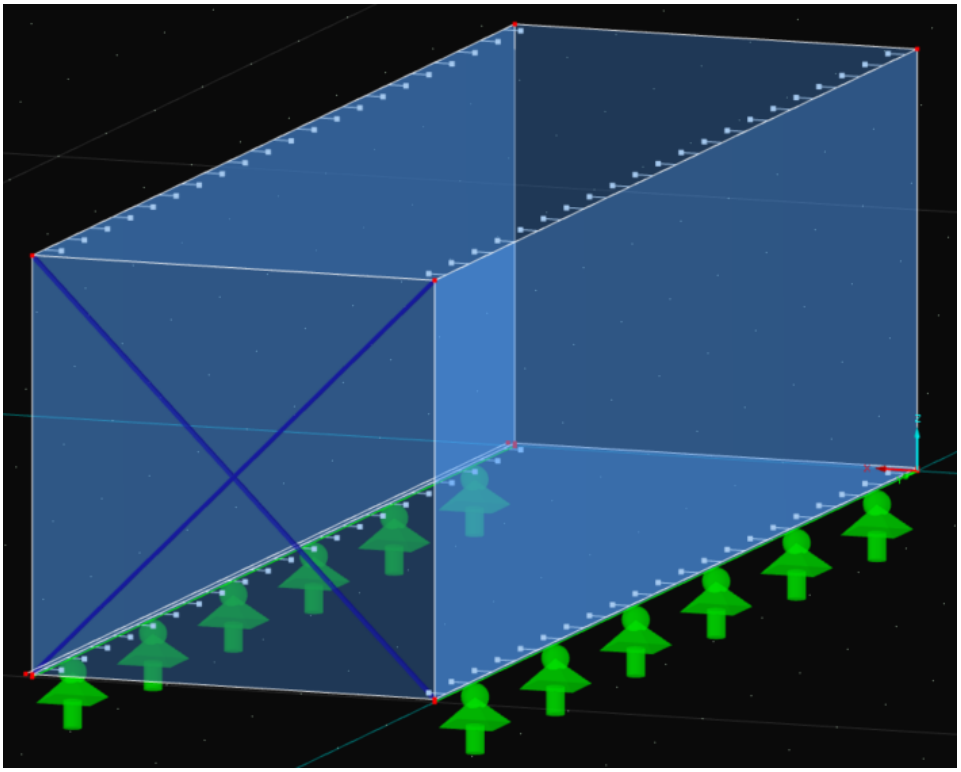

Figure 8.4: RFEM module

The stiffness of the CLT panels is modelled with a stiffness matrix for orthotopic surfaces. The stiffness matrix is generated with the RF-Laminate module. The build-up is shown in Figure 8.5:

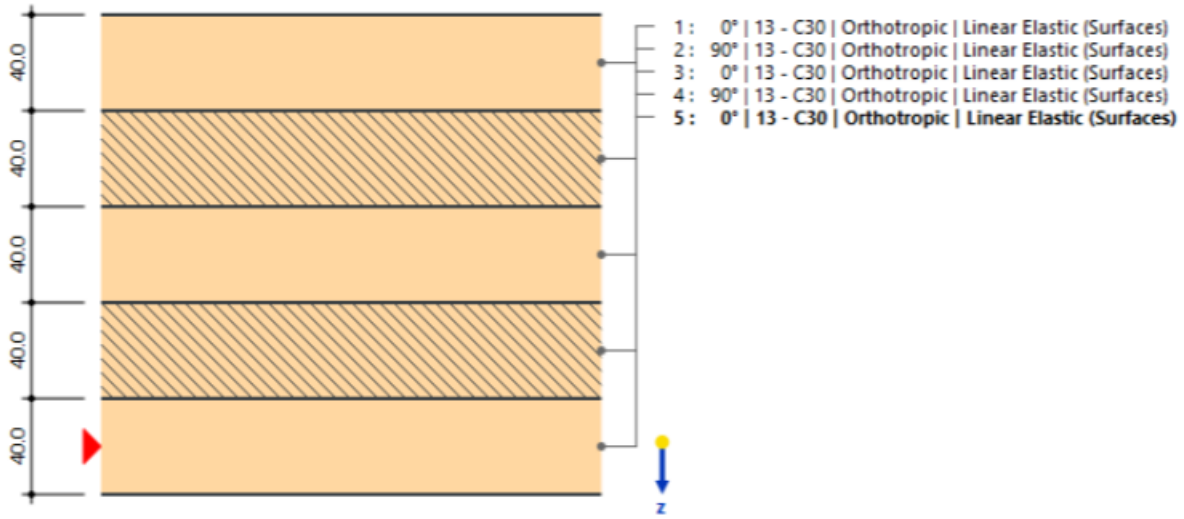

Figure 8.5: Build-up CLT in RFEM

The global stiffness matrix of the cross-section relates the strains to the stresses:

$$\begin{bmatrix} m_x \\ m_y \\ m_{xy} \\ v_x \\ v_y \\ n_x \\ n_y \\ n_x y \end{bmatrix} = \begin{bmatrix} D_{11} & D_{12} & D_{13} & 0 & 0 & D_{16} & D_{17} & D_{18} \\ & D_{22} & D_{23} & 0 & 0 & sym. & D_{27} & D_{28} \\ & & D_{33} & 0 & 0 & sym. & sym. & D_{38} \\ & & & D_{44} & D_{45} & 0 & 0 & 0 \\ & & & & D_{55} & 0 & 0 & 0 \\ & & sym. & & & D_{66} & D_{67} & D_{68} \\ & & & & & & D_{77} & D_{78} \\ & & & & & & & D_{88} \end{bmatrix} \begin{bmatrix} \kappa_x \\ \kappa_y \\ \kappa_{xy} \\ \gamma_{xz} \\ \gamma_{yz} \\ \epsilon_x \\ \epsilon_y \\ \gamma_{xy} \end{bmatrix}$$

With:
$D_{11}..D_{33}$ in Nm
$D_{44}..D_{88}$ in N/m
$D_{16}..D_{38}$ in Nm/m

Position D_{11} till D_{33} represent the bending and torsional stiffness of the cross section, so the stiffness for out-of-plane loads. Position D_{44} till D_{55} represents the shear stiffness of the cross section. D_{66} till D_{88} represents the membrane stiffness of the cross section or in other words the stiffness for in-plane loads. Position D_{16} till D_{38} represent the eccentricity component of the stiffness. For a symmetrical cross-section, this component is equal to zero. The global stiffness matrix is calculated by the RF-Laminate module and is for this specific cross-section:

$$D = \begin{bmatrix} 6392 & 0 & 0 & 0 & 0 & 0 & 0 & 0 \\ & 1875 & 0 & 0 & 0 & sym. & 0 & 0 \\ & & 500 & 0 & 0 & sym. & sym. & 0 \\ & & & 23329 & 0 & 0 & 0 & 0 \\ & & & & 14325 & 0 & 0 & 0 \\ & & sym. & & & 1472000 & 0 & 0 \\ & & & & & & 1008000 & 0 \\ & & & & & & & 150000 \end{bmatrix}$$

The advantage of using the stiffness matrix is that the CLT can be modelled with 2D elements while incorporating the different E-moduli in 3 directions. Normally for 2D elements only the E_x and E_y can be inserted, and the E modulus in third direction is calculated automatically. This results in either a wrong E-modulus for the in-plane forces or the out-of-plane forces. For hand calculations the stiffness matrix is too complex to apply therefore the properties of CLT panel are also given:

E-modulus	$[N/mm^2]$	G-modulus	$[N/mm^2]$
$E_{x,outofplane}$	9587	G_{yz}	86
$E_{y,outofplane}$	2813	G_{xz}	140
$E_{x,inplane}$	7363	G_{xy}	750
$E_{y,inplane}$	5036		

Table 8.1: Properties of the CLT panel

8.2.2. Connections

In figure 6 it can be seen that the connections are modelled as springs. The spring stiffness of each connection is calculated in Appendix B. The result for each connection is shown in the tables below. The location of the connections can be found in Chapter 7. The stiffness for the steel plate connection is given in Table 8.2

Steel plate connection			
SLS		ULS	
$K_{x,ser}$	$51475N/mm$	$K_{x,u}$	$34316N/mm$
$K_{y,ser}$	$51475N/mm$	$K_{y,u}$	$51475N/mm$
$K_{z,ser}$	$10^10N/mm$	$K_{z,u}$	$10^10N/mm$

Table 8.2: Stiffness properties of the steel plate connection

The stiffness for the shear plate connector is given in Table 8.3

Shear plate connector			
SLS		ULS	
$K_{x,ser}$	$23460N/mm$	$K_{x,u}$	$15640N/mm$
$K_{y,ser}$	$23460N/mm$	$K_{y,u}$	$15640N/mm$
$K_{z,ser}$	$0N/mm$	$K_{z,u}$	$0N/mm$

Table 8.3: Stiffness properties of the shear plate connector

The steel plate on the front of the module is not modelled as its only purpose is to create a secure connection for the shear plates. All the Vertical forces are transferred to the foundation through the sidewalls. The entire wall area serves as a continuous connection. Friction between two walls is not considered in this model.

8.2.3. Support conditions

Each bottom module is supported by a line support underneath each side wall. This connection is a hinged support where the rotation is released.

8.2.4. Loading conditions

In this model, the following loads are applied:

- Self weight
- Superimposed dead loads
- Imposed loads
- Wind loads

CC2 is used because the building is lower than 70 meter.

Self weight, superimposed dead loads and imposed loads

The self weight of the CLT of each module is applied as line loads onto each side wall. The superimposed dead loads and imposed loads are also applied as lineloads on each sidewall. The self-weight of the TGSW is applied as a point load on the edge of the sidewalls. The following line loads are used:

	Lineloads on the left sidewall:	Lineloads on the right sidewall:
Selfweight	Selfweight CLT floor 200 mm = $4,6 \cdot 0,2 \cdot \frac{2,6}{2} = 1,2kN/m$ Selfweight CLT ceiling 200 mm = $4,6 \cdot 0,2\frac{2,6}{2} = 1,2kN/m$ Selfweight CLT left wall 200 mm = $4,6 \cdot 3 \cdot 0,2 = 2,76kN/m$	Selfweight CLT floor 200 mm = $4,6 \cdot 0,2 \cdot \frac{2,6}{2} = 1,2kN/m$ Selfweight CLT ceiling 200 mm = $4,6 \cdot 0,2\frac{2,6}{2} = 1,2kN/m$ Selfweight CLT left wall 200 mm = $4,6 \cdot 3 \cdot 0,2 = 2,76kN/m$
Super imposed dead loads	Finishing and installations = $0,5 \cdot \frac{2,600}{2} = 0,65kN/m$	Finishing and installations = $0,5 \cdot \frac{2,600}{2} = 0,65kN/m$
Imposed loads	Floor loading = $1,75 \cdot \frac{2,6}{2} = 2,275kN/m$	Floor loading = $1,75 \cdot \frac{2,6}{2} = 2,275kN/m$
	Total lineload = $8,01kN/m$	Total lineload = $8,01kN/m$

Table 8.4: Decomposition of the lineloads acting on the sidewalls.

Regarding Table 8.4 some remarks must be made:

- The width of the floor and ceiling is 2,6 meters.
- For the finishing and installations a load of $0,5kN/m2$ is assumed.
- The variable loading is assumed to have a reference period of 50 years. Categorie A is used, which refers to areas for domestic and residential activities.

	Pointloads on the left sidewall:	Pointloads on the right sidewall:
Selfweight	Self weight glass pane = $\frac{1}{2} \cdot 25 \cdot 2.760 \cdot 2.760 \cdot 12 = 1,14kN$	Self weight glass pane = $\frac{1}{2} \cdot 25 \cdot 2.760 \cdot 2.760 \cdot 12 = 1,14kN$
Super imposed dead loads	-	-
Imposed loads	-	-
	Total pointload = $1,14kN$	Total pointload= $1,14kN$

Table 8.5: Decomposition of the pointloads acting on the sidewalls

Regarding Table 8.5 one remarks must be made:

- The self weight of the TGSW only consists of the glass pane. The weight of the LVL-adapter frame is neglectable.

Windloads

The wind loading is calculated according to Eurocode 1 part 4. The building is assumed to be located in a rural area 2. The terrain factor is 3. The wind load is given by:

$$q_{wind} = C_s C_d \cdot C_{pe} \cdot q_p(Z_e) \tag{8.4}$$

With:

- $C_d = 1,05$ under condition that building height < 50 meters and h/b < 5 (Dutch national annex)
- C_s varies over building height and is given in Table [C1>NB.22 – C.2<C1] of the Dutch national annex
- $C_{pe} = C_{pe}D + C_{pe}E = 0,8pressure + 0,7suction = 1,5$ parallel to the building
- $C_{pe} = C_{pe}D + C_{pe}E = 0,8pressure + 0,5suction = 1,3$ perpendicular to the building
- $q_p(Z_e)$ varies over building height given in Table NB.5 in Dutch national annex

Due to lack of correlation of wind pressures at the windward and leeward sides, the resulting force due to wind pressures at the windward and leeward side of buildings may be multiplied by a factor 0,85 according to the Eurocode. The result is shown in Table 8.6 and Table 8.7. The pressure applied to the top of the building is applied to the whole building. Although there is a variation in wind pressure, this approach can be regarded as conservative.

Height [m]	Story	$q_{wind}[kN/m^2]$
3	1	0,64
6	2	0,63
9	3	0,69
12	4	0,76
15	5	0,84
18	6	0,90
21	7	0,96
24	8	1,00

Table 8.6: Windpressure per storyheight to side of the building

Height[m]	Story	$q_{wind}[kN/m2]$
3	1	0,59
6	2	0,59
9	3	0,66
12	4	0,74
15	5	0,81
18	6	0,87
21	7	0,93
24	8	0,97

Table 8.7: Windpressure per storyheight to front of the building

8.2.5. Load combinations

According to the Eurocode the ultimate limit state should be considered when inspecting the maximum stresses in the structure. The serviceability limit state should be considered when looking at the maximum deflection. The Dutch National Annex is used for the ψ factors.

Ultimate limit state

The ultimate limit state load combinations are given in Table 8.8:

Load combination	Permanent actions		Loading variable action	Accompanying variable actions	
	Favourable	Unfavourable	Action	Main	Others
Eq 6.10a	1,35 $G_{k,sup}$	0,9 $G_{k,inf}$		1,5 ψ_0 $Q_{k,1}$	1,5 ψ_0 $Q_{k,i}$
Eq 6.10b	1,2 $G_{k,sup}$	0,9 $G_{k,inf}$	1,5 $Q_{k,1}$		1,5 ψ_0 $Q_{k,i}$

Table 8.8: Load combinations for ULS

The following ψ factors according to the Dutch national annex are used:

Action	ψ_0	ψ_1	ψ_2
Category A: Domestic, residential areas	0,4	0,5	0,3
Category H: Roofs	0	0	0
Wind loads on buildings	0	0,2	0
Snow loads on buildings	0	0,2	0

Table 8.9: Phi factors according to the Dutch national annex

Serviceability limit state

The servicability limit state load combinations are given in Table 8.10:

Load combination	Permanent action	Loading variable action	Accompanying variable actions
Characteristic	G_k	$Q_{k,1}$	$\psi_{0,i}$ $Q_{k,i}$
Frequent	G_k	$\psi_{1,1}$ $Q_{k,1}$	$\psi_{2,i}$ $Q_{k,i}$
Quasi-permanent	G_k	$\psi_{2,i}$ $Q_{k,i}$	$\psi_{2,i}$ $Q_{k,i}$

Table 8.10: Load combinations for SLS

8.2.6. The RFEM model

The model shown in Figure 8.6 is used to calculate both the deflection and the force distribution in the structure.

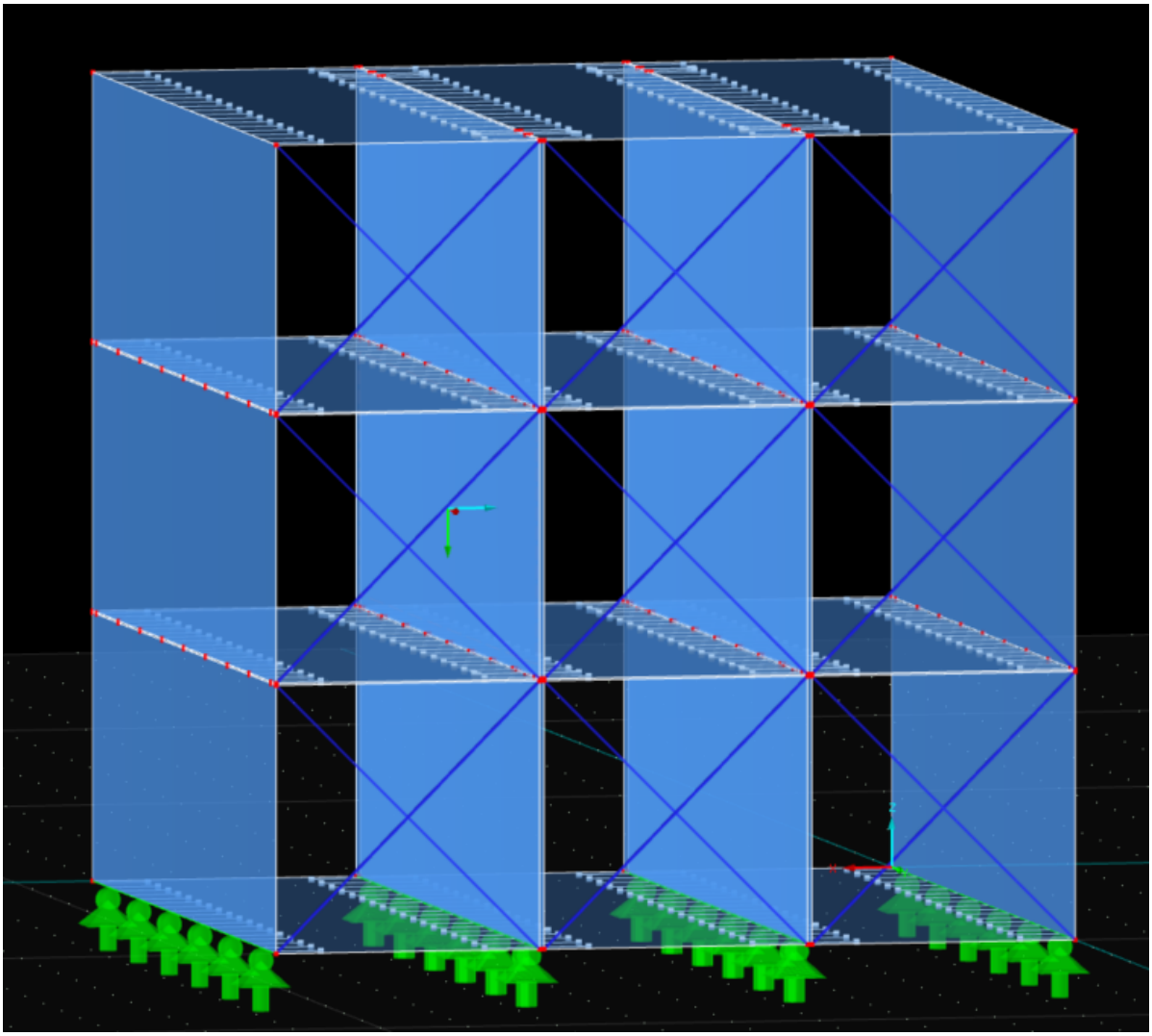

Figure 8.6: Example of a 3x3 configuration of a modular building in RFEM

In this model, the diagonal sizes are varied ranging from 3 mm by 3 mm to 30 mm by 30 mm. This corresponds to a stiffness range of the TGSW from 445 N/mm to 44550 N/mm. The cross-sectional sizes were increased by 0,5 mm for dimensions between 3 mm and 7 mm, and by 1 mm for dimensions between 7 mm and 30 mm. Consequently, each building typology is represented by a total of 32 data points. In figure 8.6 an example configuration of a 3 by 3 modules building is shown.

The results of every FEM analysis consists of the maximum displacement of the building, and the maximum force in the sum of the diagonals. This represents the load on the TGSW. Based on these two results, the strength and stiffness verification is performed for the building. The outcome of the verification's are presented in Section 8.3.1. The workflow to gather this data is explained and visualised in Figure 8.7.

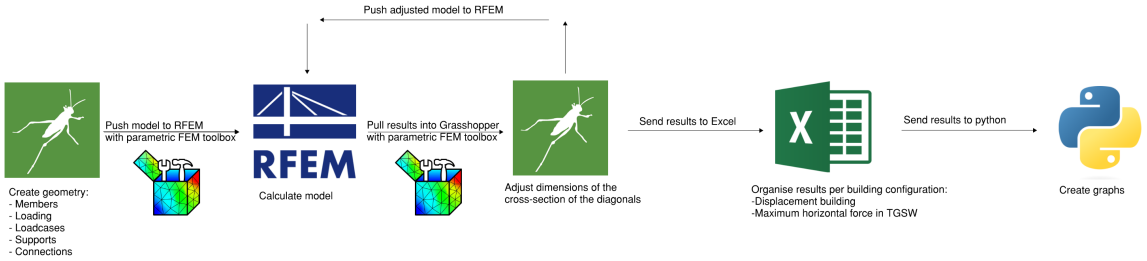

Figure 8.7: Parametric workflow for data collection

8.3. Results

In this section, the results of the model will be presented. The results are presented as design graphs for designing a TGSW, that should function as a stability element in a modular building. For each story level two design graphs are produced. The first graph compares the strength of the TGSW to the strength required to stabilise a modular building. As long as the strength of the TGSW is higher than the required strength for the stability element, the strength criterion is fulfilled. The other graph compares the deflection of the modular building to the maximum deflection limit given by the Eurocode. For buildings, the maximum displacement of the building is given by $H_{building}/500$. The other SLS requirement limits the inter-story drift and is given by $H_{story}/300$ which is for this building 10 mm. As long as the deflection of the modular building remains below this limit, the deflection criterion is fulfilled.

8.3.1. Stiffness and strength verification

As discussed, different stiffnesses of the TGSW, give different load distributions and deflections of the buildings. For the building heights of 3, 4, 5 and 6 stories and the number of adjacent modules ranging from 3 to 18 both the ULS and SLS are calculated.

3 stories building

For a 3-stories modular building, the following configurations are considered: 3 modules high by 3 modules wide till 3 modules high by 9 modules wide. For each of the configurations and different stiffnesses of the diagonals, the maximum displacement and maximum force in the diagonals is calculated. The maximum force in the sum of the diagonals represents the maximum horizontal force on the TGSW. Subsequently, the maximum horizontal force can be compared to the maximum allowable horizontal force calculated in Section 7.2.4. This is plotted in Figure 8.8

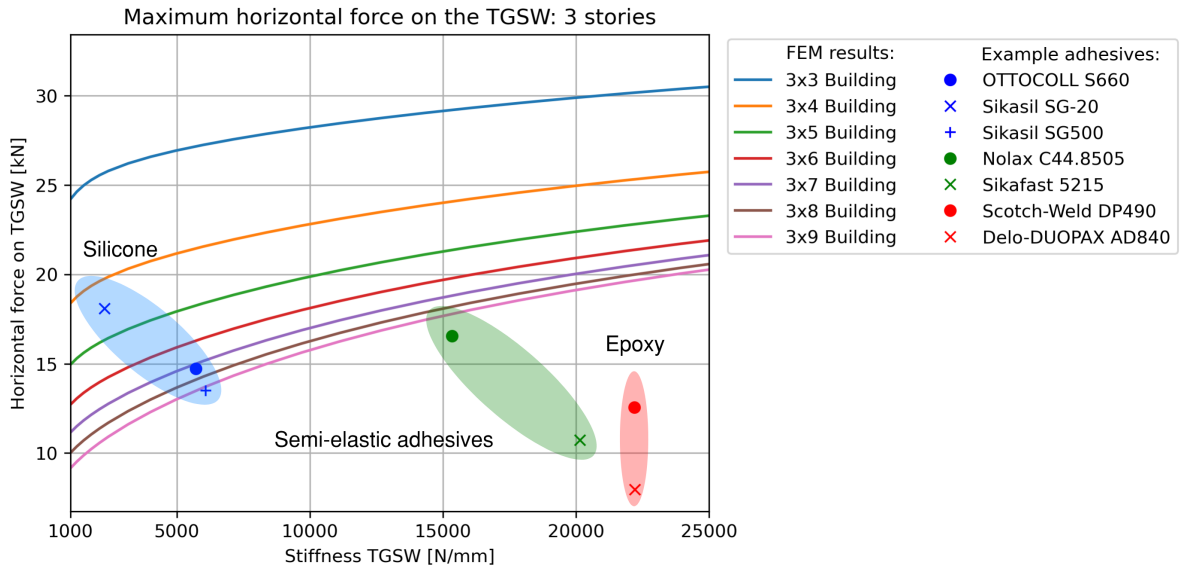

Figure 8.8: Maximum horizontal force on the TGSW: 3 stories

From Figure 8.8 the strength criterium can be verified. The FEM results can be seen as the F_{ed}. The strength of the adhesive, which governs the strength of the TGSW, can be seen as F_{rd}. The strength criterion is fulfilled if Equation 8.5 holds:

$$F_{rd} \geq F_{ed} \tag{8.5}$$

One can easily deduce this by examining the graph and determining whether the marker lies above the FEM result-line. If it does, then the strength criterion is met for that particular configuration. For example, for Sikasil SG20 any configuration with five or more adjacent modules meets the strength criterion.

In a similar way, the displacement of the building can be compared to the maximum allowable displacement ($\frac{H}{500}$). This is done for the different configurations and stiffness ranges of the diagonals. The result is shown in Figure 8.9.

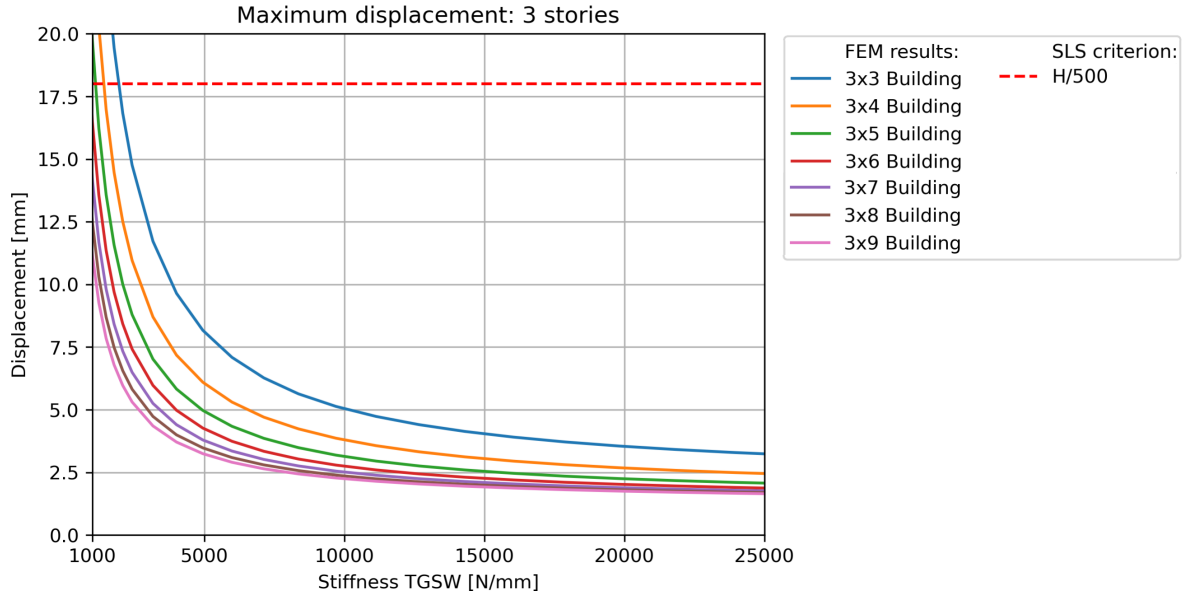

Figure 8.9: Maximum displacement of the building: 3 stories

For the displacement it can be seen that this is less governing for a 3-story building. At roughly less

than 2000 N/mm the 3x3 and 3x4 configurations start to deform too much. The other configurations, all fulfil the displacement requirement over the entire stiffness range.

4 stories building

For a 4-stories modular building, the following configurations are considered: 4 modules high by 4 modules wide till 4 modules high by 12 modules wide. The graphs are constructed in the same way as for 3 stories, therefore no further explanation is given about the graphs. The strength criterion can be verified with Figure 8.10

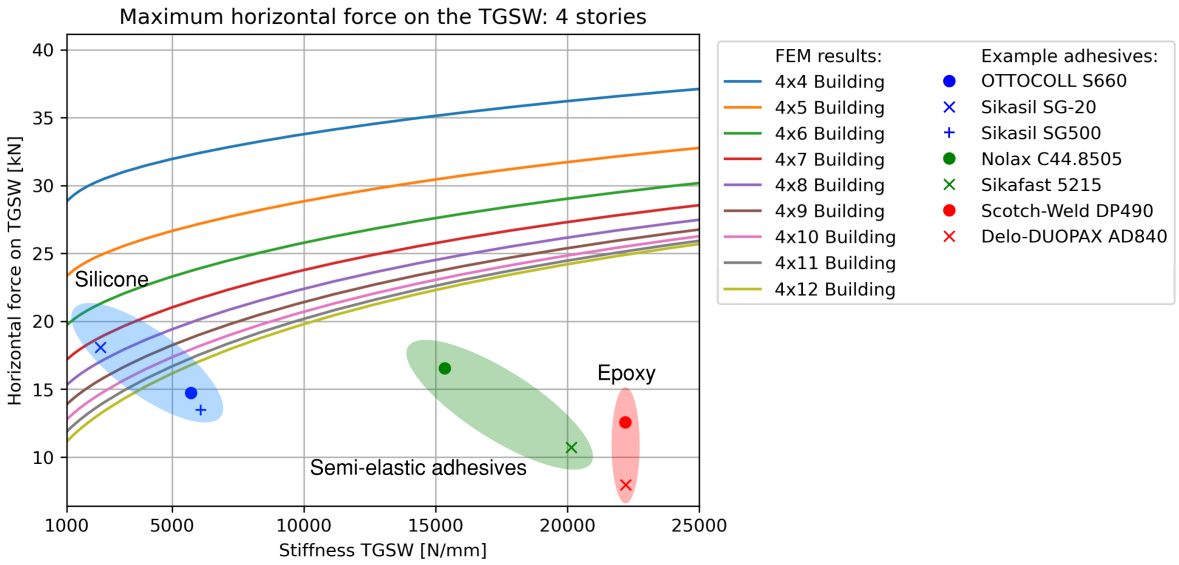

Figure 8.10: Maximum horizontal force on the TGSW: 4 stories

The displacement criterion can verified with Figure 8.11

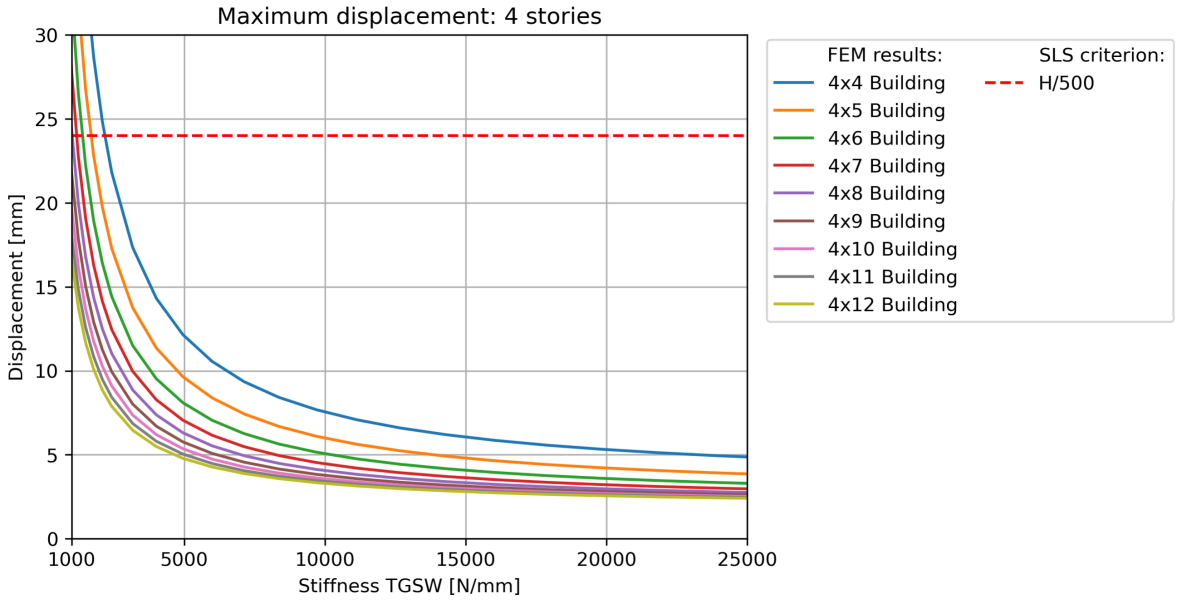

Figure 8.11: Maximum displacement of the building: 4 stories

5 stories building

For a 5-stories modular building, the following configurations are considered: 5 modules high by 5 modules wide till 5 modules high by 15 modules wide. The graphs are constructed in the same way as

for 3 stories, therefore no further explanation is given about the graphs. The strength criterion can be verified with Figure 8.12.

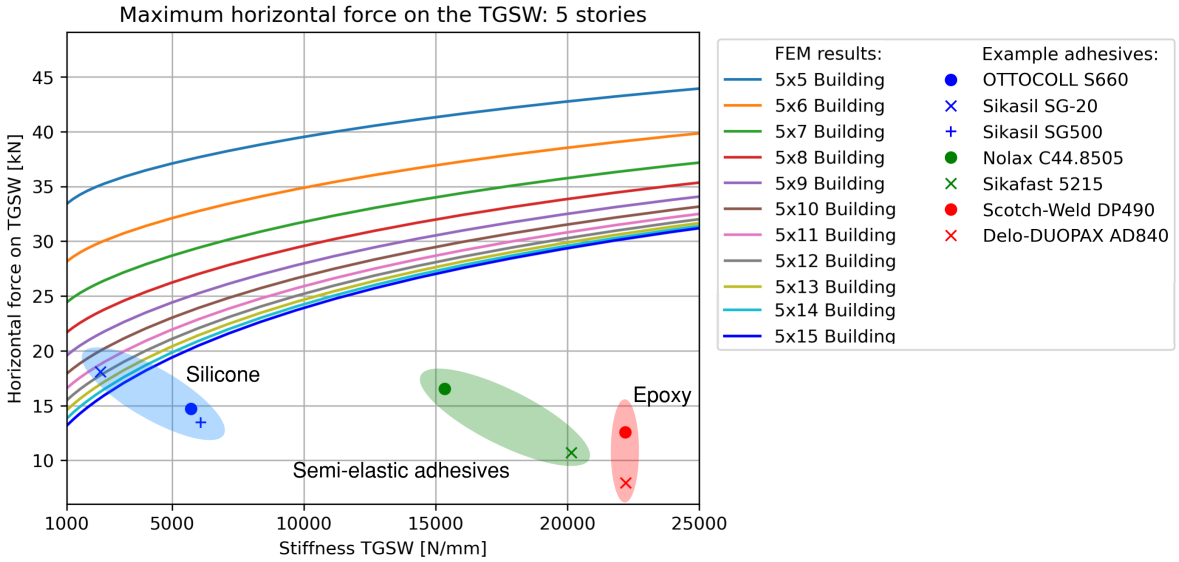

Figure 8.12: Maximum horizontal force on the TGSW: 5 stories

The displacement criterion can verified with Figure 8.13.

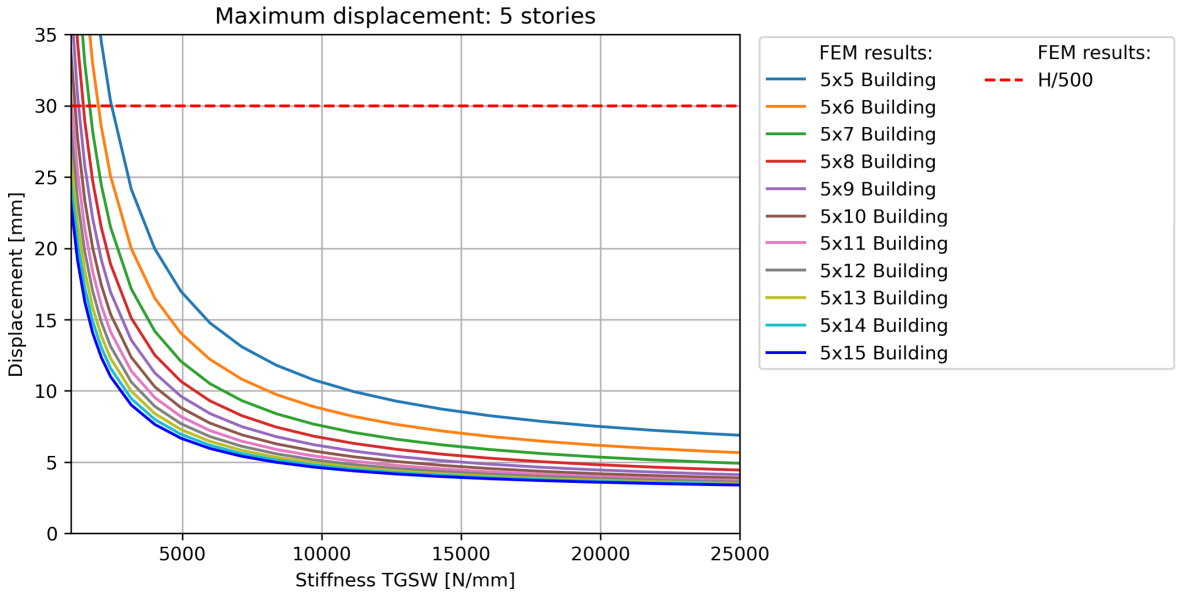

Figure 8.13: Maximum displacement of the building: 5 stories

6 stories building

For a 6-stories modular building, the following configurations are considered: 6 modules high by 6 modules wide till 6 modules high by 18 modules wide. The graphs are constructed in the same way as for 3 stories, therefore no further explanation is given about the graphs. The strength criterion can be verified with Figure 8.14.

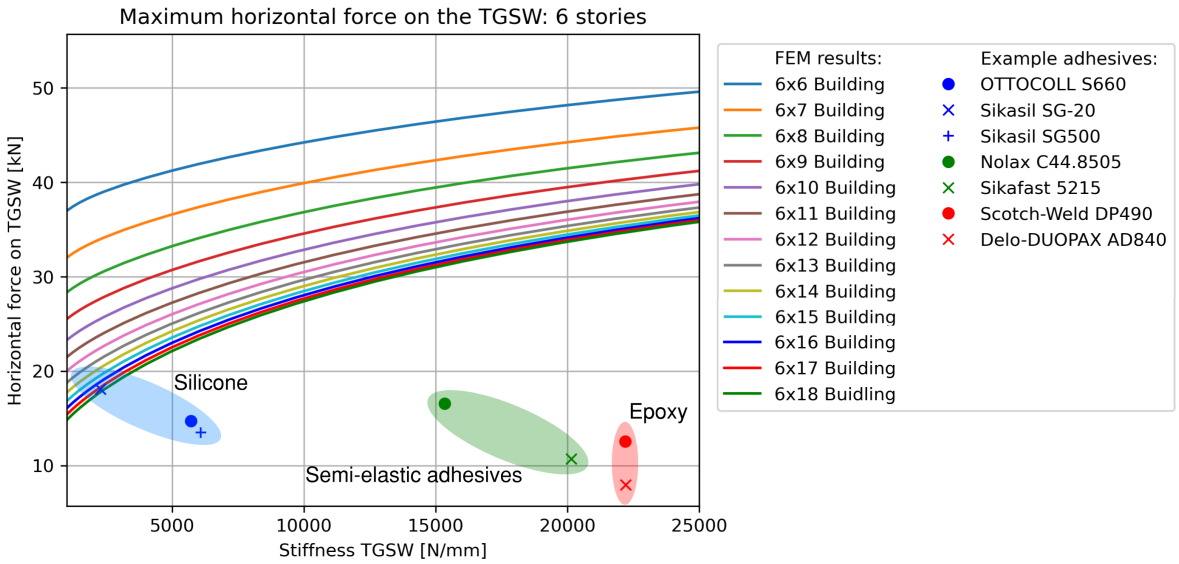

Figure 8.14: Maximum horizontal force on the TGSW: 6 stories

The displacement criterion can verified with Figure 8.15.

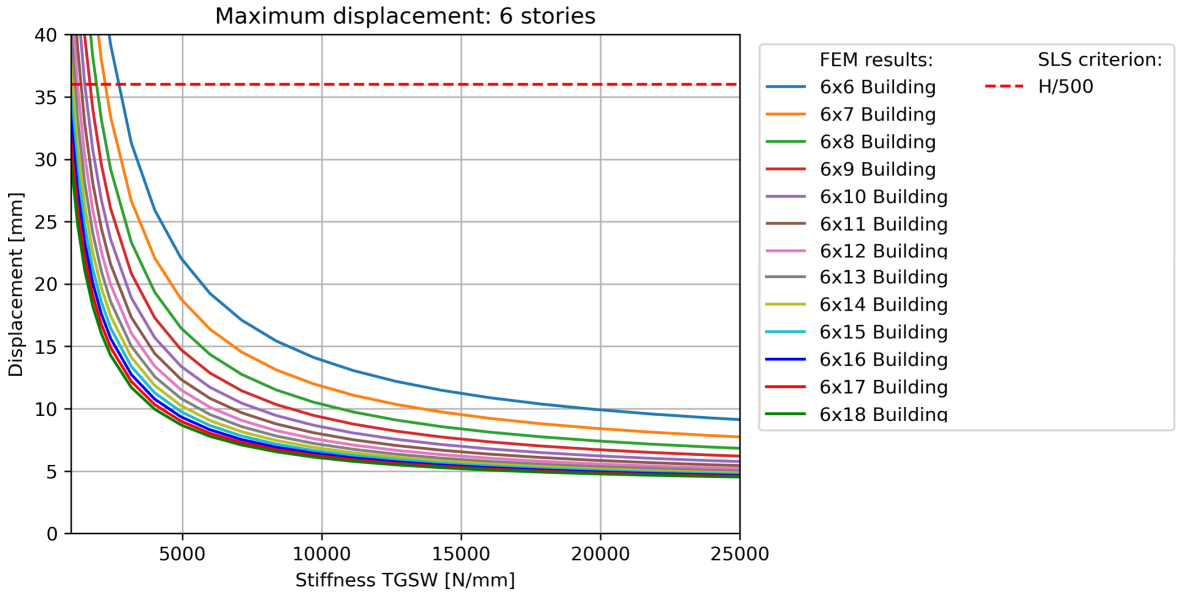

Figure 8.15: Maximum displacement of the building: 6 stories

8.4. Interpretation of the results

For the interpretation of the results, both SLS and ULS are important. In the SLS a requirement for the maximum displacement limits the design. Looking only at the SLS situation, the higher the stiffness of the TGSW, the less displacement occurs. Reducing the displacement means that the design is more likely to satisfy the displacement requirement.

The other situation is about the ULS. In this situation, the design is governed by the strength of the building. In this case, special attention is paid to the strength of the TGSW. The maximum load-bearing capacity of the TGSW was determined by the adhesive strength. This means that if the normal force exceeds the allowable stress of the adhesive, the TGSW is assumed to be broken and has no additional strength. In reality, the plastic region of TGSW will be entered. From this point of view, a stiffer module, allows for less redistribution over adjacent modules, and thus a higher force will be attracted to the first

module, increasing the chance of breaking this module.

In conclusion, the SLS criterion gives a lower limit for the stiffness of the TGSW whereas the ULS criterion gives an upper limit for the stiffness of the TGSW. As long as the upper limit is higher than the lower limit, a viable design for the TGSW can be found. If this is not the case, the TGSW cannot provide stability for the modular building.

8.4.1. Efficiency of the modules

From the previous section it can be seen that, as the stiffness of the TGSW lowers, the maximum horizontal force also lowers, while excerting the same load on the building. The reason for this decrease has everything to do with the redistribution of forces. At lower stiffnesses the forces are spread more equally over the adjacent modules. As a result, the horizontal force in the first module is closer to the value of the horizontal force of the last module. In other words, the modules are more efficiently used. The efficiency of the modules is defined as:

$$efficiency = \frac{H_{max,base}}{H_{min,base}} \tag{8.6}$$

The efficiency is always related to the modules on the bottom of the building. Another way of using this concept, could be for concluding whether it is useful to add a module if the capacity is not sufficient. If there is low efficiency, this means that little to no force will be transferred to the new module, thus having a limited impact on the redistribution of forces.

Influence of the horizontal connections

The horizontal connections play an important role in transferring horizontal forces from one module to another. Having infinitely stiff connections would mean almost equal force spread over all the modules, and thus a high efficiency. In order to quantify this effect, the stiffness of the designed connection is multiplied by a factor 2 and a factor 4. A valid design is picked for this case and happens to be 3 modules high and 8 modules wide. The result is shown in figure 8.16.

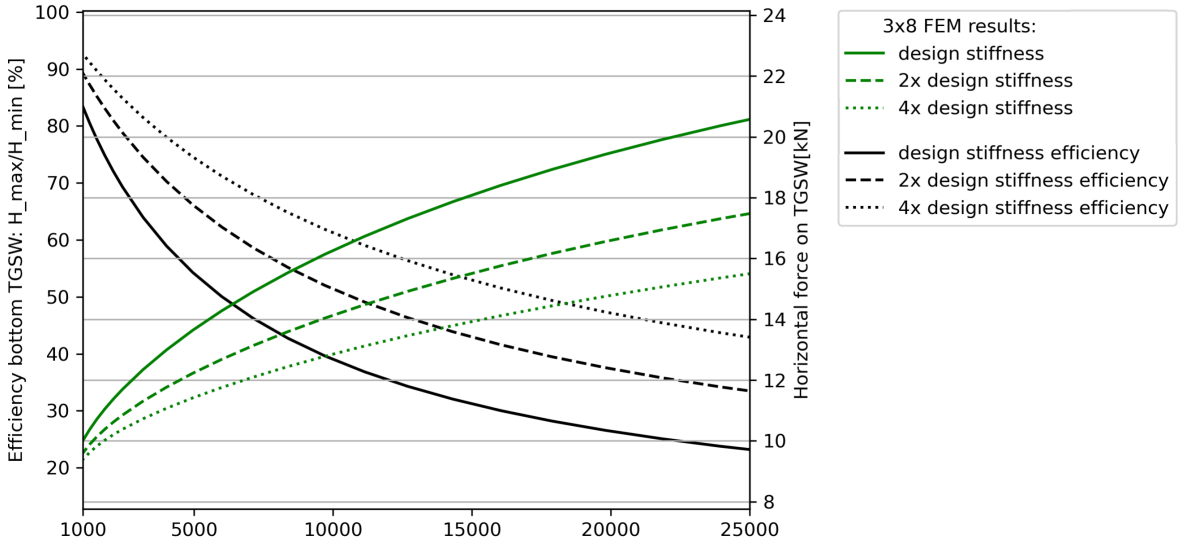

Figure 8.16: Effiency of the modules and maximum horizontal force at design stiffness, 2x design stiffness and 4x design stiffness for building configuration 3x8.

The main conclusions from this graph are:

- As the stiffness of the TGSW increases, less redistribution of forces is possible, and therefore the efficiency goes down quite rapidly. This effect can have quite an influence on the structure. Especially at the stiffer TGSW's the first module will fail whereas the last module is only loaded up to 30/40 percent.

- Increasing the stiffness of the connections, has a significant influence on the efficiency of the modules. This influence increases, as the stiffness of the TGSW increases. Although this effect is significant, the reduction of the horizontal force is only rougly 2 kN when doubling the design stiffness. Nevertheless, this could lead to a situation where a certain configuration does not fulfil the strength criterion with the original design stiffness but does fulfil the strength criterion with 4 times design stiffness. In that case, an extra solution is introduced besides, simply adding an additional module.

Number of stories

In order to investigate how the number of stories is related to the efficiency of the modules, the efficiency of configurations 3x8 and 4x8 are plotted. It can be seen that adding another story to the building, increases the efficiency of the modules. This can be explained by the fact that the forces can be transferred to the bottom modules across a greater height. The forces can redistribute more evenly on each floor level, and therefore the forces are more evenly spread over the modules at the bottom level with an increasing number of floor levels.

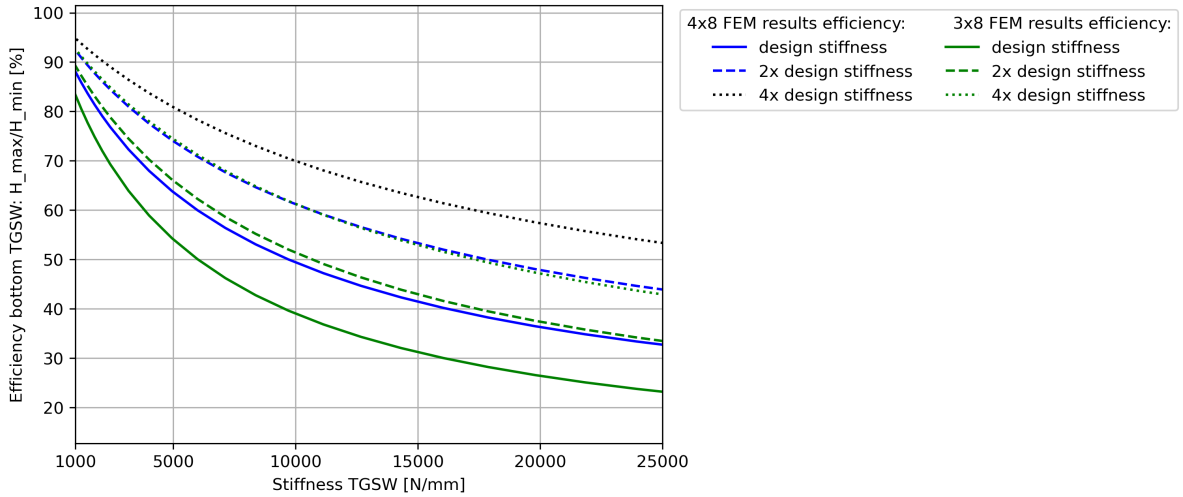

Figure 8.17: Efficiency stories influence

Number of adjacent modules

In order to investigate how the number of modules is related to the efficiency, the efficiency of configurations 3x8 and 3x5 are plotted.

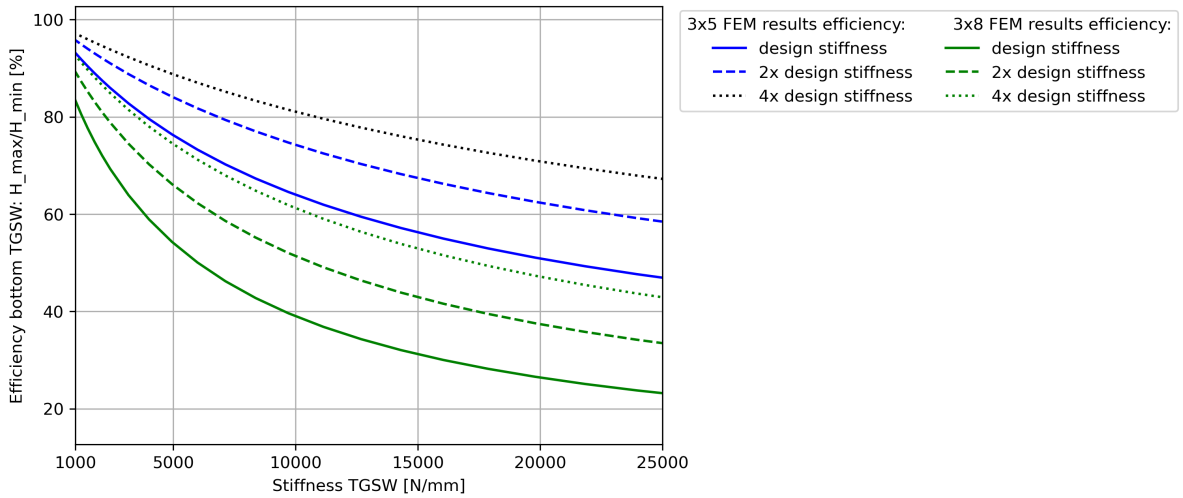

Figure 8.18: Efficiency numbers influence

In this case, it can be seen that the efficiency goes down, as the number of adjacent modules increases. First of all, increasing the number of horizontal modules, logically increases the number of horizontal connections. As these connections are modelled as springs, those springs slightly compress due to the horizontal force transferred from one module to another. Consequently, the first module should deform much more to compensate for the compression of the springs and to deform the last module. More deformation means, more normal force to the first modules compared to the last module, hence a lower efficiency.

Another reason could be that at a certain point, the force transfer is already efficiently going to the foundation. At this point, adding extra modules will not result in a different load distribution. This means that the extra module will take no extra force which means the the efficiency goes down.

8.4.2. Glass failure according to 'afkeurniveau' from NEN 8700

A realistic scenario, that could occur during the lifetime of the building, is that a glass pane breaks. This would imply that this module no longer contributes to the stability of the building, and the forces should be redistributed. During this scenario, the other modules should be able to handle the extra loading. In the Eurocode accidental loading conditions are given. For this loading combination, the windload has a ψ_0 factor of 0,2. Additionally, the safety factor of 1,5 is also left out. As the breaking of a glass pane is a very likely scenario compared to accidental loading, such as blast loads or column failure, it is decided to use 'afkeurniveau' according to NEN 8700. According to this code the wind load factor $\gamma_{Q,1}$ is reduced from 1,5 to 1,3. In addition, a lower reference period of 15 years is used for wind which also reduces the windload. In Eurocode 1991 1-4 the following equations are used to determine the reduction.

$$c_{prob} = \frac{1 - K \cdot \ln - \ln 1 - p^{n}}{1 - K \cdot \ln - \ln 0,98} = 0,93 \tag{8.7}$$

$$(1 - p) = e^{\frac{-1}{R}} = e^{\frac{-1}{15}} \tag{8.8}$$

With:
$K = 0,2$ for wind area 1
$n = 0,5$ for wind area 1
R is the reference period of 15 years.

It is assumed that a broken glass pane is renewed in one year. Nevertheless, the code prescribes a minimum reference period for 'afkeurniveau' of 15 years for CC2-buildings. For a reference period of 15 years, a reduction factor c_{prob} of 0,93 is calculated. The total reduction is roughly 20 percent compared to the ULS level. Building configurations 3x5, 4x8, 5x12 and 6x18 were the minimum configurations for each story level that complied with Eurocode. These configurations are also verified according to NEN 8700 in case of breakage of a glass pane. It is assumed that glass pane in the bottom left module breaks, as this glass is always the most heavily loaded. This is schematically visualised in Figure 8.19.

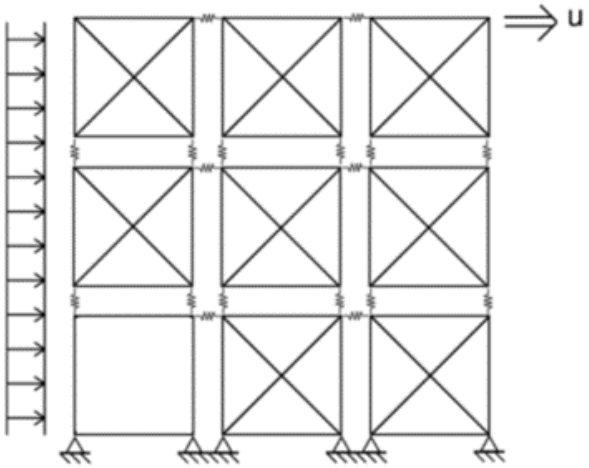

Figure 8.19: Schematic representation of a modular building with one broken glass.

The outcome, with one less TGSW and a reduced wind load, is depicted in Figure 8.20. For reference, the original situation is also depicted on the right.

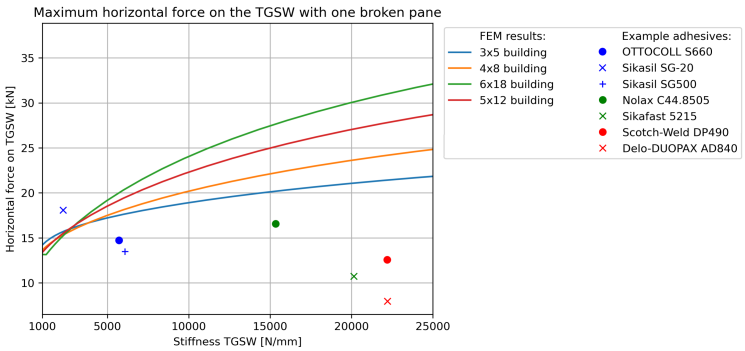

Figure 8.20: Maximum horizontal force on the TGSW with reduced windload

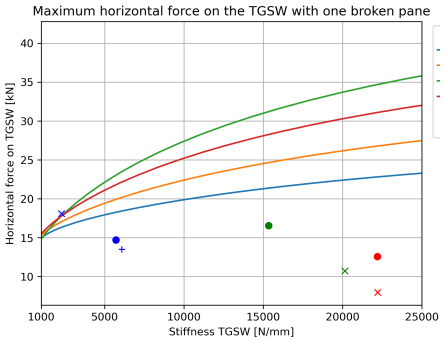

Figure 8.21: Maximum horizontal force on the TGSW: normal situation

It can be concluded that the modular building still meets the criteria set in the NEN 8700 for the 'afkeur-niveau', in case a glass pane breaks.

9

Discussion

In this section, the analytical and FEM models, results, and assumptions presented in this thesis will be discussed. First, the design graphs, which relate the strength of the TGSW to the required stability of the modular building, are discussed. Next, the intermodular connections, as well as the assumptions in modelling these connections, are elaborated on. Finally, assumptions regarding the derivation of the strength and stiffness of the TGSW are discussed, along with the limitations associated with these assumptions.

Design graphs modular building

The main results of this thesis are design graphs representing the displacement and maximum horizontal force at different stiffnesses for several building configurations. The stiffness of the TGSW ranged from 450 to 45.000 N/mm, with the number of stories varying from 3 to 6 and a height-to-width ratio of 1:1 to 1:3. Some remarks should be made about the chosen ranges and the applicability of the design graphs:

- The stiffness range: The range of the TGSW was chosen relatively early in the design process, where it was decided to aim for maximum stiffness for the TGSW. However, as the design process progressed, it became clear that stiffening the module would result in higher forces on the TGSW. This was not favorable for the design, as strength was already a governing factor. In the end, it was decided for the chosen adhesives, that the range of 25000 N/mm till 45000 N/mm, was excluded from the results. Within this range, the horizontal force was much higher than the load-bearing capacity of the TGSW and therefore not of interest.
- Configurations: In the scope of this research, midrise buildings were defined as buildings with 3 to 10 stories. In this chapter, results are only shown from 3 to 6 stories, which is fewer than the indicated 10 stories. This has two reasons. The first argument relates to the limited computational time. As the number of modules grew rapidly, due to both an increase in the number of stories and also a widening range from 1:1 to 1:3, the extra computational time didn't outweigh the extra results. The second reason is that for six stories, only the ratio 1:3 had a valid solution whereas for five stories this was roughly 1:2,5. Extrapolating this trend would indicate that there would be no valid solution for seven stories or higher within the ratio range of 1:1 to 1:3. Consequently, it was decided not to assess building levels higher than six stories.
- Relevance: It was opted to present design graphs for a modular building stabilised by the TGSW. Although these graphs have been shown, one should bear in mind that these graphs are presented for a very specific set of boundary conditions. For example, different sizes of the module or a different design of the TGSW would result in different design graphs. Nevertheless, with the theory presented in this thesis, one should be able to recreate these graphs with different parameters. Additionally, the graphs in this thesis provide an indication of the possible building configurations with a TGSW.
- Limitation: The graphs presented in this thesis cannot be directly used for the construction of a modular building as some important building aspects have not been considered. The design graphs specifically focus on the relationship between the strength and stiffness provided by the

TGSW and the strength and stiffness necessary to stabilise a modular building. For example, a more thorough assessment of the connection properties is required.

Connections

The connections chosen in this thesis were created to establish a functioning building. The main goal was to assess the strength and stiffness of the TGSW, to which the connections were not allowed to be a limiting factor. That being said, the connection do play an important role within the building design. The following remarks should be made about the connections:

- Stiffness of the horizontal connection: It was shown that the stiffness of the horizontal connection had a significant influence on the efficiency of the modules. For this thesis, the connection was purely designed for strength, and the stiffness was not of interest for the design. In hindsight, the design could be reiterated to create a connection with both the desired strength properties and the desired stiffness properties. Unlike the stiffness of the TGSW, an increased stiffness of the connection will lead to a better load distribution across the modules, thus lowering the maximum horizontal force.
- Shear plate connector: As a consequence of the design choice to create a balloon-type construction for the modules, a wall-to-wall shear connection was required. After the multi-criteria analysis, presented in Table 5.1, it was chosen that the shear plate connector was the most suitable connection for this purpose. Nevertheless, it was observed, that little to no reference projects could be found with this connection, even though this connection was presented in the Eurocode. No specific reason can be given for why there is so little use of this connection. Since the connection was presented in the Eurocode, those concerns were ignored, and it was chosen to be a 'common' connection.
- Modelling assumptions for the connections: It has been proven that the stiffness of connections can significantly contribute to the deflection of the entire modular building. As the importance of the connections was inferior to that of the TGSW, some simplifications were made to model the connections. For instance, certain connections are modelled as perfect hinges, implying infinite axial stiffness of the connection. An infinite axial stiffness will never be fully correct as slip in the connection will always cause deformation. Although this may not have a significant impact on the total deflection, it cannot be stated with certainty that it doesn't significantly contribute to the total deflection of the building. To assess the contribution of the connections to the overall deflection of the building more precisely, a more accurate modelling approach must be used.

Stiffness of the TGSW

Regarding the stiffness of the TGSW, there are two points which should be discussed:

- Stiffness parameters: For this thesis, only two parameters were varied for the stiffness calculations: the shear modulus of the adhesive and the screw spacing. These two parameters were found to be the most flexible parameters of the TGSW and would therefore have the most significant impact on the overall stiffness. Nevertheless, the other parameters could also be varied, using the theory presented in this thesis.
- Elastic zone: A prominent assumption within this thesis was that the adhesives were assumed to undergo only elastic deformation and not plastic deformation. In reality, plastic deformation is the part which would provide ductility and safety to the stability system. In this thesis, this aspect is qualitatively addressed by providing the maximum strain of the adhesives and presenting stress-strain graphs for each component to indicate the elastic-plastic region. However, the impact of these factors on the ductility of the entire TGSW is not explicitly discussed. The main reason for considering only the elastic zone is that the TGSW should return to its initial position after loading and not remain in its deformed position. This would only happen if the TGSW is loaded up to the elastic zone.

Load-bearing capacity of the TGSW

The load-bearing capacity of the TGSW was based on the weakest component composing the TGSW. Determining the load-bearing capacity of the TGSW went hand in hand with many assumptions, which will be discussed:

- The basis for modelling the TGSW in this thesis is the spring model. Several studies in the literature have examined its accuracy and concluded that it shows reasonable agreement with tests and complex numerical calculations, especially in the elastic region. For this study, larger TGSWs were used, which have not yet been presented nor verified in the literature. Nevertheless, it is assumed that the outcome of the spring model will remain in reasonable agreement with the tests, since no fundamental changes are made.
- Adhesive strength: For the strength of the adhesive, only the elastic part is considered, whereas for semi-elastic adhesives, a plastic part is also present. This additional part has a favorable effect, as there is redundant plastic capacity for these types of adhesives. However, this favorable effect was never included in this thesis, which might result in an underestimation of the performance of the semi-elastic adhesives.
- Adhesive stress concentrations: The Volkersen model is used to model stress concentrations in adhesives. One important assumption for this model is that the shear modulus of the adhesive is much lower than that of the adherent (glass and timber). As a result, the shear deformation of the adherents is neglected. Within this thesis, the shear modulus of the adhesive is a varying parameter. Relating this parameter to the previous assumption, a remark should be made about the validity of the assumption. For elastic and semi-elastic adhesives, this assumption is valid. However, for the rigid adhesives, this assumption is no longer valid and the shear deformation of timber should be included. In this thesis, another model is suggested which does include shear deformation of the adherents but is not implemented in the calculations. The main reason for this is that the rigid adhesives were already classified as unsuitable adhesives for this application from multiple aspects. Therefore, this different model is not implemented to accurately model a 'non-suitable' adhesive.
- Glass pane: The occurring stresses in the glass pane were verified with a FEM analysis presented in Section 7.2.2. In this analysis, the glass was connected to the timber frame with linear springs to determine the stress concentrations in the glass. As a consequence, the stress concentrations, which were included in the adhesive strength calculation, were not included in the FEM model. To incorporate these stress concentrations for a more precise representation, the adhesive should be modelled in a more detailed way in a FEM model. Nevertheless, maximum tensile stress in the glass, accounting for initial bow and second-order effects, was reached at a horizontal load nine times higher than the adhesive could handle. The stress concentrations in the elastic adhesives were less than a factor of two. Therefore, it is assumed that including stress concentrations will not increase the stresses to a level where glass failure will become governing. In other words, it is assumed that glass failure is not the governing factor based on this simpler FEM model.

Recommendations for improving the load-bearing capacity of the TGSW

It has been stated that the load-bearing capacity of the TGSW was the limiting factor for applying the TGSW as a stability element. Based on this work, several adjustments to the TGSW are proposed to enhance the load-bearing capacity of the TGSW:

- More research could be conducted on adhesives specifically suitable for a load-bearing application in timber-glass composites. Increasing the variety of different adhesives included in a study could lead to the discovery of more suitable adhesives, thus resulting in a higher load-bearing capacity.
- Obtain a more accurate prediction model of the stress concentrations in the adhesive. For instance, a more precise FEM model that incorporates the complex behaviour of the adhesive could be developed to model the stress concentrations. Also, the bonding properties of the glass-adhesive and timber-adhesive interface could be modelled. It was stated that the Volkersen model was conservative. Therefore, a more precise model could result in lower stress concentrations, consequently resulting in a higher load-bearing capacity.
- A final improvement would be to increase the thickness of the adhesive. In this thesis, the adhesive layer was designed to be 50 mm wide and 6 mm thick. This design choice was restricted by the fact that in the codes, it is assumed that the glass pane is supported by line hinges in case of in-plane loading. This assumption is only valid for a width-to-thickness ratio between 1:1 and 1:3. At a higher ratio, the support condition would be somewhere between a hinge and a clamped connection, meaning that extra stresses are induced on the adhesive. However, if a

more accurate FEM model is created, the width of the adhesive can be increased much more because those extra stresses are accounted for in the FEM model. This could lead to a higher load-bearing capacity of the timber-glass shear wall. On the other hand, the extra stresses could also limit this increase in load-bearing capacity.

10

Conclusions and recommendations

The main goal of this thesis was to gain insight into the structural behaviour of a TGSW and to assess if it could be applicable as a stability element in a modular building. In this chapter, the research questions formulated to achieve this goal are answered. To answer the main research question, the sub-questions will be answered first.

10.1. Subquestions

- How does the existing literature relate the in-plane stiffness and load-bearing capacity of the timber-glass shear wall to the properties of its individual components like the adhesive, glass pane, timber frame, screws, timber substructure?

In literature, two methods are provided to explore the relationship between the load-bearing capacity and the stiffness of the TGSW and it's individual components: Analytical spring model and FEM modelling. The first option is chosen for the thesis.

The stiffness of the timber-glass shear wall is described in literature as a serial system of springs where the spring stiffness of each spring represents an individual component of the TGSW. Using the theory for serial springs, the total stiffness of the system can be derived, as well as the contribution of each component to this total stiffness. From this, it can be concluded that the substructure, the timber frame, and the glass pane are generally much stiffer compared to the stiffness of the screws and the adhesive.

The overall load-bearing capacity of the TGSW is governed by its weakest component. The stress distribution is calculated using the spring model. The shear strength of the adhesive governs the TGSW's strength. As the term adhesive is very broad, three different types of adhesive with a range of properties are introduced in literature. Those three types are silicones, semi-elastic adhesives, and epoxy's.

Several examples of each type are assessed to determine which type of adhesive is most suitable for this application, considering criteria such as glass transition temperature, stress concentrations and maximum strain. Epoxy's are found to be the least suitable type of adhesive for this application by a significant margin. Overall, the silicones are the most suitable adhesives for this application, closely followed by the most flexible semi-elastic adhesives. A advantage of semi-elastic adhesives is their additional capacity in the plastic region. This provides extra safety in case of overloading.

The potential failure mechanism may shift if the screw spacing is too large. However, the spacing can easily be reduced by adding extra screws. Generally, the timber frame, glass pane, and substructure have a much higher strength compared to the adhesive strength.

- What connection can be used to create an intra-modular connection between the timber-glass shear wall and the load-bearing elements of the timber module?

The connections between the TGSW and the module should only transfer shear forces. For this connection, the most simple and well-known option is chosen, which is a screwed connection. In this way,

the screws will be laterally loaded in order to transfer the shear force. This is well-known, and thus the strength and stiffness can easily be calculated.

The other connection should provide a connection between the wall and floor, and wall and ceiling. This is also a standardised connection between a CTL wall and CLT floor/CLT ceiling. For this connection, the Titan S angle bracket from Rothoblaas is used.

- What are common solutions to create an inter-modular connection between timber modules?

In general, the timber modules should be connected both horizontally and vertically.The horizontal connection primarily transfers compressive forces but also tensile forces to create horizontal ties. The vertical connections transfer mainly shear forces but also tensile forces in order to form vertical ties.

For the horizontal connection, a very common solution is to use steel plates combined with screws or dowels to connect two modules horizontally. The steel plate is placed on top of both modules, which can transfer both compressive and tensile forces.

For the second type of connection, several options are presented in literature: glued-in rods, toothplate connector, ring plate connector, shear plate connector, steel plate and screws, and dowels. After a multi-criteria analysis, including several aspects like demountability, ductility, and required work on site, the shear plate was identified as the most suitable connection. However, this connection is not capable of forming vertical ties. Therefore steel plates with screws are added, located on the corner points of the modules. These connections are purely added to create vertical ties. It should be noted that progressive collapse is only qualitatively assessed and not in a quantitative manner. In theory, these connections can transfer tensile forces. However, it cannot be concluded that these connections, fulfil all the requirements in case of progressive collapse. This requires quantitative research into the robustness of these connections, which was beyond the scope of this research.

- How can the analytical spring-model be used to improve the in-plane stiffness and load-bearing capacity of the timber-glass shear wall within the module requirements?

The analytical spring-model can be used to predict the stiffness of TGSW based on its individual components. The two most flexible parameters were investigated as these had the most impact on the final properties of the TGSW. These parameters were the shear modulus of the adhesives and the spacing of the screws. Increasing the screw spacing increases the stiffness of the TGSW and, as long as the adhesive is weaker, has no influence on the strength of the TGSW.

For the shear stiffness of the adhesive, this is not the same. After investigating several types of adhesives, it can be concluded that there is an inverse relation between the best performing (in terms of strength) adhesive and the stiffness of this adhesive. This can be explained by the fact, that the outcome of simple shear tests was not directly used as input for the strength of the adhesive. Instead, a reduction factor based on the Volkersen theory was applied to account for stress concentrations in the adhesive. As a result, the silicones, performed better after applying this reduction factor than the much stiffer epoxy's. In other words, the stiffer the adhesive, the higher stress concentrations occur in this adhesive. Therefore, the type of adhesive results in a trade-off between maximising strength or maximising stiffness of the adhesive. For this application, it can be concluded that maximising shear strength of the adhesive is far more important than maximising the stiffness of the adhesive.

- How can the results of a finite element model be used to determine the load-bearing capacity and stiffness of a mid-rise modular timber building, including the strength and stiffness of the inter and intra-modular connections?

From a SLS point of view, the stiffness of the module should be maximised as this would reduce the total deflection of the building.

From a strength point of view, the stiffness of the module should be minimised in order to redistribute the windload as evenly as possible over the horizontal modules. This presents a conflict of interest. As the strength is the limiting factor, the stiffness should be minimised up to the boundary of H/500. In this scenario, the forces are redistributed as efficiently as possible to meet the SLS criteria. For mid-rise buildings, the strength criterion will generally be governing over the deflection criteria.

Also from an efficiency standpoint, it is preferable to minimise the stiffness of the building, while meeting the deflection criterion. Utilising all modules up to their maximum capacity is more efficient than having one module at maximum capacity while others are not. This indicates that there is unused capacity due to a lack of force redistribution. Additionally, the efficiency of the modules increases when the stiffness of the horizontal connections is increased.

10.2. Main research question

- To what extent can the structural performance of a timber-glass shear wall as a stability element in a timber module be used to accommodate for the stability of a mid-rise modular timber building?

The structural performance of a timber-glass shear wall can be used to a certain extent as a stability element in a mid-rise modular building, depending on several aspects. The aspects that should be considered when using a TGSW as a stability element in a modular timber building are as follows:

- For the adhesives and configurations assessed in this thesis, the best-performing adhesive, was Sikasil SG-20. This adhesive was the most flexible adhesive yet provided the TGSW with the highest load-bearing capacity.
- With Sikasil SG-20 the minimum number of adjacent modules required for three, four, five and six stories were respectively 5 modules, 8 modules, 12 modules, and 18 modules.
- Above six stories, no configurations could fulfil the strength criterion within the 1:1 and 1:3 height-to-width ratio.
- The design graphs 8.8 up to 8.15 can be used to design a modular building. As a starting point, one has to decide the configuration of the modular building, for example, 4 by 9 modules. From the stiffness graph, the minimum stiffness of the TGSW can be derived. This point can be found by the intersection of the right line with the 'H/500' line. For the 4 by 9 modules configuration, this is approximately 1000 N/mm. Next, one has a new adhesive which results in stiffness of 5000 N/mm and a maximum load-bearing capacity of 20 kN of the TGSW. In order to verify the strength, one should check if the marker of the adhesive is above the '4x9'line, which is the case. Therefore, it can be concluded that this design fulfils both strength and stiffness criteria.

10.3. Recommendations

During this research, various aspects were not considered. In order to improve this research, multiple recommendations are given:

- The intermodular connection could, in theory, provide horizontal and vertical ties. However, no calculations have been performed to demonstrate that this is actually the case. In further research, these calculations should be performed, and if required, the connection design should be adjusted.
- The TGSW and also the inner double glazing function as facade elements in the module. Further research could be put into the possibility of combining both the double glazing with the structural glazing in a single facade element. Additionally, it would be interesting to see how the TGSW would perform in terms of thermal insulation and how it influences the heating and cooling demand of the module.
- Fire safety was only quantitatively discussed, but no calculations were performed on the design proposed in this thesis. Additional research could provide insight into whether this design would satisfy the requirements for fire safety.
- An important horizontal force, which was out of the scope of the research, is earthquake loading. It would be interesting to see how the TGSW would perform in the case of seismic loading. Furthermore, it would be interesting to see how the design could be improved from a seismic point of view.
- The final recommendation is made regarding the breakage of a glass pane. More research should be put into the probability of a glass pane breaking during the lifetime of a TGSW. This could then solve the question of whether breakage of a glass pane can be seen as an exceptional situation such as in ALS or that the design should be up to renovation level during the replacement of a TGSW. This research could clarify the type and magnitude of loads that should be applied to the building in case a glass pane breaks.

References

172 hotelrooms - Hotel Jakarta - Ursem Modular Building systems (June 2019). URL: https://www.ursem.nl/en/projects/hotel-jakarta/.

Americana, Click (June 2021). "Mobile homes". In: *Click Americana*. URL: https://clickamericana.com/topics/home-garden/mobile-homes-hot-housing-trend-50s-60s.

Bedon, Chiara (2017). "Structural Glass Systems under Fire: Overview of Design Issues, Experimental Research, and Developments". In: *Advances in Civil Engineering* 2017. Ed. by Rafik Belarbi, p. 2120570. ISSN: 1687-8086. DOI: 10.1155/2017/2120570. URL: https://doi.org/10.1155/2017/2120570.

Blass, H J, J Ehlbeck, and M Schlager (1994). "Strength and stiffness of ring and shear-plate connections". In: *Holz als Roh-und Werkstoff* 52.2, pp. 71–76.

Blyberg, Louise (2011). "Timber/glass adhesive bonds for structural applications". PhD thesis. Institutionen för teknik, Linnéuniversitetet.

Cantournet, S., R. Desmorat, and J. Besson (June 2009). "Mullins effect and cyclic stress softening of filled elastomers by internal sliding and friction thermodynamics model". In: *International Journal of Solids and Structures* 46.11-12, pp. 2255–2264. ISSN: 00207683. DOI: 10.1016/j.ijsolstr.2008.12.025.

Derix (Dec. 2018). *Nachhaltiges Modulsystem Hotel Jakarta, Amsterdam/NL*. Tech. rep. URL: https://derix.de/wp-content/uploads/2018_12_Jakarta_DBZ.pdf.

Descamps, Pierre, Valerie Hayez, and Mahmoud Chabih (Oct. 2017). "Next generation calculation method for structural silicone joint dimensioning". In: *Glass Structures & Engineering* 2.2, pp. 169–182. ISSN: 2363-5142. DOI: 10.1007/s40940-017-0044-7.

Ellingwood, Bruce R et al. (2007). "Best practices for reducing the potential for progressive collapse in buildings". In.

EN 1991-1-7 (2006). *Eurocode 1 - Actions on structures - Part 1-7: General actions - Accidental actions*.

EN 1995-1-2 (2004). *Eurocode 5. Design of Timber Structures–Part 1–2: General–Structural Fire Design*.

EUMiesAward (n.d.). URL: https://miesarch.com/work/3224.

Fadai, Alireza, Katharina Holzinger, and Werner Hochhauser (2021). "Timber-glass composite: concepts for glued bracing floor elements". In: *Engineered Transparency Glass in Architecture and Structural Engineering* 4.6, pp. 291–300.

Fadai, Alireza, Matthias Rinnhofer, and Wolfgang Winter (May 2017). "Timber–Glass Composites Used for Bracing of Mid-Rise Timber Buildings". In: *Structural Engineering International* 27.2, pp. 175–183. ISSN: 1016-8664. DOI: 10.2749/101686617X14881932435655.

Feldmann, Markus et al. (2014). "Guidance for European structural design of glass components". In: *Publications Office of the European Union*, pp. 1–196.

Ferdous, Wahid et al. (2019). "New advancements, challenges and opportunities of multi-storey modular buildings – A state-of-the-art review". In: *Engineering Structures* 183, pp. 883–893. ISSN: 0141-0296. DOI: https://doi.org/10.1016/j.engstruct.2019.01.061. URL: https://www.sciencedirect.com/science/article/pii/S0141029618334175.

Floor, J H J (2014). *Structural Adhesive Bonded Steel-to-Steel Connections: An Introduction for Structural engineering*. URL: https://repository.tudelft.nl/islandora/object/uuid:4650e727-703c-46be-b408-24a45aeefbf7?collection=education.

Franke, Steffen, Bettina Franke, and Annette M Harte (2015). "Failure modes and reinforcement techniques for timber beams–State of the art". In: *Construction and Building Materials* 97, pp. 2–13.

Gilbert, Benoit P. et al. (Sept. 2017). "Strength modelling of Laminated Veneer Lumber (LVL) beams". In: *Construction and Building Materials* 149, pp. 763–777. ISSN: 09500618. DOI: 10.1016/j.conbuildmat.2017.05.153.

Gunawardena, Tharaka (2016). "Behaviour of prefabricated modular buildings subjected to lateral loads". In: *Department of Infrastructure Engineering*.

Hiziroglu, Salim (July 2016). *Laminated Veneer Lumber (LVL) as a Construction Material*. URL: https://extension.okstate.edu/fact-sheets/laminated-veneer-lumber-lvl-as-a-construction-material.html.

Huber, Johannes A. J. et al. (Mar. 2019). "Structural robustness and timber buildings – a review". In: *Wood Material Science & Engineering* 14.2, pp. 107–128. ISSN: 1748-0272. DOI: 10.1080/17480272.2018.1446052.

Huß, Wolfgang, Matthias Kaufmann, and Konrad Merz (June 2019). *Building in Timber - Room Modules*. DOI: 10.11129/9783955534950. URL: https://doi.org/10.11129/9783955534950.

J. Maljaars and A.J. Breunese (2015). *Fire Safety Design CIE 5131*.

Källsner, Bo and Ulf Arne Girhammar (Apr. 2009). "Analysis of fully anchored light-frame timber shear walls—elastic model". In: *Materials and Structures* 42.3, pp. 301–320. ISSN: 1359-5997. DOI: 10.1617/s11527-008-9463-x.

Kaufmann bausysteme (n.d.). *Student residences WOODIE, Hamburg (D)*. URL: https://kaufmannbausysteme.at/en/studentenheim-woodie-hamburg-d.

Klippel, Michael and Joachim Schmid (2017). "Design of Cross-Laminated Timber in Fire". In: *Structural Engineering International* 27.2, pp. 224–230. DOI: 10.2749/101686617X14881932436096. URL: https://doi.org/10.2749/101686617X14881932436096.

Knuppe, Joep (2022). "Robustness of Modular Timber Buildings: An investigation into alternative load paths in volumetric timber post and beam modules". en. In: URL: https://repository.tudelft.nl/islandora/object/uuid%3Af6bf1b27-322b-4f2c-9d15-d96604a2e946.

Kozłowski, Marcin (Nov. 2014). "Experimental and numerical analysis of hybrid timber-glass beams". PhD thesis. DOI: 10.13140/RG.2.2.25895.85923.

Kreuzinger, Heinrich and Peter Niedermaier (2005). "Glas als Schubfeld". In: *Tagungsband Ingenieurholzbau, Karlsruher Tage*.

Lawson, Mark, Ray Ogden, and Chris Goodier (Feb. 2014). *Design in Modular Construction*. CRC Press. ISBN: 9780203870785. DOI: 10.1201/b16607.

Lawson, P. M. et al. (Feb. 2008). "Robustness of light steel frames and modular construction". In: *Proceedings of the Institution of Civil Engineers - Structures and Buildings* 161.1, pp. 3–16. ISSN: 0965-0911. DOI: 10.1680/stbu.2008.161.1.3.

Lindberg, G A (Nov. 2023). *What is Tg, the glass transition temperature for adhesives?* URL: https://www.galindberg.se/en/Inspiration_and_knowledge/what-is-Tg-adhesive#:~:text=The%20glass%20transition%20temperature%20for%20an%20adhesive%20is%20the%20temperature,from%20being%20glassy%20to%20rubbery..

María Francisca González (July 2018). "Hotel Jakarta / SeARCH". In: *ArchDaily*. URL: https://www.archdaily.com/899081/hotel-jakarta-search.

Metsä (n.d.). *kerto-manual-lvl-mechanical-properties*. URL: https://www.metsagroup.com/metsawood/products-and-services/design-tools/kerto-lvl-manual/.

Ministerie van Algemene Zaken (June 2023). *900.000 nieuwe woningen om aan groeiende vraag te voldoen*. URL: https://www.rijksoverheid.nl/onderwerpen/volkshuisvesting/nieuwe-woningen.

Mocibob, Danijel (2008). "Glass panel under shear loading use of glass envelopes in building stabilization". In: p. 170. DOI: https://doi.org/10.5075/epfl-thesis-4185. URL: http://infoscience.epfl.ch/record/125889.

Modular-T (n.d.). URL: https://bauart.ch/projects/modular-t-neuchatel-en/.

Mohammad, Mohammad et al. (2018). "Design approaches for CLT connections". In: *Wood and Fiber Science*, pp. 27–47.

Moulds, Richard J. (2006). "Design and Stress Calculations for Bonded Joints". In: pp. 197–231. DOI: 10.1016/S1874-5695(06)80014-X.

NEN-EN 13501-2 (2023). *Fire classification of construction products and building elements - Part 2: Classification using data from fire resistance and/or smoke control tests, excluding ventilation services*.

NEN-EN 15998 (2020). *Glass in building - Safety in case of fire, fire resistance - Glass testing methodology for the purpose of classification*.

NEN-EN 912 (2011). *Timber fasteners - Specifications for connectors for timbers*.

Nick Bertram et al. (June 2019). *Modular construction: From projects to products*. Tech. rep. McKinsey \& Company.

Nicklisch, F, J Giese-Hinz, and B Weller (2016). “Experimental and numerical study on glass stresses and shear deformation of long adhesive joints in timber-glass composites”. In: *Challenging Glass Conference Proceedings*. Vol. 5, pp. 295–304.

Nicklisch, Felix (June 2016). “Ein Beitrag zum Einsatz von höherfesten Klebstoffen bei Holz-Glas-Verbundelementen”. PhD thesis.

Nicklisch, Felix, Michael Dorn, et al. (Nov. 2014). “Joint study on material properties of adhesives to be used in load-bearing timber-glass composite elements.” In.

Nicklisch, Felix, Sebastian Hernandez, et al. (May 2015). “Development of load-bearing timber-glass composite shear wall elements”. In.

Niedermaier, Peter (2004). *Holz-Glas-Verbundkonstruktionen. Ein Beitrag zur Aussteifung von filigranen Holztragwerken.* Tech. rep. Technische Universität München.

Niedermaier Peter and Kreuzinger Heinrich (2005). “Glas als Schubfeld”. In: *Karlsruher Tage*.

NVN-CEN/TS 19100-1 (n.d.). *Design of glass structures - Part 1: Basis of design and materials*.

Park, Hyung Keun and Jong-Ho Ock (2016). “Unit modular in-fill construction method for high-rise buildings”. In: *KSCE Journal of Civil Engineering* 20, pp. 1201–1210.

Piculin, Sara, Felix Nicklisch, and Boštjan Brank (Oct. 2016). “Numerical and experimental tests on adhesive bond behaviour in timber-glass walls”. In: *International Journal of Adhesion and Adhesives* 70, pp. 204–217. DOI: 10.1016/j.ijadhadh.2016.06.012.

PietersBouwtechniek (n.d.). *Hotel Jakarta*. URL: https://www.pietersbouwtechniek.nl/projecten/hotel-jakarta.

Pölzl, Franz (2017). “Mechanical Behavior of Cold-Bent Insulating Glass Units”. PhD thesis. Graz University of Technology.

Raghvendra Gopal (Nov. 2021). *Glass Transition Temperature (TG)*. URL: https://www.corrosionpedia.com/definition/593/glass-transition-temperature-tg.

Rijksoverheid (Apr. 2023). *Hoofdstuk 2. Technische bouwvoorschriften uit het oogpunt van veiligheid*. URL: https://rijksoverheid.bouwbesluit.com/Inhoud/docs/wet/bb2012/hfd2.

Sandhaas, Carmen et al. (2018). “Design of connections in timber structures”. In: *Shaker-Verlag GmbH*.

StoraEnso (June 2016). *3–8 Storey Modular Element Buildings*. Tech. rep. URL: https://www.storaenso.com/-/media/Documents/Download-center/Documents/Product-brochures/Wood-products/Design-Manual-A4-Modular-element-buildings20161227finalversion-40EN.pdf.

Štrukelj, Andrej, Boštjan Ber, and Miroslav Premrov (Sept. 2015). “Racking resistance of timber-glass wall elements using different types of adhesives”. In: *Construction and Building Materials* 93, pp. 130–143. ISSN: 09500618. DOI: 10.1016/j.conbuildmat.2015.05.112.

Tsai, M Y, D W Oplinger, and J Morton (1998). “Improved theoretical solutions for adhesive lap joints”. In: *International Journal of Solids and structures* 35.12, pp. 1163–1185.

Uibel, Thomas and Hans Joachim Blaß (2013). “Joints with dowel type fasteners in CLT structures”. In: *Focus solid timber solutions-European conference on cross laminated timber (CLT), Bath*, pp. 119–136.

Voulpiotis, Konstantinos (2021). “Robustness of Tall Timber Buildings”. PhD thesis. ETH Zurich. DOI: https://doi.org/10.3929/ethz-b-000526211.

Wiesner, Felix and Luke Bisby (2019). “The structural capacity of laminated timber compression elements in fire: A meta-analysis”. In: *Fire Safety Journal* 107, pp. 114–125. ISSN: 0379-7112. DOI: https://doi.org/10.1016/j.firesaf.2018.04.009. URL: https://www.sciencedirect.com/science/article/pii/S0379711218301759.

Ye, Zhihang et al. (Jan. 2021). “State-of-the-art review and investigation of structural stability in multi-story modular buildings”. en. In: *Journal of Building Engineering* 33, p. 101844. ISSN: 2352-7102. DOI: 10.1016/j.jobe.2020.101844. URL: https://www.sciencedirect.com/science/article/pii/S235271022033477X.

Zandbergen, T (2016). *Fire resistance of existing structures: Assessing the fire resistance of existing concrete buildings*. URL: https://repository.tudelft.nl/islandora/object/uuid:5637b420-d8b5-4321-b0c4-7f556a7e69ed?collection=education.

A

Appendix A

In this appendix, an extended description of the case studies can be found. The following projects are reviewed:

- Hotel Jakarta
- Puukuokka
- Woodie Student Hostel
- Sara Cultural center

For each case study the loadbearing structure is described. Furthermore, the fire safety measures in the buildings are discussed and the type of foundation is presented.

Hotel Jakarta, Netherlands

A famous example of a modular timber building in the Netherlands is Hotel Jakarta. This is the highest modular timber building in the Netherlands and is located on Java-Eiland in Amsterdam. The start of the design was in 2014 and four years later, in 2018, the construction was finished. The building consists of 176 modules placed on-site in a period of just 4 weeks. The hotel rooms with precast concrete floors and cross-laminated timber walls and roofs were stacked partly up to four layers, and partly up to eight layers. According to the structural engineer PietersBouwtechniek n.d., the first two floors of the building are made of a table concrete construction that provides stability for the lower part. The timber modules are placed on top of this concrete table structure and stabilised by three concrete cores highlighted in red in Figure A.1.

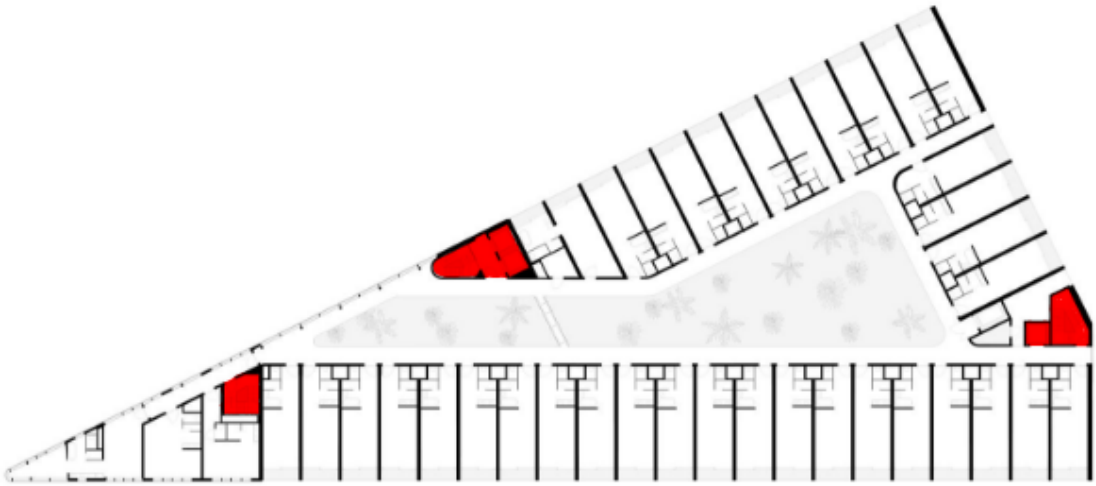

Figure A.1: Hotel Jakarta: Floorplan of the 4th floor (María Francisca González 2018)

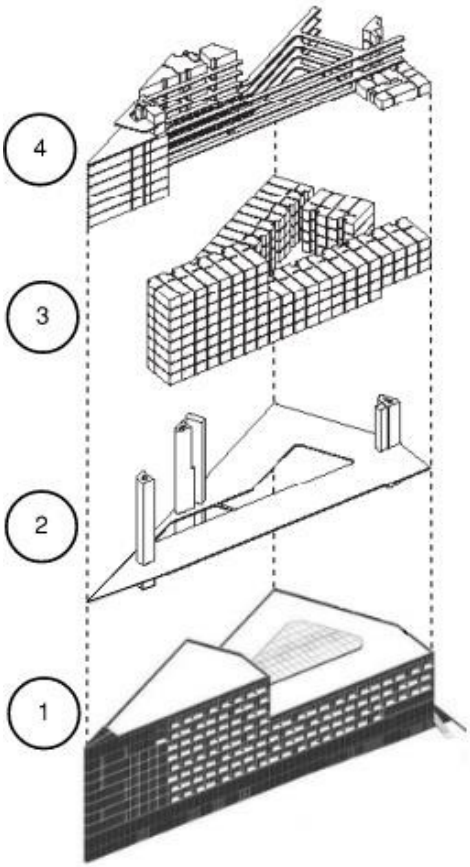

Figure A.2: Hotel Jakarta: Building extracted view (Derix 2018)

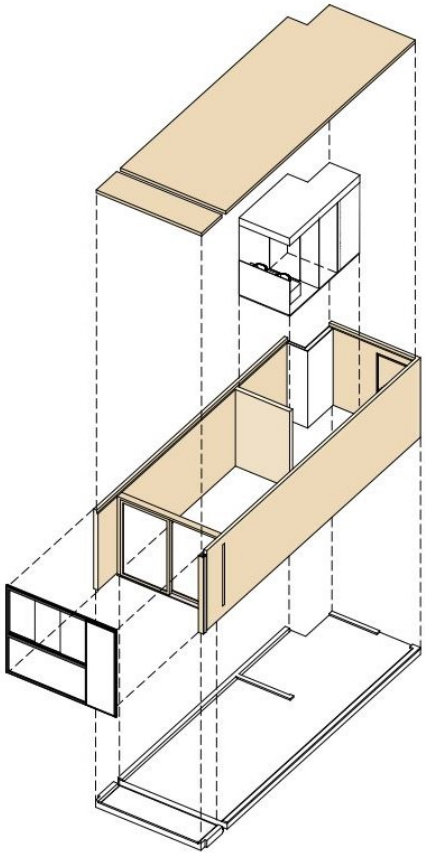

Figure A.3: Hotel Jakarta: Timber module extracted view (Derix 2018)

In Figure A.2 an exploded view is given of the building. In the second layer, the concrete cores and the construction of the concrete table are shown, providing stability for the timber modules. Portals supporting the concrete table are not shown. The third layer shows the configuration and varying

height over the cross-section of the building of the timber modules. The fourth layer shows additional structural components supporting, for example, the glass facade and the walkways inside the hotel. In Figure A.3 An exploded view of the timber module itself is given. The module is constructed of five prefabricated elements: concrete flooring, timber walls, window frame, a bathroom pod, and timber ceiling. The modules do not contribute to the global stability of the building, but the modules are self-stabilised. In addition, the walls function as load-bearing components, therefore the modules can be considered load-bearing modules. Concrete flooring was chosen for multiple reasons including fire safety, acoustics, intensive cleaning, and the presence of a wet bathroom pod.

Puukuoka One, Finland

In Finland, the Puukuoka complex, comprised of three wooden buildings, offers 186 single-family apartments. The buildings are six to eight stories high and construction was finished in respectively 2015, 2017 and 2018 for buildings Puukuoka One, Puukuoka Two and Puukuoka Three. Puukuoka One was the first eight-story wooden building constructed in Finland. The building is constructed with 116 prefabricated CLT modules made of Spruce creating 58 apartments. Each apartment is made of two modules: 'the room module' accommodates the living room, balcony, and bedroom, while the 'technical module' accommodates the bathroom, kitchen, and foyer area. The use of prefabricated modules allowed for the mechanical, electrical and plumbing (MEP) services to be integrated into the wall structure in the hallway making it easily accessible for maintenance purposes. The modules are manufactured in a local factory less than two hours from the construction site. Using prefabricated modules, the building time on site is cut down to six months per building.

Figure A.4: Puukuokka: Floorplan of the 4th floor (*EUMiesAward* n.d.)

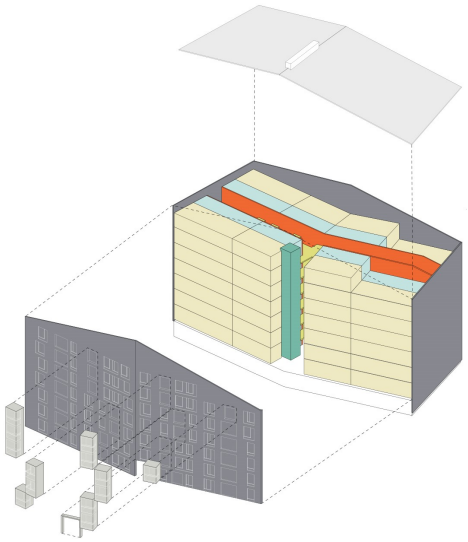

Figure A.5: Puukuokka axonometric diagram (*EUMiesAward* n.d.)

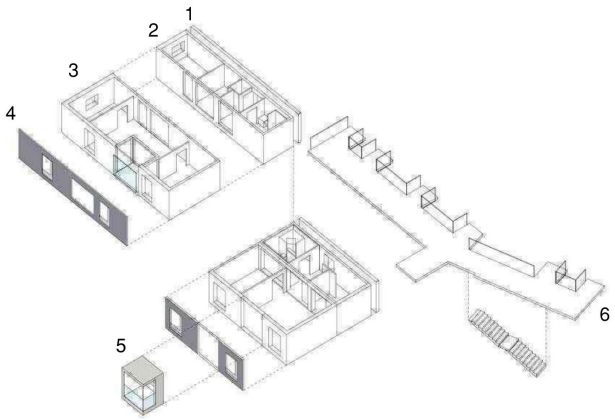

Figure A.6: Puukuokka modular unit (StoraEnso 2016)

The building has a concrete foundation with an indoor parking garage on the basement level. The rest of the load-bearing structure is made of massive wood integrated into the volumetric modules. This means that both the lateral forces and the vertical forces are transferred via the modules. A floorplan is shown in Figure A.4 in which the shear walls are indicated in red and the walls transferring only vertical forces shown in blue. In addition, the central elevator shaft is manufactured in timber and acts as a small core. In Figure A.6 the build-up of the modules is shown: 1) the wall for technical installations, 2) the technical module, 3) the room module, 4) the facade system with window frames, 5) the balcony with CLT structure, and 6) corridor with CLT slab.

Woodie student hostel, Germany

In 2017 the Woodie Student Hostel in Hamburg was opened. The building provides 371 student flats, making it the current largest residential building made of timber room modules. The modules are stacked up to six layers on top of an expressive table-like reinforce concrete structure. The ground floor structure and the three service cores are manufactured in conventional reinforced concrete with an additional outer shell of exposed concrete. The installation rate of the modules was twelve modules per day while the unique timber facade was mounted later. The total construction on-site was finished in ten months and the result is shown in Figure A.7.

Figure A.7: Woodie Student Hostel in Hamburg (Huß et al. 2019)

As mentioned the reinforced concrete table structure is responsible for carrying the stacked modules and providing stability to the building. More specifically the three concrete cores, which also house the elevator shafts and staircases, are designed to resist the horizontal loads. The three cores, to which the modules are attached for the transfer of horizontal forces, are shown in Figure A.8. The load-bearing parts of the module consist of five layered cross-laminated timber. With respect to fire safety, the load-bearing parts of the modules are designed to be fireproof in terms of load-bearing capacity, space enclosure, and thermal insulation for at least 90 minutes (REI 90). A computer drawing of the module can be seen in Figure A.10. The building sequence is depicted from right to left in Figure A.9. It starts with constructing the prefabricated concrete table structure and core. Subsequently, the modules were stacked and mounted to the concrete elements. Finally, the facade panels and roof are built, to conceal the outside of the monotonic CLT modules.

Figure A.8: Woodie Student Hostel: Floorplan of standard floor (Huß et al. 2019)

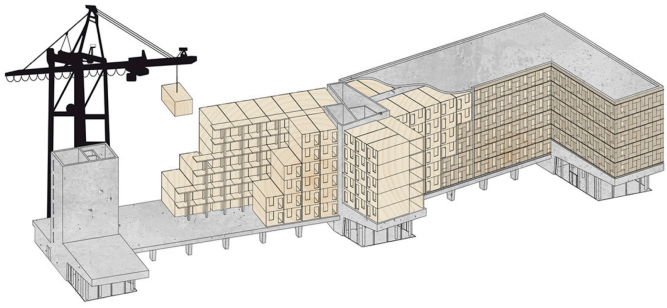

Figure A.9: Woodie Student Hostel: Building sequence (Kaufmann bausysteme n.d.)

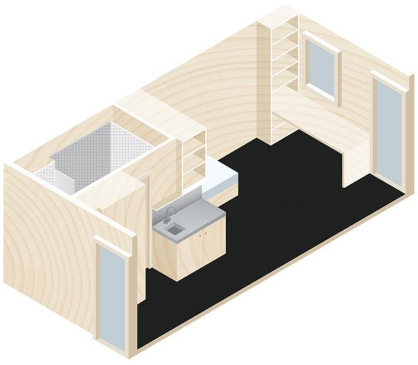

Figure A.10: Woodie modular unit (Kaufmann bausysteme n.d.)

Sara cultural center, Sweden

In Sweden, the partly modular building named Sara cultural center was delivered in 2021. The 20-story building combines a theatre, museum, art gallery, public library, conference and hotel. The part of the building of interest for the research is the hotel since it is composed of prefabricated solid CLT modules. The structure is 72.8 meters high and is made of both Glulam and CLT.

Figure A.11: Sara cultural center

The tower is constructed of 13 layers of CLT modules stacked between two elevator cores, one at each end of the tower, which are also made out of CLT. To accommodate the desired flexibility and openness of the ground floor beneath the hotel, the tower structure was essentially designed as if it were supported on stilts. The weight of all the stacked modules is transferred to the stilts via hybrid timber-steel trusses. In addition to the self-weight of the modules, they also carry the load of the facade and the corridor. An issue in the design was meeting the stability requirement for the tower, as the stiffness of the building was relatively low due to the lightweight of the timber. This was solved in two ways: The first was by integrating the posts within the four corners of the module and tying each module into those adjacent modules with four steel brackets to form a sort of structural lattice. The second was by adding two concrete slabs at the two top floors which adds weight and thus acts as a damper. This reduces the buildings' acceleration due to wind.

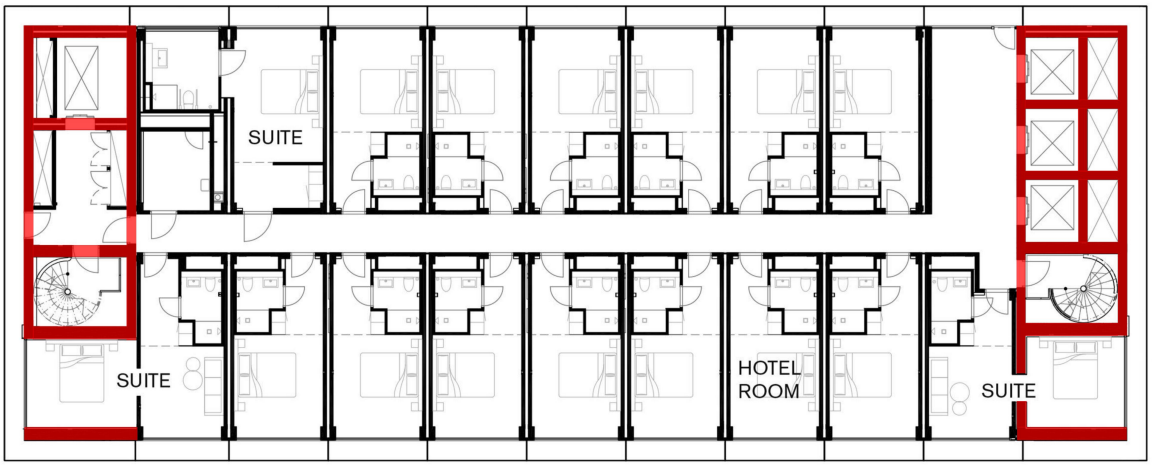

Figure A.12: Sara cultural center: Floorplan 9th floor

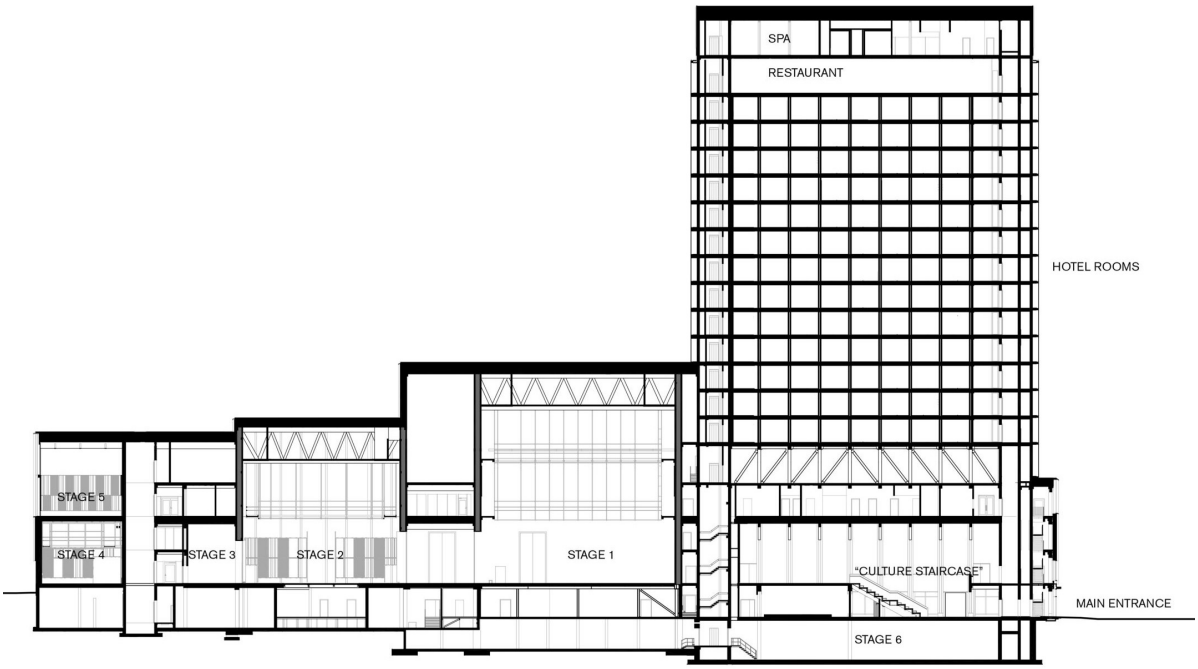

Figure A.13: Sara cultural center: Section

Figure A.14: Sara cultural center: Picture of the module in the factory

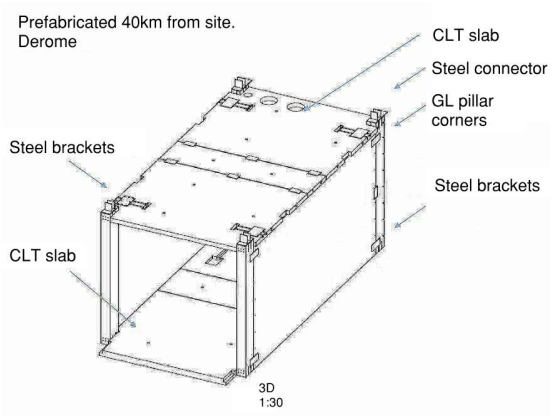

Figure A.15: Sara cultural center: Schematic drawing of the module

The corner-supported modules are entirely made of CLT and the dimensions of the posts do not vary over the height of the building for simplicity reasons. Consequently, almost all the modules are over-dimensioned as the load on the upper modules is lower than on the bottom modules. According to the architect: 'The reduced costs of lesser material for varied modules didn't outweigh the costs associated with additional complexity in engineering and construction.' With regard to fire safety, the CLT is over-dimensioned to include an additional 10-centimeter layer of CLT wrapped in insulation to meet the fire safety regulation in Sweden. In addition, each module is equipped with a sprinkler system for increased fire protection.

B

Calculations of the strength and stiffness of the connections

First an overview is given of all the inter-modular connections:

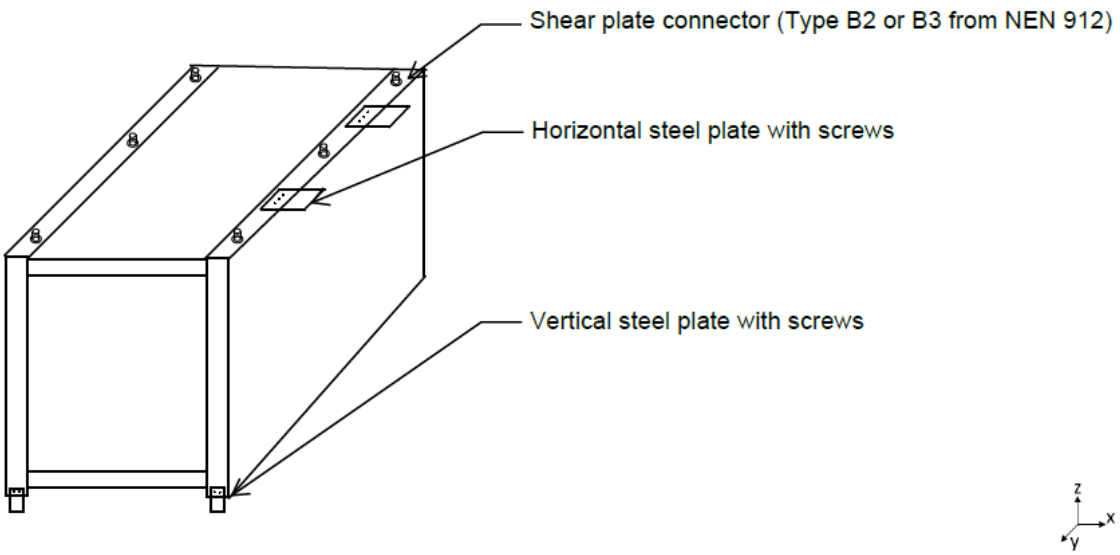

Figure B.1: Overview of the connections

B.1. Horizontal steel plate with screws

The first connection is the horizontal steel plate.

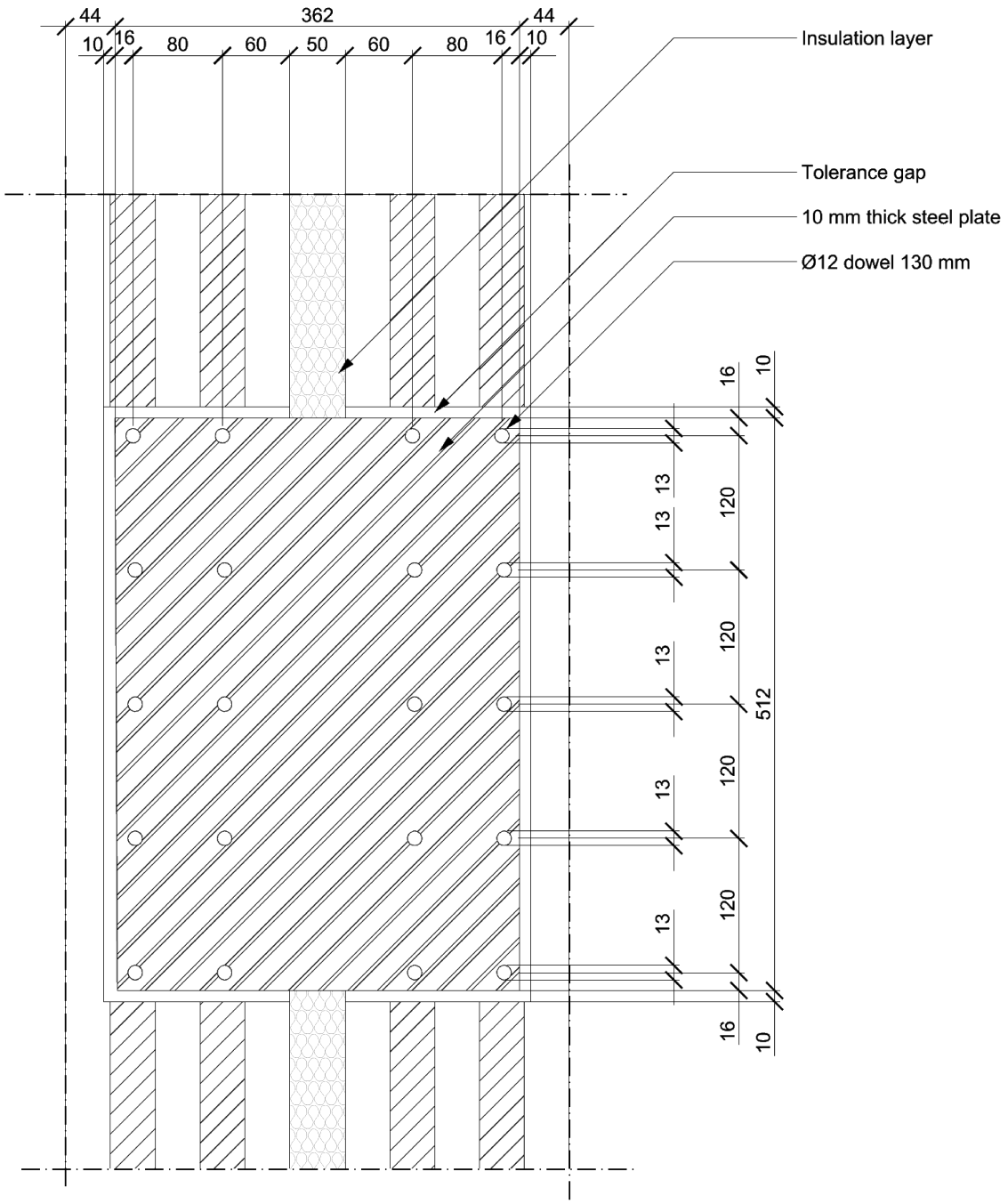

Figure B.2: Horizontal steel plate with screws

The following properties are used for the screws, plate and CLT:

Screw properties	Plate properties	CLT C30 properties
$l_{screw} = 120mm$	$t_{plate} = 10mm$	$\rho_k = 380kg/m^3$
$d_{screw} = 12mm$	$b_{plate} = 362mm$	$\rho_m = 460kg/m^3$
$d_0 = d_{screw} + 1 = 13mm$	$l_{plate} = 512mm$	$t_i = 40mm$
$f_{u,k} = 800N/mm^2$	$f_u = 355N/mm^2$	
$f_{y,k} = 640N/mm^2$	$E_s = 210GPa$	
$n_y = 5screws$		
$n_x = 2screws$		

B.1.1. Strength of the connection

The strength of the connection is given by the minimum value of the strength of:

- The dowels
- The steel plate

Steel to timber joint in single shear

The embedment strength parallel to the grain is:

$$f_{h,0,k} = 0,082 \cdot (1 - 0,01 \cdot d_{screw}) \cdot \rho_k = 0,082 \cdot (1 - 0,01 \cdot 12) \cdot 380 = 27,42MPa$$

The embedment strength perpendicular to the grain is:

$$f_{h,90,k} = \frac{f_{h,0.k}}{k_{90} \cdot \sin(\alpha)^2 + \cos(\alpha)^2} = \frac{27,42}{1,53 \cdot \sin(90)^2 + \cos(90)^2} = 17,92MPa$$

With:

$k_{90} = 1,35 + 0,015 \cdot d_{screw} = 1,35 + 0,015 \cdot 12 = 1,53$ for softwoods

The bending strength of the screw is:

$$M_{y,Rk} = 0,3 \cdot f_{u,k} \cdot d_{screw}^{2,6} = 0,3 \cdot 800 \cdot 12^{2,6} = 153490MPa$$

The strength of the steel-to-timber joint in single shear depends on the thickness of the steel plate as this determines the possible failure modes. The following five failure modes:

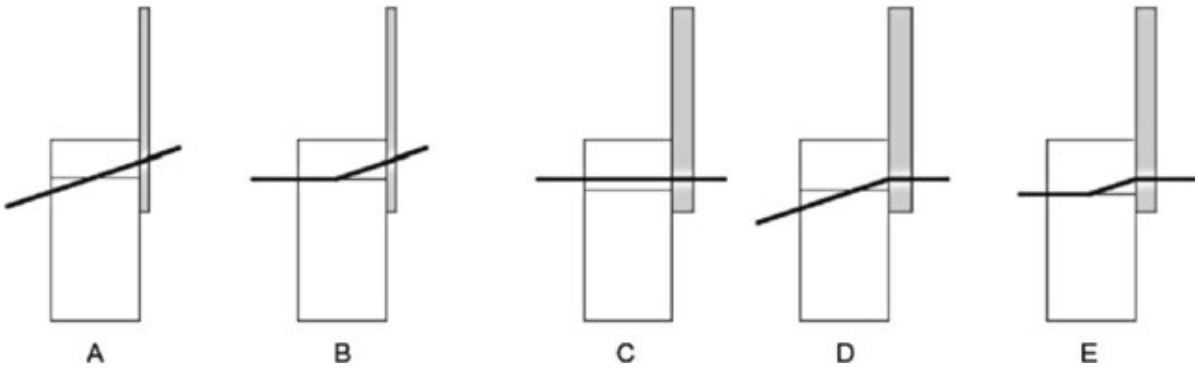

Figure B.3: Failure modes fasteners in single shear

For a timber-to-steel connection with thin plates ($t_{plate} \leq 0,5d_{screw}$) failure mechanisms (a) and (b) can occur. Thick steel plates ($t_{plate} < d_{screw}$) result in failure modes (c), (d) and (e). For this connection the plate is qualified as thick steel plate.

Thin steel plates:

$$F_{v,rk,A} = 0,4 \cdot f_{h,90,k} \cdot d_{screw} \cdot l_{screw} = 0,4 \cdot 17,92 \cdot 12 \cdot 120 = 10,3\ kN$$

$$F_{v,rk,B} = 1,15\ \sqrt{2 \cdot M_{y,Rk} \cdot f_{h,90,k} \cdot d_{screw}} + \frac{F_{ax,Rk}}{4} = 1,15\ \sqrt{2 \cdot 153491 \cdot 17,92 \cdot 12} + \frac{F_{ax,Rk}}{4} = 9,34\ kN$$

$$F_{v,rk,thin} = min(F_{v,rk,A}; F_{v,rk,B}) \ = \ min(10,3; 9,34) = 9,34\ kN$$

Thick steel plates:

$$F_{v,rk,C} = f_{h,90,k} \cdot l_{screw} \cdot \ d_{screw} = 17,92 \cdot 120 \cdot \ 12 = 25,8\ kN$$

$$F_{v,rk,D} = f_{h,90,k} \cdot l_{screw} \cdot d_{screw} \cdot \quad \left[\sqrt{2 + \frac{4 \cdot M_{y,Rk}}{f_{h,90,k} \cdot d_{screw} \cdot {l_{screw}}^2}} - 1\right] + \frac{F_{ax,Rk}}{4}$$
$$= 17,92 \cdot 120 \cdot 12 \cdot \left[\sqrt{2 + \frac{4 \cdot 153490}{17,92 \cdot 12 \cdot 120^2}} - 1\right] + \frac{F_{ax,Rk}}{4} = 12,46kN$$

$$F_{v,rk,E} = 2,3 \cdot \sqrt{2 \cdot M_{y,Rk} \cdot f_{h,90,k} \cdot d_{screw}} + \frac{F_{ax,Rk}}{4} = 2,3 \cdot \sqrt{2 \cdot 153490 \cdot 17,92 \cdot 12} + \frac{F_{ax,Rk}}{4} = 18,68kN$$

$$F_{v,rk,thick} = min(F_{v,rk,C}; F_{v,rk,D}; F_{v,rk,E}) \ = \ min(25,8; 12,46; 18,68) = 12,46\ kN$$

The design load per fastener is:

$$F_{v,rd} = k_{mod} \cdot \frac{F_{v,rk}}{\gamma_m} = 1,1 \cdot \frac{12,46}{1,3} = 10,54kN$$

Edge and space distances

For the definition see Figure 4.9. The end- and space distances for $d_{screw} = 12mm$ in CLT are given Table B.1.

Fastener type	Position	a_1	a_2	$a_{3,t}$	$a_{3,c}$	$a_{4,t}$	$a_{4,c}$
Self-tapping screws	Face	$48mm$	$30mm$	$72mm$	$72mm$	$72mm$	$30mm$
	Edge	$120mm$	$36mm$	$144mm$	$84mm$	$60mm$	$60mm$
Design	Edge	$120mm$	$80mm$	$-$	$>>$	$-$	$60mm$

Table B.1: Edge and space distance: Horizontal steel plate

The end- and space distances for $d_{screw} = 12mm$ in a steel plate are given in Table B.1.

	e_1	e_2	p_1	p_2
Required	$16mm$	$16mm$	$29mm$	$32mm$
Design	$16mm$	$16mm$	$120mm$	$80mm$

Table B.2: End and spacing distance: Horizontal steel plate connection

Steel plate strength buckling

The connection is loaded in compression to divide the lateral loads across all adjacent modules. Therefore buckling of the steel plate must be considered as a failure mode.

$$I_{plate} = \frac{1}{12} \cdot l_{plate} \cdot {t_{plate}}^3 \ = \frac{1}{12} \cdot 512 \cdot 10^3 = 42667\ \text{mm}^4$$

Buckling length is assumed to be the centre-to-centre distance between the inner screws. Then the Euler buckling load is given by:

$$N_{cr} = \frac{\pi^2 \cdot E_s \cdot I_{plate}}{{L_{cr}}^2} = \frac{\pi^2 \cdot 210000 \cdot 42667}{170^2} = 3060\ kN$$

$$A_{plate} = l_{plate} \cdot t_{plate} = 512 \cdot 10 = 5120\ \text{mm}^2$$

$$\lambda = \sqrt{\frac{A_{plate} \cdot f_y}{N_{cr}}} = \sqrt{\frac{5120 \cdot 355}{3060 \cdot 10^3}} = 0,77$$

$$\Phi = 0,5 \cdot [1 + \alpha \cdot (\lambda - 0,2) + \lambda^2] = 0,5 \cdot [1 + 0,49 \cdot (0,77 - 0,2) + 0,77^2] = 0,94$$

$$\chi = \frac{1}{\Phi + \sqrt{\Phi^2 - \lambda^2}} = \frac{1}{0,94 + \sqrt{0,94^2 - 0,77^2}} = 0,68$$

$$N_{b,rd} = \frac{\chi \cdot A_{plate} \cdot f_y}{\gamma_{M1}} = \frac{0,68 \cdot 2720 \cdot 355}{1} = 1236kN$$

Steel plate net area

The net area of the steel plate is:

$$A_{net} = (l_{plate} - n_y \cdot (1 + d)) \cdot t_{plate} = (512 - 5 \cdot (1 + 12)) \cdot 10 = 4340\ \text{mm}^2$$

$$N_{net,rd} = A_{net} \cdot f_y = 4340 \cdot 355 = 1540,7\ kN$$

Compressive strength calculation

The connection is designed to transfer compressive forces. The compressive strength of the plate is given by:

$$F_{v,rd} = min(N_{net,rd}; N_{b,rd}; F_{v,rd} \cdot n_x \cdot n_y) = min(1236; 1540,7; 10,54 \cdot 2 \cdot 5) = 105,4\ kN$$

This means that the screws govern the connection's strength.

Shear strength calculation

The connection is also designed to transfer shear forces. It should be noted that a shear force, does not only result in a normal force in the screws but also introduces a bending moment. It is assumed that the eccentricity of the shear force is equal to the distance between the centroidal axis of the screws. This is visualised in Figure B.4

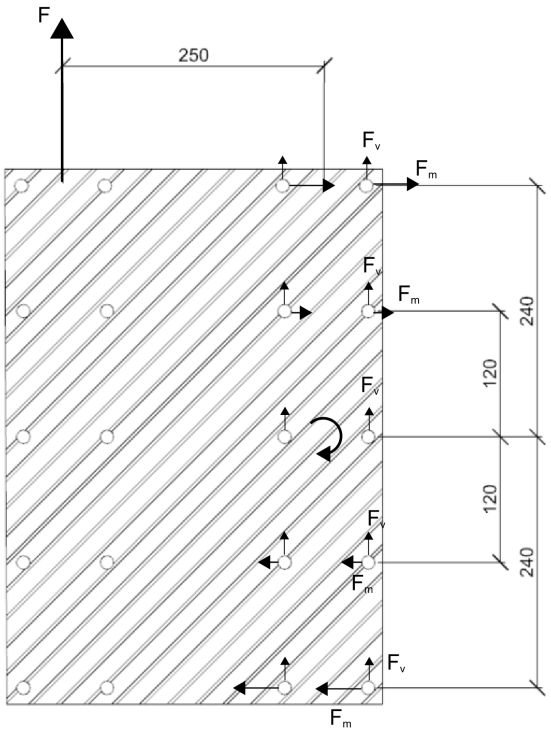

Figure B.4: Decomposition of the shearforce into F_v and F_m

$$M = e \cdot F = 0,25 \cdot F$$

Most stressed bolts are the outer ones. The force related to the moment and the distance r_i is:

$$F_m = \frac{r_3}{4 \cdot r_1^2 + 4 \cdot r_2^2 + 4 \cdot r_3^2} \cdot M = \frac{240}{4 \cdot 0^2 + 4 \cdot 120^2 + 4 \cdot 240^2} \cdot 0,25F = 0,2075F$$

$$F_v = \frac{n}{F} = \frac{10}{F} = 0.1F$$

Combining both the shear force and the normal force due to the bending moment results in the maximum shear stress that is allowed for the connection.

$$\sqrt{F_m^2 + F_v^2} = F_{v,rd} = \sqrt{(0,2075F)^2 + (0.1F)^2} = 10,54kN -> 0,23F = 10,54kN$$

Solving this for F results in a maximum shear force of $F = 45,83kN$.

In reality it is not solely a compressive force or purely a shear force acting on the connecting, but a combination of both. The normal force and shear force are therefore combined and compared to the resistance of the screws.

$$\sqrt{(F_m + F_n)^2 + F_v^2} = F_{e,d}$$

The connections in RFEM are checked for a combination of compression and shear. For the configurations 3x5, 4x8, 5x12 and 6x18 a unity check is calculated to verify the strength of the connection. The size of the diagonal was 7 mm by 7 mm which corresponds to the stiffness of Sikasil SG-20 as this was the only valid design. The outcome is presented in Table B.3.

	Horizontal steel plate with screws				
Configuration	Normal force [kN]	Shear y [kN]	$F_{e,d}$	$F_{r,d}$	U.C
3x5	11,22	2,3	1,62	10,54	0,15
4x8	13,22	1,88	1,72	10,54	0,16
5x12	15,04	1,72	1,87	10,54	0,18
6x18	16,35	1,63	1,98	10,54	0,19

Table B.3: Verification: Horizontal steel plate

It can be seen that the connections are highly over dimensioned. This was caused by the fact that the connections, where not allowed to be governing for the design. In addition, the connections were designed in an early stage of the project, where the load-bearing capacity of the TGSW was assumed to be much higher. After several reductions of the load-bearing capacity of the TGSW, the connections were not adjusted, hence the overcapacity.

B.1.2. Stiffness of the connection

The stiffness of a single screw for a timber-to-steel connection in SLS is:

$$K_{ser} = 2 \cdot {\rho_m}^{1,5} \cdot \frac{d}{23} = 2 \cdot 460^{1,5} \cdot \frac{12}{23} = 10294 \; N/mm$$

The total stiffness of the connection can be derived by applying the stiffness in parallel for the screws on one side of the connection and in series with the screws on the other side of the connection:

$$K_{ser,total} = \frac{1}{\frac{1}{n \cdot K_{ser}} + \frac{1}{n \cdot K_{ser}}} = \frac{1}{\frac{1}{10 \cdot 10924} + \frac{1}{10 \cdot 10924}} = 51474 \; N/mm$$

The stiffness of a single screw for a timber-to-steel connection in ULS is:

$$K_u = \frac{2}{3} \cdot K_{ser} = \frac{2}{3} \cdot 10294 N/mm$$

The total stiffness is:

$$K_{u,total} = \frac{2}{3} \cdot K_{ser,total} = \frac{2}{3} \cdot 51474 = 34316 N/mm$$

B.2. Vertical steel plate with screws

The connection with dimensions is presented in Figure B.5

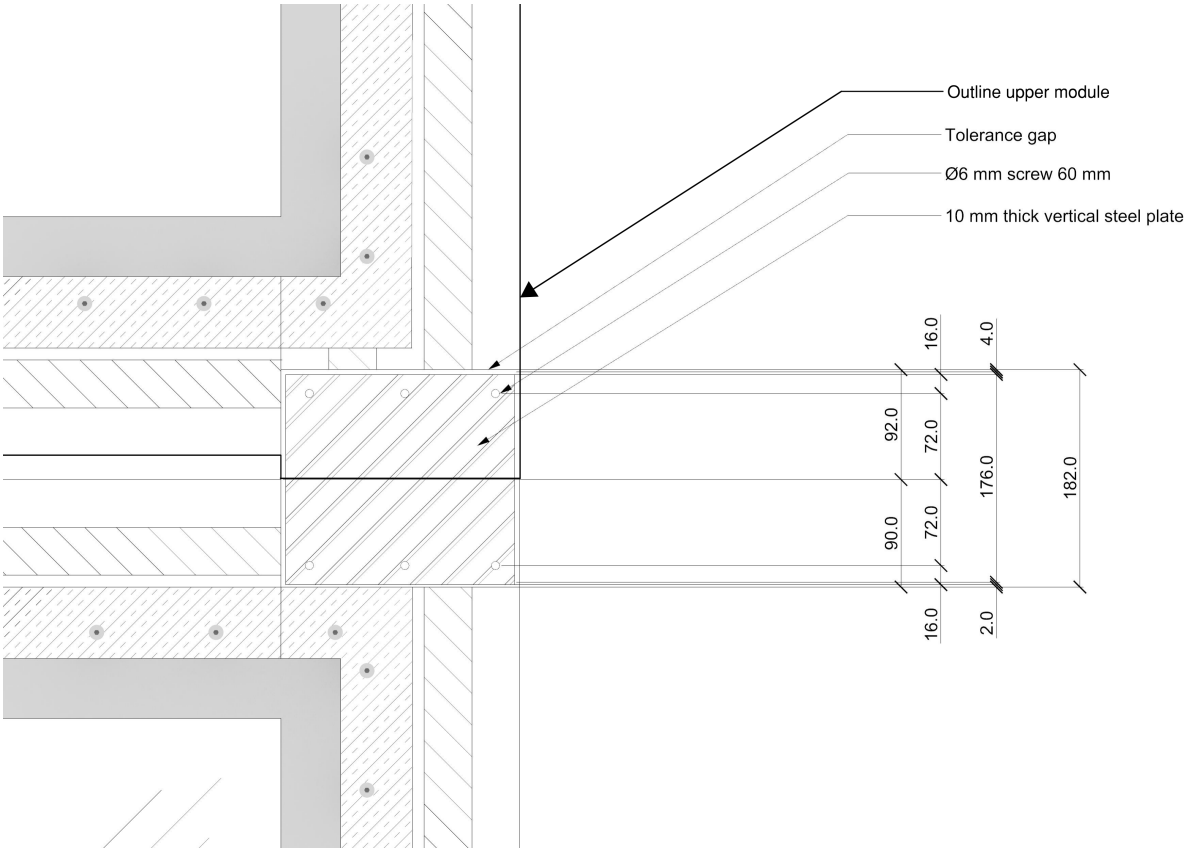

Figure B.5: Vertical steel plate with screws

The following properties are used for the screws, steel plate, and CLT.

Screw properties	Plate properties	CLT C30 properties
$l_{screw} = 60mm$	$t_{plate} = 10mm$	$\rho_k = 380kg/m^3$
$d_{screw} = 6mm$	$b_{plate} = 192mm$	$\rho_m = 460kg/m^3$
$d_0 = d_{screw} + 1 = 7mm$	$l_{plate} = 164mm$	$t_i = 40mm$
$fu, k = 800N/mm^2$	$f_u = 355N/mm^2$	
$fy, k = 640N/mm^2$	$E_s = 210GPa$	
$n_y = 3screws$		
$n_x = 1screws$		

B.2.1. Strength of the connection

Steel to timber joint in single shear

The embedment strength parallel to the grain is:

$$f_{h,0,k} = 0,082 \cdot (1 - 0,01 \cdot d_{screw}) \cdot \rho_k = 0,082 \cdot (1 - 0,01 \cdot 6) \cdot 380 = 29,29MPa$$

The embedment strength perpendicular to the grain is:

$$f_{h,\alpha,k} = \frac{f_{h,0.k}}{k_{90} \cdot \sin(\alpha)^2 + \cos(\alpha)^2} = \frac{29,29}{1,44 \cdot \sin(90)^2 + \cos(90)^2} = 20,34MPa$$

With:

$k_{90} = 1,35 + 0,015 \cdot d_{screw} = 1,35 + 0,015 \cdot 6 = 1,44$ for softwoods

The bending strength of the screw is:

$$M_{y,Rk} = 0,3 \cdot f_{u,k} \cdot d_{screw}^{2,6} = 0,3 \cdot 800 \cdot 6^{2,6} = 25316MPa$$

The strength of the steel-to-timber joint in single shear depends on the thickness of the steel plate as this determines the possible failure modes. The following five failure modes:

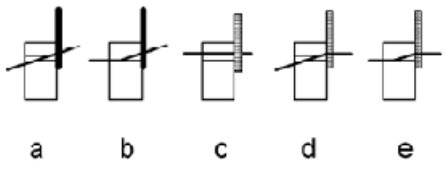

Figure B.6: Failure modes fasteners in single shear

For a timber-to-steel connection with thin plates (t <= 0,5d) failure mechanisms (a) and (b) can occur. Thick steel plates (t<d) result in failure modes (c), (d) and (e). As the thickness of the steel plate is between thin and thick plates, linear interpolation between the governing failure modes is applied. For thin plates the characteristic strength is calculated:

$$F_{v,rk,A} = 0,4 \cdot f_{h,90,k} \cdot d_{screw} \cdot l_{screw} = 0,4 \cdot 18,70 \cdot 10 \cdot 100 = 7,48\ kN$$

$$F_{v,rk,B} = 1,15\ \sqrt{2 \cdot M_{y,Rk} \cdot f_{h,90,k} \cdot d_{screw}} + \frac{F_{ax,Rk}}{4} = 1,15\ \sqrt{2 \cdot 95545 \cdot 18,70 \cdot 10} + \frac{F_{ax,Rk}}{4} = 6,87\ kN$$

For thick plates the characteristic strength is calculated:

$$F_{v,rk,C} = f_{h,90,k} \cdot l_{screw} \cdot\ d_{screw} = 18,70 \cdot 100 \cdot\ 10 = 18,70\ kN$$

$$F_{v,rk,D} = f_{h,90,k} \cdot l_{screw} \cdot d_{screw} \cdot \left[\sqrt{2 + \frac{4 \cdot M_{y,Rk}}{f_{h,90,k} \cdot d_{screw} \cdot {l_{screw}}^2}} - 1\right] + \frac{F_{ax,Rk}}{4}$$
$$= 18,70 \cdot 100 \cdot 10 \cdot \left[\sqrt{2 + \frac{4 \cdot 95545}{18,70 \cdot 10 \cdot 100^2}} - 1\right] + \frac{F_{ax,Rk}}{4} = 9,06kN$$

$$F_{v,rk,E} = 2,3 \cdot \sqrt{2 \cdot M_{y,Rk} \cdot f_{h,90,k} \cdot d_{screw}} + \frac{F_{ax,Rk}}{4} = 2,3 \cdot \sqrt{2 \cdot 95545 \cdot 18,70 \cdot 10} + \frac{F_{ax,Rk}}{4} = 13,75kN$$

The characteristic strength of the connection assuming thin steel plates is:

$$F_{v,rk,thin} = min(F_{v,rk,A}; F_{v,rk,B}) = min(7,48; 6,87) = 6,87\ kN$$

$$F_{v,rk,thick} = min(F_{v,rk,C}; F_{v,rk,D}; F_{v,rk,E}) = min(18,70; 9,06; 13,75) = 9,06\ kN$$

Linear interpolation between 0,5 d_{screw} and d_{screw} results in:

$$F_{v,rk} = F_{v,rk,thin} + \frac{F_{v,rk,thick} - F_{v,rk,thin}}{d_{screw} - 0,5 \cdot d_{screw}} \cdot (t_{plate} - 0,5 \cdot d_{screw}) =$$
$$9,34 + \frac{12,46 - 9,34}{12 - 0,5 \cdot 12} \cdot (10 - 0,5 \cdot 12) = 9,06kN$$

The design load per fastener is:

$$F_{v,rd} = k_{mod} \cdot \frac{F_{v,rk}}{\gamma_m} = 1,1 \cdot \frac{9,06}{1,3} = 7,67kN$$

B.2.2. Edge and spacings

For the definition see Figure 4.7. The end- and space distances for $d_{screw} = 6mm$ in CLT are given in Table B.4

Fastener type	Position	a_1	a_2	$a_{3,t}$	$a_{3,c}$	$a_{4,t}$	$a_{4,c}$
Self-tapping screws	Face	$24mm$	$15mm$	$36mm$	$36mm$	$36mm$	$15mm$
	Edge	$60mm$	$18mm$	$72mm$	$42mm$	$30mm$	$30mm$
Design	Edge	$70mm$	$29mm$	$72mm$	$-$	$-$	$30mm$

Table B.4: Edge and space distance: Vertical steel plate connection

Steel plate net area

The net area of the steel plate is:

$$A_{net} = (b_{plate} - n_x \cdot (1+d)) \cdot t_{plate} = (192 - 3 \cdot (1+10)) \cdot 10 = 1590 \text{ mm}^2$$

$$N_{net,rd} = A_{net} \cdot f_y = 1590 \cdot 355 = 565\ kN$$

Tensile strength calculation

The connection is designed to transfer compressive forces. The compressive strength of the plate is given by:

$$F_{v,rd} = min(N_{net,rd}; F_{v,rd} \cdot n_x) = min(565; 7,67 \cdot 3) = 23\ kN$$

This means that the screws govern the connection's strength.

B.2.3. Stiffness of the connection

The stiffness of a single screw for a timber-to-steel connection in SLS is:

$$K_{ser} = 2 \cdot {\rho_m}^{1,5} \cdot \frac{d}{23} = 2 \cdot 460^{1,5} \cdot \frac{10}{23} = 8579\ N/mm$$

The total stiffness of the connection can be derived by applying the stiffness in parallel for the screws on one side of the connection and in series with the screws on the other side of the connection:

$$K_{ser,total} = \frac{1}{\frac{1}{n \cdot K_{ser}} + \frac{1}{n \cdot K_{ser}}} = \frac{1}{\frac{1}{3 \cdot 8579} + \frac{1}{3 \cdot 8579}} = 12868,5\ N/mm$$

The stiffness of a single screw for a timber-to-steel connection in ULS is:

$$K_u = \frac{2}{3} \cdot K_{ser} = \frac{2}{3} \cdot 5719 N/mm$$

The total stiffness is:

$$K_{u,totoal} = \frac{2}{3} \cdot K_{ser,total} = \frac{2}{3} \cdot 51474 = 8579 N/mm$$

B.3. Shear plate connector

The third connection is the shear plate connector and is shown in Figure B.7 .

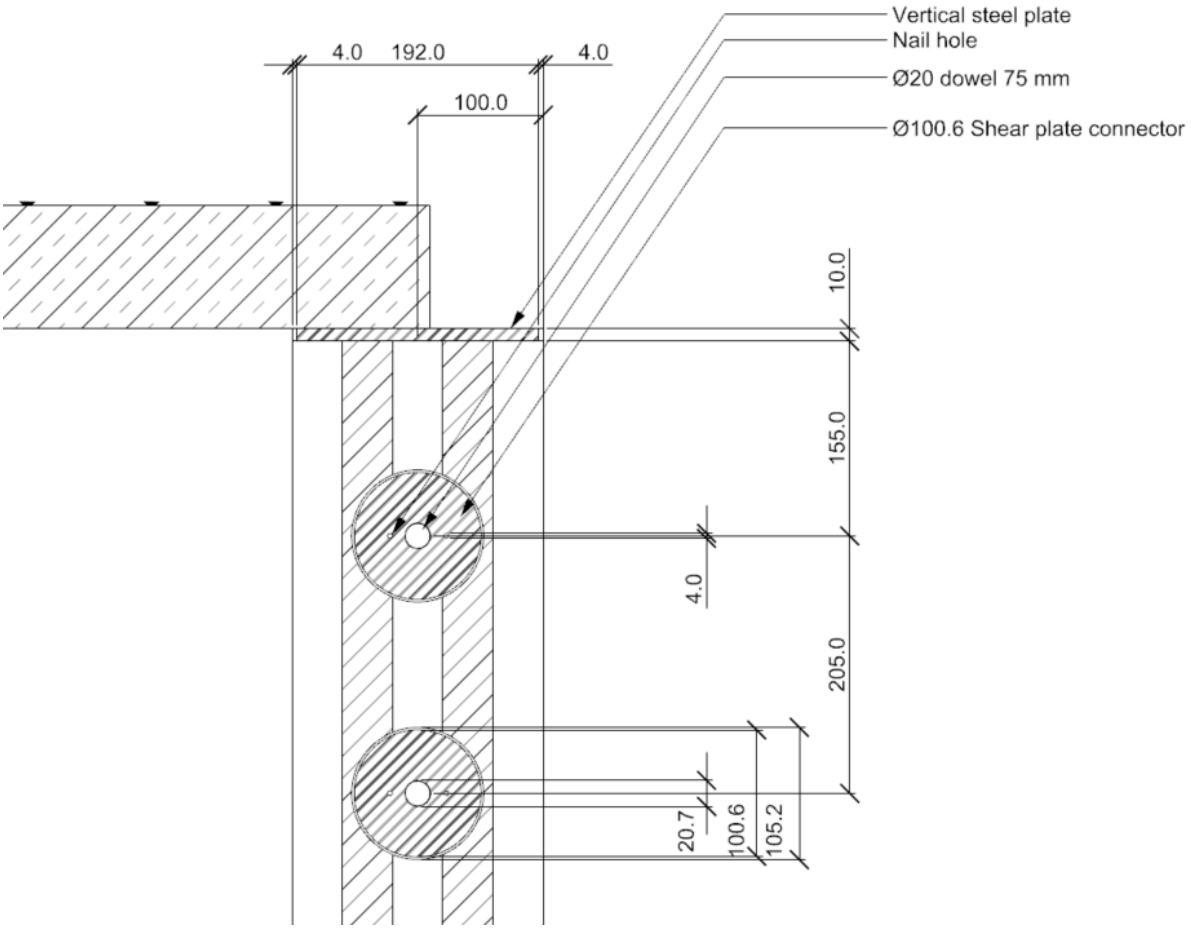

Figure B.7: Shear plate connector

The following properties are used:

Shear plate properties	Dowel properties	CLT C30 properties
$d_{shearplate} = 102mm$	$t_{dowel} = 20mm$	$\rho_k = 380kg/m^3$
$t_{shearplate} = 15,7mm$	$l_{dowel} = 75mm$	$\rho_m = 460kg/m^3$
	$fy,k = 640N/mm^2$	$t_i = 40mm$
	$fu,k = 800N/mm^2$	

B.3.1. Strength of the connection

$$F_{v,\alpha,Rk} = \frac{F_{v,Rk}}{k_{90} \cdot \sin(\alpha)^2 + \cos(\alpha)^2} = \frac{39,16}{1,402 \cdot \sin(90)^2 + \cos(90)^2} = 27,93kN$$

Where:

$$k_{90} = 1,3 + 0,001 \cdot d_c = 1,3 + 0,001 \cdot 102 = 1,402$$

$$F_{v,0,Rk} = min \begin{cases} k_1 \cdot k_2 \cdot k_3 \cdot k_4 \cdot 35 \cdot d_c^{1,5} = 1 \cdot 1 \cdot 1,086 \cdot 1 \cdot 35 \cdot 102^{1,5} = 39,16kN \\ k_1 \cdot k_3 \cdot h_e \cdot 31,5 \cdot d_c = 1 \cdot 1,086 \cdot 15,7 \cdot 31,5 \cdot 102 = 54,78kN \end{cases} = 39,16kN$$

Where:

$$k_1 = min \begin{cases} 1 \\ \frac{t_1}{3h_c} = \frac{50}{3 \cdot 15,7} = 1,06 \end{cases} = 1$$

k_2 applies for a loaded end ($-30° \leq \alpha \leq 30°$):

$$k_2 = min \begin{cases} k_a = 1,0 \\ \frac{a_{3,t}}{2d_c} = \frac{250}{204} = 1,22 \end{cases} = 1$$

$$k_a = \begin{cases} 1,25 & \text{for connections with one connector per shear plane} \\ 1,0 & \text{for connections with more than one connector per shear plane} \end{cases} = 1$$

For other values of α, $k_2 = 1$.

$$k_3 = min \begin{cases} 1,5 \\ \frac{\rho_k}{350} = \frac{380}{350} = 1,086 \end{cases} = 1,086$$

$$k_4 = \begin{cases} 1,0 & \text{for timber-to-timber connections} \\ 1,1 & \text{for steel-to-timber connections} \end{cases} = 1$$

The design load per fastener is:

$$F_{v,rd} = k_{mod} \cdot \frac{F_{v,rk}}{\gamma_m} = 1,1 \cdot \frac{27,93}{1,3} = 23,63kN$$

The shear force in both directions is combined by vector addition:

$$F_{ed} = \sqrt{{V_x}^2 + {V_y}^2}$$

Taking into account shear forces act in two directions and their magnitude don't necessarily need to be the same, the direction of the resultant shear force may vary. The strength of the timber is evaluated with respect to its angle perpendicular to the grain. As this angle might change, this also effects the strength of the timber, and thus the unity check. For instance, an angle closer parallel to the grain would have an positive influence the strength capacity of the timber ($f_{h,\alpha,k}$). Nevertheless, this effect is disregarded as the connection already results in a unity check far below 1. Therefore this is a conservative outcome. The RFEM-model is used to derive the maximum shear forces present in the connections. For the configurations 3x5, 4x8, 5x12 and 6x18 a unity check is calculated to verify the strength of the connection. The size of the diagonal was 7 mm by 7 mm which corresponds to the stiffness of Sikasil SG-20 as this was the only valid design. The F, rd-part is times two, since there are two shear plate connectors at each edge of the module. The outcome is presented in Table B.5

Shear plate connector					
Configuration	Shear x [kN]	Shear y [kN]	$F_{e,d}$	F, v, rd	U.C
3x5	7,50	8,21	11,12	47,26	0,24
4x8	8,73	11,94	14,79	47,26	0,31
5x12	9,56	15,63	18,32	47,26	0,39
6x18	9,77	19,24	21,57	47,26	0,46

Table B.5: Verification: Shear plate connector

B.3.2. Stiffness of the connection

$$K_{ser} = 2 \cdot \rho_m \cdot \frac{d_c}{4} = 2 \cdot 460 \cdot \frac{102}{4} = 23460N/mm$$

The total stiffness of the connection can be derived by multiplying with a factor 2, as two shear plate connectors are used.

$$K_{ser,total} = 2 \cdot K_{ser} = 2 \cdot 23460N/mm = 46920N/mm$$

Comparing this to other mechanical fasteners, this results in a stiff connection considering only two dowels are used. In case the density of the connected timber elements differ, Equation 4.14 can be used to calculate ρ_m.

$$\rho_m = \sqrt{\rho_{m,1} \cdot \rho_{m,2}}$$

The stiffness of a single shear plate connector in ULS situation is given by:

$$K_u = \frac{2}{3} \cdot K_{ser} = \frac{2}{3} \cdot 23460 = 15640 N/mm$$

For the total connection, the stiffness in ULS is:

$$K_{u,total} = \frac{2}{3} \cdot K_{ser,total} = \frac{2}{3} \cdot 46920 = 31280 N/mm$$

B.4. TGSW to module connection

The TGSW is connected to the CLT-module with screws. Dependend on the screw spacing the total capacity of the connection is determined. In this section the $F_{v,rd}$ of a single screw is calculated.

Timber to timber connection

The following properties are used for the screws, CLT and LVL:

Screw properties	LVL properties	CLT C30 properties
$l_{screw} = 160mm$	$\rho_k = 380kg/m^3$	$\rho_k = 380kg/m^3$
$l_{screw,CLT} = 80mm$	$\rho_m = 460kg/m^3$	$\rho_m = 460kg/m^3$
$l_{screw,LVL} = 80mm$		$t_i = 40mm$
$d_{screw} = 6mm$		
$d_0 = d_{screw} + 1 = 7mm$		
$f_{u,k} = 800N/mm^2$		
$f_{y,k} = 640N/mm^2$		

The embedment strength of CLT parallel to the grain is:

$$f_{h,0,k} = 0,082 \cdot (1 - 0,01 \cdot d_{screw}) \cdot \rho_k = 0,082 \cdot (1 - 0,01 \cdot 6) \cdot 380 = 29,29 MPa$$

The embedment strength of CLT perpendicular to the grain is:

$$f_{h,\alpha,k} = \frac{f_{h,0.k}}{k_{90} \cdot \sin(\alpha)^2 + \cos(\alpha)^2} = \frac{29,29}{1,44 \cdot \sin(90)^2 + \cos(90)^2} = 20,34 MPa$$

With:

$k_{90} = 1,35 + 0,015 \cdot d_{screw} = 1,35 + 0,015 \cdot 6 = 1,44$ for softwoods

The embedment strength of LVL parallel to the grain is:

$$f_{h,0,k} = 0,082 \cdot (1 - 0,01 \cdot d_{screw}) \cdot \rho_k = 0,082 \cdot (1 - 0,01 \cdot 6) \cdot 480 = 36,99 MPa$$

The embedment strength of LVL perpendicular to the grain is:

$$f_{h,\alpha,k} = \frac{f_{h,0.k}}{k_{90} \cdot \sin(\alpha)^2 + \cos(\alpha)^2} = \frac{36,99}{1,39 \cdot \sin(90)^2 + \cos(90)^2} = 20,34 MPa$$

With:

$k_{90} = 1,30 + 0,015 \cdot d_{screw} = 1,30 + 0,015 \cdot 6 = 1,39$ for softwoods

The bending strength of the screw is:

$$M_{y,Rk} = 0,3 \cdot f_{u,k} \cdot d_{screw}^{2,6} = 0,3 \cdot 800 \cdot 6^{2,6} = 25316MPa$$

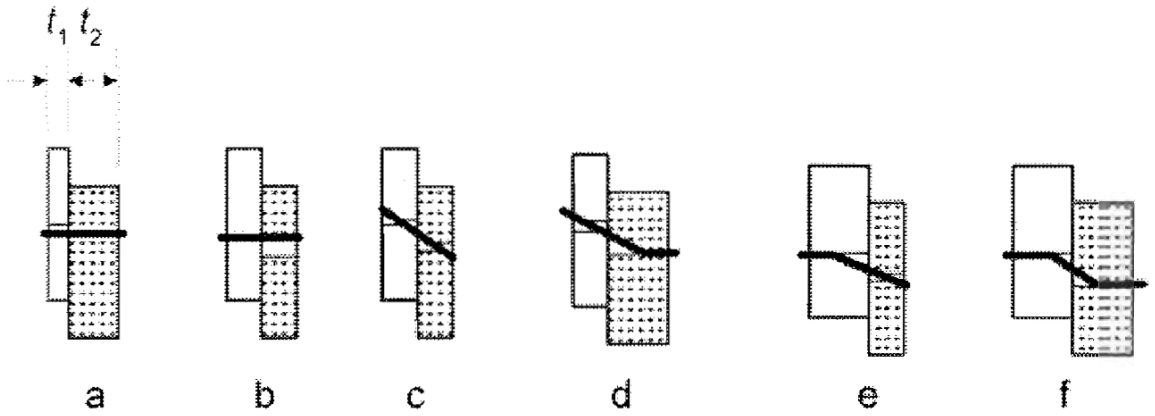

Figure B.8: Failure modes timber to timber connection

$$F_{v,Rk} = \text{min} \begin{cases} f_{h1,k} \cdot t_1 \cdot d & (a) \\ f_{h2,k} \cdot t_2 \cdot d & (b) \\ \frac{f_{h1,k} \cdot t_1 \cdot d}{1+\beta}[\sqrt{\beta + 2\beta^2[1 + \frac{t_2}{t_1} + \frac{t_2}{t_1}^2] + \beta^3(\frac{t_2}{t_1})^2} - \beta(1 + \frac{t_2}{t_1})] + \frac{F_{ax,Rk}}{4} & (c) \\ 1,05\frac{f_{h1,k} \cdot t_1 \cdot d}{2+\beta}[\sqrt{2\beta(1+\beta) + \frac{4\beta(2+\beta)M_{y,Rk}}{f_{h,1,k} \cdot d \cdot t_1^2}} - \beta] + \frac{F_{ax,Rk}}{4} & (d) \\ 1,05\frac{f_{h1,k} \cdot t_2 \cdot d}{1+2\beta}[\sqrt{2\beta^2(1+\beta) + \frac{4\beta(1+2\beta)M_{y,Rk}}{f_{h,1,k} \cdot d \cdot t_2^2}} - \beta] + \frac{F_{ax,Rk}}{4} & (e) \\ 1,15\sqrt{\frac{2\beta}{1+\beta}}\sqrt{2M_{y,Rk} \cdot f_{h,1,k} \cdot d} + \frac{F_{ax,Rk}}{4} & (f) \end{cases}$$

$$= \begin{cases} 20,34 \cdot 80 \cdot 6 = 9763,47kN \\ 26,62 \cdot 80 \cdot 6 = 17759,2kN \\ \frac{20,34 \cdot 80 \cdot 6}{1+1,31}[\sqrt{1,31 + 2 \cdot 1,31^2[1 + \frac{80}{80} + \frac{80}{80}^2] + 1,31^3(\frac{80}{80})^2} - 1,31 + \frac{80}{80})] + \frac{F_{ax,Rk}}{4} = 4655,8kN \\ 1,05\frac{20,34 \cdot 80 \cdot 6}{2+1,31}[\sqrt{2 \cdot 1,31(1+1,31) + \frac{4 \cdot 1,31(2+1,31)25316}{20,34 \cdot 6 \cdot 80^2}} - 1,31] + \frac{F_{ax,Rk}}{4} = 3907,5kN \\ 1,05\frac{20,34 \cdot 80 \cdot 6}{1+2 \cdot 1,31}[\sqrt{2 \cdot 1,31^2(1+1,31) + \frac{4 \cdot 1,31(1+2 \cdot 1,31)25316}{20,34 \cdot 6 \cdot 80^2}} - 1,31] + \frac{F_{ax,Rk}}{4} = 3907,5kN \\ 1,15\sqrt{\frac{2 \cdot 1,31}{1+1,31}}\sqrt{2 \cdot 25316 \cdot 20,34 \cdot 6} + \frac{F_{ax,Rk}}{4} = 3043,8kN \end{cases} = 3043,8kN$$

Where:

$$\beta = \frac{f_{h,2,k}}{f_{h,1,k}} = \frac{26,62}{20,34} = 1,31 \quad \text{(B.1)}$$

The design load per fastener is:

$$F_{v,rd} = k_{mod} \cdot \frac{F_{v,rk}}{\gamma_m} = 1,1 \cdot \frac{3043,8}{1,3} = 2575,5kN$$

C

Appendix C: Verification of the FEM model

C.1. Analytical verification of the FEM model

To verify the results of the FEM model, analytical calculations are made to compare the results. Different levels of simplification are used to see the influence of each modelling choice.

C.1.1. Analytical solution vs RFEM solution with rigid connections and rigid floors

The building can be schematised as clamped Timoshenko beams with a bending stiffness EI and shear stiffness GA. The beams are coupled by the connections splitting the load equally over 'n' number of modulin case rigid links are used as connections. Formulas used for the shear beam which is clamped at one edge:

$$k \cdot \frac{d^2w}{dx^2} = -q \tag{C.1}$$

Solving for the boundary conditions:

- at x = 0 -> w = 0
- at x = L -> V = 0

The result is:

$$w_{shear} = \frac{q \cdot x \cdot (2L - x)}{2GA} \tag{C.2}$$

For the diagonals, which are 7,0 mm x 7,0 mm rectangles made of steel, the stiffness can be derived by the equivalent diagonal theory. This results in a GA of 7275 kN or a k of 2425 N/mm.

Formulas used for the bending beam which is clamped at one edge:

$$EI \cdot \frac{d^4w}{dx^4} = q \tag{C.3}$$

solving for the boundary conditions:

- at x = 0 -> w = 0 and ϕ = 0
- at x = L -> M = 0 and V = 0

The result is:

$$w_{bending} = \frac{q * L^4}{8 \cdot EI \cdot n} \tag{C.4}$$

The stiffness is derived by looking at a single module. A section of the module is used as a cross section for the stiffness of the 'beam'. The stiffness if given by:

$$EI = E_{equivalent,shear} \cdot \frac{1}{12} \cdot b \cdot ((w + h)^3 - (w - h)^3) \tag{C.5}$$

The E-modulus of the cross section is the E_y of the timber CLT panel.

The torsion effect is considered because the shear wall is placed asymmetrically. The distributed torsional moment is given by the eccentricity of the windload related to the shear centre of the building. In this case the eccentricity is 5 meter. This results in a torsional moment of 150 kN. The steel plates on top of the modules provide a shear connection meaning that the torsional moment is divided by the width of the building. The torsional moment is resisted by the timber walls perpendicular to the windload. The torsional moment results in a distributed load on the side of the timber walls. This simplifies to a shear wall loaded by a distributed load. The deflection of the shear wall is presented in Equation C.2 The deflection of the shear wall in x direction results in a rotation, this rotation causes the building an additional deflection in y-direction. The rotation and deflection are given by:

$$\phi = 2 \cdot w_x/(n * 3000 + (n-1) * 50) \tag{C.6}$$

$$w_{y,torsion} = \phi \cdot 10000 \tag{C.7}$$

Comparing the results of the analytical calculations to the results in RFEM indicate accurate results. The difference is presented in Table C.1:

Configuration	u_{shear} [mm]	$u_{bending}$ [mm]	$u_{torsion}$ [mm]	$u_{analytical}$ [mm]	$u_{RFEM,rigidfloor/connection}$ [mm]	Difference [%]
3x5	7,12	0,02	0,1	7,79	7,8	0,13
4x8	9,4	0,05	0,06	9,52	9,6	0,84
5x12	10,82	0,1	0,02	10,94	11,1	1,45
6x18	11,13	0,15	0,03	11,31	11,4	0,79

Table C.1: Deflection from analytical calculations vs deflection vs RFEM-model

C.1.2. RFEM analysis of the connections stiffness and floor stiffness

In the previous section, the connection stiffness and floor stiffness was not included in the RFEM model, as this enables the results to be verified with hand calculations. For a better approximation of the building, those aspects should also be included. As these aspects also introduce effects, based on redistribution of forces, which can't be checked with simple hand calcuculations. Those effects will be described in a qualitative way and quantified by the RFEM model. First, the floor stiffness is introduced, after which also the stiffness of the connections is considered.

RFEM model including floor stiffness excluding connection stifffness

An infinite floor stiffness prevents the floor from bending. As the floor is hingedly connected to the walls, the walls can only deform equally over the cross-section. This equal deformation, enables full use of the wall cross-section. This is also reflected in the calculation of the bending stiffness EI calculation. In reality, the floor is not infinitely stiff but can bend. This bending results in a non-uniform deflection of the wall due to a point load. In other words, not the full cross-section of the wall is used. This causes extra deformation as parts of the wall are more heavily loaded, compared to others. The effect results in an increase of roughly 8 percent deformation compared to an infinitely stiff floor.

Configuration	$u_{RFEM,rigidfloor/connection}$ [mm]	$u_{RFEM,rigidconnection}$ [mm]	Difference [%]
3x5	7,8	8,3	6,2
4x8	9,6	10,2	6,1
5x12	11,1	12	7,8
6x18	11,4	12,5	9,2

Table C.2: Difference in deflection due to rigid floors

RFEM model including floor stiffness and connection stifffness

Transferring forces from one module to another, both horizontally and vertically, is done via the connections. Due to the loading of the connection the connection deforms slightly resulting in additional deformation of the total building. The difference between a building with rigid floors and rigid connections, and a building where the stiffness of the floors and connections is presented in Table C.3. It can be seen that the building, deflects roughly 10 to 25 % more compared to the calculations.

Configuration	$u_{RFEM,rigidfloor/connection}$ [mm]	u_{RFEM} [mm]	Difference [%]
3x5	7,8	8,9	13,2
4x8	9,6	11,1	14,5
5x12	11,1	13,2	17,3
6x18	11,4	14,4	23,3

Table C.3: Difference in deflection due to rigid connections

D

Appendix C: Verification of the spring model

D.1. Verification of the load-bearing capacity and stiffness of the spring model

Both methods for estimating the load-bearing capacity and stiffness of the timber-glass shear wall are theoretical approaches used to model its behaviour. In order to verify the theoretical methods they are compared to experimental tests. In this case, the results presented in the paper of Felix Nicklisch, Hernandez, et al. 2015 are used. First, the set-up that is used will be explained. A schematic of the set-up is given in D.1

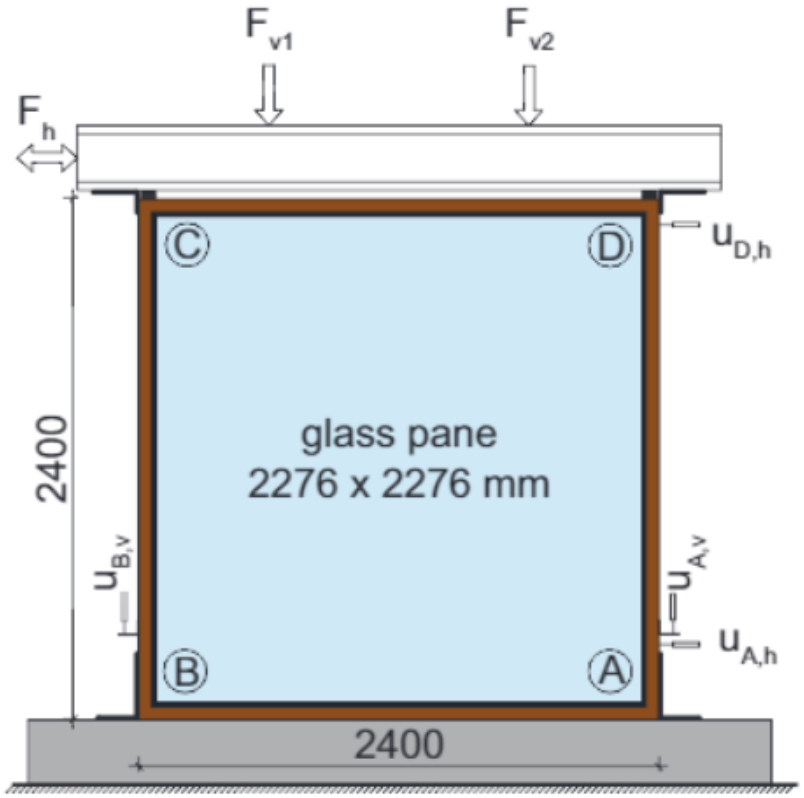

Figure D.1: Set-up experiment timber glass shear wall (Felix Nicklisch, Hernandez, et al. 2015)

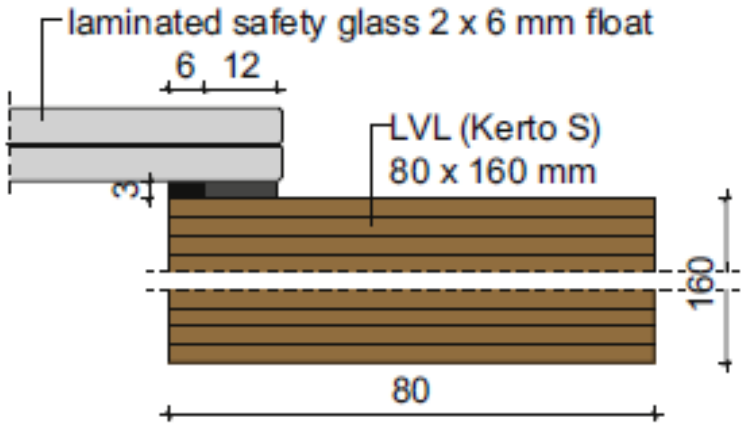

Figure D.2: Set up experiment timber glass shear wall detail(Piculin et al. 2016)

In total 4 tests were performed of which one was a monotonic test. The other tests were cyclically tested and showed similar failure behaviour. The graphs from the cyclic tests are not shown. According to Felix Nicklisch, Hernandez, et al. 2015 the test was performed in the following way: 'The specimen is loaded by a combination of the horizontal load F_h and two vertical loads F_v. In the monotonic static test the horizontal load is applied with an average loading rate of 0.1 mm/s until the ultimate load Fh, max is reached.'

D.1.1. Comparison of the theoretical stiffness vs the experimental stiffness

The spring model is a theoretical approach to model the behaviour of the timber-glass shear wall. In order to verify this theoretical approach it is compared to physical tests. In this case, the results presented in the paper of Felix Nicklisch, Hernandez, et al. 2015 are used.

The input for the theoretical bi-linear stiffness is presented in tables D.1 and D.2:

Component	Index	G [N/mm^2]	b [mm]	d [mm]	$c_{equivalent}$ [N/mm^2]
Adhesive	τ	6,4	12	3	25,6
Adapter frame	KL	270	80	160	135
Glass pane	G	28455	2276 x 2276	12	600,1
C_{total}					20,77
K_{shear}					15761

Table D.1: Input for the equivalent spring stiffness

Component	Index	G [N/mm^2]	b [mm]	d [mm]	$c_{equivalent}$ [N/mm^2]
Adhesive	τ	1,61	12	3	6,44
Adapter frame	KL	270	80	160	135
Glass pane	G	28455	2276 x 2276	12	600,1
C_{total}					6,08
K_{shear}					4616

Table D.2: Input for the equivalent spring stiffness

$C_{equivalent,shear}$ is calculated with Equation 3.13. Subsequently, K_{shear} can be calculated with Equation 3.19. Besides the experimental force-displacement diagram, the theoretical stiffness is shown in Figure D.3

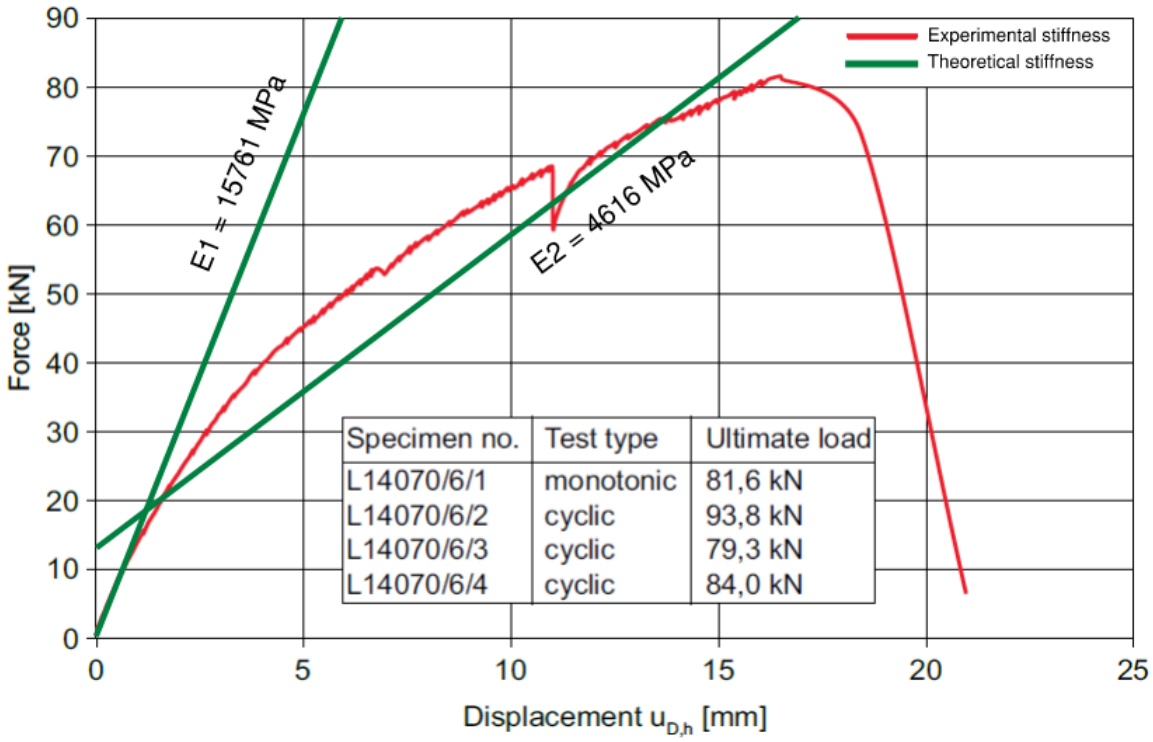

Figure D.3: Theoretical and experimental force-displacement diagram of the timber-glass shear wall (Felix Nicklisch, Hernandez, et al. 2015).

Only the monotonic test type is plotted, but the other cyclically loaded specimens showed similar failure loads. The stiffness outcome of the spring model presented in Table D.1 and Table D.2 is plotted in green in Figure D.3. It can be observed that the bi-linear approximation of the stiffness is reasonably accurate. Especially in the elastic zone of the graph, the deviation between the experimental result and the theoretical result is accurate enough for this research. Another observation that can be made is that the elastic load-bearing capacity of the shear wall is roughly 4,5 times lower than the plastic load-bearing capacity. This reduction is purely caused by the elastic-plastic behaviour of the adhesive.

D.1.2. Comparison of the theoretical load-bearing capacity vs the experimental load-bearing capacity

All the required parameters are presented so Equations 3.25 till 3.36 can be used to calculate the strength of each component. Based on the strength of the individual components, an estimation can be made of the load-bearing capacity of the timber-glass shear wall. Furthermore, the governing failure mechanism can be predicted. The theoretical maximum loads are given in Table D.3

Component	Type of failure	Failure load [kN]
Glass	Shear failure	1229
	Buckling	300
Adhesive	Shear failure	90
LVL Kerto-s	Tensile failure	448
	Shear	62,8

Table D.3: Theoretical failure loads of the test set-up

Based on the ultimate failure loads, it is expected that the timber-glass shear wall to fail in shear splitting of the LVL.

In Figure D.3 it is stated that the ultimate failure load in the case of monotonic loading is 81,6 kN. Furthermore, the failure mechanism is described as: 'The LVL timber frame split in shear deformation

parallel to the grain. The splitting started on the tension end of the wall and continued throughout to the compression end. In some parts, the timber section did not split apart but fibres of the upper ply were torn out. The glass did not break.'

The difference between the calculated failure load and the tested failure load can be explained by several factors. First of all the characteristic shear strength was used to predict the ultimate load. This value is defined as the 5 percent fractile of the strength distribution of a material. In other words, 95 percent of the tested timber has a higher strength than the characteristic value. Therefore it is likely that the ultimate load in testing will result in a higher value. The distribution is also shown in Figure D.4

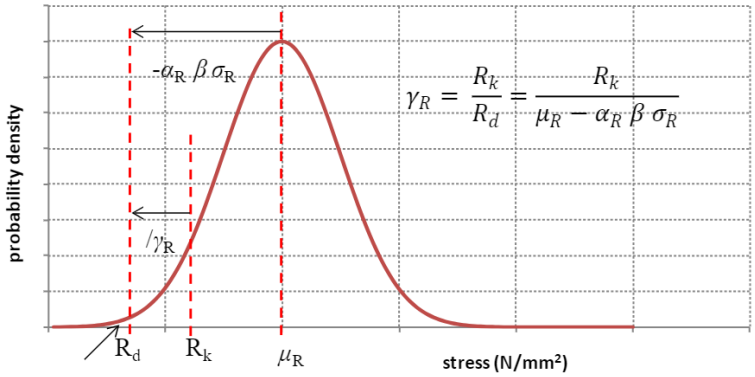

Figure D.4: Relationship between the characteristic strength value and the design strength

For this test, the particular LVL Kerto-s beams is likely to have a higher strength than the characteristic strength of LVL Kerto-s beams.

Another reason could be that the adhesive layer was slightly wider due to tolerances. Especially on a smaller scale tolerances have a higher impact. A wider adhesive layer results in a slightly greater shear area, thus decreasing the shear stress in the timber. For a better representation of the reality, more tests should be performed to limit the impact of statistical deviations especially with wood products.

Nolax C44.8505

Many tests have been performed in literature but for this application, nolax C44.8505 is selected. Nolax C44.8505 is a two-part silane-modified epoxy which is identified as semi-elastic. On this material small-scale tests have been performed, resulting in a large amount of data available on the stress-strain behaviour of the adhesive. Furthermore, full-scale tests have been performed on a timber glass shear wall using this adhesive. This allows for a comparison between the theoretical modal and the physical tests. Thus, enabling verification of the theoretical model. Nolax C44.8505 has the following properties:

Property	Value	Unit
Density	-	kg/m^3
Young's modulus (T = -20 °C)	37,8	MPa
Young's modulus (T = 23 °C)	17,9	MPa
Tangent modulus (T = 23 °C, ϵ = 6,6 %)	4,5	MPa
Young's modulus (T = 80 °C)	15,3	Mpa
Maximum elongation (ϵ_{max})	200 %	-
Poisson's ratio (T = 23 °C)	0,4	-
Shear modulus (T = 23 °C)	6,4	MPa
Average shear strength small-size specimen ($\tau_{m,small}$)	5,2	MPa
Average shear strength mid-size specimen ($\tau_{m,mid}$)	3,3	MPa

Table D.4: General properties of nolax C44.8505

The Young's modulus and Poisson's ratio are used to calculate the shear modulus of the isotropic adhesive:

$$E = 2G(1 + \mu) \tag{D.1}$$

In small-scale tensile tests by Nicklisch et al. 2016 the stress-strain relation of Nolax C44.8505 is found. Tests are carried out at a loading rate of 1 mm/min up to a maximum elongation of 50 % strain. The adhesive did not fail within this strain range. The observed nonlinear behaviour is approximated by bilinear behaviour. The initial stiffness of the adhesive is assumed to be valid up to till 6,6 % strain. This stiffness is calculated from the results between 0,05% and 0,25%. After 6,6 % strain, a much lower stiffness is observed. This stiffness is assumed to be equal to the tangent of the linear segment of the curve. It is assumed that the elastic region corresponds to the region where the initial stiffness is valid. After the kink, the tangent modulus is valid and plastic deformation is assumed. This is shown in Figure D.5

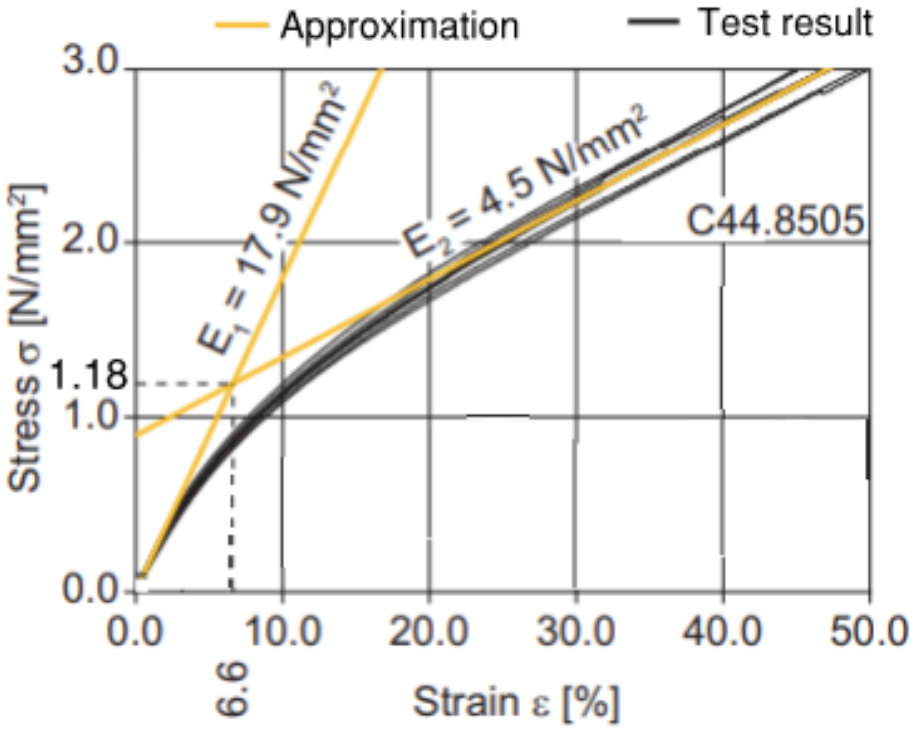

Figure D.5: Bi-linear approximation and experimental stress-strain relation of Nolax C44 8505 (Nicklisch et al. 2016)

The initial stiffness and tangent stiffness at 6,6% are respectively 17,9 N/mm^2 and 4,5 N/mm^2. It is assumed that the Poissons's ratio remains constant during elongation. As a consequence, Equation D.1 can be applied to calculate the shear modulus for both the initial Young's modulus and the Tangent modulus. This results in a shear modulus of 6,4 N/mm^2 and 1,61 N/mm^2 respectively.

Regarding the strength of this adhesive, a distinction is made between the maximum stress and the elastic limit stress. The elastic limit stress corresponds to the stress level up to which the adhesive shows elastic behaviour. When the load is removed, the adhesive will return to its initial position and no permanent deformation will occur. Research has shown that plastic deformation results in limited life to be expected (Moulds 2006). From the graph shown in Figure D.5, the elastic stress limit of 1,18 N/mm^2 is derived.

The adhesive is loaded in shear and therefore the elastic shear stress should be used instead of the elastic stress. In shear test by Piculin et al. 2016 the relation between the shear stress and the displacement of the specimen was found. The tests were performed with Birch plywood. It is assumed that this data can also be used for LVL. The main argument for this is that the failure was either related to failure was related either to failure of the adhesive- timber adhesion or to a combined failure of both timber and adhesion. The maximum stress of the LVL is known and therefore shear failure is included in the calculations. The difference between plywood and LVL is that the ply layers are rotated 90 degrees whereas this is not the case for LVL. This difference has no influence on the strength of the adhesion

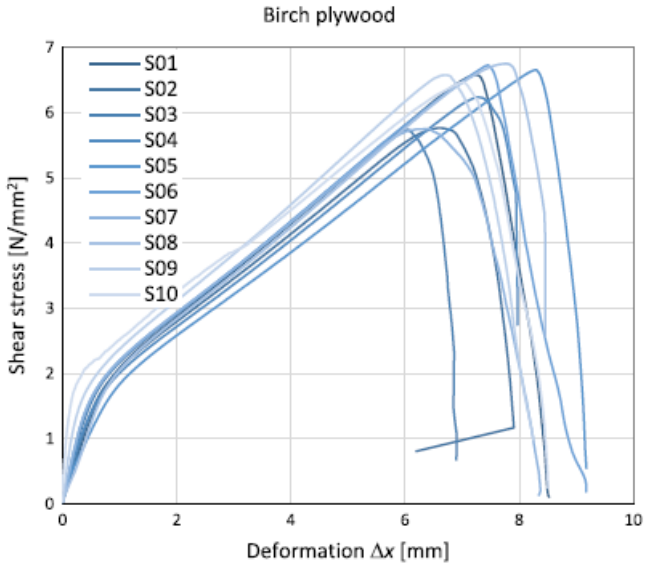

Figure D.6: Results of shear test on small specimens

between the timber and the adhesive and therefore it is assumed that Figure D.6 can be used. Again, bi-linear stress-strain behaviour can be observed. Similar to the axial tests, up to the first part of the shear-strain diagram elastic behaviour is assumed. The second part is assumed to be within the plastic region of the material. With this assumption, it can be stated that the maximum elastic shear stress is equal to roughly 1.8 N/mm2 for small specimens. The timber-glass shear wall is regarded as a midsize specimen and therefore a reduction in strength is applied. The ultimate shear strength of Nolax for small-size specimens was 5,2 MPa whereas for mid-size specimens 3,3 Mpa was used. This results in a reduction factor of 1,57. This reduction factor is also applied to the elastic shear strength and results in an elastic shear strength for mid-size specimens of 1,14 Mpa.